ΕΘΝΙΚΟ ΜΕΤΣΟΒΙΟ ΠΟΛΥΤΕΧΝΕΙΟ
Δ.Π.Μ.Σ.
"Σχεδιασμός και Κατασκευή Υπογείων Έργων"
Συνεργαζόμενες σχολές: Πολιτικών Μηχανικών και Μηχανικών Μεταλλείων Μεταλλουργών

SIMULATION OF A CYLINDRICAL SHAFT WITH F.E.M.

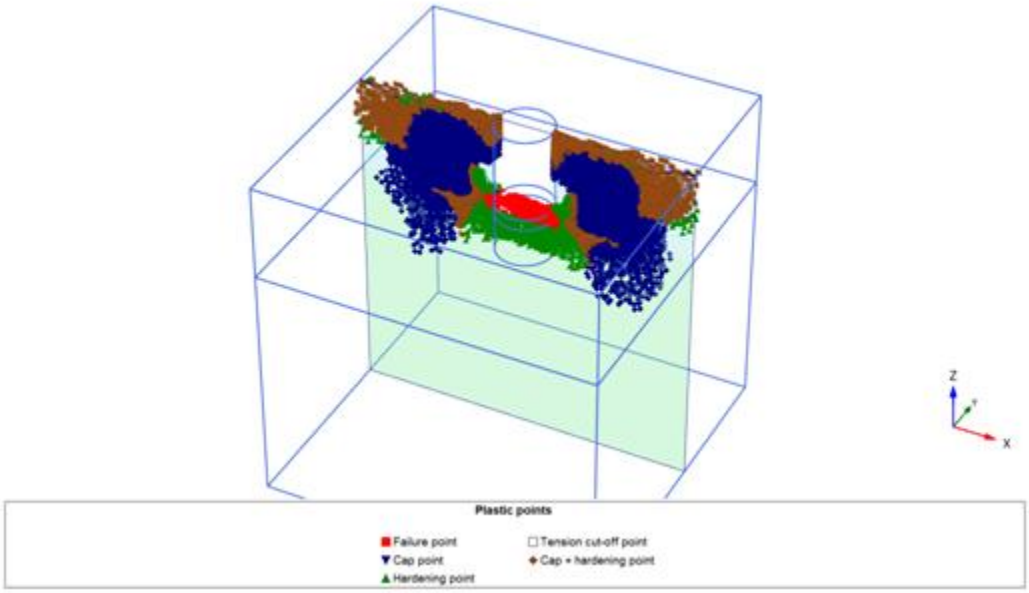

Διπλωματική εργασία του: **Ενρίκο Μουστάκιο**

Επιβλέπουσα: Καθηγήτρια **Βασιλική Γεωργιάννου**

ΑΘΗΝΑ, ΑΠΡΙΛΙΟΣ 2019

SIMULATION OF A CYLINDRICAL SHAFT WITH F. E. M.

"Nature is always smarter than some of us and sometimes smarter than all of us"

"Tunneling brings the engineer into confrontation with the infinite variety and complexity of nature"

ACKNOWLEDGEMENTS

The present postgraduate diploma thesis is presented for the completion of the Interfaculty Postgraduate Master Program “Design and Construction of Underground Works”, which is realized and actively supported by the Schools of Civil Engineering and Mining and Metallurgical Engineering of the National Technical University of Athens (N.T.U.A.).

At this point, I would like to express my sincere gratitude to my supervisor, Dr. Vasiliki Georgiannou, professor at the Faculty of Civil Engineering at the N.T.U.A. for my introduction to the subject of this postgraduate dissertation and continuous support, motivation and knowledge. The present work was the reason for further deepening into one of the most demanding parts of the civil engineering’s science, that of geotechnical engineering.

In addition, I would like to express my acknowledgements to the professor Dr. Nikos Gerolymos, for his valuable knowledge and guidance especially using specialized finite element programs as well as the interpretation of the results.

Misters D. Papadopoulos, Engineering Geologist, M.Sc. and A. Serafis, Civil Engineer, M.Sc. for the excellent and well documented analysis of the project that is as well, analyzed in this postgraduate work. The postgraduate theses of the aforementioned, which were carried out in the framework of the same postgraduate course of studies, were the beginning for my own further study and analysis.

Finally, I would like to thank my friends and family, who in their own special way contributed to the completion of my postgraduate studies.

ABSTRACT

The overall objective of this Master Thesis is to simulate the process of excavation and construction of a 24m deep circular shaft in a two layer ground; each one representing a different soil formation, mainly consisting of low cohesion values.

The above mentioned shaft provides ventilation and access to an underground infrastructure. In the analysis a constant shaft diameter of 10m is considered. The excavation phases and the respective support, consisting of segmented circular prefabricated concrete rings, are numerically simulated with sixteen to seventeen construction stages.

Three finite element method programs are used in order to simulate the excavation and the subsequent construction process, namely “PLAXIS 2D” and “PHASE 2D” for the two-dimensional analysis and “PLAXIS 3D” for a three-dimensional analysis. In the two-dimensional analysis the shaft is analyzed as an axisymmetric problem.

The Mohr Coulomb (MC) and the Hardening Soil (HS) constitutive models, both available in the 2D and 3D versions of PLAXIS are adopted in order to simulate the soil behavior and the respective results of the analyses are compared. Extensive literature review regarding the applications of these soil models is presented.

Furthermore, an attempt is made to replicate the construction process in the presence of a water regime leading to flow and to quantify the effects of flow on the observed stress and deformation development. Maximum hoop forces, bending moments, shear stresses and maximum values of deformations, as well as settlements are reported.

In this MSc Thesis water flow was induced through the installation of wells. Special attention was paid on the deformations associated with lowering the water table and seepage.

ΠΕΡΙΛΗΨΗ

Ο απώτερος στόχος της παρούσας Μεταπτυχιακής Διπλωματικής Εργασίας είναι η προσομοίωση της διαδικασίας εκσκαφής και κατασκευής ενός κυκλικού φρέατος βάθους 24 μέτρων σε ένα υπέδαφος αποτελούμενο από δυο στρώσεις. Η κάθε μία στρώση αντιπροσωπεύει ένα διαφορετικό εδαφικό σχηματισμό, αποτελούμενο κυρίως από έδαφος χαμηλής συνεκτικότητας.

Το προαναφερθέν φρέαρ παρέχει αερισμό και προσβασιμότητα σε μια υπόγεια υποδομή. Στην ανάλυση θεωρείται μια σταθερή διάμετρος φρέατος ίση με 10 μέτρα. Η εκσκαφή και η αντίστοιχη υποστήριξη, αποτελούμενη από τμηματικούς κυκλικούς προκατασκευασμένους δακτυλίους από σκυρόδεμα, προσομοιώνονται ανάλογα με τη διαδικασία κατασκευής με δεκαέξι ως δεκαεπτά φάσεις.

Τρία λογισμικά προγράμματα πεπερασμένων στοιχείων χρησιμοποιούνται για την προσομοίωση της εκσκαφής και της ακόλουθης διαδικασίας κατασκευής, συγκεκριμένα τα “PLAXIS 2D” και “PHASE 2D” για τη δυδιάστατη ανάλυση και το “PLAXIS 3D” για την τρισδιάστατη προσομοίωση. Στη δυσδιάστατη ανάλυση το πρόβλημα προσομοιώνεται ως αξονοσυμμετρικό.

Τα καταστατικά μοντέλα Mohr Coulomb (MC) και Hardening Soil (HS) είναι και τα δυο διαθέσιμα στις 2D και 3D εκδόσεις του PLAXIS. Προσαρμόζονται για να προσομοιώσουν τη συμπεριφορά του εδάφους και τα αντίστοιχα αποτελέσματα συγκρίνονται. Εκτενής βιβλιογραφική αναφορά γίνεται για να δικαιολογηθούν οι προαναφερθείσες επιλογές.

Επιπρόσθετα, εξετάζεται και να αναπαράγεται η διαδικασία κατασκευής υπό την παρουσία υδατικής ροής και συγκρίνεται με ξηρές συνθήκες. Προσδιορίζονται οι μέγιστες εφαπτομενικές δυνάμεις “Hoop Forces”, οι καμπτικές ροπές, οι διατμητικές τάσεις, και οι μέγιστες τιμές των παραμορφώσεων καθώς και οι καθιζήσεις της κατασκευής.

Η παρούσα Διπλωματική Εργασία δεν αντιμετωπίζει μόνο θέματα σχετικά με την αλληλεπίδραση εδάφους κατασκευής. Καταβάλλεται προσπάθεια να αντιμετωπιστούν ζητήματα που σχετίζονται με τις συνθήκες υδατικής ροής, προτείνοντας ως λύση την εγκατάσταση πηγαδιών. Τα πηγάδια εξετάζονται εκτενώς ως μέσο επίλυσης του προβλήματος και εκτιμάται η επίδραση της χρήσης τους, ιδίως μέσω των προκαλουμένων καθιζήσεων.

CONTENTS

LIST OF FIGURES

OUTPUTS - PLAXIS 2D, DEFORMATION ANALYSIS, MOHR-COULOMB MODEL

OUTPUTS - PLAXIS 2D, STRESS ANALYSIS, MOHR-COULOMB MODEL

OUTPUTS - PLAXIS 2D, DEFORMATION ANALYSIS, HARDENING SOIL MODEL

CURVES- PLAXIS 2D, STRESS ANALYSIS, HARDENING SOIL MODEL

PHASE2 8.0

OUTPUTS- PHASE2 8.0, DEFORMATION ANALYSIS, MOHR-COULOMB MODEL

OUTPUTS- 4 PLAXIS 2D, DEFORMATION ANALYSIS, HARDENING SOIL MODEL IN WATER FLOW CONDITIONS

OUTPUS- PLAXIS 2D, STRESS ANALYSIS, HARDENING SOIL MODEL IN WATER FLOW CONDITIONS

CURVES- PLAXIS, DEFORMATION ANALYSIS, HARDENING SOIL MODEL IN WATER FLOW CONDITIONS

EMPLOYMENT OF WELLS

PLAXIS 3D, STRESS ANALYSIS, HARDENING SOIL MODEL IN DRY CONDITIONS

LIST OF TABLES

CHAPTER I
INTRODUCTION

1.1 VENTILATION SHAFT, AN UNDERGROUND STRUCTURE

There is no denying the fact that modern world is under continuous development. That means that modern era cities need more room to expand, although there is no room left on the surface. Consequently the construction of underground structures, structures built beneath the earth's surface, is increasing in most of the industrially developed world employing particular construction methods, structural elements determined by the structure's function and the properties of the surrounding soil or rock. Urban underground structures are of several types, mainly transportation engineering structures and are an integral part of metropolitan areas. In the absence of strong stable rock permanent structures made of cast concrete, reinforced concrete and precast reinforced concrete are built.

One of the major concerns of geotechnical engineering is the study of soils and the interaction with any type of structure which they are able to support. The aim of this dissertation is to study closely the construction of an underground structure, in particular of a 24m deep cylindrical excavation and the excavation support structure; consisting of segmented circular concrete rings providing stability to the excavation and opposing the movements induced by the soil pressures.

It is often the case that cylindrical structures such as shafts are employed. There is a growing engineering interest in deep shafts, as in the recent years the scale and depth of underground projects have grown. That means a more detailed study of the design and techniques used for shaft excavation in a more safe and rational manner.

1.2 SCOPE AND OBJECTIVES

The results of numerical analyses using sophisticated finite element packages such as "PLAXIS 2D", "PHASE 2D" and "PLAXIS 3D" to simulate the excavation and construction process are analyzed.

Primarily, the main objectives are:

1) To review the available theoretical background regarding the modern construction of shafts.
2) To create and develop 2D and 3D FEM models capable of simulating the excavation and the structural response of a circular shaft.
3) To determine and accurately select the soil model parameters.
4) To model the full axisymmetric 2D configuration of a cylindrical shaft.
5) To perform parametric studies and compare their results, namely, displacements, axial, shear and hoop forces and bending moments distributions.

6) To model the shaft configuration in the presence of water flow conditions.
7) Last but not least, to propose practical and pragmatic solutions such as the use of wells in the construction process.

1.3 THESIS STRUCTURE

The present MSc Thesis is subdivided into (7) Chapters each addressing, a separate aspect of the study. Nevertheless, all Chapters including the Introduction in Chapter I contribute to the understanding of shaft behavior. Below a brief description of each Chapter is presented in more detail:

Chapter II contains an extensive literature review regarding the construction of shafts. Various criteria for selecting the most suitable approach to the problem are mentioned, while a special reference is made to circular shafts. Chapter III is dedicated to water flow through soil materials whilst, the concept of permeability is dominating the chapter. The concept of watering is synonym to the use of wells.

Chapter IV refers to the basic concepts of the finite element method and the use of FEM analysis in geotechnical projects. The notion of axisymmetry also discussed.

The project inputs and assumptions are reported in Chapter V. A detailed explanation of the various constitutive models used is made; additionally to assumptions regarding the soil parameters and the construction techniques.

Emphasis is placed on axisymmetric models and studies conducted in Chapter VI. Two dimensional analyses using PLAXIS 2D and PHASE 2 are performed, simulating the staged excavation procedure and the sequential construction. Model settings and computational results are incorporated.

In Chapter VII full models, instead of axisymmetrical conditions examined in previous chapters are used and simulation models are set up in the presence of water flow. Three dimensional analyses using PLAXIS 3D are conducted, simulating the staged excavation procedure and the vertical shaft sequential construction as previously analyzed. Water flow was induced via a group of wells and their performance during construction is examined.

Finally, in Chapter VIII the conclusions and a summary of the analyses' outputs are reported.

CHAPTER II
SHAFTS

2.1 INTRODUCTION

A shaft can be defined as an underground vertical or inclined passageway entered through a manhole. According to Muramatsu and Abe (1996) from an engineering viewpoint, a shaft is defined as a structure with a depth larger than its width, in contrast with earth retaining structures by open cutting of a long and narrow shape or those having a large planar shape.

Shafts are mainly built to facilitate the construction of a tunnel, to provide ventilation to a tunnel or underground structure, as a drop shaft for sewerage or water tunnel and for access or escape route to an underground structure. The traditional use of shafts is to provide a launch chamber for new excavations.

There are a number of construction techniques for the assemblage of shafts. The most common include the application of sheet piles, diaphragm walls or bored piles to construct a rectangular shaft, while segmented lining installed by underpinning or caisson sunk is utilized to form a circular shaft. In the latter case, the excavation proceeds incrementally. Generally, shafts are circular or elliptical in section for structural efficiency reasons, even though more complex geometries may be applied. The multiplicity of the existing methods for excavating and supporting a shaft on civil engineering projects is making them an integral part of almost all underground projects.

There is a necessity to clearly define the nature and scope of the excavation support system and to identify what technical guidance is available for its design, construction and maintenance. The selection of the most suitable construction technique depends on many aspects including the type of ground, the working place needed, the depth of the tunnel horizon, the underground water table, the allowable settlements in particular in urban densely populated areas, the overall cost ect.

Technical challenges during the construction are often experienced, including variable soil and rock profiles, high groundwater tables and limitations imposed by the surrounding built environment.

2.2 SHAFTS CONSTRUCTION METHODS

There are several different shaft support methods found in the international literature, each one representing a series of advantages and disadvantages, depending on the uniqueness of the conditions that are encountered during a shaft construction. It should be underlined that some of these methods are restricted by the depth of the excavation, the ground conditions, that means soil or rock and the groundwater level,

as constructing underneath it is problematic. According to Boyce in Rush (2012) the most common shaft construction methods, from simplest to complex are:

- Trench boxes and speed slide rails
- Soldier piles and wood lagging (or steel plates)
- Liner plates
- Precast segments
- Conventional excavation with rock dowels and shotcrete
- Sheet piles
- Secant piles
- Drilled shafts
- Cutter soil mixing
- Slurry walls
- Ground freezing
- Caissons

For example soldier piles with wood lagging are a common method of shaft construction, allowing for flexibility in shaft size and dimensions while secant piles are small-diameter (3 ft) concrete columns drilled side-by-side, an effective way to build a watertight shaft. In addition drilled shafts are used for smaller diameter shafts (<10 ft) and ground freezing is required in the presence of groundwater or partially saturated ground of high permeability. It is not unusual for methods to be used in combination, depending on the complexity and the applicability of the methods. Designers and builders of excavation supports rely heavily on past experience as well as company-specific design and construction guidelines to perform their work.

2.3 SELECTION OF A SUITABLE SHAFT SUPPORT METHOD

The excavation support structures aim to prevent a collapse of the earth walls that surrounds an open excavation. Its design remains one of the most specialized areas in the engineering and construction field. As stated above not every support construction technique is always suitable. A critical reasoning must be made based on various parameters. The choices available are in turn determined primarily by the prevailing ground conditions and the purpose of the shaft. The most significant ones are briefly mentioned below.

In addition, excavation support always involves a certain amount of risk based on the unknown. Underground conditions are difficult to predict with complete accuracy.

2.3.1 GEOTECHNICAL CONDITIONS

The most important parameter in the selection of the most suitable support method is the existing geological conditions, signifying the various conditions that represent the geotechnical characteristics taken into account in the verification of the performance

of the shaft and its reliability. Geotechnical and hydrogeological conditions incorporate stratigraphical conditions of the ground, including depth of the bearing strata, depth of the thickness of weak strata, water level and hydraulic conductivity, degree of compaction, consolidation characteristics, shear characteristics, liquefaction potential, ect.

According to Aye et al. (2014) for a material mainly dominated by cemented to semicemented, dense and generally low permeability soil including some localized sand lenses, it is expected that the soil can have sufficient standup time during the excavation and may not induce significant ground movement if the face is left unsupported for a short period of time prior to installation of the supporting elements. Such a ground condition is suitable for adopting the caisson method.

2.3.2 PURPOSE OF THE COSTRUCTION

Ventilation shafts, buildings used for providing fresh air, are commonly widely used in engineering structures. Circular, mainly, shafts are designed to facilitate the launching of tunnel boring machines (TBMs) for the construction of metro in metropolitan areas at some part of the alignment. In such cases an extended diameter is chosen as a project parameter. Shafts provide access between underground and aboveground structures such as underground sewage treatment facilities, hydraulic and power facilities, underground storage tanks. They might have even a temporary use (temporary shafts) supporting the logistics for the tunnels, lowering pipes, utilities and other tunnel related installations and services. In such cases the dimension of the shaft is determined based on the functionality, providing access between underground and aboveground structures.

2.3.3 SHAPE OF THE SHAFT

Many, if not almost every shaft construction method can be adapted to both circular and rectangular shapes. Elliptical or even more complex forms can be found. Specifically, elliptical forms are applied in very deep shafts. Zhang et al., (2013) suggested that combined shapes are adopted in special geological conditions to achieve given functions. In relatively high crustal stress area if the maximum principal stress is much higher than the minimum principal stresses, an elliptical shape with the long axis parallel to the maximum principal stress is the best choice for stability. According to Holl & Fairon, (1973), historically, the typical shape of the shaft in the horizontal plane has changed from being rectangular to circular due to the development of new construction techniques.

2.4 CIRCULAR SHAFTS

A review of the literature sources related to this particular civil engineering structure reveals valuable and sufficient information. It can be concluded that a circular shaft is structurally stable. The earth loads applied to this geometry place the support in ring compression. The reinforcement in the structural elements can be reduced, benefiting the structure and the need for internal support is limited. The shape is typically vertical, for obvious reasons. That means to minimize the overall length of the excavation and consequently the comprehensive cost.

According to Kunagai et al. (1999) circular building shape due to their structural superiority and the benefit of not requiring any bracing systems, result in a large decrease in construction cost and time.

Zhang et al. (2013) affirm that, circular shape is widely used for vertical shaft due to its unique feature, which cannot converge freely when radially loaded. When the wall is subjected to an axisymmetrical pressure 'p' the reaction to the external pressure produces a compressive hoop force in the wall which resists the tendency to converge and no extra support from the internal shaft is needed to balance the external pressure. This is the reason why circular supporting structures are inherently stable under an axisymmetrical pressure provided the hoop force does not exceed the limits of the material properties.

Aye et al. (2014) stated that a circular structure is preferred as it is structurally stable and can be constructed with no struts spanning across the excavation, hence providing a relatively obstruction free area for excavation works. Also, by taking the ground loading through hoop forces (circular shape), a circular shaft can minimize the ground displacement during excavation.

Muramatsu and Abe (1996) conducted an empirical study and it was made clear that cylindrical shafts tend to decrease diaphragm wall displacement more than rectangular earth retaining structures on the same scale without regard to the aspect ratio of a shaft or the hardness of the ground excavated.

The behavior of a vertical shaft is affected and near the surface is dominated by gravitational forces (Wong and Kaiser, 1988 in Kim et al., 2013). It is a truly three-dimensional problem and all three stress components (σ′ t, σ′ v, σ′ r) are important. The stress concentrations near a vertical shaft would cause yielding due to the stress difference between vertical (σ'_v) and radial (σ'_r) stresses around a shaft. Tangential, vertical and radial stresses (Wong and Kaiser, 1998) are schematically represented below (Wong and Kaiser, 1998).

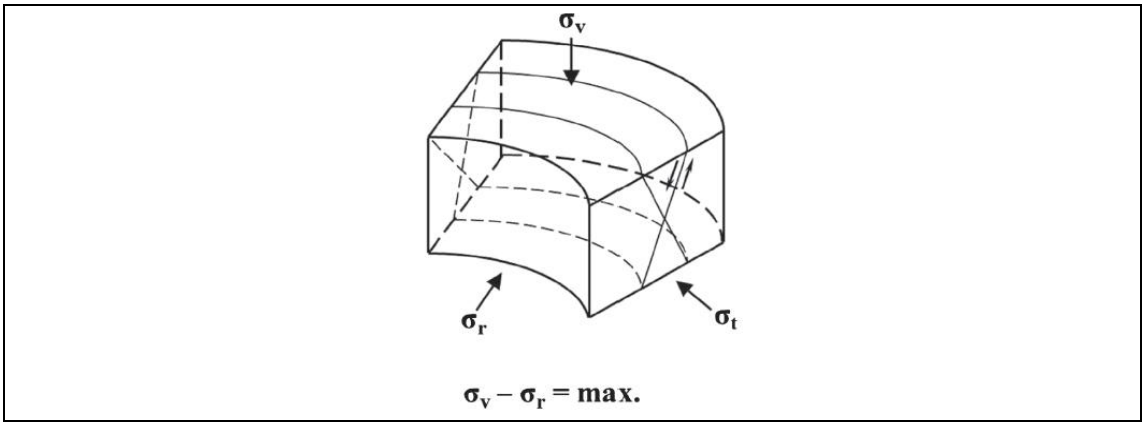

Figure.1 Behavior of the soil around vertical circular shaft, mode of yielding (Wong and Kaiser, 1988).

According to Kim et al. (2013) since Terzaghi in 1920 started to examine the effect of lateral earth pressure acting on a plane wall, much work has been done in the area of soil–structure interaction of plane retaining walls. Relatively little work has been done on flexible and circular walls such as in vertical shafts, and hardly anything on earth pressure distribution on vertical circular shaft. Soil-circular wall interaction is complicate since many complex construction sequences, different soil conditions, initial conditions, and arching effect are involved. Additionally, previous studies are not applicable to the multi-layered and/or c–φ soils. The authors studied the distribution of lateral earth pressures along the depth, simulating a cylindrical shaft construction using F.E. models. It can be concluded that proper estimation of earth pressures is a key factor in design of vertical circular shafts. The behavior of a vertical shaft is a three dimensional problem. Because of three dimensional arching effects, i.e. convex arching and/or inverted arching, the earth pressure acting on a circular type of vertical shaft is less than in other types.

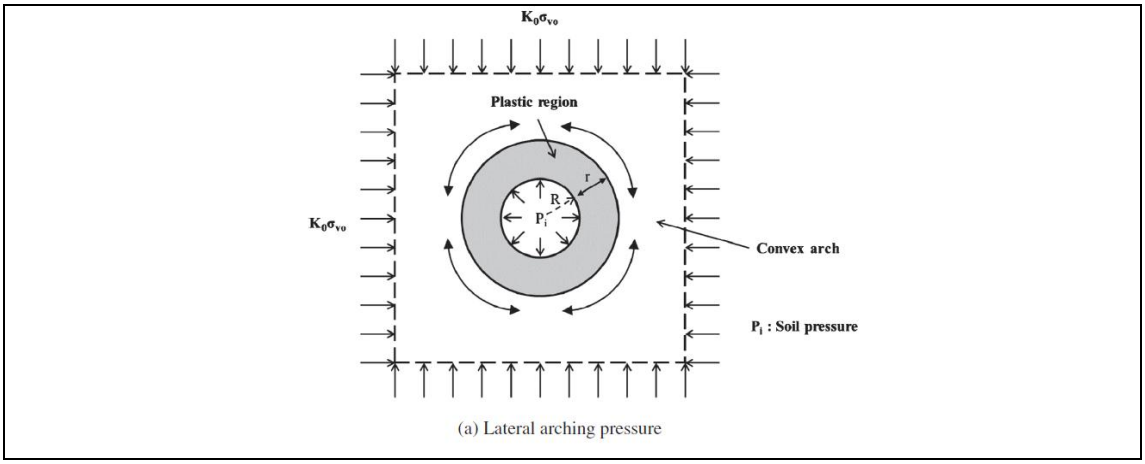

Figure.2 Lateral and vertical arching effect of vertical circular shaft, lateral arching pressure (Kim et al., 2013).

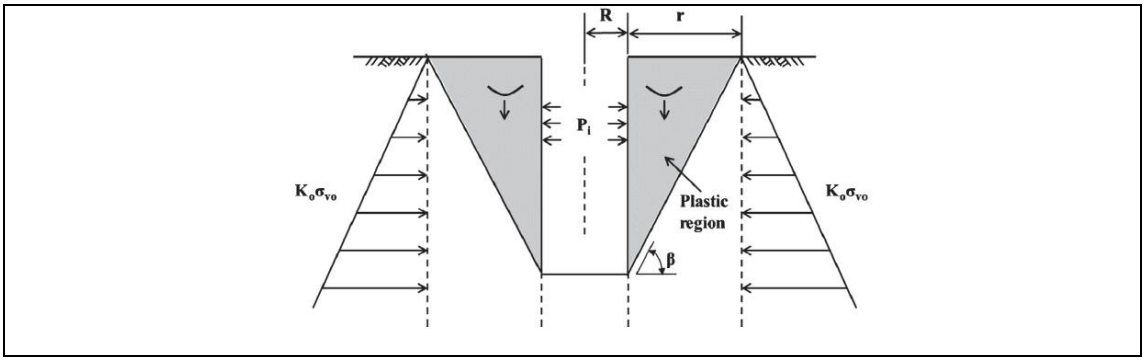

Figure.3 Lateral and vertical arching effect of vertical circular shaft, vertical arching pressure (Kim et al., 2013).

As it is shown above, it is necessary to consider an accurate shape for the slip surface in the formulation for the earth pressure.

Although a circular retaining system is known to be one of the most stable and economic retaining system, during the construction several building challenges may occur. Maintaining the circularity of the shaft is another important design consideration to take into account.

2.5 EARTH PRESSURE DISTRIBUTION ALONG A CYLINDRICAL STRUCTURE

In the last decades the state of stress around a vertical axisymmetric excavation in soft ground has been theoretically studied by several authors. All methods predict that horizontal stresses are less than the active values. The distribution of earth pressure differs considerably.

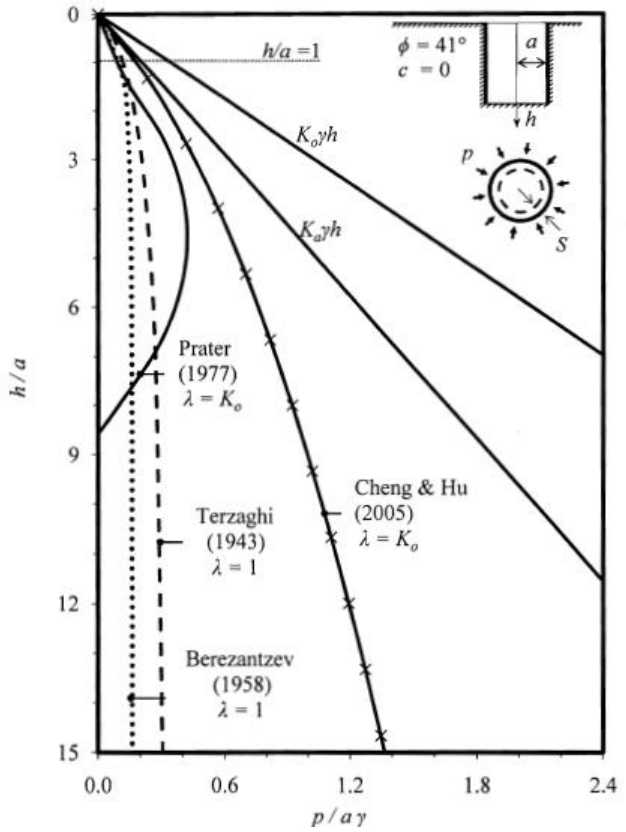

Figure.4 Earth pressure distribution using different theoretical methods (Cheng and Hu, 2005).

The above figure shows a comparison of the calculated earth pressure distribution along a shaft of radius α and depth h, using some of the above methods, namely: Terzaghi (1943), Berezantzev (1958), Prater (1977) and Cheng and Hu (2005). To be mentioned that λ is a coefficient of lateral earth pressure for the active conditions defined as the ratio of tangential to normal stresses acting on radial plates $\lambda = \sigma_\theta/\sigma_r$. According to Meftah et al. (2018), it can also be observed that Prater, Terzaghi and Berezantzev‘s methods are easy to apply but underestimate the active pressure. Moreover, Coulomb's theory and Rankine’s theory for the prediction of the active earth pressure on the shaft are easy to apply but they an overestimate of these pressures.

2.6 SEQUENTIAL EXCAVATION METHOD

The Sequential Excavation Method has been, in the past, typically used for the excavation of tunnels and recently has been adapted for the excavation of shafts. The earth removal is usually performed sequentially either in small benches or as a fully fixed depth cycle depending on the shaft dimensions and shaft properties.

According to Aye et al. (2014) the sequential excavation method is selected to construct the large diameter shafts. The shaft excavation area is divided into several

parts around the shaft with a center core. The casting of rings is carried out sequentially upon completion of the excavation at a particular area. Dias at al. (2013), stated that Excavation of shafts with this technique in residual soils implies usually that the water table is lowered, creating a non-saturated condition with important consequences, both in the mechanical and hydraulic behavior of the excavation. The procedure in vertical direction is briefly explained below and schematically shown in the following figure (Figure 5).

1) The 1st phase can involve water table (WT) variations and the WT lowering can happen before or while the excavation takes place. At the same time takes place the construction of the capping beam;
2) Excavation of the 1st ring;
3) Construction of the support of the 1st ring;
4) Repeat phase 2 and 3 to the remaining rings ending with the excavation of the last ring and construction of the respective support.

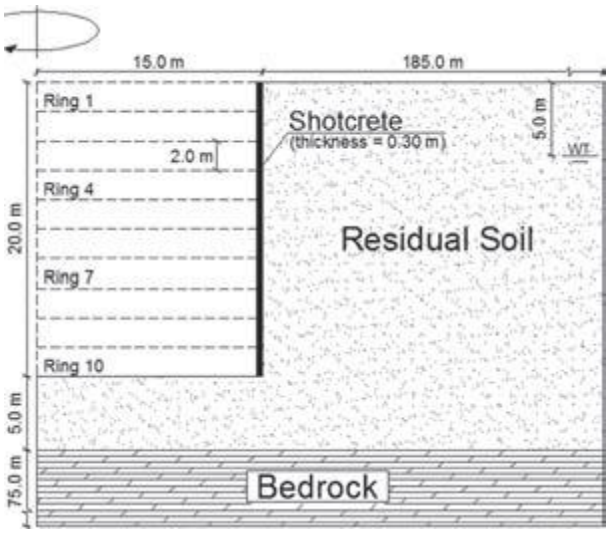

Figure.5 Geometry of the hydromechanical calculation (Dias et al., 2013).

2.7 PRECAST SEGMENTS

Precast segments represent an economical and safe solution for permanent and temporary underground structures making them ideal for a variety of applications including ventilation shafts. The main advantages are:

- Cost saving.
- Innovative design.
- Safe work environment.
- Minimal environmental impact.

An arcuate shaft or tunnel lining segment includes a precast concrete body divided into angularly adjoining segment parts that are held fastened together. It is common practice to describe circular shafts using terminologies like ‘‘segmental shafts’’, ‘‘caisson shafts’’ or ‘‘segmentally lined shafts’’. There are various techniques available to install a precast concrete shaft segment, including the caisson method, the underpin method and/or a combination of the two.

Figure.6 Erection of pre-cast segments for Ref. National Grid (2015). The ground is exposed prior to erecting the shaft lining (Faustin et al., 2013).

In the above figure the underpin method of shaft installation is shown. According to Humes, the underpin method can be used in self supported soil where caisson installation is not possible. In this method, the precast concrete elements are progressively installed at the base of the excavation. Segmental rings are built and the annulus between their outside perimeter and the excavated ground is immediately grouted. To be distinguished from the caisson method, used in softer soils with or without the presence of ground water t he precast concrete elements are erected at the surface and are then lowered into the ground whilst excavation progresses.

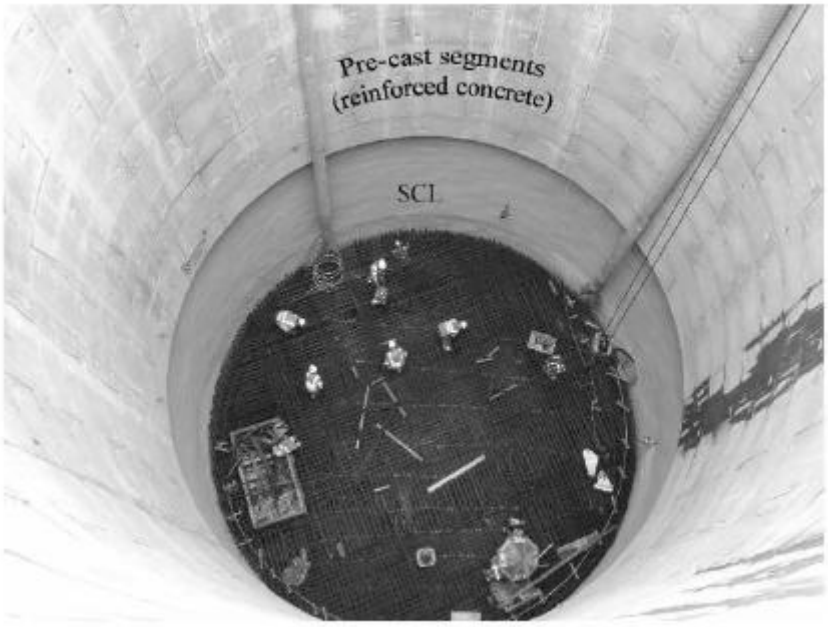

Figure.7 EBS shaft construction for National Grid's London Power Tunnels project (Ref. National Grid (2015) (Faustin et al., 2013).

2.8 COMMON FAILURES

It is often the case that civil engineering projects are threatened by a potential risk of excessive water ingress that might be encountered when the ground is exposed during excavations. In particular the finer soil elements might be washed out, dragged by the high water flow provoking face instability. Unbalanced lateral pressure due to the different soil type might act on the shaft in a way that the supporting system could not withstand. Moreover, uneven topography and geological conditions, additional loadings due to the site activities and unbalanced loading due to construction activities could damage irreversibly the project.

2.9 SETTLEMENTS

The construction process unavoidably reduces the horizontal stress in the ground and causes movement of the adjacent soil. Settlements might occur not only during the installation of shaft lining, but even during the formation of the cavity of the shaft. In the international bibliography there is a limited number of well documented studies regarding ground movements related to the construction of cylindrical shafts. The origin of the settlements could be:

- Excavation induced settlements.
- Settlements due to the installation of the supporting system.
- Dewatering settlements.

According to Faustin et al. (2018), the field observations show that settlements arising from excavation of circular shafts are critically dependent on the method of shaft construction. More specifically, from a case study the interpretation of the field observations showed that settlements are much more significant for excavation before support shaft construction than for support before shaft excavation, although settlement arising from installation of pre-installed walls or dewatering operations should not be overlooked.

Even more critical could be the occurrence of differential settlements, occurring when parts of the building settle at different rates resulting in cracks, potentially affecting the structural integrity of the building.

CHAPTER III
WATER FLOW

3.1 INTRODUCTION

In the subsoil the water may be under static conditions without flow. When the underground water is in a state of rest, the water pressures are hydrostatic. However, when there is a water flow in the ground, the conditions are no longer hydrostatic and the water pressure depends on the flow conditions. There are many cases where groundwater is initially in an at rest state, turning to steady state flow as a result of various activities such as water pumping to a certain extent, during underground construction ect.

3.2 WATER FLOW THROUGH SOIL MATERIAL

The problem of water flow across the soil is of particular interest to the geotechnical engineer. In some cases, the aquatic flow through the soil is desirable, for example pumping to supply water from the underground horizon. All soil elements are permeable as the voids of their pores communicate and form continuous passages. Subsequently, water moves through interconnecting voids. In granular materials all the voids communicate with each other regardless of their placement pattern as bead experiments have shown. The water flow velocity through the voids depends on their size and layout, resulting in the variation of the soil materials permeability. Differences in the permeability of different soil materials are purely quantitative, i.e. other materials have high permeability (for example gravels and coarse sands) while other have very low values (clays).

One of the major problems where the water flow into soil is involved is the amount of water that is infiltrated into the interior of the excavation below the phreatic horizontal line. In this case the infiltrating waters, apart from the fact that it obstructs the construction process inside the excavation, loosen the soil, with consequent collapse of the excavation sides, loosening of the bottom of the shaft, ect.

3.3 PERMEABILITY

Permeability can be defined as the ability of a porous mass to allow passage of water through the medium. Determining permeability enables to study fluid flow characteristics through a soil mass, as understanding permeability means understanding the structure of the soil.

Permeabilities **kx**, **ky** and **kz** or coefficients of permeability (hydraulic conductivity) have the dimensions of velocity (unit of length per unit of time). In particular, the higher the permeability factor, the greater the flow rate in the soil material, if the remaining sizes are kept constant. This factor depends on the size of the soil materials and therefore it is not a property of the material but changes when the degree of its condensation changes. For example, a particular sand has much greater permeability when it is loose, rather than when condensed, assuming a very dense structure. The input of permeability parameters is required for seepage and consolidation calculations. In such calculations, it is necessary to specify the coefficient of permeability for all drained and undrain clusters in the FE analyses.

3.3.1 LABORATORY DETERMINATION OF PERMEABILITY

The two important methods for determining permeability in the laboratory are the constant-head permeameter and the variable-head permeameter methods.

- Constant-Head Permeameter
  The principle is that the hydraulic head causing the flow is maintained constant. The quantity of water flowing in a given time through a soil specimen of known cross-sectional area and length is measured. Since adequate quantity of water gets collected in a relatively short time in pervious soils only, this set-up is mainly used for sandy soils. If Q is the quantity of water collected in the measuring jar after flowing through the soil in an elapsed time t, from Darcy's law, the rate of flow or discharge

$$q = \frac{Q}{T} = ki\,A$$

Therefore, $$k=\frac{Q}{t}.\frac{l}{iA} = \frac{Q}{t}.\frac{L}{Ah} = \frac{QL}{thA}$$

where k is the coefficient of permeability, L and A are length and cross section of soil specimen and h is the hydraulic total head difference causing the flow. The water should be collected only after a steady state of flow has been established.

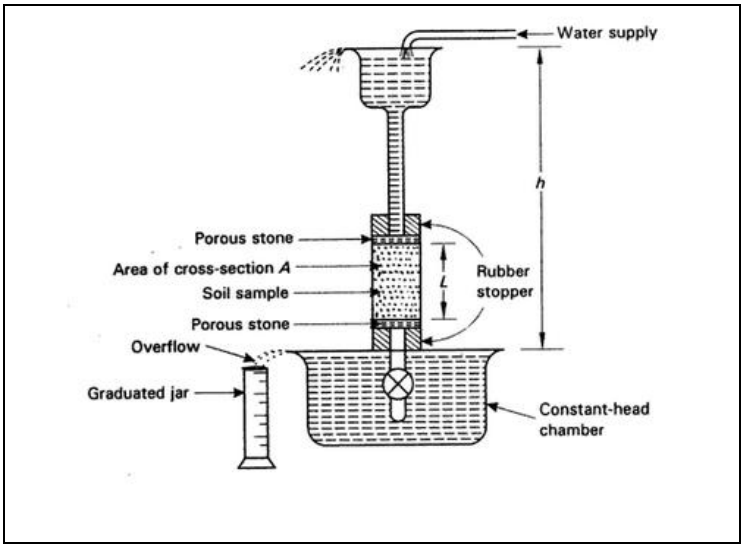

Figure.8 Schematic diagram of constant-head permeameter (Venkatramaiah, 1995).

- Variable head permeameter (falling head permeameter)
  The water level in the stand pipe falls continuously as water flows through the soil specimen. After steady flow is established, if the head or height of water level in the stand pipe above that in the constant head chamber falls from h_o to h_1, corresponding to elapsed times t_o and t_1, the coefficient of permeability k can be shown to be

$$k=\frac{2{,}303aL}{A(t1-to)}\log10\left(\frac{ho}{h1}\right)$$

  where a is the area of the cross section of the stand pipe and L and A are the length and cross section of the soil, respectively (Venkatramaiah, 1995).

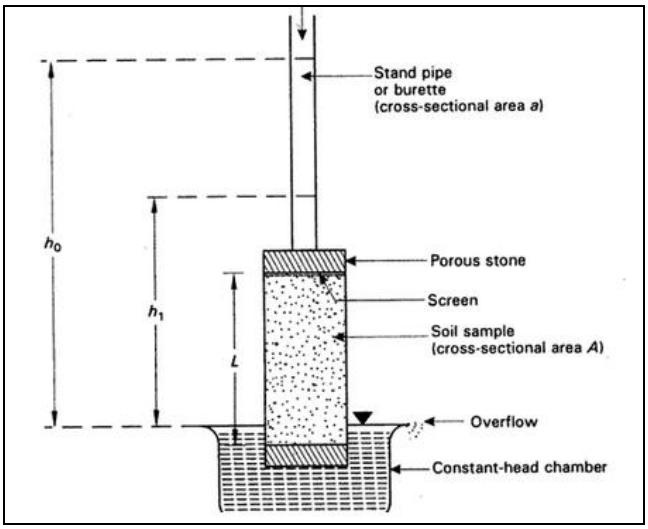

Figure.9 Schematic diagram of variable-head permeameter (Venkatramaiah, 1995).

Soil type	k (m/sec)
clear sands	10^{-2}-10^{-5}
silty sands	10^{-5}-10^{-8}
silts, clay silts	10^{-8}-10^{-9}

Table.1 Typical values of the coefficient of permeability for various soil formations (Kavvadas, 2005).

3.4 DEWATERING

Dewatering becomes an issue any time an excavation will proceed below the ground water table. Two basic solutions are available for ground water control. The first is to select a watertight support method such as continuous steel sheet piles or slurry walls. The second option is to temporarily or permanently alter the level of the water table (Chini and Genauer, 1997).

According to Datta et al (2005), when construction operations have to be executed below the ground water level, it is desirable to temporarily lower the water table such that work can proceed in relatively dry conditions by:

a. Collecting water in sumps and pumping out.
b. Installing wellpoints (small sized wells) or deep wells and pumping out groundwater.
c. Using special techniques in fine grained soils, such as vacuum dewatering and electroosmosis.

For a more dry working area, the two methods used most often for lowering water table below the excavation level are the **wellpoint** method and the **deep well** method. The former is economical and useful for lowering the water table by 15 meters or less, whereas the latter is used for lowering the water table by more than 15 meters. Both methods are based on the fact that removal of water by continuous pumping from well causes the water table level to become depressed and results in the formation of a drawdown curve. Wellpoints can usually lower the water table by only 6-7 meters because the pump, which is located at the ground surface and connected to a group of wellpoints through a header pipe cannot lift water from a higher depth.

As it is clear from the above, there are many methods of lowering the phreatic surface. The selection of the most suitable one depends on many factors such as the level of the phreatic surface, depth and extend of the excavation, depth of the impermeable substrate, nature of the soil with particular reference to the granulometry ect.

In the study of groundwater hydraulics some simplifications are generally proposed for the theoretical approach of the problem of dewatering. According to Chiesa

(1994), problems related to the uptake of groundwater can be studied considering a transient or stationary regime. In the transient regime the cone of influence expands during pumping while in the steady state, the depression cone reaches a geometry that remains fixed over time. Regarding water drainage works, only the stationary regime is considered since these works generally drain for long periods of time. In such conditions the stationary regime is reached. The following simplifications are proposed:

i. The flow of the water must be considered laminar, thus making Darcy's law valid.
ii. The aquifer must be devoid of proper motion and therefore its surface must be horizontal.
iii. The thickness of the aquifer must be considered constant.
iv. The aquifer must be considered continuous, homogeneous and isotropic.
v. The aquifer must be considered of infinite extension.
vi. The flow velocity must not vary along the depth and therefore the equipotential lines must be a vertical network.
vii. The vertical component of the velocity must be considered as null, ie the flow lines must be represented by horizontal straight lines.
viii. The well or the drainage points must have an efficiency of 100% and therefore there must be no difference in pressure drop between the well and the aquifer.

It is obvious that, the conditions listed above are difficult to find in nature where the hydraulic characteristics of the soil can present strong variations in space.

Should be noted that, aquifer is a permeable formation which allows a significant quantity of water to move through it. Aquifers may be unconfined, in which case the ground water table is the upper surface of the zone of saturation and it lies within the test stratum, or confined, in which case groundwater remains entrapped under pressure greater than the hydrostatic pressure by overlying relatively impermeable strata. The latest is called artesian acquifer.

3.5 WELLS

A water well is a hole shaft, or excavation used for the purpose of extracting ground water from the surface. Water may flow to the hole naturally after excavation of the hole or shaft. Such a well is known as a flowing artesian well. More commonly, water must be pumped out of the well.

The overall objective of the design is to create a structurally stable, long-lasting, efficient well that has enough space to house pumps or other extraction devices, allows ground water to move effortlessly and sediment free from the aquifer into the well at the desired volume and quality and prevents bacterial growth and material decay in the well (Harter, 2003).

It is common that a group of wells is used. In the case of water excavation from the subsoil through a group of wells, the overlapping of the draining effects must be taken into account. That means, that when the wells are located at a mutual distance, less than their radius of influence R, each well interferes with the other neighboring wells and therefore, the lowering of the groundwater level is equal to the algebraic sum of the lowering produced by every single well (Chiesa, 1994).

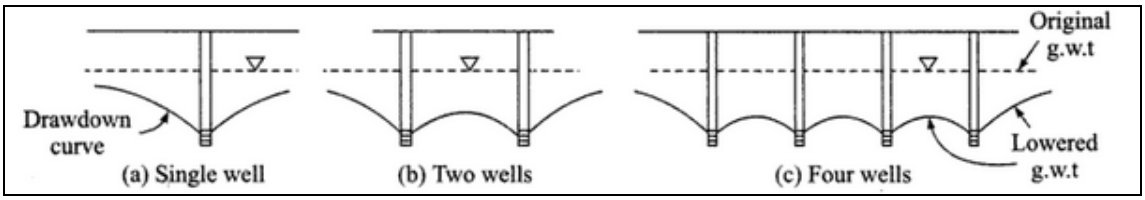

Figure.10 Drawdown curves for a single well, two wells and four wells (Datta et al, 2005).

In the Figure 11 are reported some plan views of groups of wells of various geometrical configurations are shown. In particular, wells placed at the vertices of a square, wells along a circumference, wells set along two parallel lines and wells placed along the sides of a rectangle. In the case of wells along a circumference, the lowering is equal to that given by a well placed in the center and with a capacity of nQ, where n the number of wells and Q the total discharge of every single well (m^3/s).

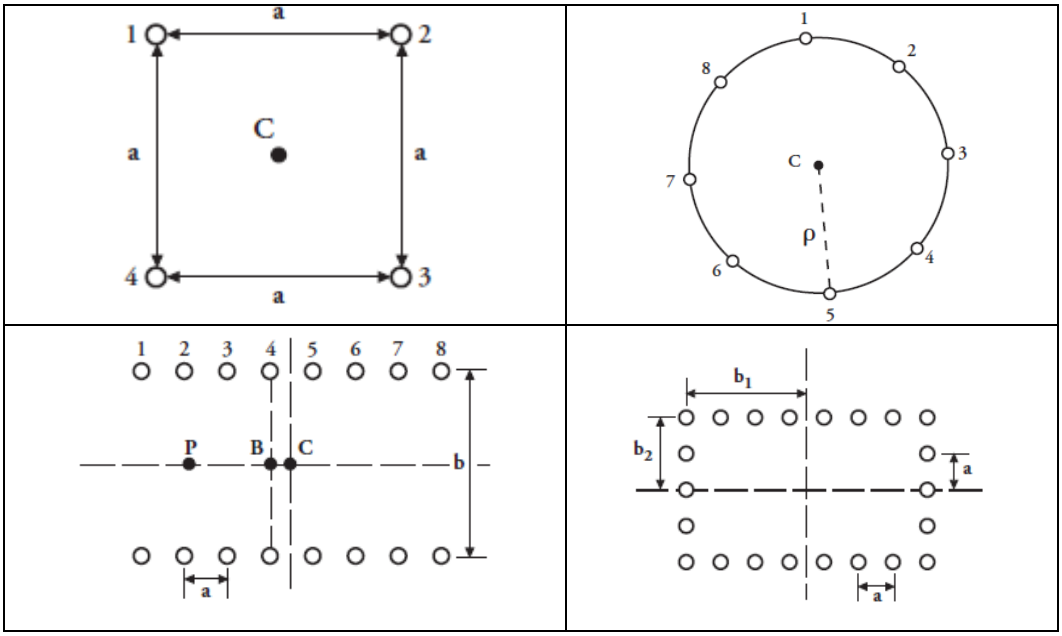

Figure.11 Some examples of groups of wells (Chiesa, 1994).

Last but not least, it should be kept in mind that, when wells are utilized, there is always the fear of unacceptable settlements induced around nearby existing buildings and of environmental concerns such as groundwater withdrawal and recharge. Additionally, difficulties in controlling the excavation process often results in larger ground settlements around the well.

CHAPTER IV
F.E.M.

4.1 INTRODUCTION OF BASIC CONCEPTS OF THE FINITE ELEMENT METHOD

The finite element method (FEM), sometimes referred to as finite element analysis (FEA), is a computational technique used to obtain approximate solutions of boundary value problems in engineering. Simply stated, a boundary value problem is a mathematical problem in which one or more dependent variables must satisfy a differential equation everywhere within a known domain of independent variables and satisfy specific conditions on the boundary of the domain. Boundary value problems are also sometimes called field problems. The field is the domain of interest and most often represents a physical structure. The field variables are the dependent variables of interest governed by the differential equation. The boundary conditions are the specified values of the field variables (or related variables such as derivatives) on the boundaries of the field. Depending on the type of physical problem being analyzed, the field variables may include physical displacement, temperature, heat flux, and fluid velocity to name only a few (Hutton, 2004).

The finite element formulation of the problem results in a system of simultaneous algebraic equations for solution rather than requiring the solution of differential equations. These numerical methods yield approximate values of the unknown at discrete numbers of points in the continuum. Hence this process of modeling a body by dividing it into an equivalent system of smaller bodies or units (finite elements) interconnected at points common to two or more elements (model points or nodes) and/or boundary lines and/or surfaces is called discretization. In the finite element methods instead of solving the problem for the entire body in the operation we formulate the equations for each finite element and combine them to obtain the solution of the whole body (Logan, 2011).

The solution for structural problems typically refers to determining the displacement at each node and the stresses within each element making up the structure that is subjected to applied loads.

In Figure 12, the following types of elements used in discretization are shown in sequence respectively, a) simple two dimensional elements with corner nodes, typically used to represent plane stress/strain and higher order two dimensional elements with intermediate nodes along the side, b) three dimensional elements typically used to represent three dimensional stress state and higher order three dimensional elements with intermediate nodes along edges, and simple axisymmetric triangular and quadrilateral elements used for axisymmetric problems.

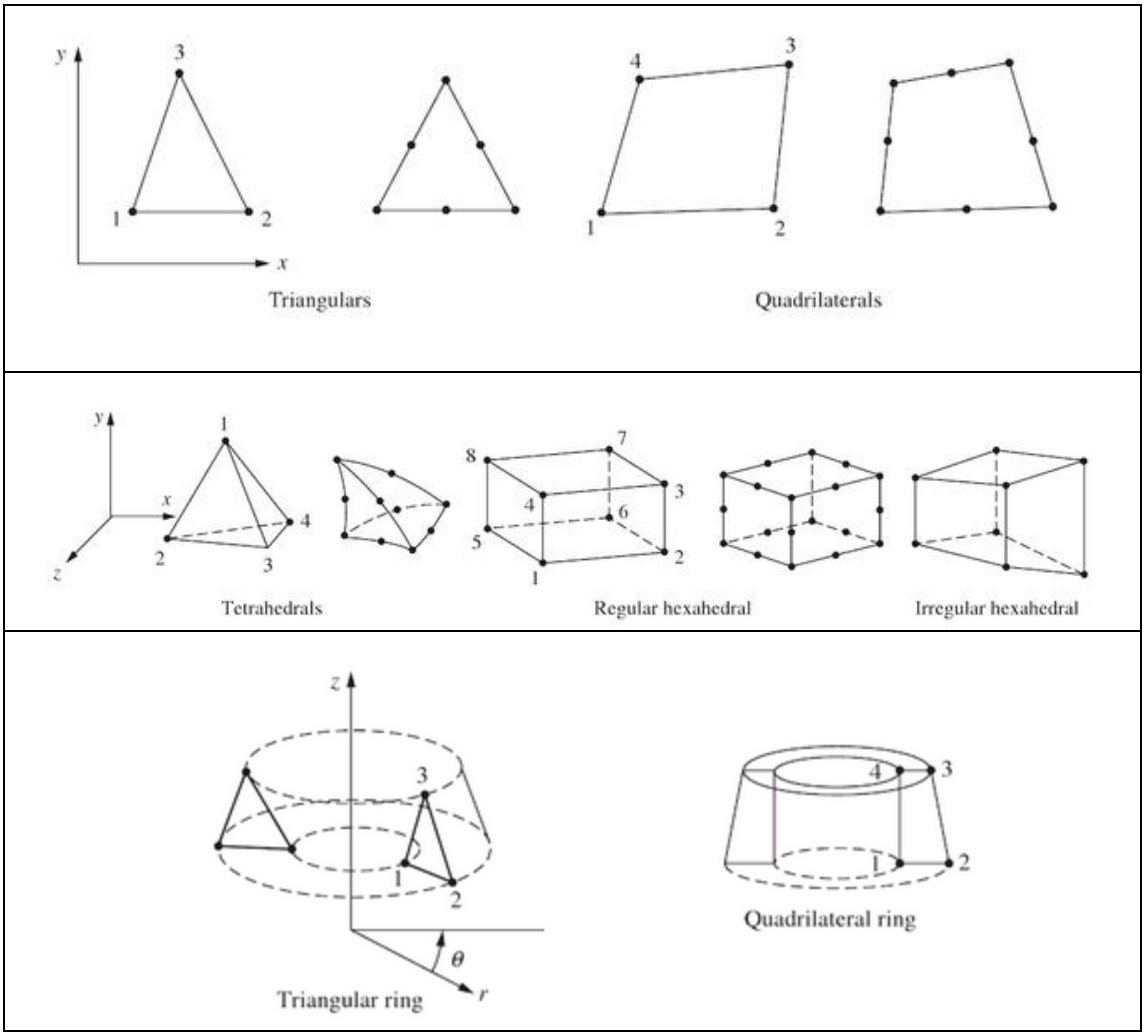

Figure.12 From top to bottom, two-dimensional, three-dimensional and simple axisymmetric and quadrilateral elements (Logan, 2011).

4.2 FINITE ELEMENT ANALYSIS IN GEOTECHNICAL PROJECTS

The finite element method has been used in many fields of engineering practice. Recently it has begun to be widely used for analyzing geotechnical problems. The method when properly used can produce realistic results which are of great value to realize civil engineering problems. One of the most important aspects of a finite element analysis of a geotechnical problem is an appropriate soil constitutive model.

According to Potts and Zdravkovic (2001) to perform useful geotechnical finite element analysis, an engineer requires specialist knowledge in a range of subjects:

- Firstly a sound understanding of soil mechanics and finite and finite element theory is required.
- Secondly, an in-depth understanding and appreciation of the limitations of the various constitutive models that are currently available is needed.

- Lastly, users must be fully conversant with the manner in which the software they are using works.

4.3 FINITE ELEMENT ANALYSIS AND SYMMETRY

Geotechnical problems involving three dimensional structures necessitate a three dimensional analysis fully representing the structure's geometry, loading conditions and variations in ground conditions. This is not always a practical proposition with current personal computers.

For a twodimensional and axisymmetric analysis the assumption is frequently made that there is an axis of symmetry about the centerline of an excavation and that only a half selection needs to be modeled. In the case of a three dimensional analysis two planes of symmetry are often assumed and a quarter section is considered. This clearly reduces the size of the problem and the number of finite elements needed to represent it. However, for such an analysis to be truly representative there must be complete symmetry about the center line of the excavation. This symmetry includes geometry, construction sequence, soil properties and ground conditions (Potts and Zdravkovic 2001).

In plane stress problems, stresses exist only in the x-y plane. In axisymmetric problems, the radial displacements develop circumferential strains that induce stresses σ_r, σ_θ, σ_z and τ_{rz}, where r, θ and z indicate the radial, circumferential and longitudinal directions respectively. Triangular elements are often used to idealize the axisymmetric system because they can be used to simulate complex surfaces and are simple to work with (Logan, 2011).

4.4 PLAXIS 2018 ® 2D

The initial purpose of developing Plaxis was that, because of its many sea dikes and river embankments, the Nederlands have a special interest in geotechnical research. Computational geotechnics were needed for making results of geotechnical research operational. Computer codes then extended to a well documented computer code.

PLAXIS 2017 ® 2D is a special purpose two-dimensional finite element program used to perform deformation, stability and flow analysis for various types of geotechnical applications. Real situations may be modeled either by a plane strain or an axisymmetric model. The program uses a conventional graphical user interface that enables users to quickly generate a geometry model and finite element mesh based on a representative vertical cross section of the situation at hand. The interface consists of two sub programs:

A. The INPUT program, is a pre-processor , which is used to define the problem geometry to create the finite element mesh and to define calculation phases.
B. The OUTPUT program, is a post processor which is used to inspect the results of calculations in a two dimensional view or in cross sections and to plot graphs (curves) of output quantities of selected geometry points.

4.4.1 AXISYMMETRIC ANALYSIS IN PLAXIS 2D

The finite element model in Plaxis 2D can be

- Plain strain
  This type of model is used for geometries with a (more or less) uniform cross section and corresponding stress state and loading scheme over a certain length perpendicular to the cross section (z direction). Displacements and strains in z direction are assumed to be zero. However normal stresses in z-direction are fully taken into account.

- Axisymmetric
  An axisymmetric model is used for circular structures with a (more or less) uniform radial cross section and loading scheme around the central axis, where the deformation and stress state are assumed to be identical in any radial direction. Note that for axisymmetric problems the x-coordinate represents the radius and the y-axis corresponds to the axial line of symmetry. Negative x-coordinates cannot be used.

4.4.2 SOIL ELEMENTS

The user may select either 6-node or 15-node triangular elements (Figure 13) to model soil layers and other volume clusters. The 15-node triangle is a very accurate element that has produced high quality stress results for difficult problems as for example in collapse calculations for incompressible soils. The 15-node triangle is particularly recommended to be used in axi-symmetric analysis, like the one performed as part of the present thesis.

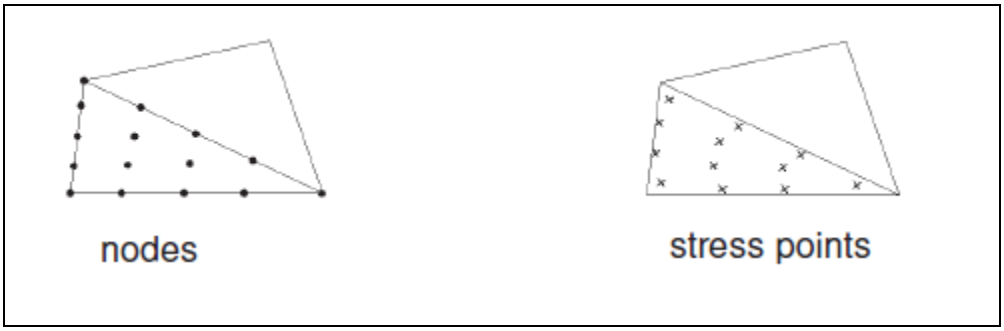

Figure.13 Nodes and stress points in a 15-node triangle element (Plaxis 3D-4-Scientific-1.pdf).

4.4.3 STRUCTURAL ELEMENTS

Plates which are actually beam elements, are structural objects used to model slender structures in the ground with a significant flexural rigidity (or bending stiffness) and a normal stiffness. The most important parameters are the flexural rigidity (bending stiffness) EI and the axial stiffness EA. For these two parameters an equivalent plate thickness $d_{eq}=\sqrt{12(\frac{EI}{EA})}$ is calculated from the equation.

Plates in the 2D finite element model are composed of beam elements (line elements) with three degrees of freedom per node, two transitional degrees of freedom (u_x,u_y) and one rotational degree of freedom.

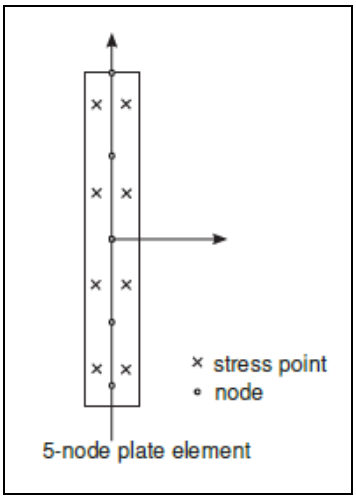

Figure.14 Position of nodes and stress points in plate elements. 5-nodes beam elements are used together with the 15-node soil elements (Plaxis 3D-4-Scientific-1.pdf).

4.4.4 INTERFACE ELEMENTS

Interfaces are joint elements to be added to plates to allow for a proper modeling of soil-structure interaction. Interfaces may be used to simulate the thin zone of intensely shearing material at the contact between a plate and the surrounding soil. Each interface has assigned to it a 'virtual thickness' which is an imaginary dimension used to define properties of the interface. The higher the virtual thickness is, the more elastic deformations are generated. In general interface elements are supposed to generate very little elastic deformations and therefore the virtual thickness should be small.

Interfaces are composed of interface elements. Figure 15 shows how interface elements are connected to soil elements. When using 15-node elements the corresponding interface elements are defined by five pairs of nodes.

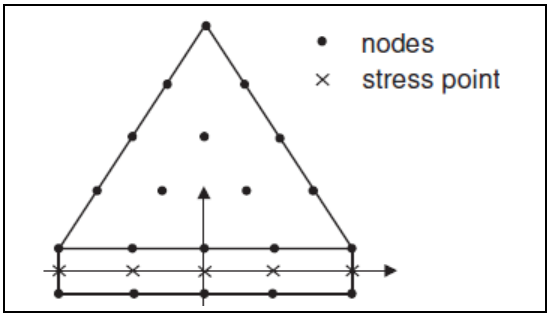

Figure.15 Distribution of nodes and stress points in interface elements and their connection to a 15-node soil elements (Plaxis 3D-4-Scientific-1.pdf).

One 15-node element can be thought of as a composition of four 6-node elements, since the total number of nodes and stress points is equal. Nevertheless, one 15-node element is more powerful than four 6-node elements.

4.5 PLAXIS 2018 ® 3D

Plaxis 3D is a full three dimensional finite element program which combines an easy to use interface with full 3D modeling facilities. Like Plaxis 2D, is a program for geotechnical applications in which soil models are used to simulate the soil behavior with a full 3D pre-processor that allows CAD objects to be imported and further processed within a geotechnical context. The program is supplied as an extended package, including static elastoplastic deformation, advanced soil models, stability analysis, consolidation, safety analysis, updated mesh analysis and steady state groundwater flow.

4.5.1 SOIL ELEMENTS

The soil volume in the program is modeled by means of 10-node tetrahedral elements, as depicted in Figure 16. The 10-node tetrahedral elements are created in the 3D mesh procedure. This type of element provides a second-order interpolation of displacements.

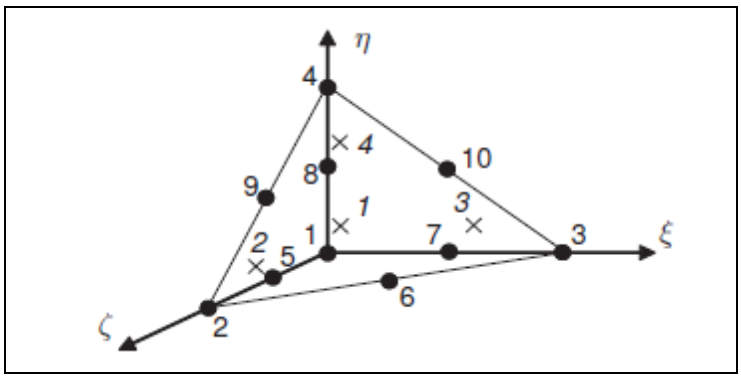

Figure.16 Local numbering and positioning of nodes (•) and integration points (x) of a 10-node tetrahedral element (Plaxis 3D-4-Scientific-1.pdf).

4.5.2 STRUCTURAL ELEMENTS

Plates which are actually shell elements are structural objects used to model thin two-dimensional structures in the ground with a significant flexural rigidity (bending stiffness). After meshing plates are composed of 6-node triangular plate elements (Figure 17) with six degrees of freedom per node:

- Three translational degrees of freedom (u_x,u_y and u_z).
- Three rotational degrees of freedom (φ_x,φ_y and φ_z).

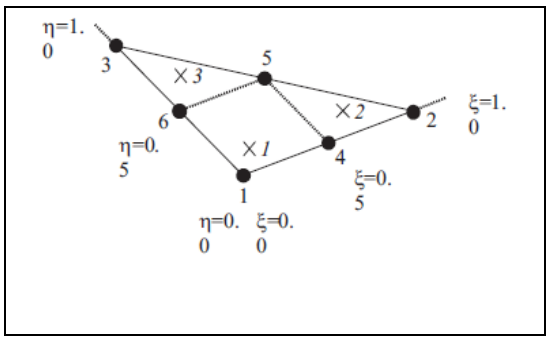

Figure.17 Local numbering and positioning of nodes (•) and integration points (x) of a 6-node plate triangle (Plaxis 3D-4-Scientific-1.pdf).

4.5.3 INTERFACE ELEMENTS

As stated above, interfaces are joint elements to be added to plates to allow a proper modeling of soil-structure interaction. After meshing, interfaces are composed of 12-node interface elements consisting of pairs of nodes, compatible with the 6-noded triangular side of a soil element or plate elements. The distance between the two nodes of a node pair is zero. Each node has three translational degrees of freedom (u_x,u_y,u_z). As a result, interface elements allow for differential displacements between the node pairs (slipping and gapping).

4.6 PHASE2 v8.00

Phase2 v8.00 is a 2D finite element program for calculating stresses, displacements and estimating support around underground excavations. Is a powerful 2D elasto-plastic finite element stress analysis program for underground or surface excavations in rock or soil. It can be used for a wide range of engineering projects and includes support design, finite element slope stability, groundwater seepage and probabilistic analysis. It faces a wide range of mining and civil engineering problems involving plain strain and axisymmetry, elastic or plastic materials, multiple materials and staged excavations up to 50 stages. The PHASE2 program consists of 3 program modules:

- MODEL
  Model is the pre-processing module used for entering and editing the model boundaries, support, in-situ stresses, boundary conditions, material properties, and creating the finite element mesh.

- COMPUTE.
  The Compute option will carry out the finite element stress analysis for the current model. The Compute option is not enabled unless the finite element mesh exists.

- INTERPRET.
  The Interpret option is enabled as soon as the finite element mesh is generated, however, the user must of course run Compute on a file before it is possible to look at the results in Interpret. When Interpret is started from Model, the active file in Model will automatically be opened in Interpret. Furthermore, the user can return back to Model using the Model button in Interpret. This allows to switch back and forth between Model and Interpret, so that you can edit a model, re-compute and view new results.

MODEL, COMPUTE and INTERPRET will each run as standalone programs. They also interact with each other as illustrated in the schematic of Figure 18 below:

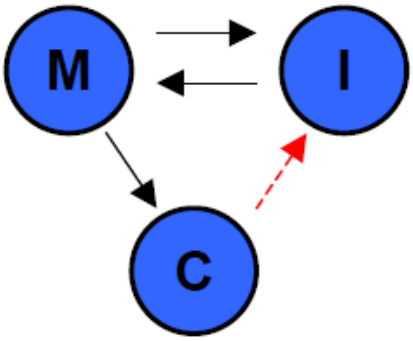

Figure.18 Model, compute and interpret programs interacting with each other (Phase2 Model Reference).

Compute and Interpret can both be started from within Model. Compute must be run on a file before results can be analyzed with Interpret while Model can be started from Interpret.

4.6.1 AXISYMMETRIC ANALYSIS IN PHASE2

Axisymmetric modeling allows to analyze a 3-D excavation which is rotationally symmetric about an axis. The input is 2-dimensional, but the analysis results apply to the 3-dimensional problem. Two different types of analysis can be selected, Plane Strain or Axisymmetric analysis.

- Plane Strain Analysis.
  Plane Strain assumes that the excavation(s) are of infinite length normal to the plane section of the analysis. In a Plane Strain analysis PHASE2 calculates the major and minor in-plane principal stresses (Sigma 1 and Sigma 3), the out-of-plane principal stress (Sigma Z) and in-plane displacements and strains. By definition, the out-of-plane displacement is zero in a Plane Strain analysis.

- Axisymmetric Analysis.
  Only an EXTERNAL boundary is required, the shape of the EXTERNAL boundary implicitly defines the excavation. The mathematical formulation of an Axisymmetric finite element is actually similar to Plane Strain (and plane stress) problems. By symmetry, the two components of displacement in any plane section of the excavation through its axis of symmetry define completely the state of strain, and therefore, the state of stress. Instead of analyzing a unit out-of-plane depth, the analysis is performed on a unit radian. There are though, several restrictions on the use of axisymmetric modeling in Phase 2:

I. The Field Stress must be axisymmetric ie. aligned in the axial and radial directions. Out of plane (or circumferential) field stress exists, but is equal to the radial stress and cannot be independently varied.
II. Cannot be used with Groundwater (ie. Piezometric lines, Water Pressure Grid, Finite Element Seepage Analysis).
III. Cannot be used with Bolts (however liners are permitted).
IV. Cannot be used with Joints.
V. All materials must have Isotropic elastic properties (cannot use Transversely Isotropic or Orthotropic elastic properties).
VI. The true orientation of the excavation can be arbitrary. However, for the purpose of the Axisymmetric analysis, the coordinates will have to be mapped so that the model is symmetric about the X=0 axis, since all finite elements are rotated about this axis.
VII. To form a closed excavation, one edge of the mesh must be coincident with the X=0 (vertical) axis. If this is not the case, the excavation will be ‘open-ended’.
VIII. All other Phase2 modelling options can be used with an xisymmetric model, however, always should be kept in mind the nature of an Axisymmetric model (for example, when defining loads, boundary conditions, etc.).

CHAPTER V
PROJECT INPUTS AND ASSUMPTIONS

5.1 INTRODUCTION

In any realistic simulation model, appropriate constitutive models are used to represent the behavior of the structural components and the behavior of the ground. Over the past decades, as research progressed, numerous constitutive models have been developed for simulating and modeling the behavior of soils. These models are used in the calculation of soil-structure interaction problems, as the one studied in this thesis, under axisymmetric, plain strain and general three-dimensional conditions. Many models that have been formulated have a purely theoretical base while others are based on experimental evidence. The determination of the right model is not always an easy task.

According to Lade (2005), it is a paramount to employ realistic constitutive models that can reproduce the important aspects of the soil-strain behavior under various loading conditions. To develop such models requires advanced experiments to study the soil behavior under various loading conditions and it requires employment of mathematical tools based on sound theoretical frameworks such e.g., elasticity and plasticity theories.

5.2 LINEAR ELASTIC MODEL

The Linear Elastic model is based on Hooke's law of isotropic elasticity, involving two basic elastic parameters, i.e. Young's modulus (E) and Poisson's ratio (ν). It is used to model the precast segments (plates), representing the side "lining" and the "lean concrete" constituting the thin concrete layer at the bottom of the excavation. In this particular case study the following materials are used:

- Precast concrete segments **C40/50**.
- Lean concrete **C16/20**.
- Reinforced steel **B500C**.

Having the below tabled characteristics:

	Nomenclature	Lining	Lean concrete	Unit
Material model		Linear elastic	Linear elastic	
Drainage Type		Non porous	Non porous	
Unit weight above phreatic level	γ_{sat}	25	25	kN/m^3
Normal stiffness	EA	$10.5*10^6$	$4.125*10^6$	kN/m
Flexural rigidity	EI	78750	7734	kNm^2/m
Effective Poisson's ratio	ν	0.2	0.2	
Ko determination		Automatic	Automatic	
Concrete thickness	d	0.3	0.3	m

Table.2 Material properties having a "linear elastic" behavior.

5.3 MOHR-COULOMB MODEL

The Mohr-Coulomb model is a simple and well known linear elastic perfectly plastic model which can be used as a first approximation of soil behavior, estimating the deformations and describing the strain distribution during soil failure. The linear elastic part of the Mohr-Coulomb model is based on Hooke's law of isotropic elasticity. The perfectly plastic part is based on the Mohr-Coulomb failure criterion, formulated in a non-associated plasticity framework. This model and its yield criterion typically involves Coulomb's hypothesis which postulates a linear relationship between shear strength on a plane and the normal stress acting on it.

$$\tau=c+\sigma_n*\tan\varphi$$

Defining τ as the shear strength, σ_n the normal stress, φ the angle of internal friction and c cohesion intercept. The Mohr-Coulomb failure criterion in terms of principal stresses can be graphically represented combining the Coulomb criterion with Mohr's circle (Figure 19).

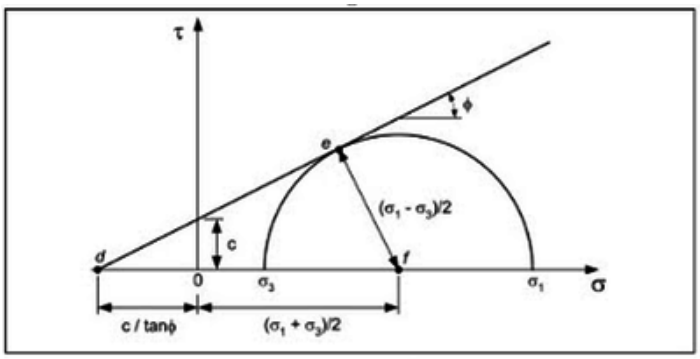

Figure.19 Graphical representation of the Coulomb criterion with Mohr's circle.

In three-dimensional principal stress space, shown in Figure 20 the Mohr–Coulomb yield criterion is an hexagonal pyramid whose central axis lies along the hydrostatic axis.

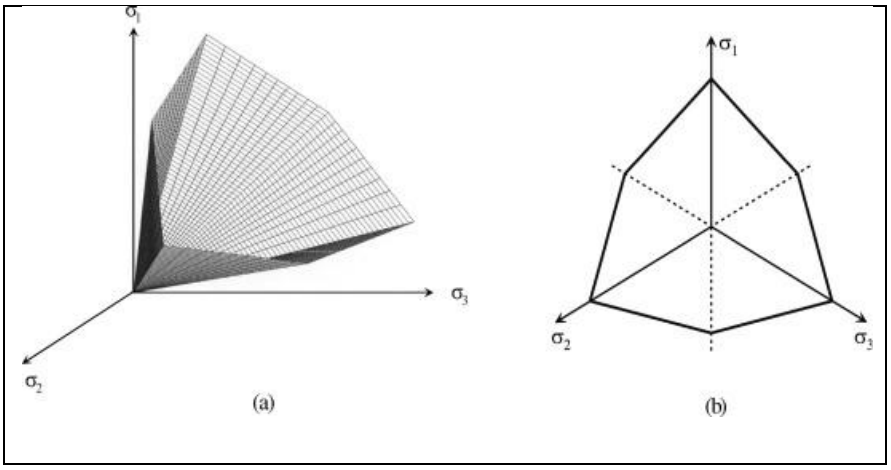

Figure.20 Mohr-Coulomb failure criterion in (a) principal stress space and (b) in the octahedral plane (Abbo et al., 2011).

According to Abbo et al. (2011), other more sophisticated constitutive models for predicting the behavior of soil have been developed over the past three decades, however the complexity of these models, as well as the additional testing required to determine the various soil parameters involved, minimizes their utility for practicing geotechnical engineers. The Mohr–Coulomb yield function is also of importance to finite element researchers and practitioners as it forms the basis of many analytical solutions. These analytical solutions serve as crucial benchmarks for validating numerical algorithms and software.

	Nomenclature	Soil 1	Soil 2	Unit
Material model		Mohr-Coulomb	Mohr-Coulomb	
Drainage Type		Drained	Drained	
Unit weight above phreatic level	γ_{unsat}	16.0	17.0	kN/m^3
Unit weight below phreatic level	γ_{sat}	20.0	20.0	kN/m^3
Effective Young's modulus	E'	30.000	20.000	kN/m^2
Effective Poisson's ratio	N	0.3	0.3	
Cohesion intercept	c'	5	25	kN/m^2
Friction angle	φ'	30	24	°
Dilatancy angle	Ψ	0	0	°
Data set		Standard	Standard	
Soil type		Coarse	Medium	
<2μm		10	19	%
2μm-50 μm		13	41	%
50 μm-2mm		77	40	%
Set parameters to defaults		Yes	Yes	
Permeability in horizontal direction	k_x,ky	10^{-7}	$5*10^{-8}$	m/s
Permeability in vertical direction	k_z	10^{-7}	$5*10^{-8}$	m/s
Interface strength		Manual	Manual	
Interface reduction factor	R_{inter}	0.9	0.9	
Interface friction angle	φ'	0	0	°
K0 determination		Automatic	Automatic	
Lateral earth pressure coefficient	Ko	0.5	0.5	

Table.3 Geotechnical characteristics, the two soil layers behave according to the Mohr-Coulomb model.

5.4 HARDENING SOIL MODEL

In many cases of daily geotechnical engineering one has good data on strength parameters but little or no data on stiffness parameters. In such a situation, it is no help to employ complex stress-strain models for calculating geotechnical boundary value problems. Instead of using Hooke's single stiffness model with linear elasticity in combination with an ideal plasticity according to Mohr-Coulomb a new constitutive formulation using a double stiffness model for elasticity in combination

with isotropic strain hardening is used (Schanz et al., 1999). In contrast to an elastic perfectly-plastic model, the yield surface of a hardening plasticity model is not fixed in principal stress space, but it can expand due to plastic straining. The Hardening Soil model is an advanced model for simulating the behavior of different types of soil, both soft soil and stiff soil (Schanz, 1998 in Plaxis Material Model Manual, 2019).
Some parameters of the hardening model coincide with those of the classical non-hardening Mohr-Coulomb model. These are the failure parameters φ_p, c and ψ_p. Additionally basic parameters for the soil stiffness used:

(E_{50}^{ref}) secant stiffness in standard drained triaxial test,
(Eo_{ed}^{ref}) tangent stiffness for primary oedometer loading,
(m) power for stress level dependency of stiffness.

This set of parameters is completed by the following advanced parameters:

(E_{ur}^{ref}) unloading/reloading stiffness,
(ν'_{ur}) Poisson's ratio for unloading/reloading,
(P^{ref}) reference stress for stiffness,
(k_0^{nc}) k_0 value for normal consolidation and
(R_f), failure ratio q_f/q_u.

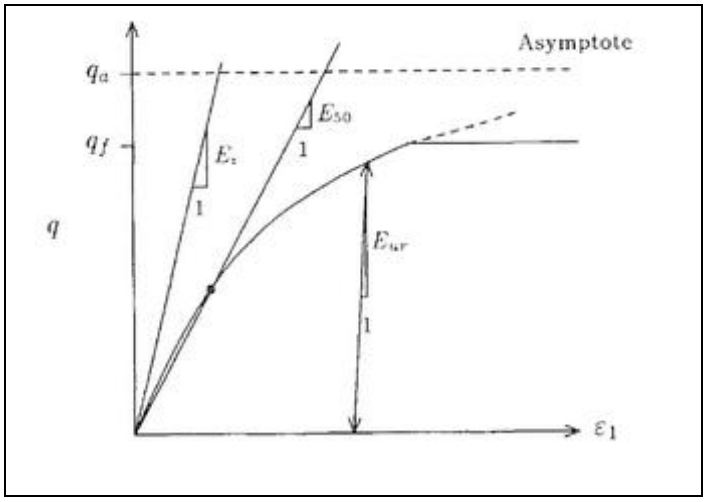

Figure.21 Hyberbolic stress-strain relation in primary loading for a standard drained triaxial test (Schanz et al., 1999).

When subjected to primary deviatoric loading, soil shows a decreasing stiffness and simultaneously irreversible plastic strain develop. In the special case of a drained triaxial test the observed relationship between the axial strain and the deviatoric stress can be well approximated by a hyperbola as shown in Figure 21.

As part of this thesis, the following average values for various soil types are used as indicated in Table 4 also including the soils' geotechnical characteristics: $Eoed^{ref} = E50^{ref}$ and $Eur^{ref} = 3\ E50^{ref}$.

	Nomenclature	Soil 1	Soil 2	Unit
Material model		Hardening soil	Hardening soil	
Drainage Type		Drained	Drained	
Unit weight above phreatic level	γ_{unsat}	16.0	17.0	kN/m^3
Unit weight below phreatic level	γ_{sat}	20.0	20.0	kN/m^3
Secant stiffness for CD triaxial test	$E50^{ref}$	30.000	20.000	kN/m^2
Tangent oedemeter stiffness	$Eoed^{ref}$	30.000	20.000	kN/m^2
Unloading/Reloading stiffness	Eur^{ref}	90.000	60.000	kN/m^2
Power for stress level dependency of stiffness	m	0.5	0.5	
Poisson's ratio	ν'ur	0.2	0.2	
Cohesion	c'	5	25	kN/m^2
Friction angle	φ'	30	24	°
Dilatancy angle	ψ	0	0	°
Reference stress for stiffness	Pref	100	100	kN/m^2
Stress ratio in normally consolidated state	k_0^{nc}	0.45	0.45	
Data set		Standard	Standard	
Soil type		Coarse	Medium	
<2μm		10	19	%
2μm-50 μm		13	41	%
50 μm-2mm		77	40	%
Set parameters to defaults		Yes	Yes	
Permeability in horizontal direction	k_x, k_y	10^{-7}	$5*10^{-8}$	m/s
Permeability in vertical direction	k_z	10^{-7}	$5*10^{-8}$	m/s
Interface strength		Manual	Manual	
Interface reduction factor	R_{inter}	0.9	0.9	
Interface friction angle	φ'	0	0	°

Consider gap closure		Yes	Yes	
K0 determination		Automatic	Automatic	
Lateral earth pressure coefficient	Ko	0.5	0.5	
Over-consolidation ratio	OCR	1.0	1.0	
Pre-overburden pressure	POP	0	0	kN/m^2

Table.4 Geotechnical characteristics, the two soil layers behave according to the Hardening Soil model.

The initial stresses may involve pre-loading or over-consolidation. In particular, advanced soil models may take the effects of overconsolidation into account. This requires information about the overconsolidation ratio (OCR) or the pre-overburden pressure (POP).

$K0^{nc}$, the K0 procedure is a special calculation method to define the initial stresses for the model, taking into account the loading history of the soil. In practice, the value of K0 for a normally consolidated soil is often assumed to be related to the friction angle through Jaky's empirical expression $K0=1-\sin\varphi$ for the Mohr-Coulomb model. For the Hardening Soil advanced model, the default value is based on the $K0^{nc}$ parameter and is influenced by the overconsolidation ratio (OCR) or the pre-overburden pressure (POP) (Plaxis23D-3-Material-Models.pdf).

5.5 SOIL ASSUMPTIONS

As far as the aforementioned Soil 1 and Soil 2 are concerned, a hypothesis is made. In particular Soil 1 is assumed to be Silty Sand and Soil 2 Sandy Silt. Their mechanical characteristics are based on an assumption, reasonable until a certain point.

Natural sands generally contain significant amounts of silt and/or clay. The properties of clean sand, for example shear strength and stiffness, are studied extensively and considered known. However, natural sands have a different mechanical behavior from that of clean sands. The comprehension of the mechanical characteristics of such soil is very useful for practical applications and theoretical models, like the one examined in the present thesis, based on constitutive models and the material's response is analyzed.

According to Salgado et al. (2000), it is clear that the shear modulus of sand decreases dramatically with fines content. The stiffness reduction with fines content may be partially explained by the way in which the fines interact with the sand matrix. If the fines are positioned within the sand matrix in such a way that they do not have well developed contacts with the sand particles, shear waves (or static stresses) are not

effectively transferred through the fine particles. Moreover, although small-strain stiffness drops, peak and critical-state strengths increase with increasing fines content. This may be interpreted as follows: initially the fine particles are not positioned in a way to provide optimum interlocking and small shear strains are imposed on the soil with greater ease than if the fines were not present. As shearing progresses, the fines reach more stable arrangements and ultimately increase interlocking, dilatancy, and shear strength.

These observations from the addition of fines, indicate that where clean values are used, can be a significant error.

5.6 PERMEABILITY COEFFICIENT ASSUMPTION

According to Venkatramaiah (1995), the average permeability of a soil deposit or stratum in the field may be somewhat different from tests on laboratory samples. Field determination of permeability is often required because permeability depends very much on the microstructure, the arrangement of soil grains and the macrostructure, such as stratification and also because of the difficulty in obtaining undisturbed soil samples.

As part of this thesis, the following hypothesis is made regarding the permeability coefficients in order to proceed with the simulation:

Silty sand	$k=10^{-7}$ m/s
Sandy silt	$k=5*10^{-8}$ m/s

5.7 CONSTRUCTION TECHNICS

As described in detail in the first chapter the sequential excavation method is selected to construct shafts having a relatively large diameter. The aforementioned method is applied in two similar ways, each one corresponding to a different type of analysis:

- **Deformation**.
  The excavation proceeds in steps of usually 1-1,5 meters and the lining is installed during the next step. Therefore, full soil deformations take place.
- **Stresses**.
  Lining is installed simultaneously with the excavation and consequently maximum stresses are induced on the lining. Soil deformations are limited.

CHAPTER VI
2DIMENSIONAL ANALYSES USING PLAXIS 2D 2018 AND PHASE2 8.0

6.1 INTRODUCTION

The overall objective is to simulate the staged excavation procedure and the sequential support, using precast concrete segments of a vertical shaft. Two-dimensional analyses are performed applying commercial finite element software, in particular Plaxis 2D 2018 and Phase2 8.0. The various assumptions, model setting and results are reported and explained where necessary.

6.2 ASSUMPTIONS

- ✓ **Axisymmetric model**.
  An axisymmetric instead of a plain strain model is selected as this particular representation of the proposed structure, allows to analyze a 3-D excavation which is rotationally symmetric about an axis. The input is 2dimensional but the analysis results apply to the 3dimensional problem. The two components of displacement in any plane section of the excavation through its axis of symmetry define completely the state of strain and therefore the state of stress.
- ✓ **Horizontal soil layers**.
  The soil layers are speculated perfectly horizontal as the models used are symmetrical.
- ✓ **Absence of the groundwater table**.
  The analyses are completed in dry conditions. It is advisable that flow condition related problems are not performed in 2dimensional axisimmetric model analyses. In dry conditions, theoretically the value of pore pressure at the upper level and the value of the pore pressure at the bottom level of the layer would be zero and no pressure would be generated in the layer.
- ✓ **Number of steps**.
  The supposition of the depth of each step is based on the dimension of the segmented concrete rings adopted i.e. 1.5 meters of height and 30 centimeter of thickness.
- ✓ **Mohr Coulomb and Hardening Soil constitutive models**.
  These two appropriate constitutive models are used to represent the behavior of the ground. Mohr Coulomb is chosen for its simplicity and familiarity, while Hardening Soil as a more sophisticated, complex and advanced stress-strain model.
- ✓ **Area extension x_{min}=0, x_{max}=30 and y_{min}=-60, y_{max}=0.**
  The assumed model extensions in width and depth should not, at any case, influence the model outputs and deviations should be negligible. That implies that the dimensions considered should be neither too short, affecting the model, nor excessive. Subsequently, a relatively large number of finite

elements constituting the materials are created, resulting in a computational inefficiency. To summarize, simple geometrical assumptions are adopted that it is believed that would have minor effect in the results.

6.3 ANALYSES OVERVIEW

An effort is made to reproduce the construction procedure using various calculation models and draw the relevant conclusions. For the purpose of the simulation the following 2dimensional representations on scale are set up and analyzed, schematically:

No	Software Applied	Constitutive Model	Analysis Type
1	PLAXIS 2D	Mohr-Coulomb	Deformation
2	PLAXIS 2D	Mohr-Coulomb	Stress
3	PLAXIS 2D	Hardening-Soil	Deformation
4	PLAXIS 2D	Hardening-Soil	Stress
5	PHASE8.0	Mohr-Coulomb	Deformation
6	PHASE8.0	Mohr-Coulomb	Stress

Table.5 Two-dimensional models set up and run as part of the analysis.

The calculation steps relying on the analysis type are listed below in Table 6:

		Segmented plate installation	
Step (1.5m)	**Overall Excavation (m)**	**Deformation (Analysis type)**	**Stress (Analysis type)**
1	-1.5		-1.5
2	-3.0	-1.5	-3.0
3	-4.5	-3.0	-4.5
4	-6.0	-4.5	-6.0
5	-7.5	-6.0	-7.5
6	-9.0	-7.5	-9.0
7	-10.5	-9.0	-10.5
8	-12.0	-10.5	-12.0
9	-13.5	-12.0	-13.5
10	-15.0	-13.5	-15.0
11	-16.5	-15.0	-16.5
12	-18.0	-16.5	-18.0
13	-19.5	-18.0	-19.5
14	-21.0	-19.5	-21.0
15	-22.5	-21.0	-22.5
16	-24.0	-22.5	-24.0 and installation of the lean concrete covering on foundation level
17		-24.0 and installation of the lean concrete covering on foundation level	

Table.6 Comparison between calculation steps of the model deformation and stress analysis.

6.4 TWO-DIMENSIONAL ANALYSIS USING PLAXIS 2D

1. PROJECT PROPERTIES

Initially, a new project is created and the basic model parameters are defined. An axisymmetric model is used for shafts, with a uniform radial cross section around the central axis. The x-coordinate represents the radius and the y-axis corresponds to the axial line of symmetry. The 15 node, that is adopted, is a very accurate element elected for axisymmetric models. The default units, as suggested by the program are used.

2. SOIL STRATIFICATION/ SOIL MATERIAL PROPERTIES

In the following phase, the soil stratigraphy, the general water level and the initial conditions of the soil layers are defined (Figure 22). The top boundary of an under-laying layer is defined by the lower boundary of the overlaying layer. Once the soil properties are defined, they are assigned to the corresponding soil layer. Each soil layer is composed of its unique properties. Groundwater and pore pressure are neglected in the present analysis as a dry state is adopted. The initial stresses state is generated using the K_0 procedure.

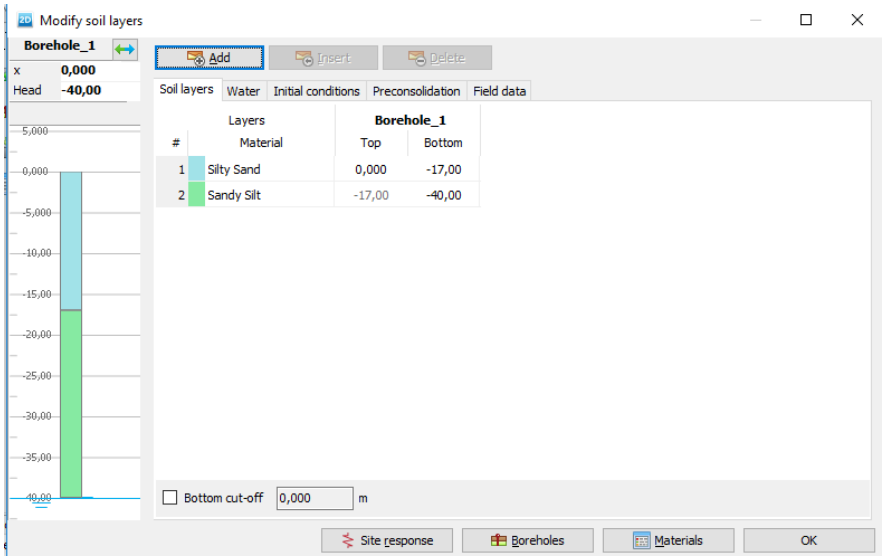

Figure.22 Soil stratification properties.

3. STRUCTURES

In the third phase, the geometric entities and the structural elements in the project are defined, being the basic components of the physical model as in Figure 23. Plates are used to simulate the influence of the geotechnical structures i.e. the segmented concrete rings and the base lining. Once the plates are created, the respective properties are assigned. The isotropic option is chosen to ensure that both stiffness, in-plane and out-of plan are equal.

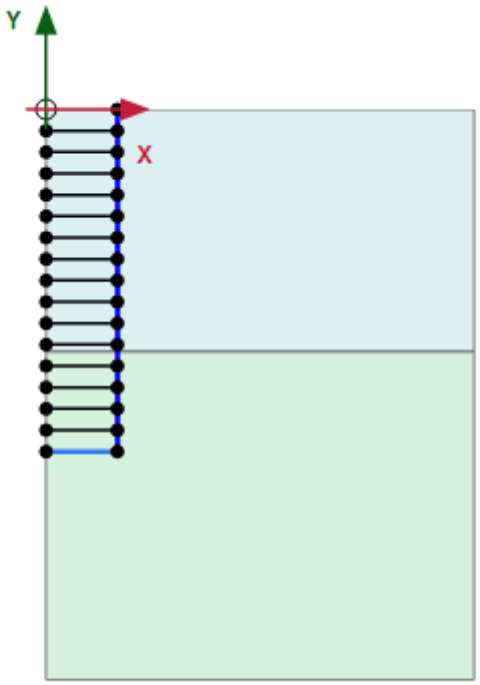

Figure.23 Construction procedure and delimitation of the structure.

4. INTERFACES

Interfaces are created and added to allow for a proper modeling of soil-structure interaction. They simulate the thin zone of intensely shearing material at the contact between a plate and the surrounding soil. Interfaces are created adjacent to the plates with a creation process similar to the creation of a line, placed at both sides of a plate enabling a full interaction indicated by a plus sign (+) and/or a minus sign (-) as indicated in Figure 24.

R_{int} (interface reduction factor) represents the strength reduction factor, modeling the roughness of the interaction. A suitable value should be chosen.

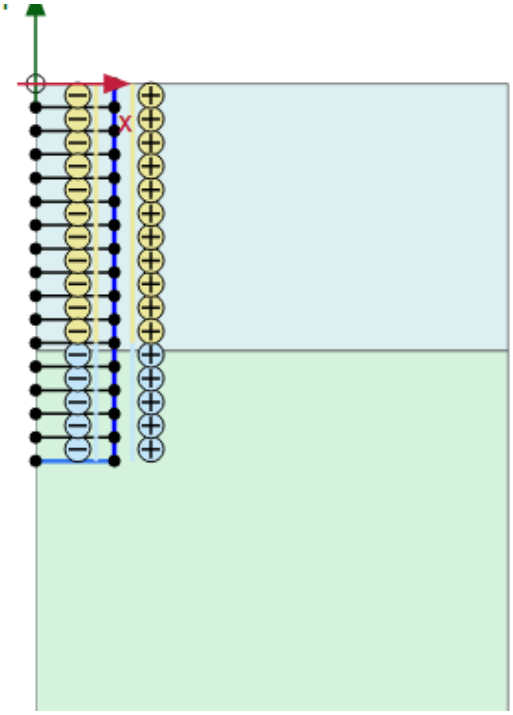

Figure.24 Negative (+) and positive (-) interfaces adjacent to the plates.

5. MESH

Once the geometry modeling process is complete the calculations may proceed. This consists of the generation of mesh and definition of the construction stages. To perform the finite element calculations, the geometry of the problem should be divided into elements. The composition of finite elements is called a mesh. The mesh is chosen to be sufficiently FINE to obtain accurate numerical results (Figure 25). PLAXIS permits the automatic creation of the mesh and the generation procedure takes into account the stratification of the soil as well as all structural elements. The mesh creation is based on a reliable triangulation procedure, a fact that leads to non-symmetric mesh output, resulting in better prediction outcomes.

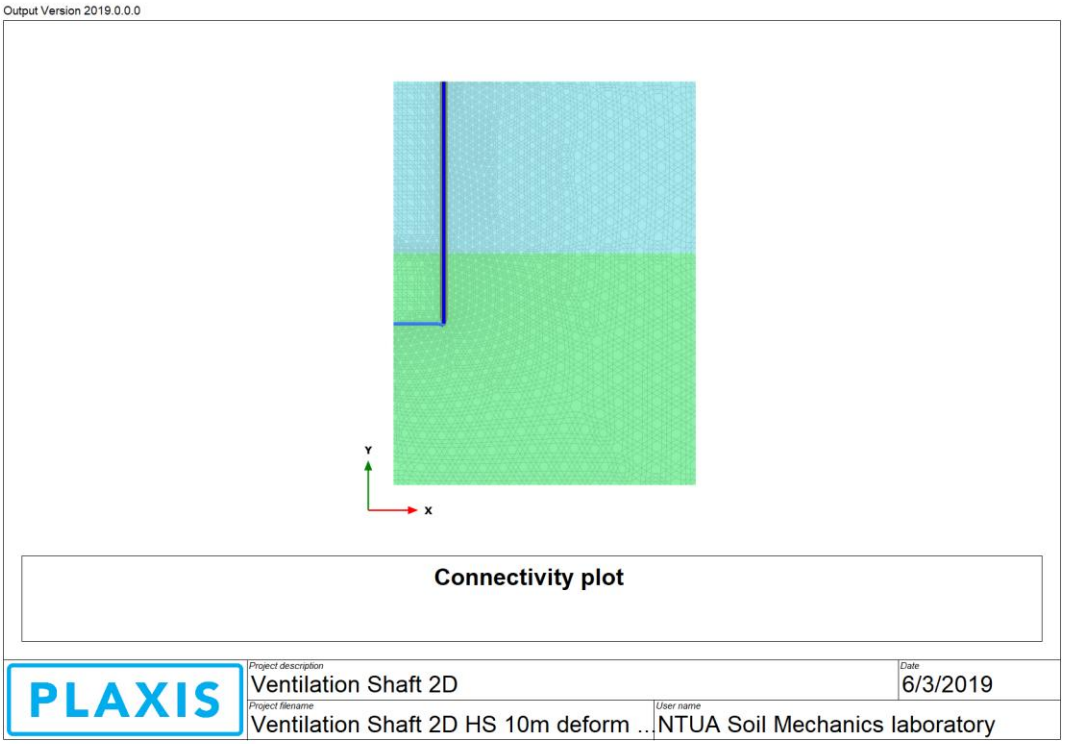

Figure.25 Generated Mesh output.

6. STAGED CONSTRUCTION

Like in engineering practice, a project is divided into project phases. Similarly, a calculation process in PLAXIS is also divided into calculation phases (Figure 26). Finite element calculations are divided into several calculation phases, each one corresponding to a particular construction stage.

The calculation type selected in the Initial Phase is the K_0 procedure, meaning generally the direct generation of initial effective stresses, pore pressures and state parameters. In the first calculation phase, following the initial phase, the option “reset displacements to zero” is selected by default, disregarding irrelevant displacements of previous calculation step, so that the new calculation starts from a zero displacement field not considering deformations that are physically meaningless.

Soil volumes and structural objects are respectively deactivated and activated to simulate the process of excavation and construction. Sequentially, all these modifications are transformed into elaborations on an element level.

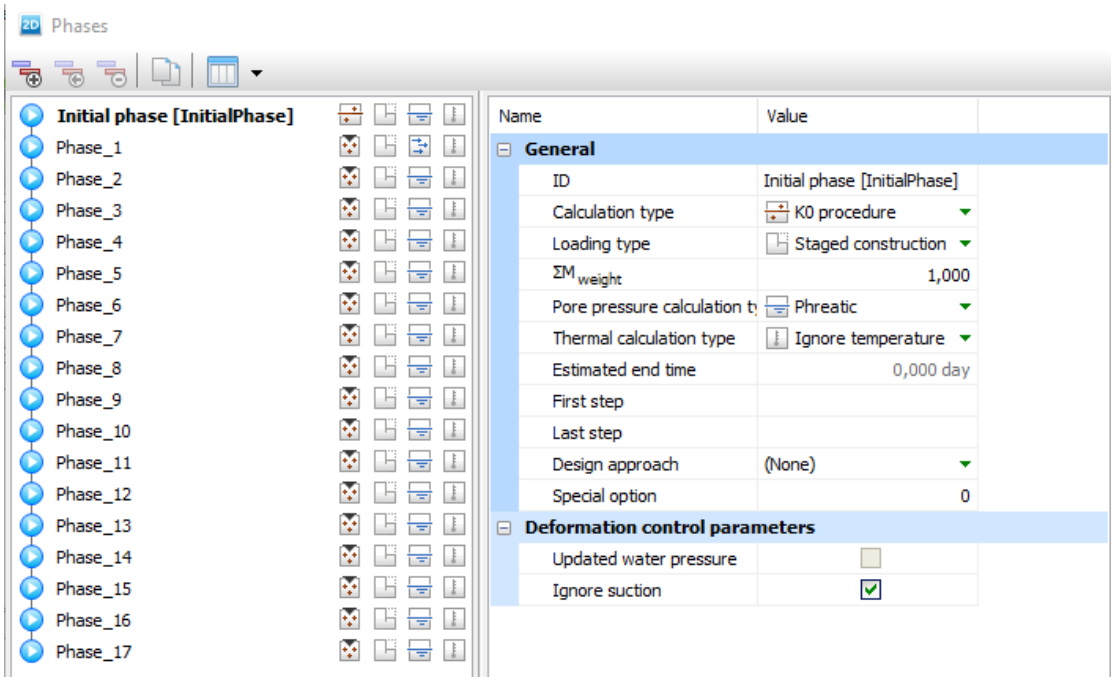

Figure.26 Staged construction phases and Initial phase general settings.

6.5 OUTPUTS USING PLAXIS 2D

After the calculation process has finished, the calculation list is updated. The main output quantities of a finite element calculation are the displacements and the stresses. In addition when a finite element model involves structural elements, the structural forces in these elements are calculated.

6.5.1 DEFORMATIONS

Deformations/displacements are visualized in Figures 27-31. Displacements are contained in the nodes of the finite element mesh. The main graphical representations consist of:

- **Deformed Mesh** which is a plot of the finite element model in the deformed shape. By default the deformations are scaled up to give a plot that might be read conveniently.
- **Total Displacements** that contain the different components of the accumulate increments in the whole calculation phase. Practically, these are the differential displacements between the end of the current calculation phase and the end of the previous calculation phase.

6.5.2 STRESSES

Stress points are usually presented in integration points. The main graphical representations are:

- **Effective stresses**. It should be noted that total stresses are equal to the effective stresses as there is complete absence of water.
- **Plastic Points** showing the stress points that are in a plastic state displayed in a plot of the undeformed geometry. The failure points, colored in red, indicate that the stresses lie on the surface of the failure envelop. Tension point is a point that fails in tension. These points will develop when the tension-cut-off is used in any of the material set in the model.

6.5.3 RESULTING FORCES IN PLATES

The resulting forces in plates are Axial forces, Shear forces and Bending Moments. For axisymmetric models the forces applied include the forces in the out-of plane direction, named Hooped Forces. Hoop forces are expressed in unit of force per unit of length. The values are constant over the circumference. Integration of the hoop forces over the in-plane length of the plate will give the total hoop force. The axial forces or hoop forces are positive when they generate tensile stresses.

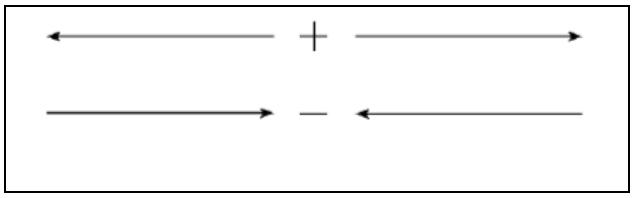

Figure.27 Sign convention for axial forces and hoop forces in plates (Plaxis2D-3-Material-Models.pdf).

In summury the resulting forces/moments in plates are:

- **Axial force (N)**, the axial force along the element axis.
- **Shear force (Q)**, the in-plane XY shear force.
- **Bending Moment (M)**, the bending moment due to bending over the out-of-plane axis Z.
- **Hoop forces (Nz)**.

Figures 32 to 64 show deformation, stresses, plastic point results from various analyses based on deformation and/or stress control and soil model variation (Mohr-Coulomb vs Hardening Soil).

6.5.4 PLAXIS 2D, DEFORMATION ANALYSIS, MOHR-COULOMB MODEL

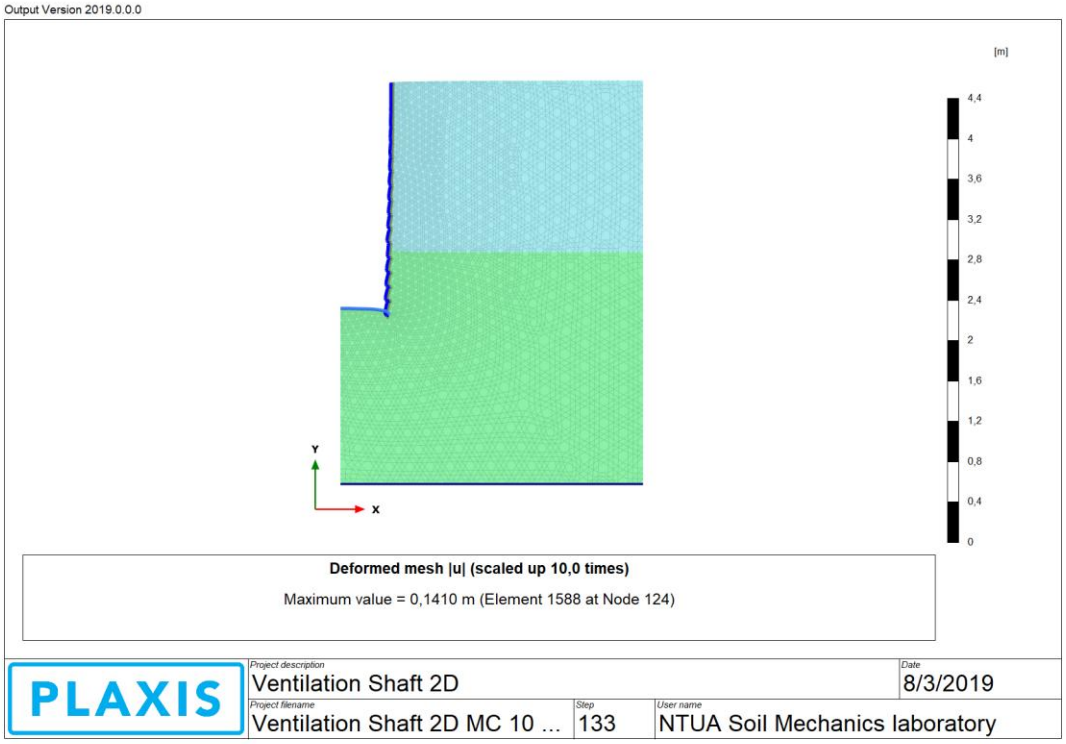

Figure.28 Deformed Mesh at the last stage (phase 17).

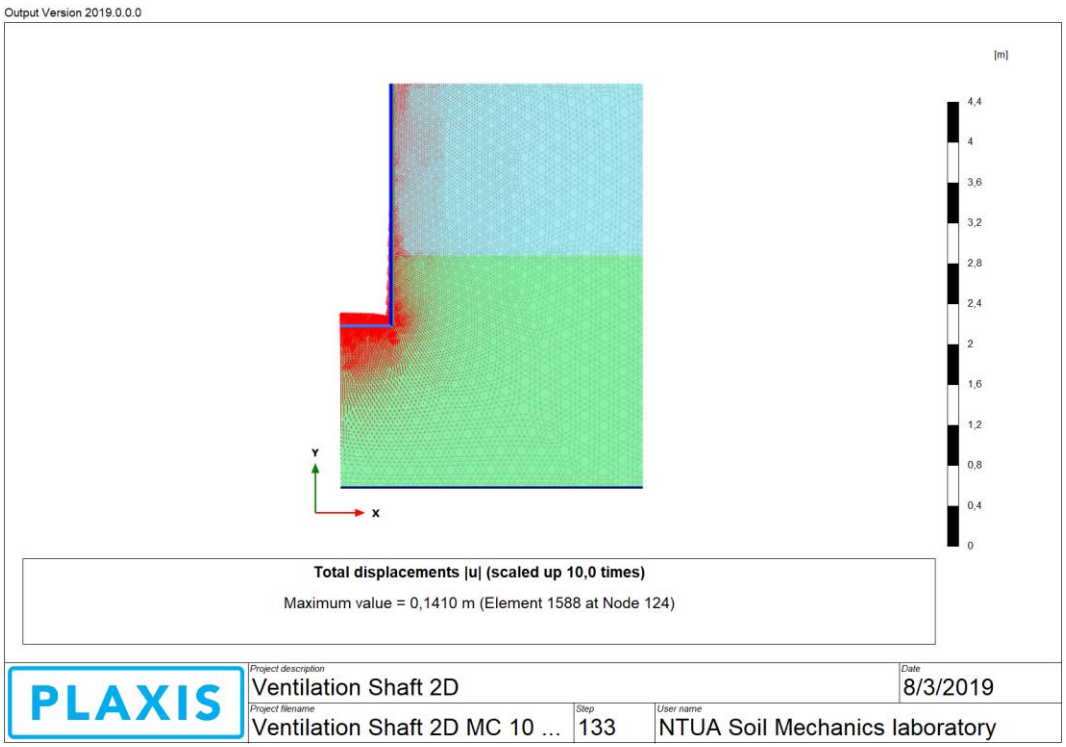

Figure.29 Total Displacements (absolute value) at the last stage (phase 17).

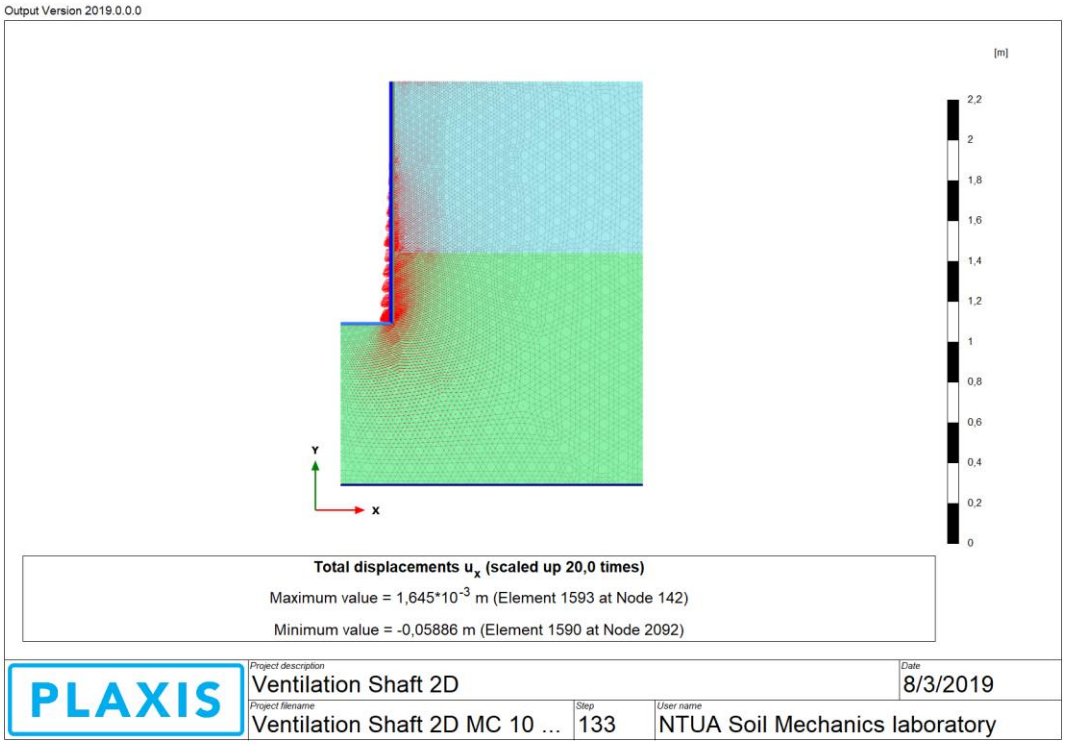

Figure.30 Maximum Horizontal Displacements (u_x) at the last stage (phase 17).

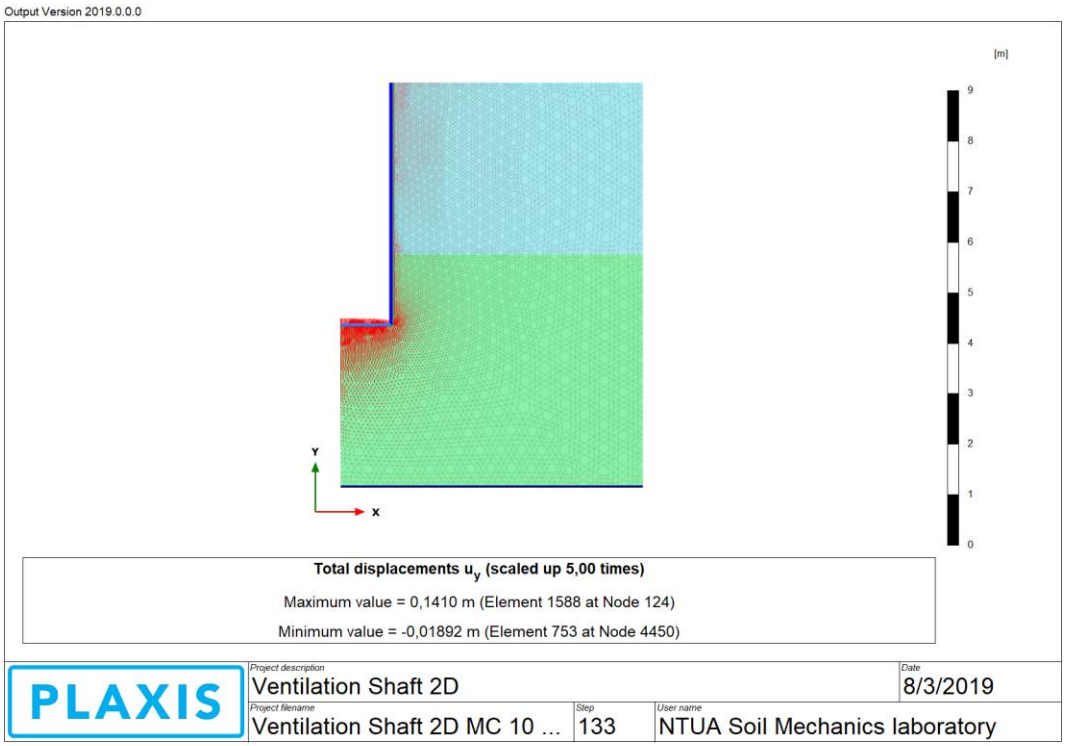

Figure.31 Maximum Vertical Displacements (u_y) at the last stage (phase 17).

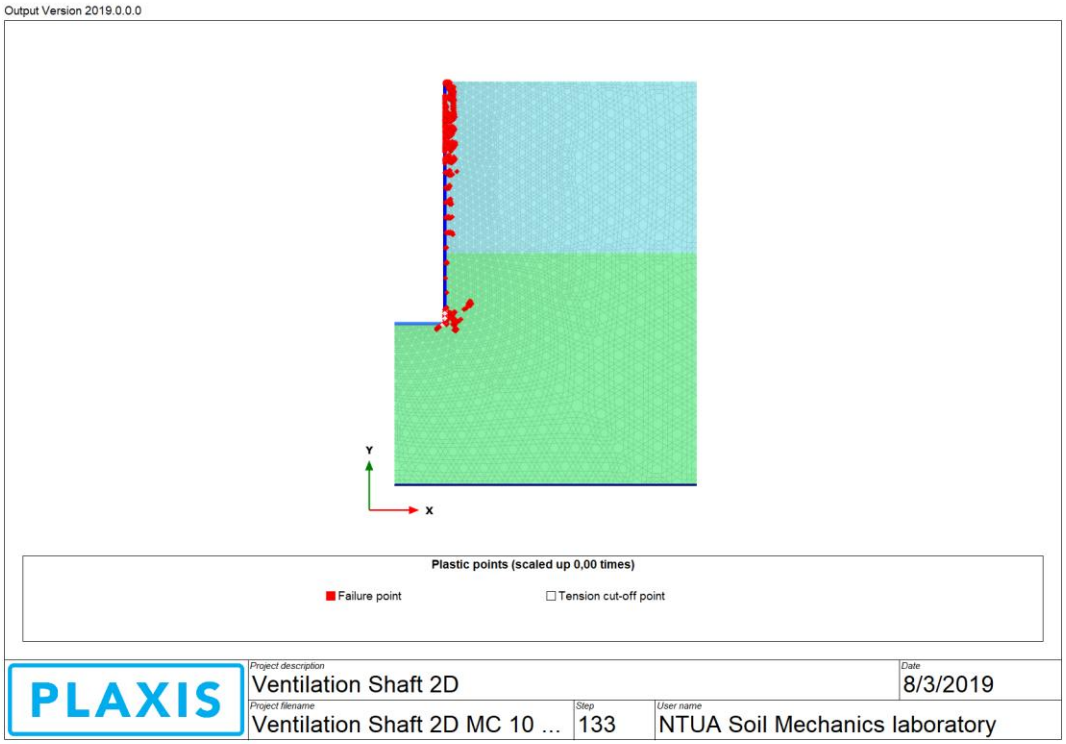

Figure.32 Plastic Points at the last stage (phase 17).

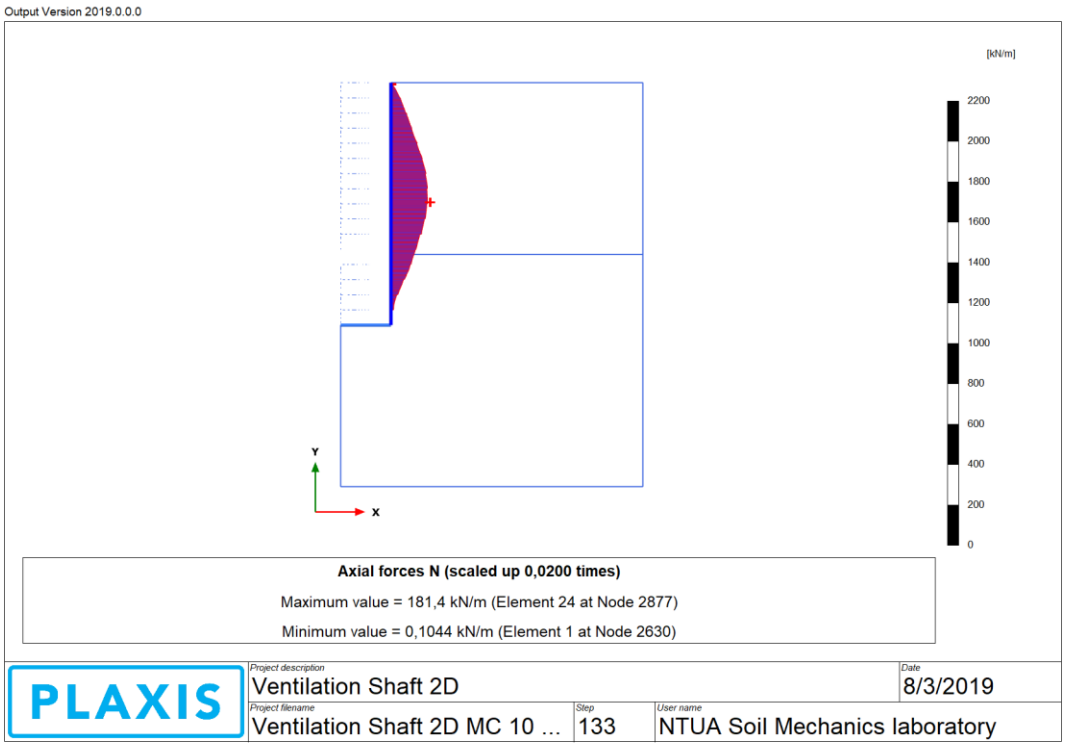

Figure.33 Axial Force (N) distribution, maximum and minimum values at the last stage (phase 17).

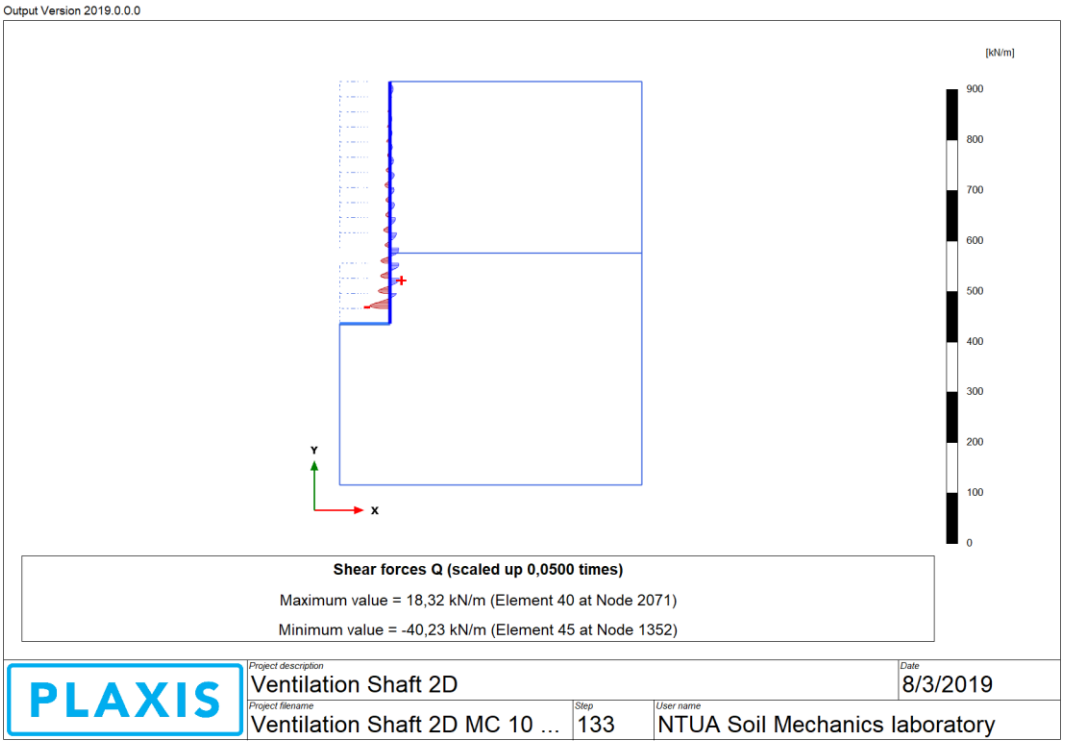

Figure.34 Shear Force (Q) distribution, maximum and minimum values at the last stage (phase 17).

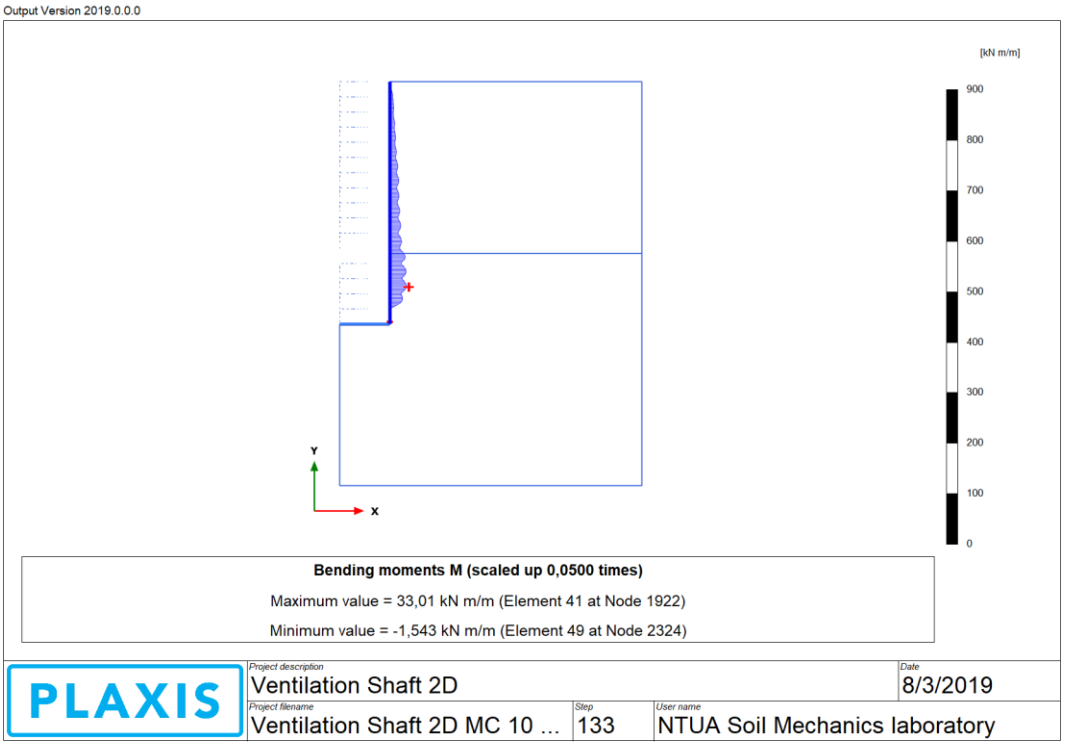

Figure.35 Bending Moment (M) distribution, maximum and minimum values at the last stage (phase 17).

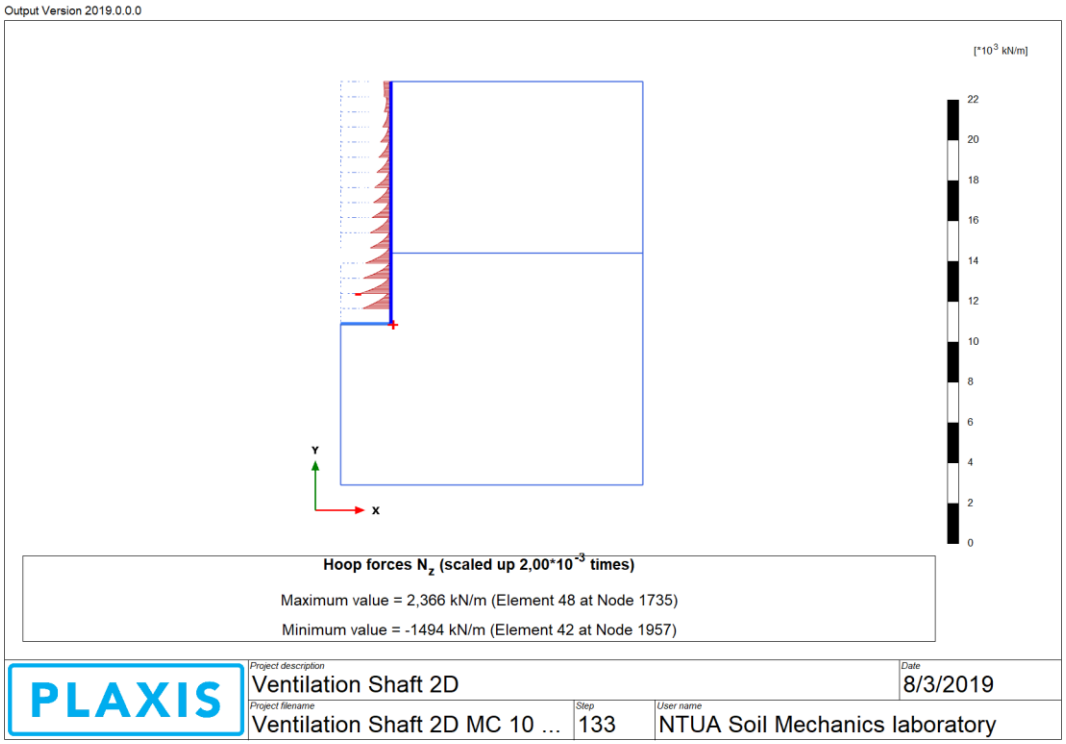

Figure.36 Hoop Force (N_z) distribution, maximum and minimum values at the last stage (phase 17).

6.5.5 PLAXIS 2D, STRESS ANALYSIS, MOHR-COULOMB MODEL

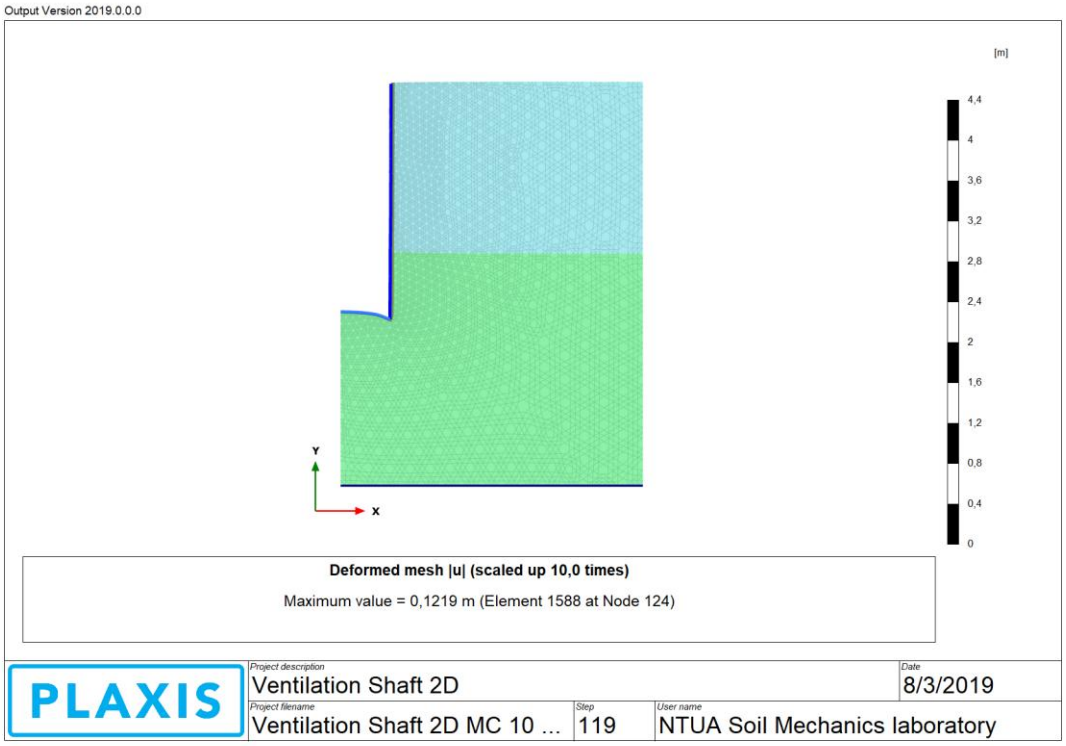

Figure.37 Deformed mesh at the last stage (phase 16).

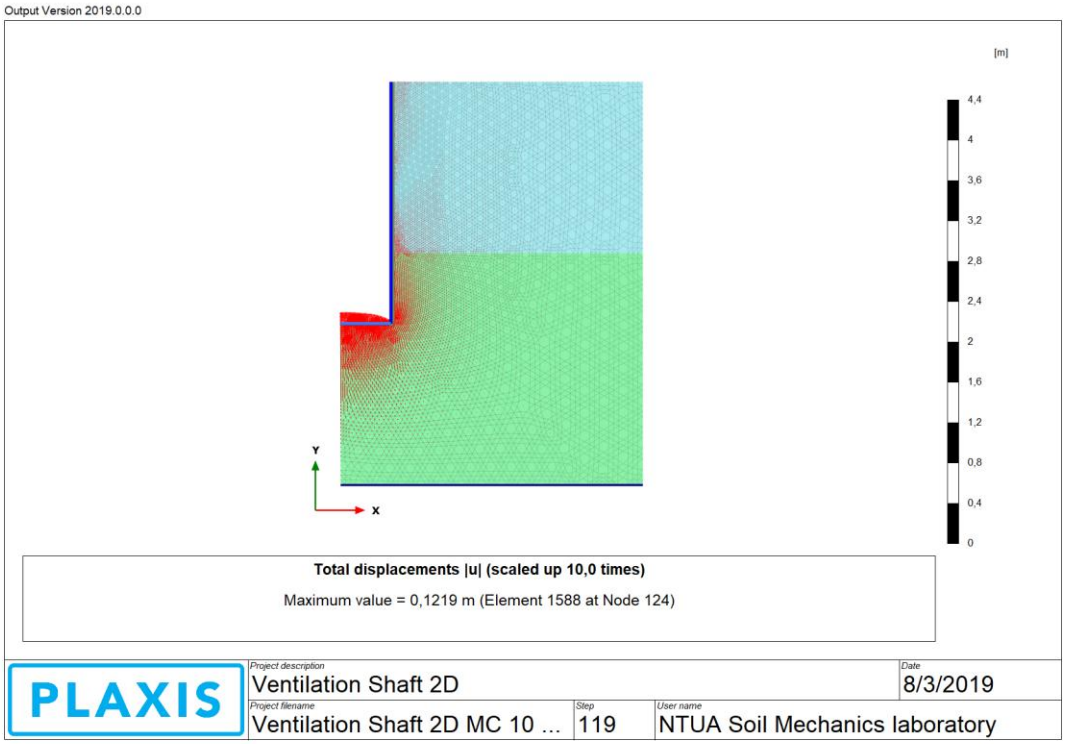

Figure.38 Total Displacements (absolute value) at the last stage (phase 16).

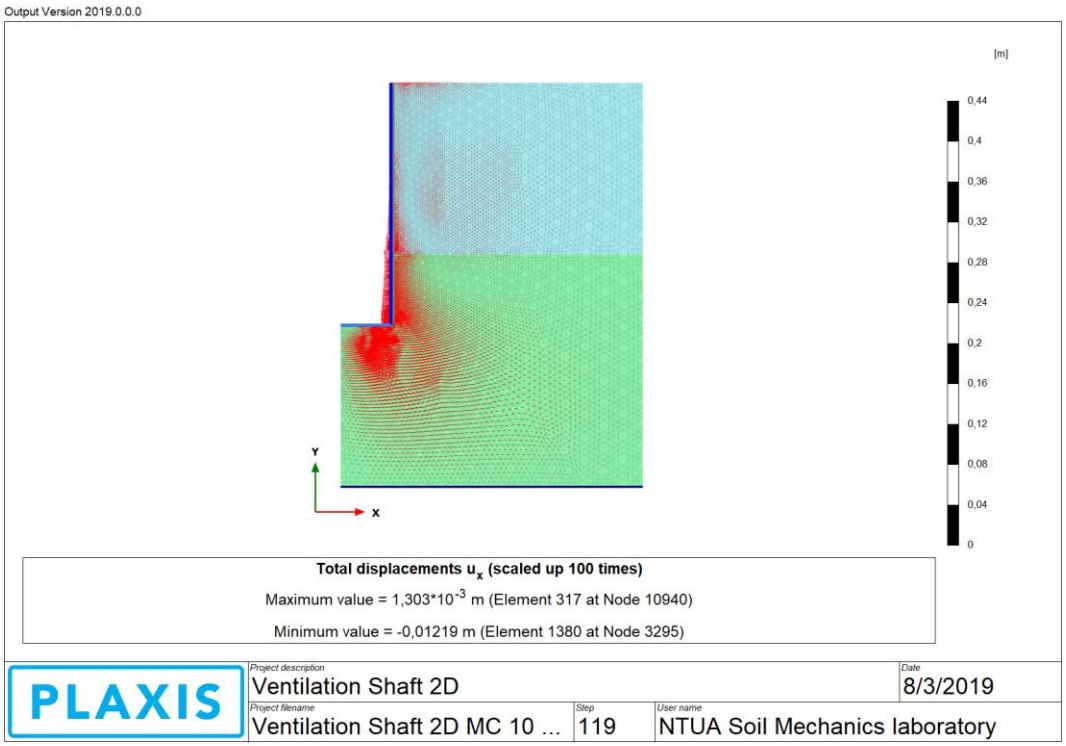

Figure.39 Maximum Horizontal Displacements (u_x) at the last stage (phase 16).

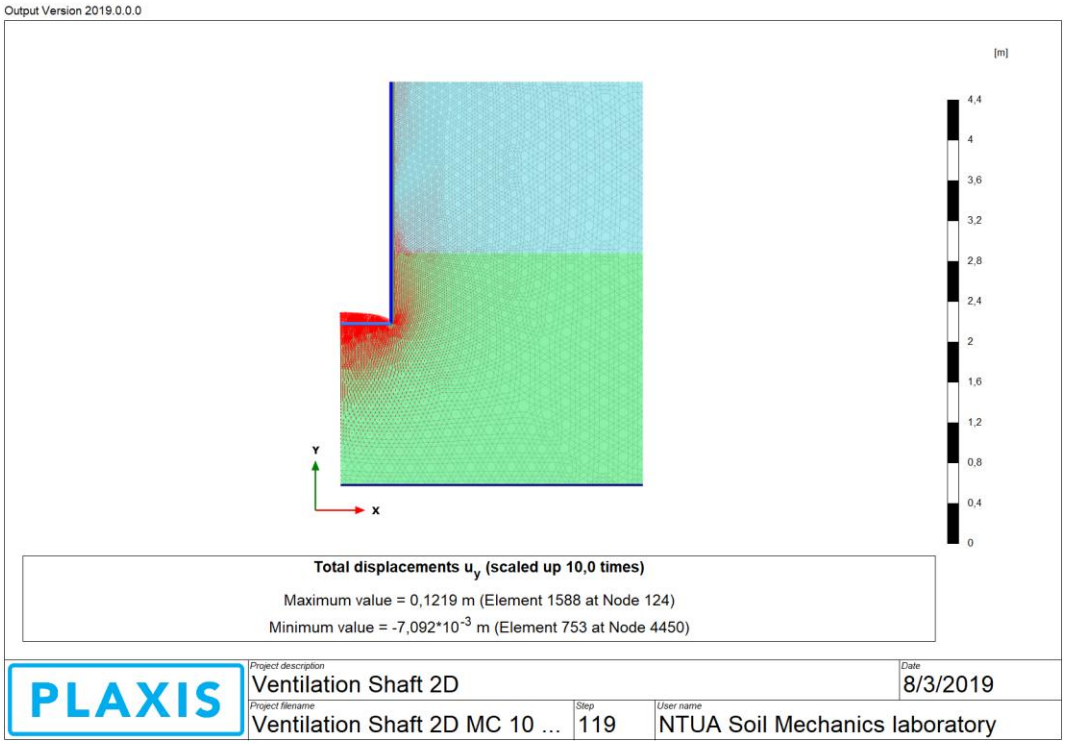

Figure.40 Maximum Vertical Displacements (u_y) at the last stage (phase 16).

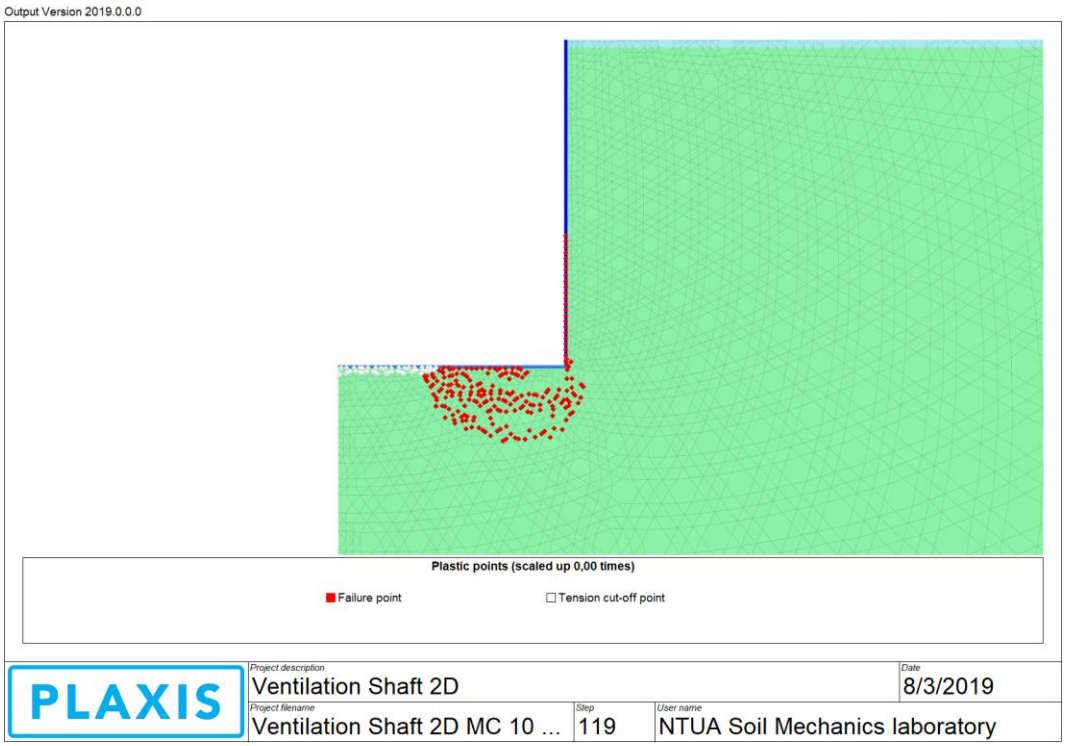

Figure.41 Plastic Points at the last stage (phase 16).

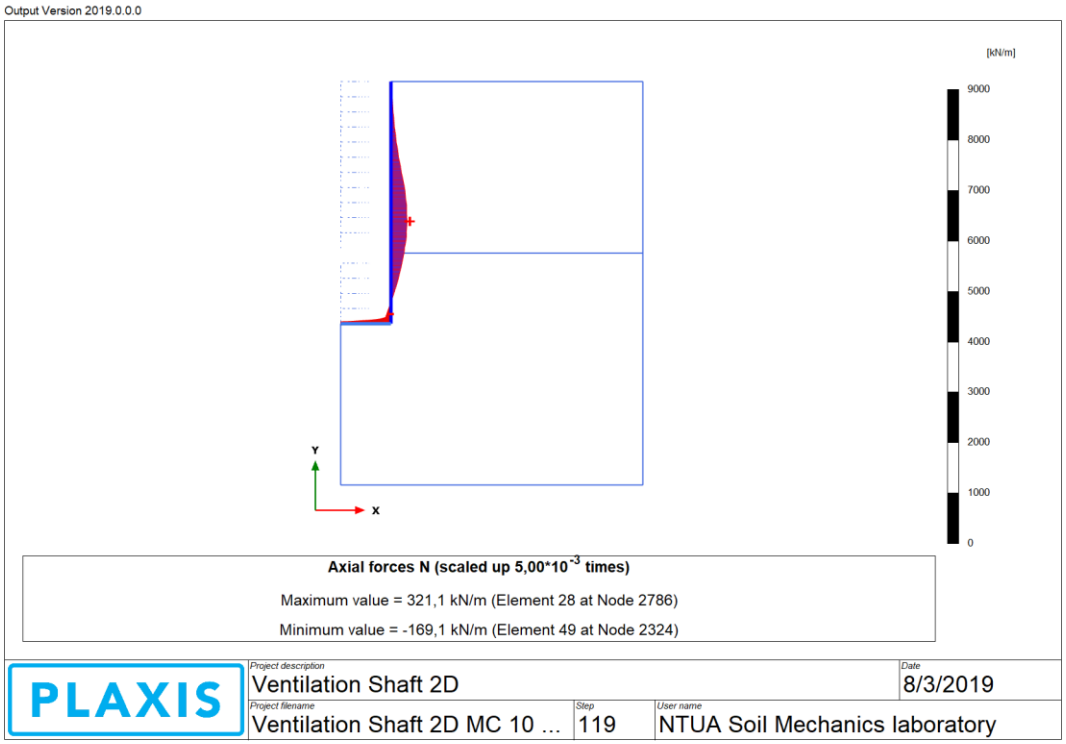

Figure.42 Axial Force (N) distribution, maximum and minimum values at the last stage (phase 16).

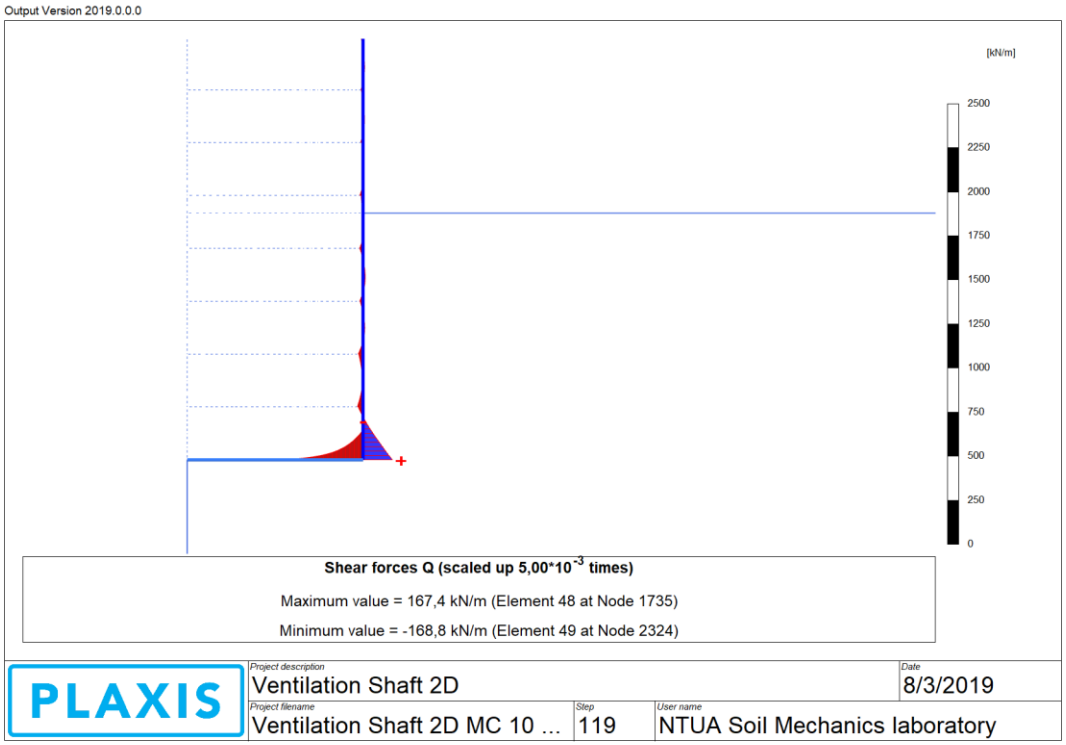

Figure.43 Shear Force (Q) distribution, maximum and minimum values at the last stage (phase 16).

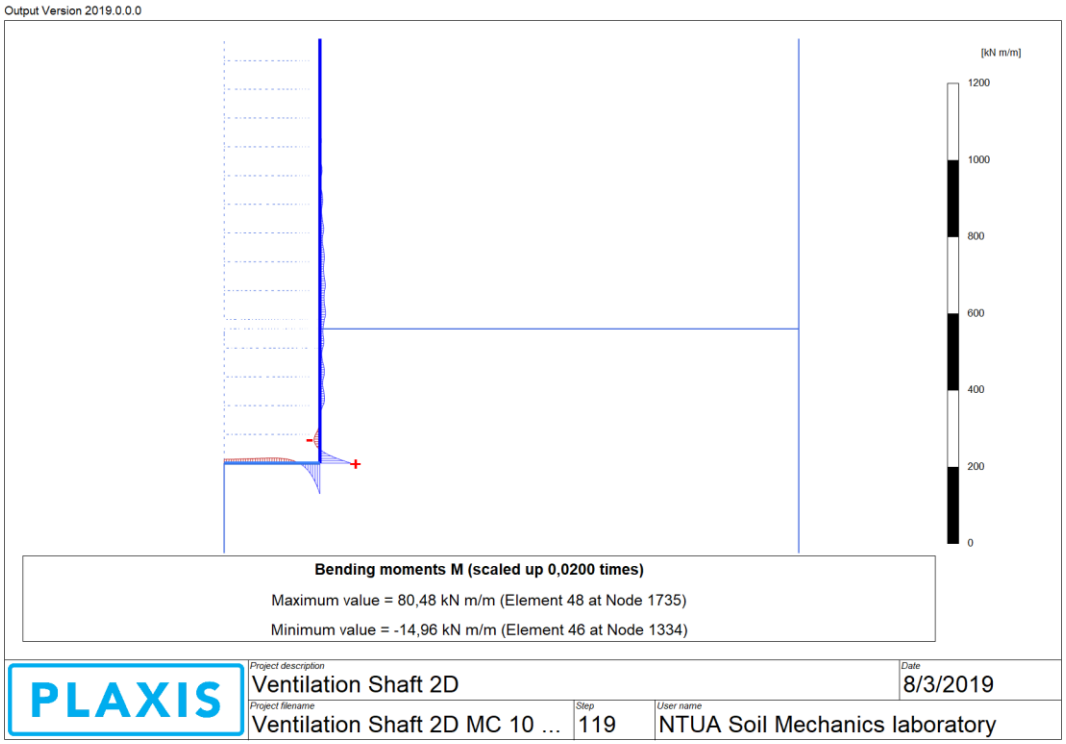

Figure.44 Bending Moment (M) distribution, maximum and minimum values at the last stage (phase 16).

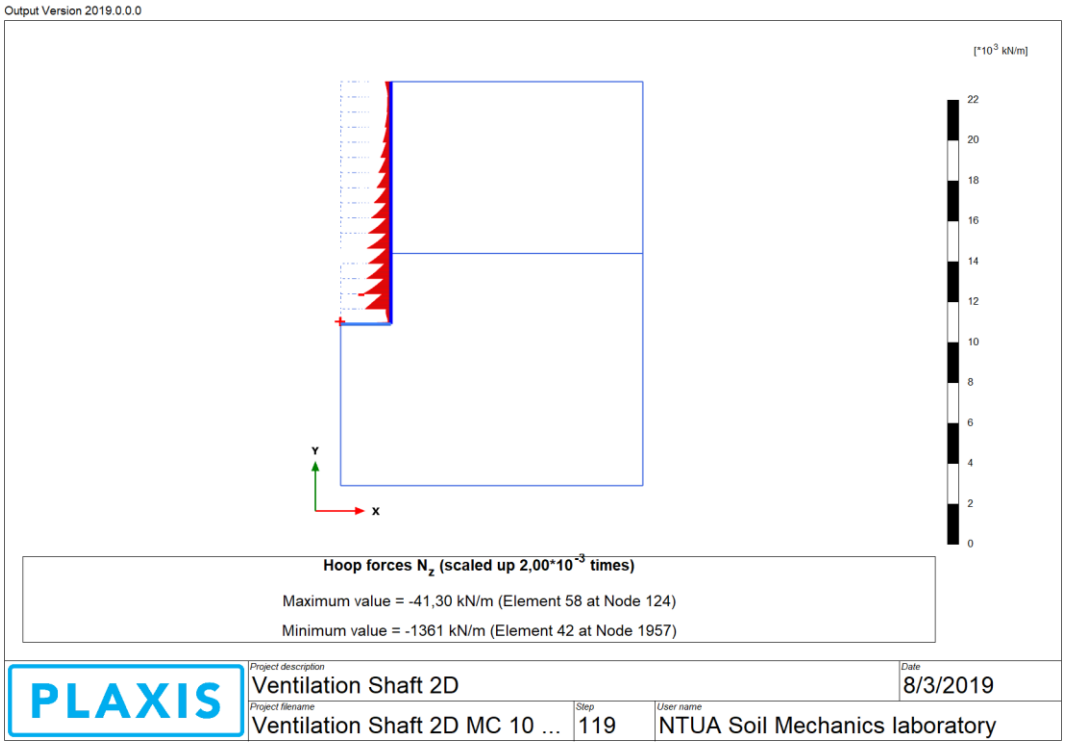

Figure.45 Hoop Axial Force (Nz) distribution, maximum and minimum values at the last stage (phase 16).

6.5.6 PLAXIS 2D, DEFORMATION ANALYSIS, HARDENING SOIL MODEL

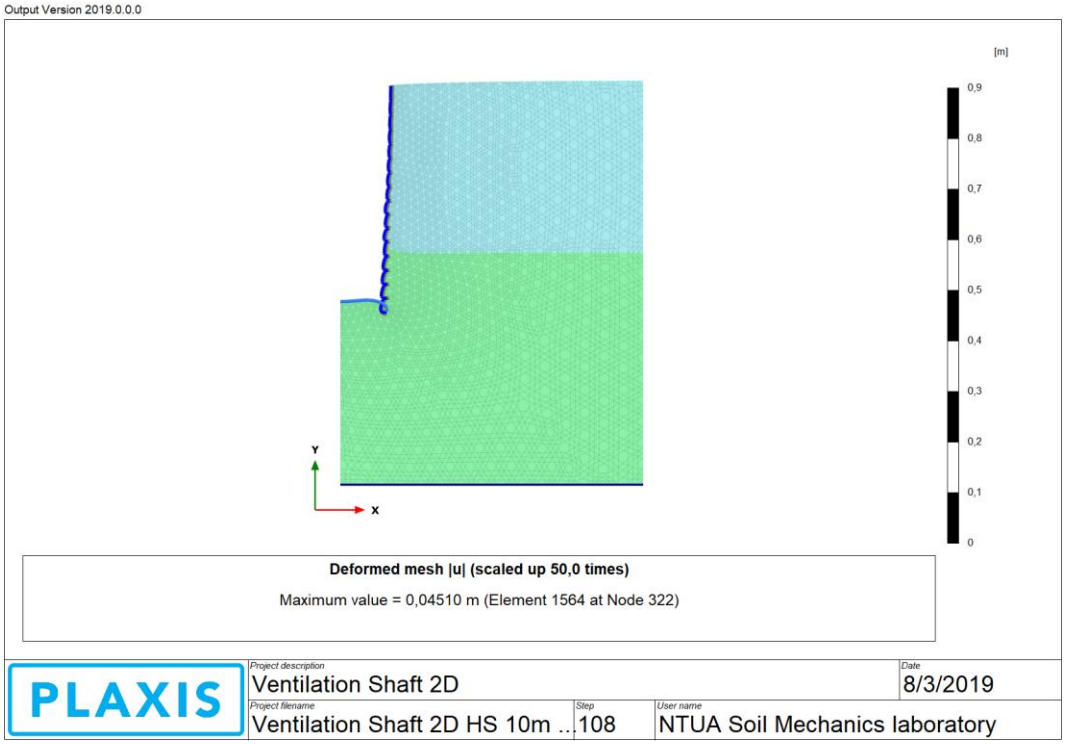

Figure.46 Deformed mesh at the last stage (phase 17).

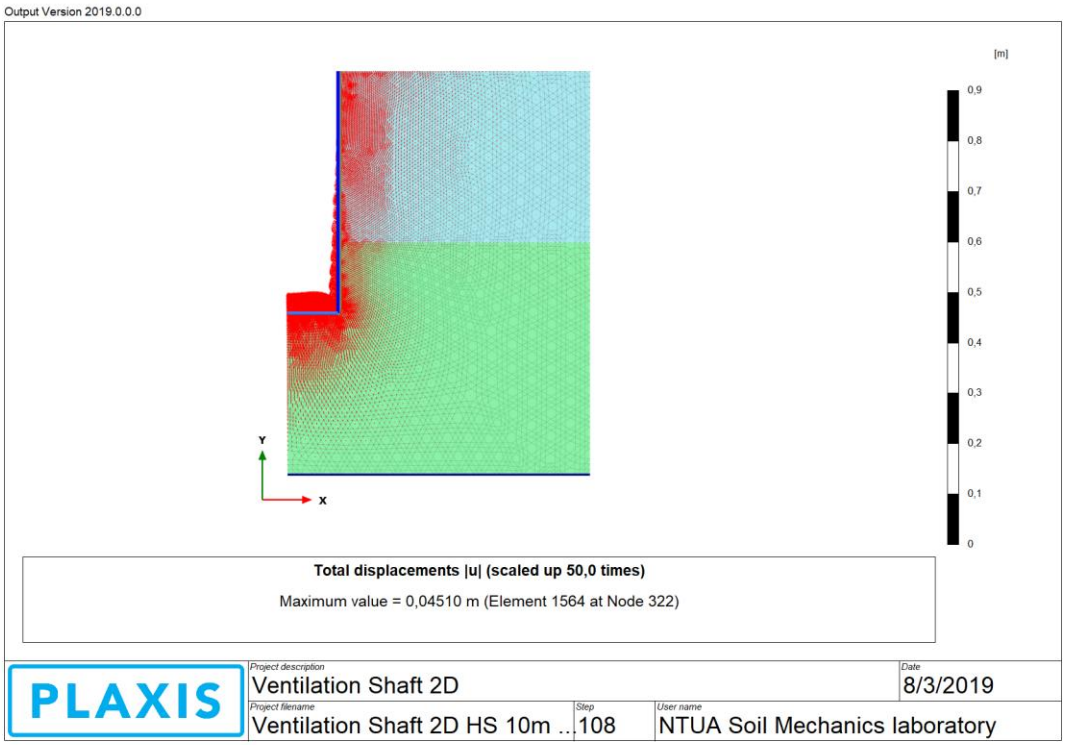

Figure.47 Total Displacements (absolute value) at the last stage (phase 17).

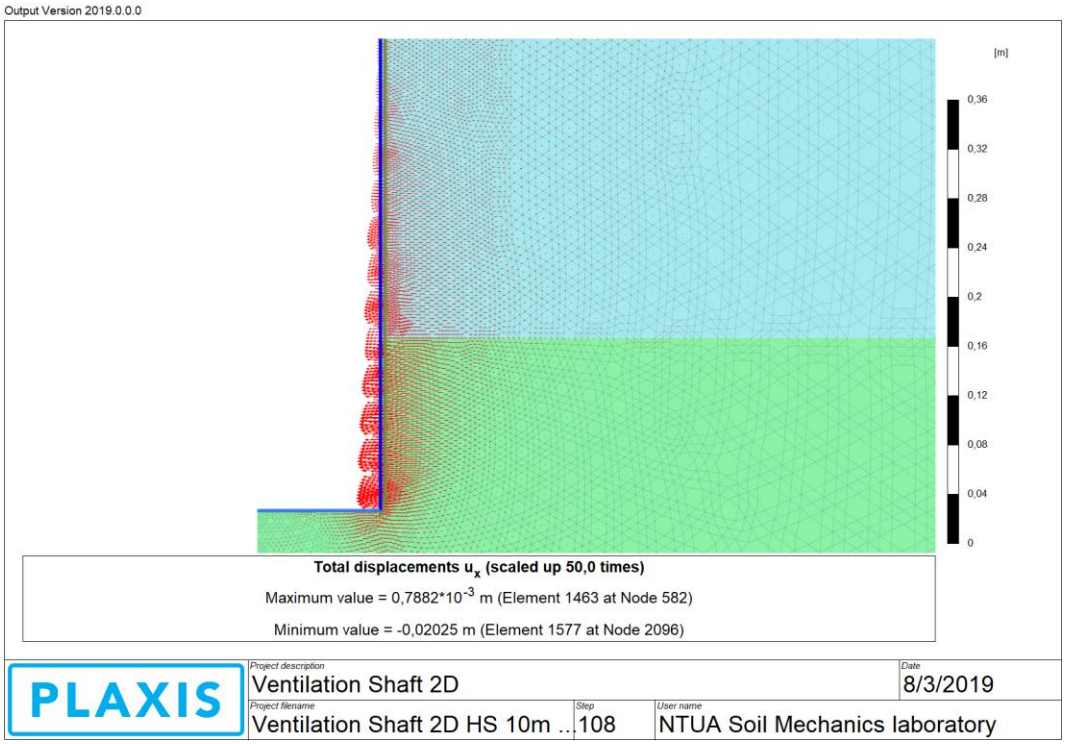

Figure.48 Maximum Horizontal Displacements (u_x) at the last stage (phase 17).

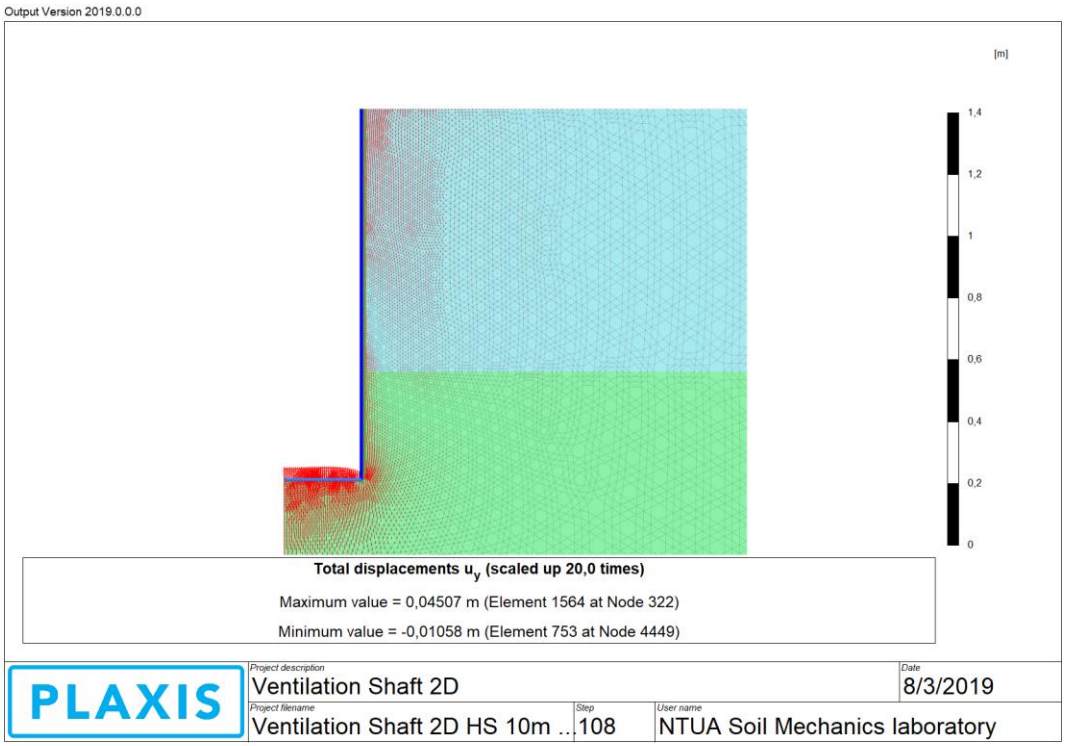

Figure.49 Maximum Vertical Displacements (u_y) at the last stage (phase 17).

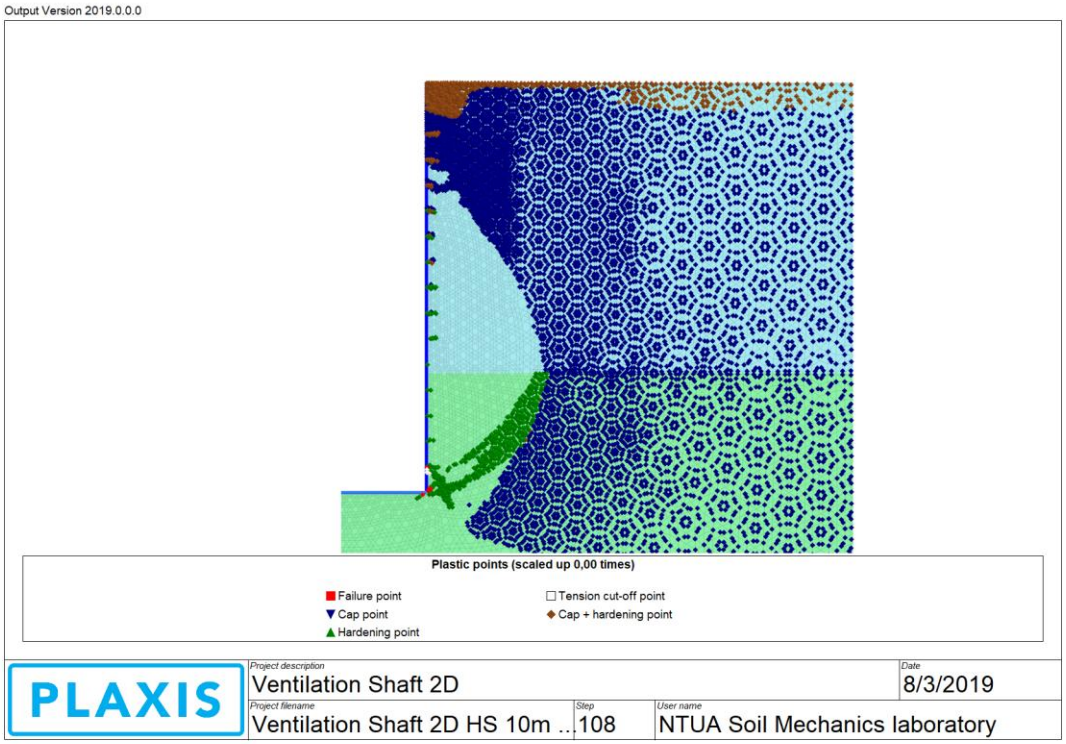

Figure.50 Plastic Points at the last stage (phase 17).

Plastic points show the stress points that are in a plastic state, displayed in a plot of the undeformed geometry. A red cube failure point indicates that the stresses lie on the surface of the failure envelop. To clarify that a "**Cap Point**" occurs if the stress state in a point is equivalent to the pre-consolidation stress, i.e. the maximum stress level that has previously been reached (OCR≤1) while a "**Hardening Point**" occurs when a stress state in a point corresponds to the maximum mobilized friction angle that has previously been reached. Cap and Hardening plastic points can only occur in the Hardening Soil model.

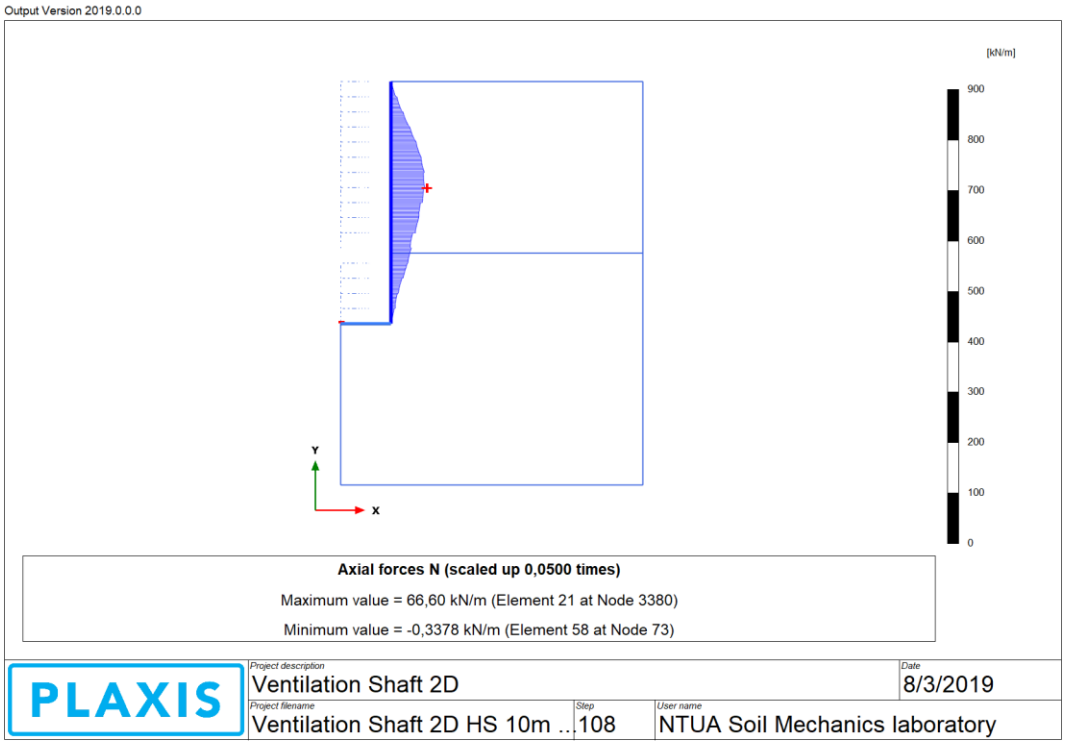

Figure.51 Axial Force (N) distribution, maximum and minimum values at the last stage (phase 17).

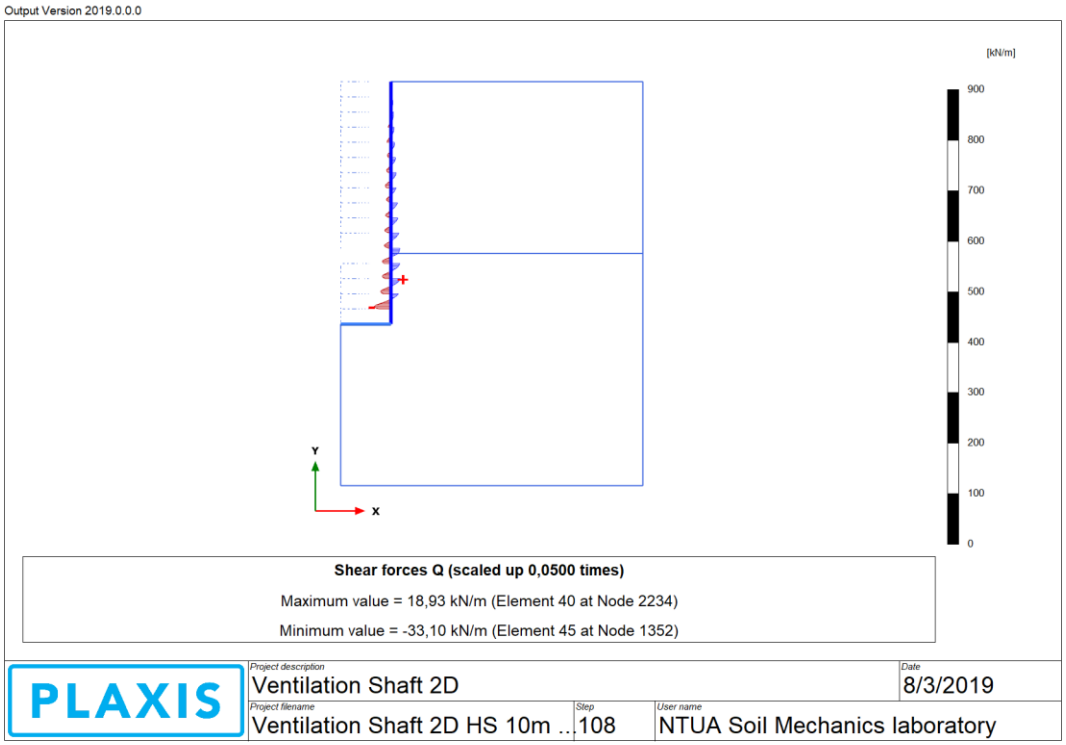

Figure.52 Shear Force (Q) distribution, maximum and minimum values at the last stage (phase 17).

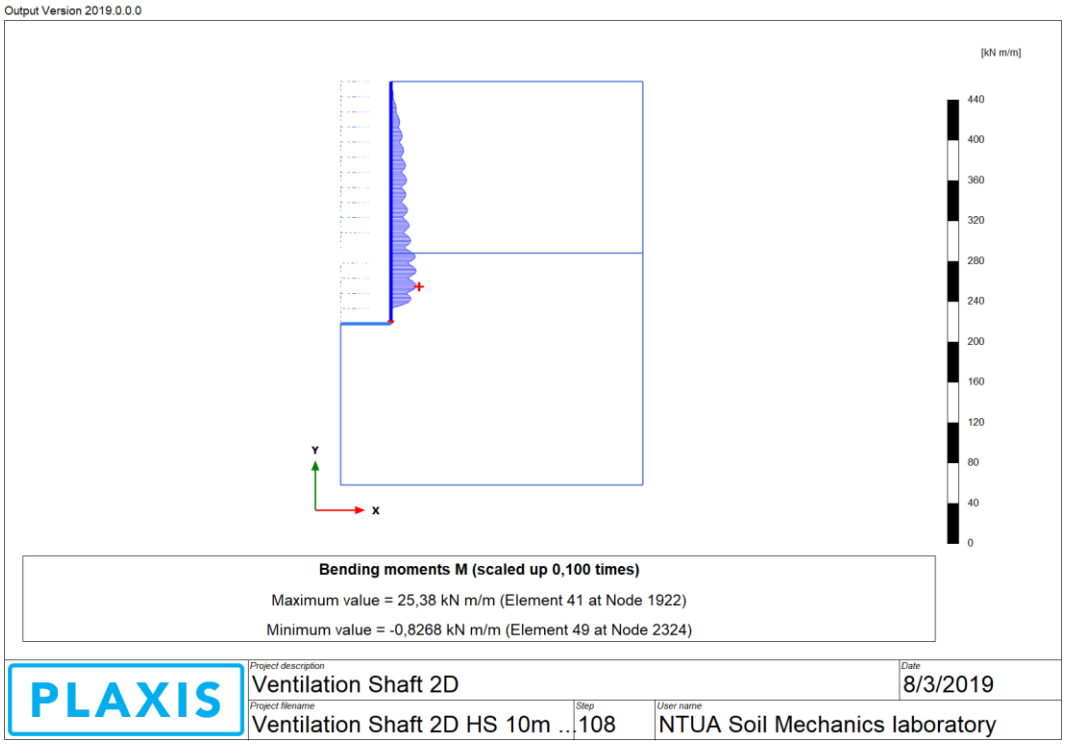

Figure.53 Bending Moment (M) distribution, maximum and minimum values at the last stage (phase 17).

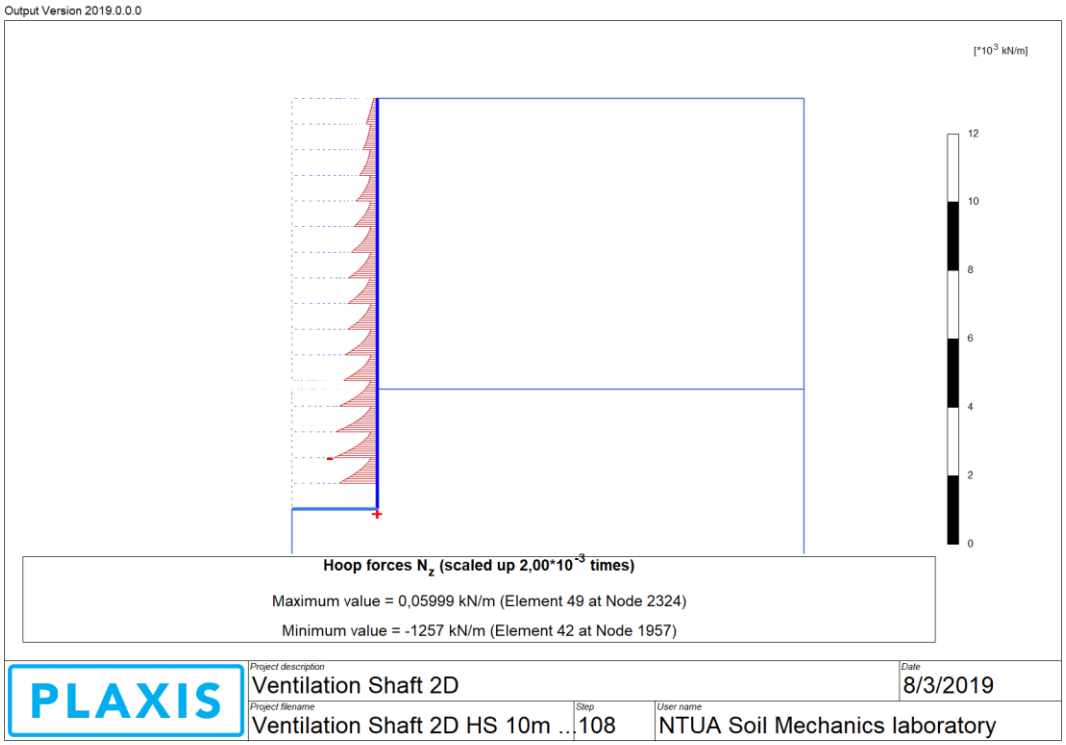

Figure.54 Hoop Axial Force (Nz) distribution, maximum and minimum values at the last stage (phase 17).

6.5.7 PLAXIS 2D, STRESS ANALYSIS, HARDENING SOIL MODEL

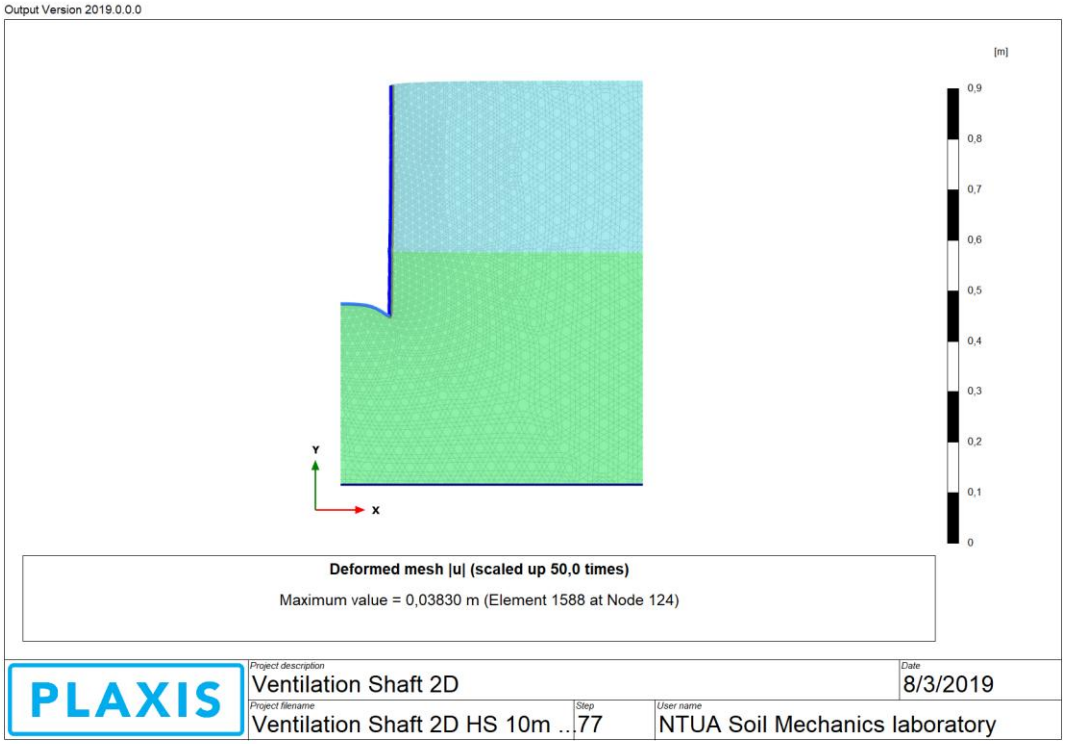

Figure.55 Deformed mesh at the last stage (phase 16).

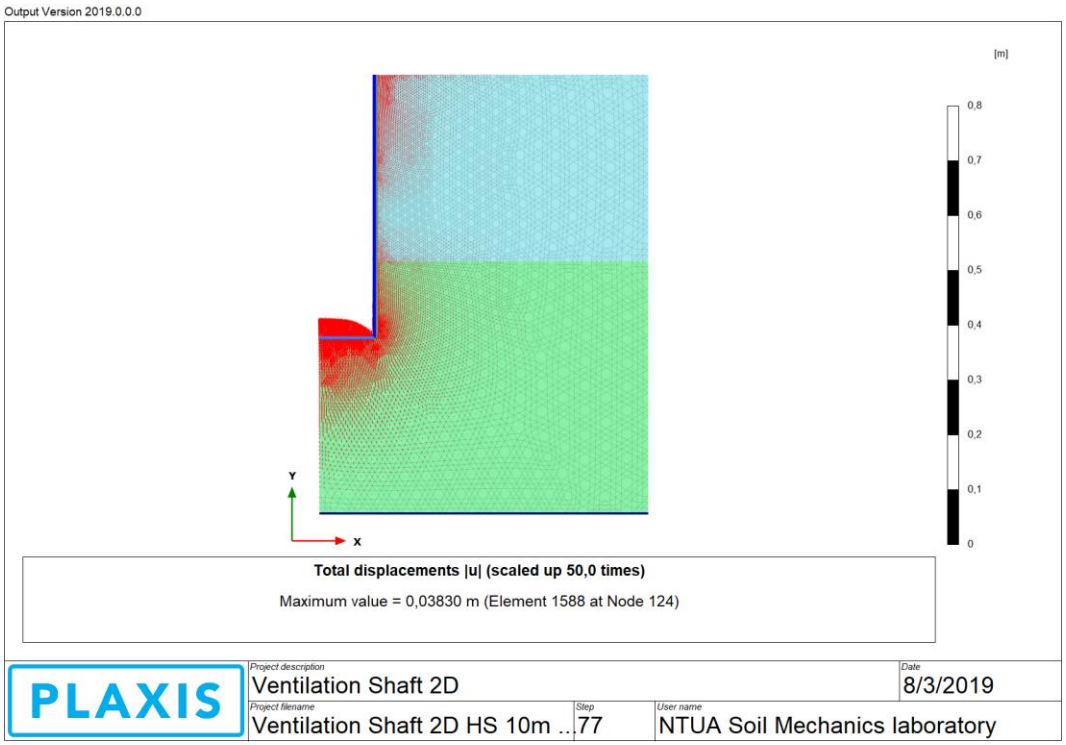

Figure.56 Total Displacements (absolute value) at the last stage (phase 16).

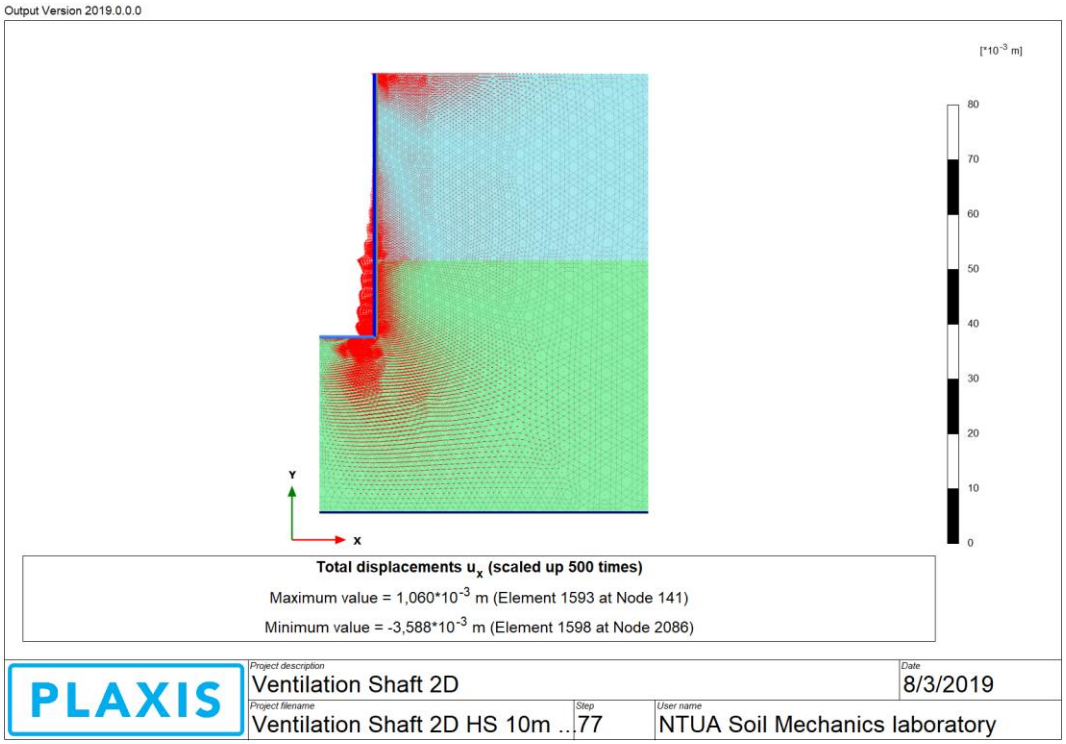

Figure.57 Maximum Horizontal Displacements (u_x) at the last stage (phase 16).

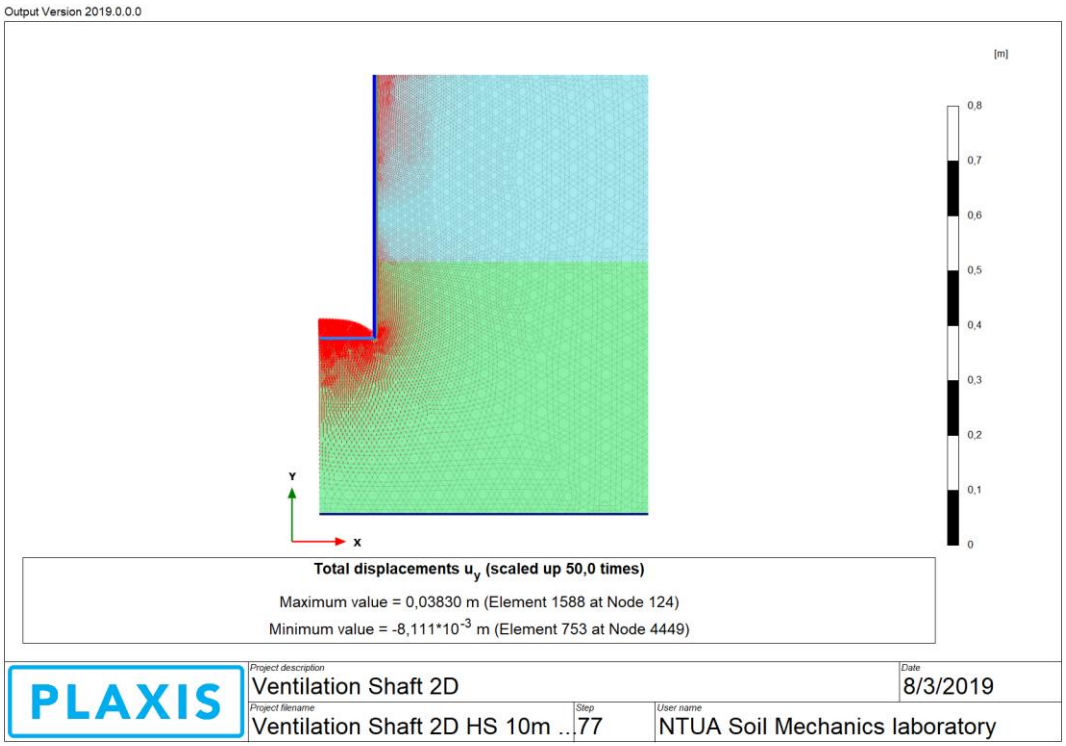

Figure.58 Maximum Vertical Displacements (u_y) at the last stage (phase 16).

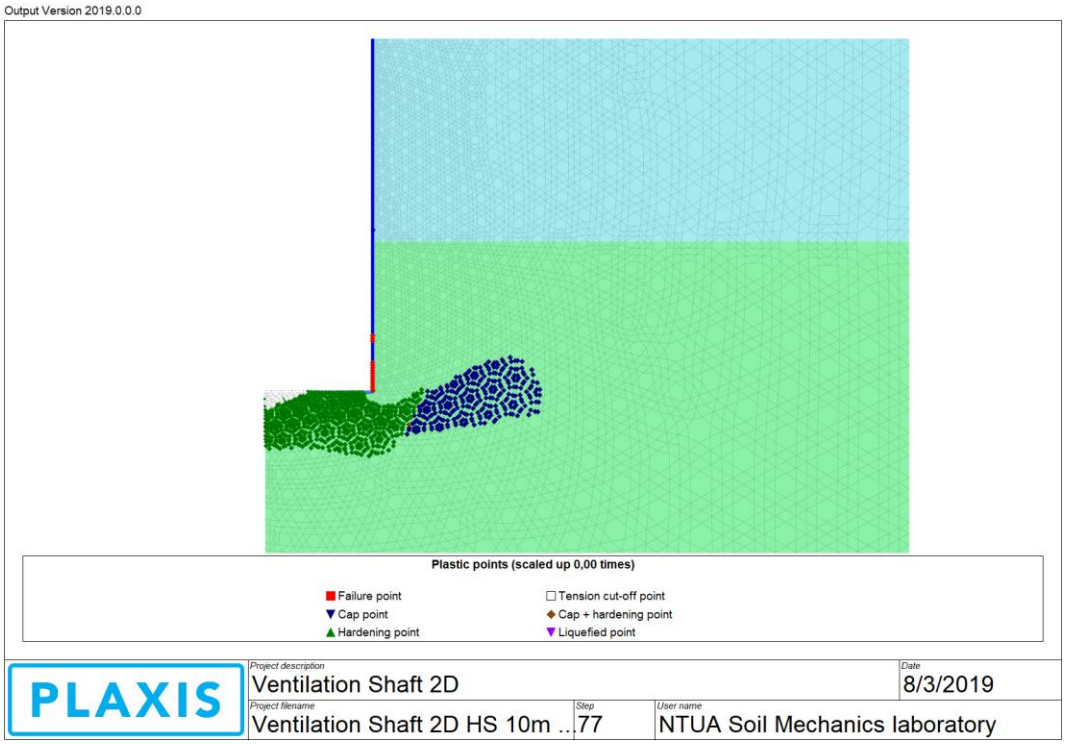

Figure.59 Plastic Points at the last stage (phase 16).

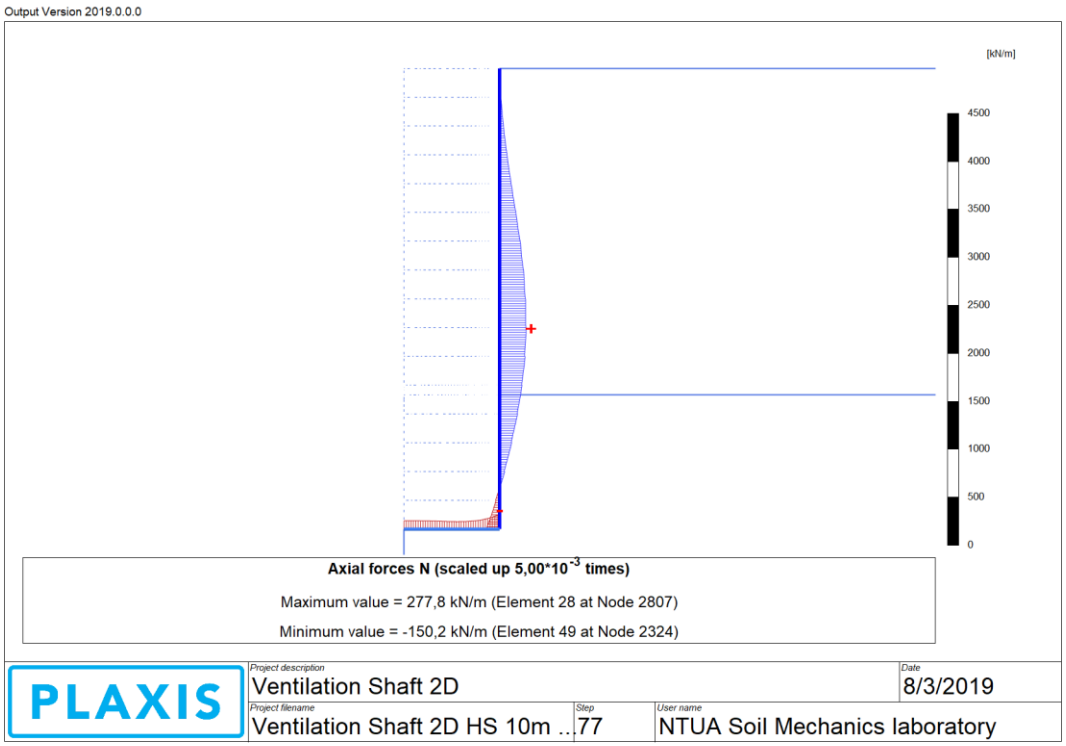

Figure.60 Axial Force (N) distribution, maximum and minimum values at the last stage (phase 16).

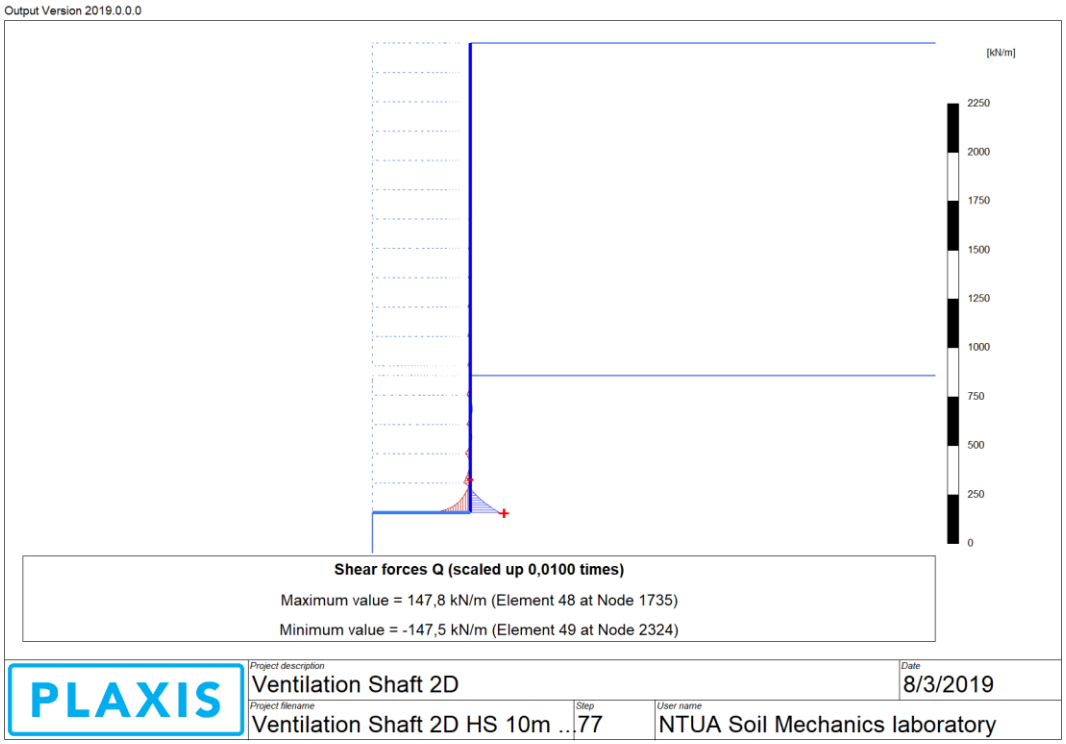

Figure.61 Shear Force (Q) distribution, maximum and minimum values at the last stage (phase 16).

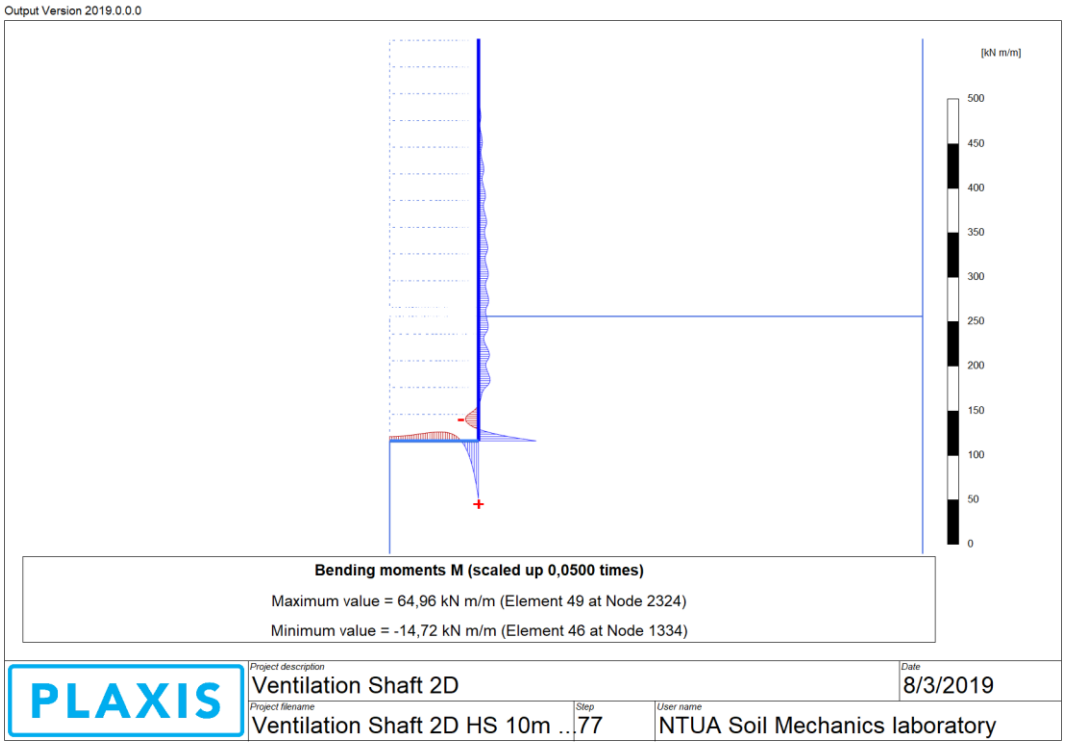

Figure.62 Bending Moment (M) distribution, maximum and minimum values at the last stage (phase 16).

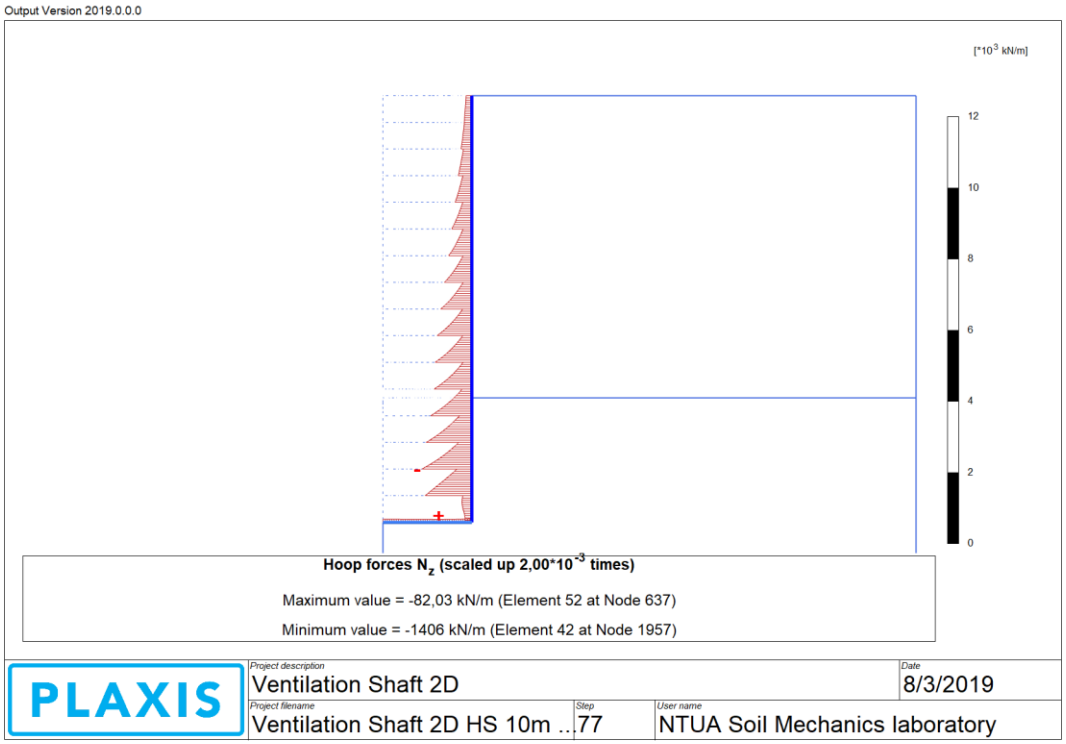

Figure.63 Hoop Axial Force (Nz) distribution, maximum and minimum values at the last stage (phase 16).

6.6 CURVES

Curves enable the recording of the development of quantities over multiple calculation steps at a specified location in the model. After the calculation phases have been defined and before the calculation process is started some points may be selected for the generation of load displacements curves or stress path ect. Nodes should be selected to plot displacements and stress points to plot stresses and strain.

Moreover, stress and strain diagrams can be used to visualize the development of stress (stress path) and strain (strain paths) of the stress-strain behavior of the soil in a particular selected point. These curves are useful to analyze the local behavior of the soil. Stress strain diagrams represent the idealized behavior of the soil according to the selected soil model. Since soil behavior is stress-dependent and soil models do not take all aspects of stress-dependency into account, stress paths are useful to validate previously selected model parameters.

Characteristically, as node points, are selected points at the ground surface 2,5 meters apart for a distance of 30 meters to evaluate the settlements and to represent them diagrammatically and gradually after the last excavation stage; more points are at the bottom of the horizontal support where the greatest uplift occurs and plastic deformation phenomena are intense. As far as stress points are concerned, the point at the greatest depth is selected, where the soil behavior is examined. Once the curve

points are selected, curves are scribed at a later stage as indicated in Figures 64 to 77 for stress and deformation analyses using Mohr-Coulomb and Hardening Soil model for the soil.

6.6.1 PLAXIS 2D, DEFORMATION ANALYSIS, MOHR-COULOMB MODEL

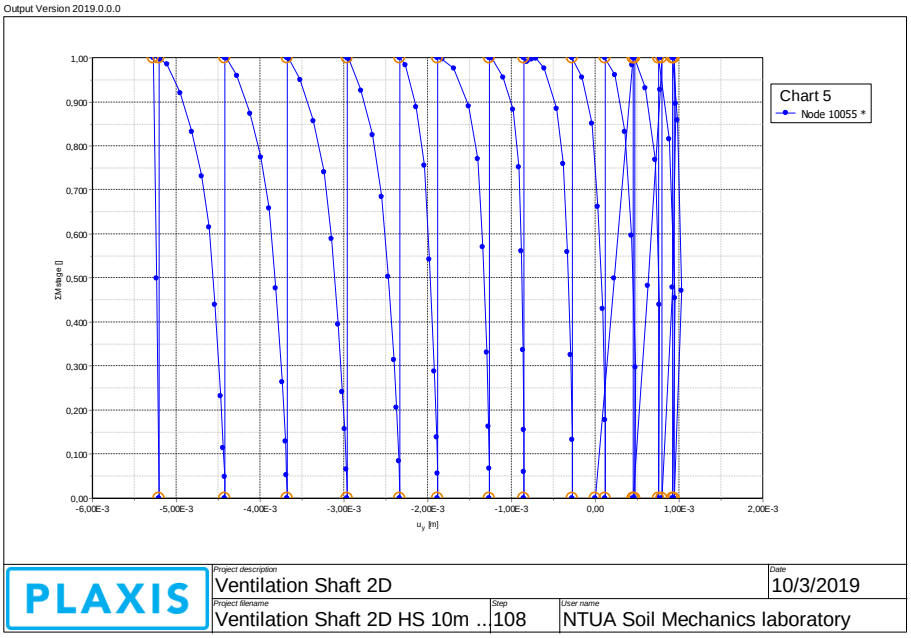

Figure.64 Vertical displacements (uy) PLAXIS Output Curves of the Node 10055 (10.2,0) for all the simulation phases.

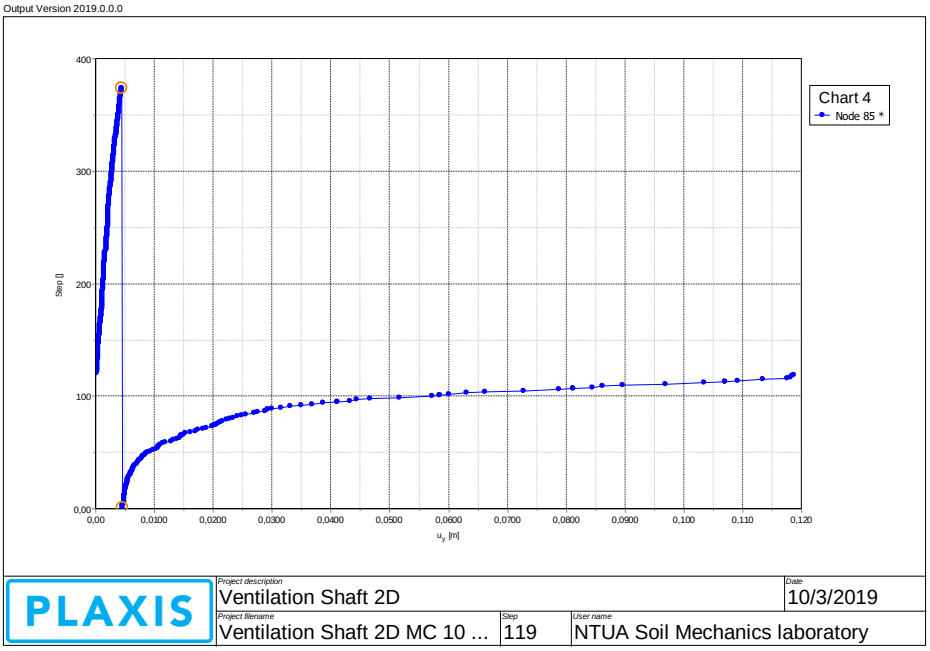

Figure.65 Vertical displacements (uy) /Progressive Uplift at the shaft's excavation bottom expressed in meters during various excavation and construction phases.

It apparent from Figure 66 that in the first construction phases for all selected points a limited uplift is documented that later it is transformed in settlement; as the distance from the excavation limit is increasing the vertical displacement (settlement) diminishes (not according to a linear distribution). This small uplift is possibly attributed to the placement of the first concrete plates. The vertical displacements corresponding to the latest stage are noted by a circle.

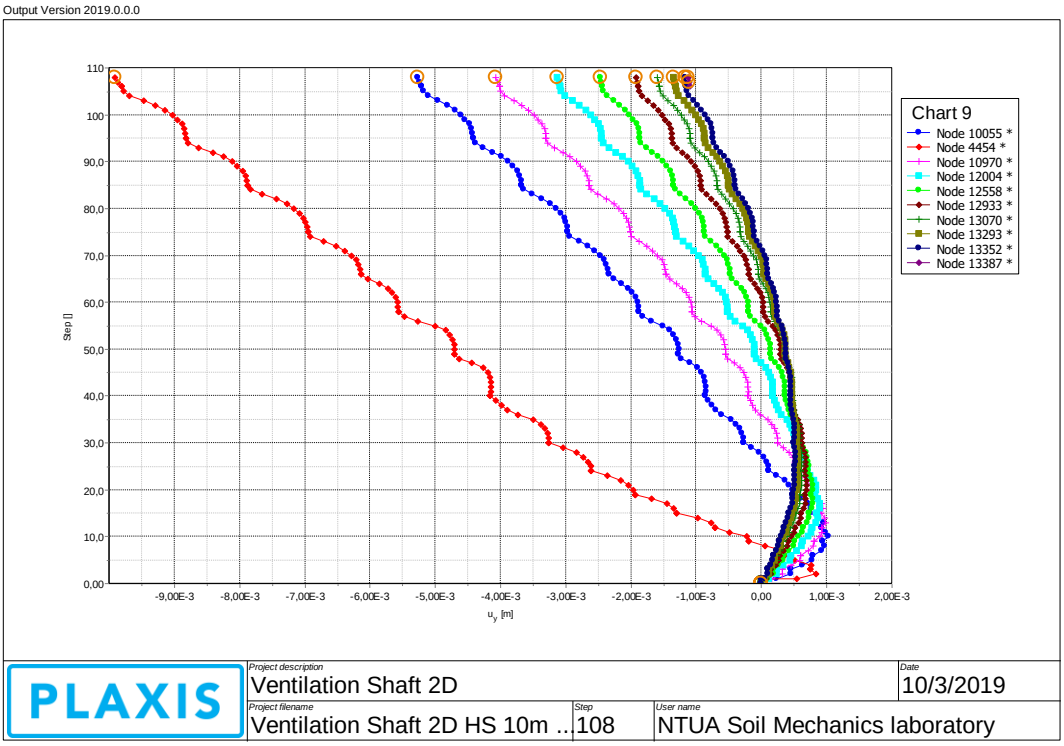

Figure.66 Vertical displacements expressed in meters during progressive excavation/construction phases for various points at the ground surface.

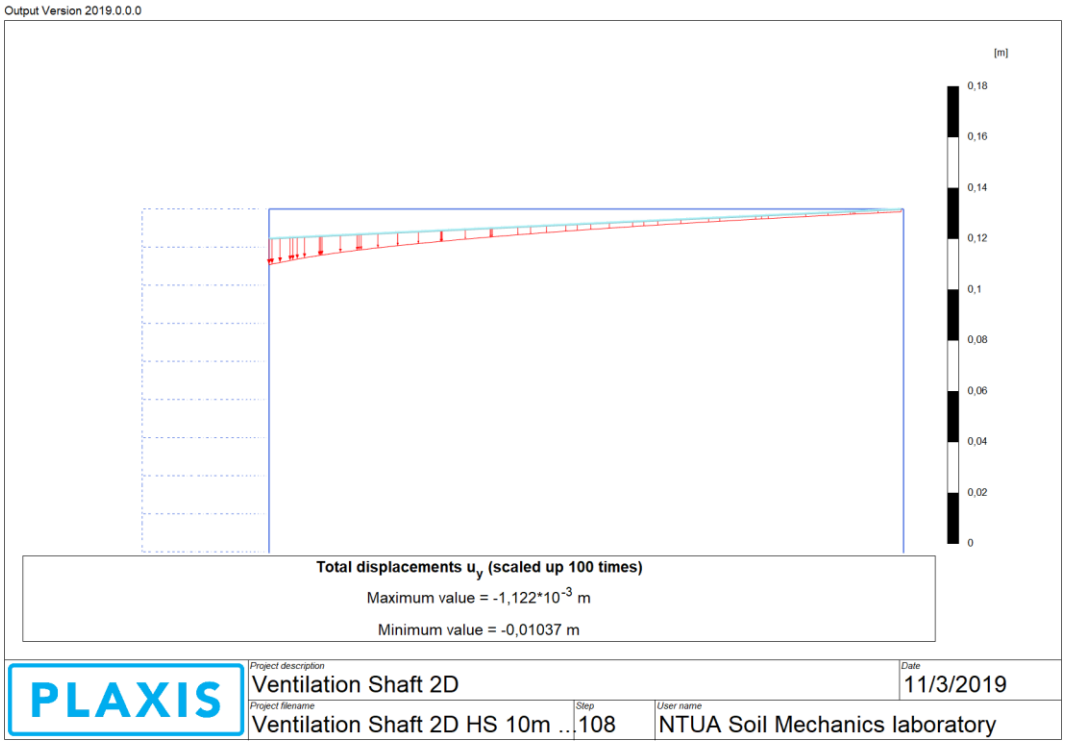

Figure.67 Settlements/Vertical Displacements (u_y) along the ground surface for a distance of 30 meters after the last construction phase.

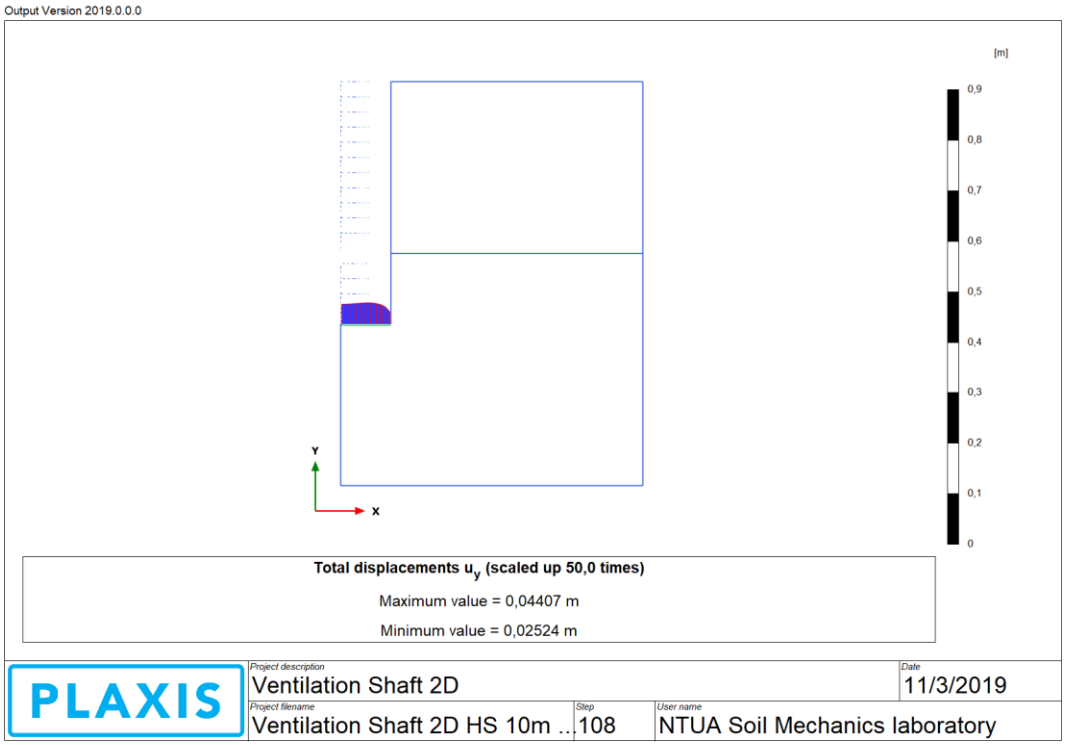

Figure.68 Uplift/ Vertical Displacements (u_y) at the shaft's excavation bottom starting from the axis of axisymmetry.

6.6.2 PLAXIS 2D, STRESS ANALYSIS, MOHR-COULOMB MODEL

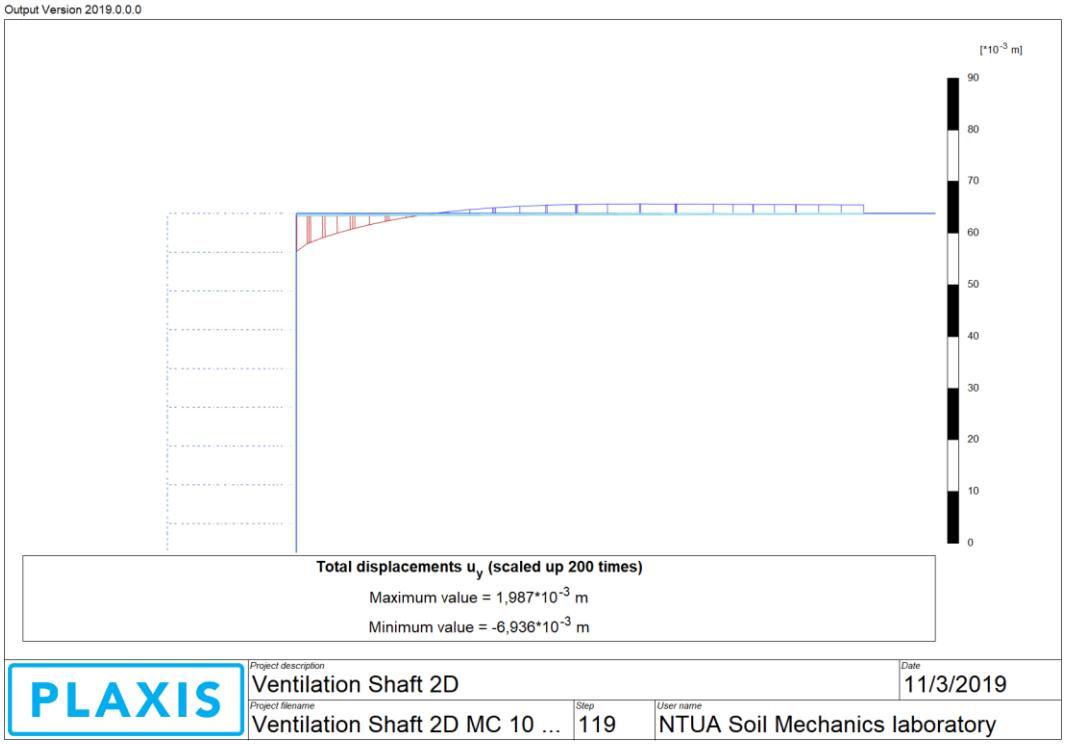

Figure.69 Settlements/Vertical Displacements (u_y) along the ground surface for a distance of 30 meters after the last construction phase.

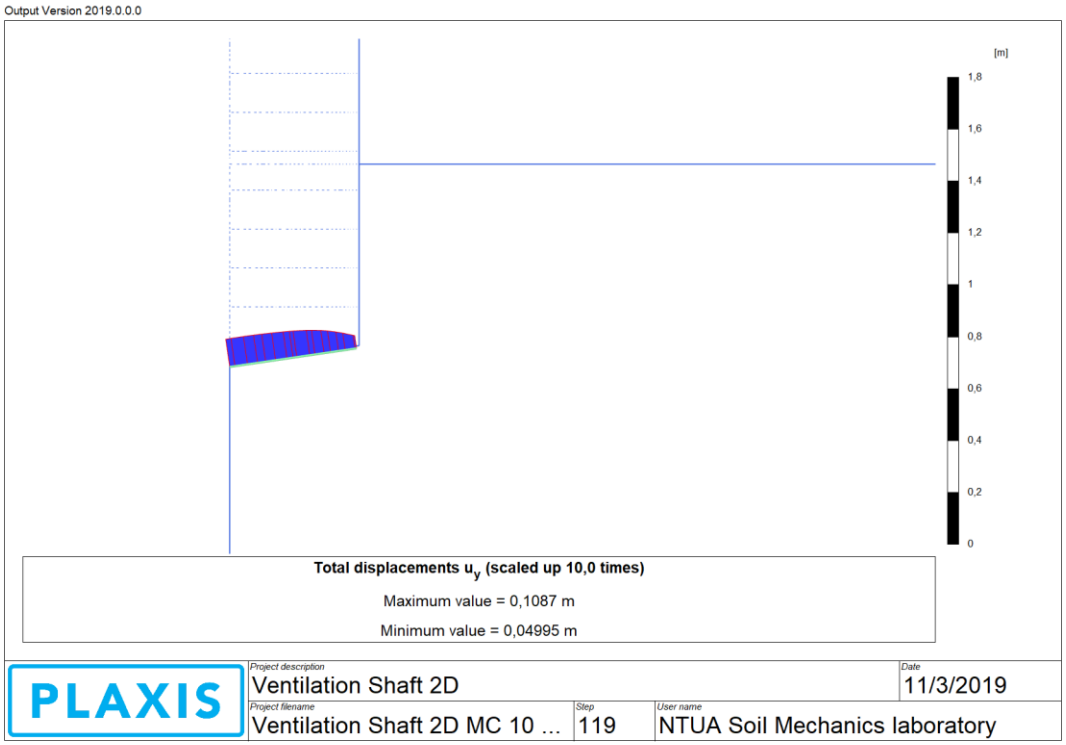

Figure.70 Uplift/ Vertical Displacements (u_y) at the shaft's excavation bottom starting from the axis of axisymmetry.

6.6.3 PLAXIS 2D, DEFORMATION ANALYSIS, HARDENING SOIL MODEL

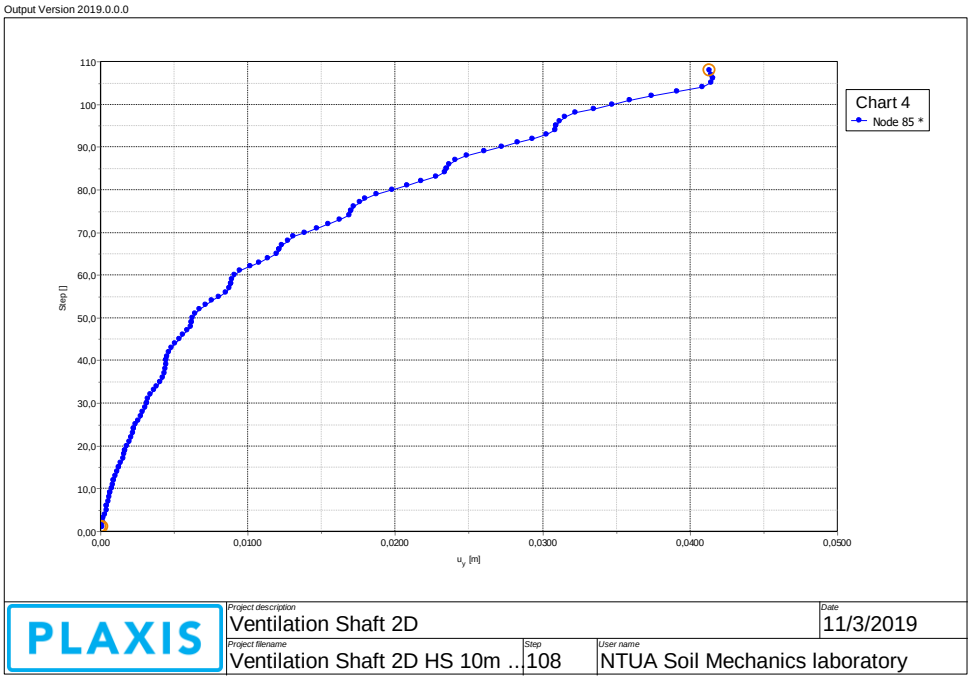

Figure.71 Vertical displacements (uy) / Progressive Uplift at the shaft's excavation bottom expressed in meters during various excavation and construction phases.

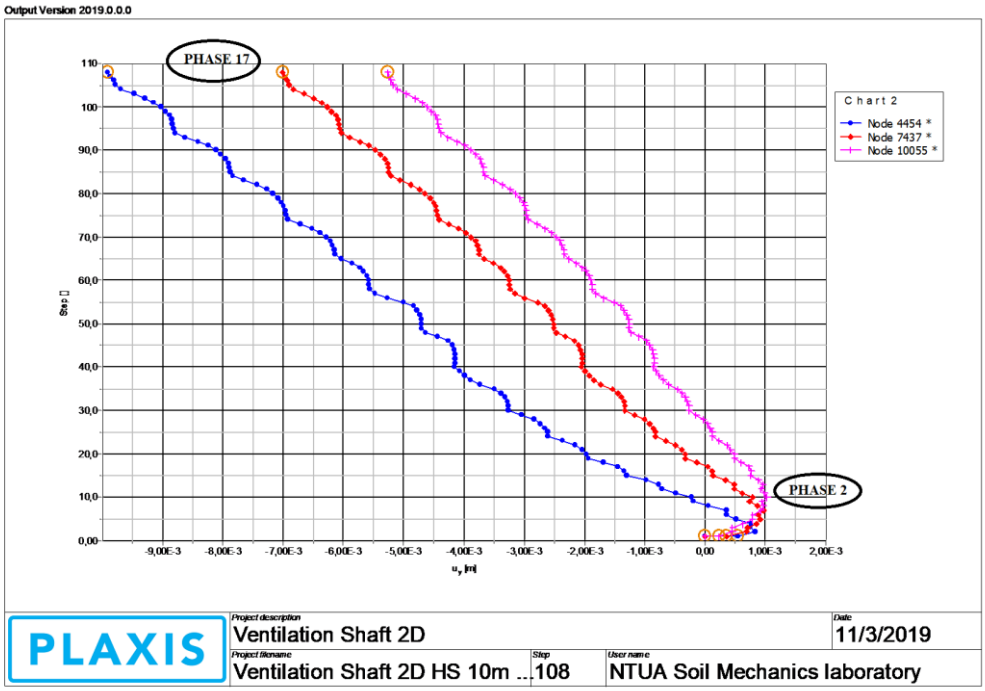

Figure.72 Vertical displacements expressed in meters during progressive excavation/construction phases for three nodes (5.125,0-7.519,0-10.027,0) distancing respectively 5, 7.5 and 10 meters from the excavation border.

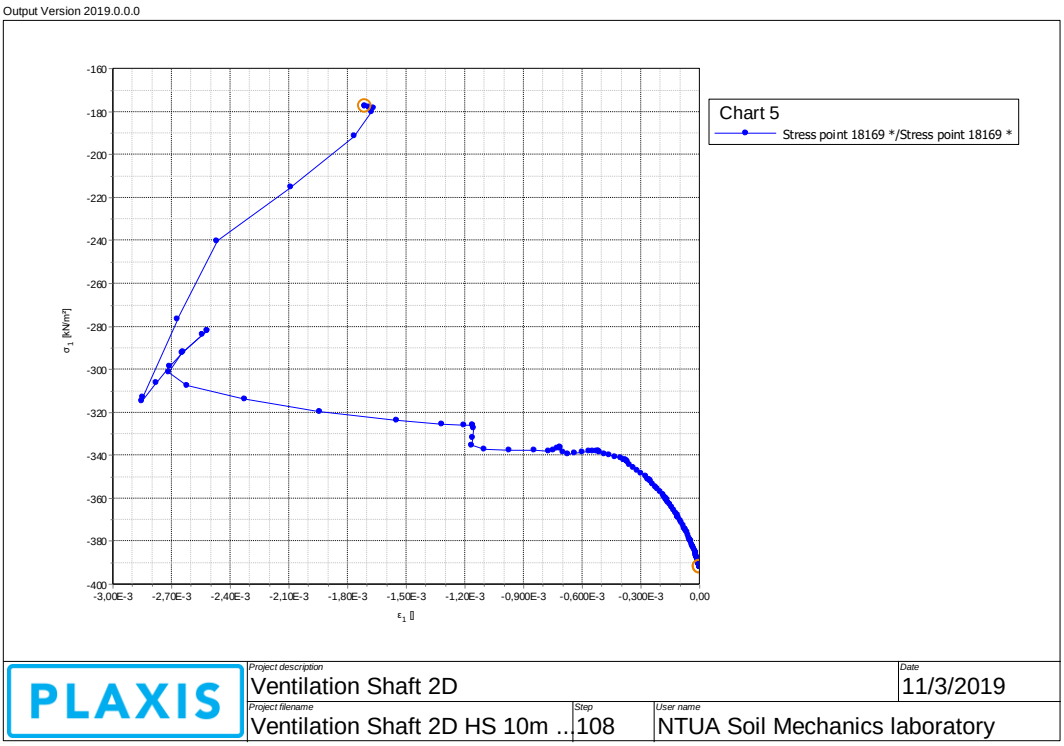

Figure.73 Total strains (σ1)-Principal total stresses (ε1) diagram during various excavation phases corresponding to a stress point (5.034,-24) at the bottom of the excavation close to the last plate (concrete ring).

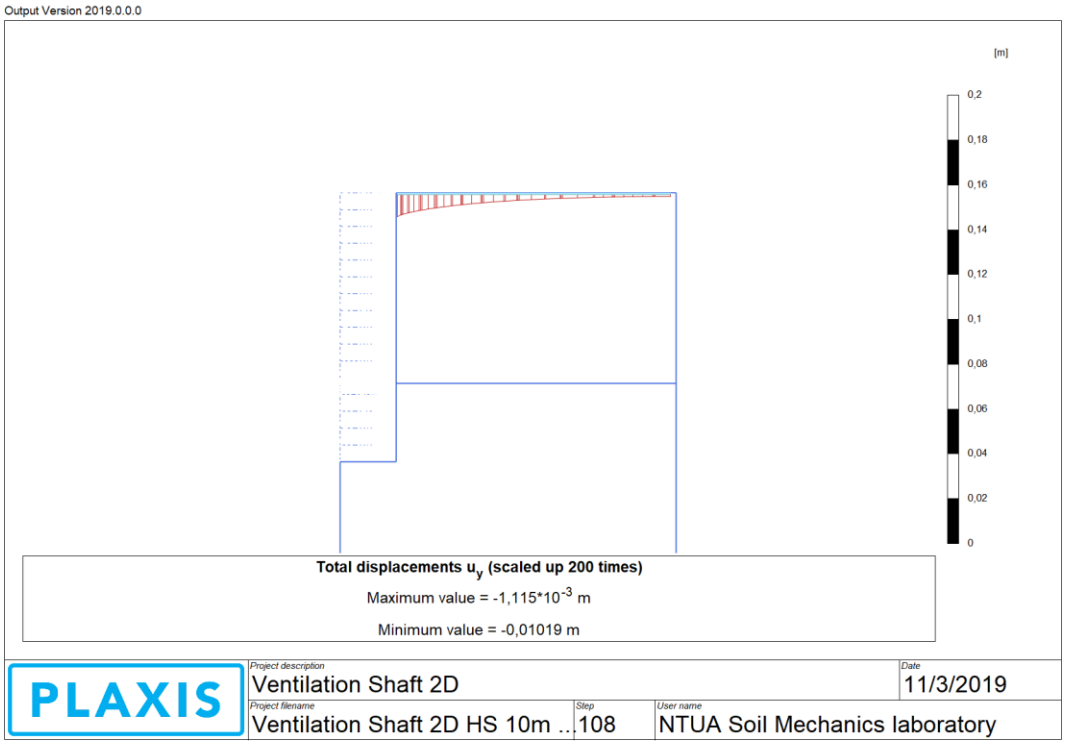

Figure.74 Settlements/Vertical Displacements (u_y) along the ground surface for a distance of 30 meters after the last construction phase.

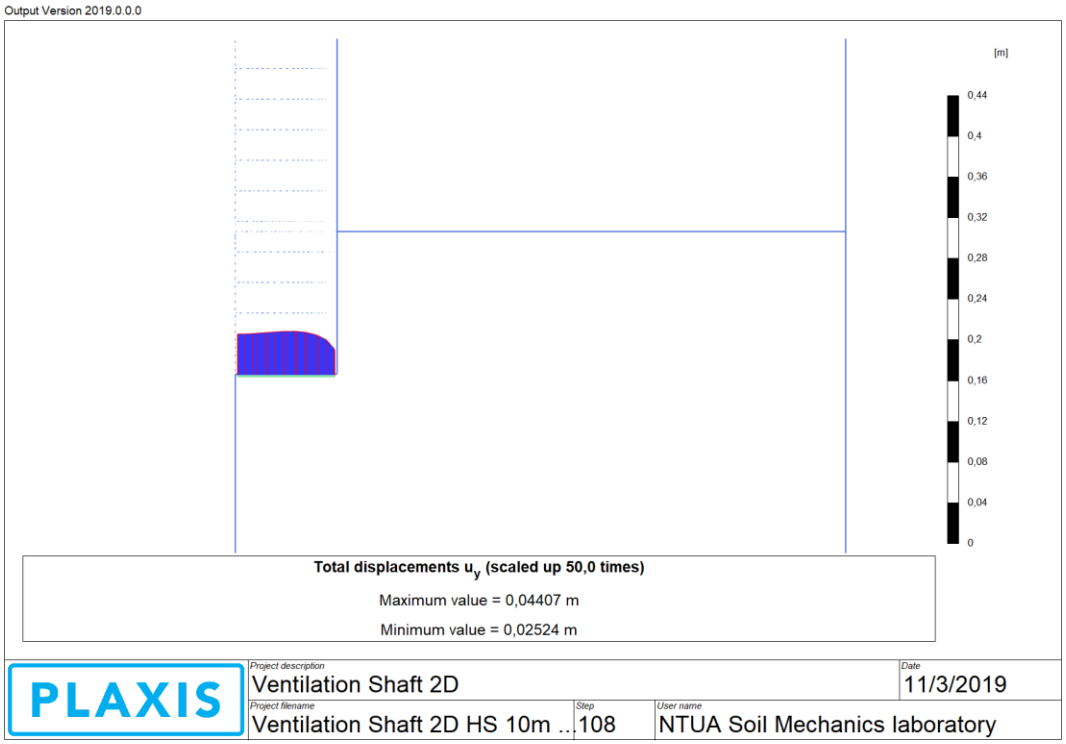

Figure.75 Uplift/ Vertical Displacements (u_y) at the shaft's excavation bottom starting from the axis of axisymmetry.

6.6.4 PLAXIS 2D, STRESS ANALYSIS, HARDENING SOIL MODEL

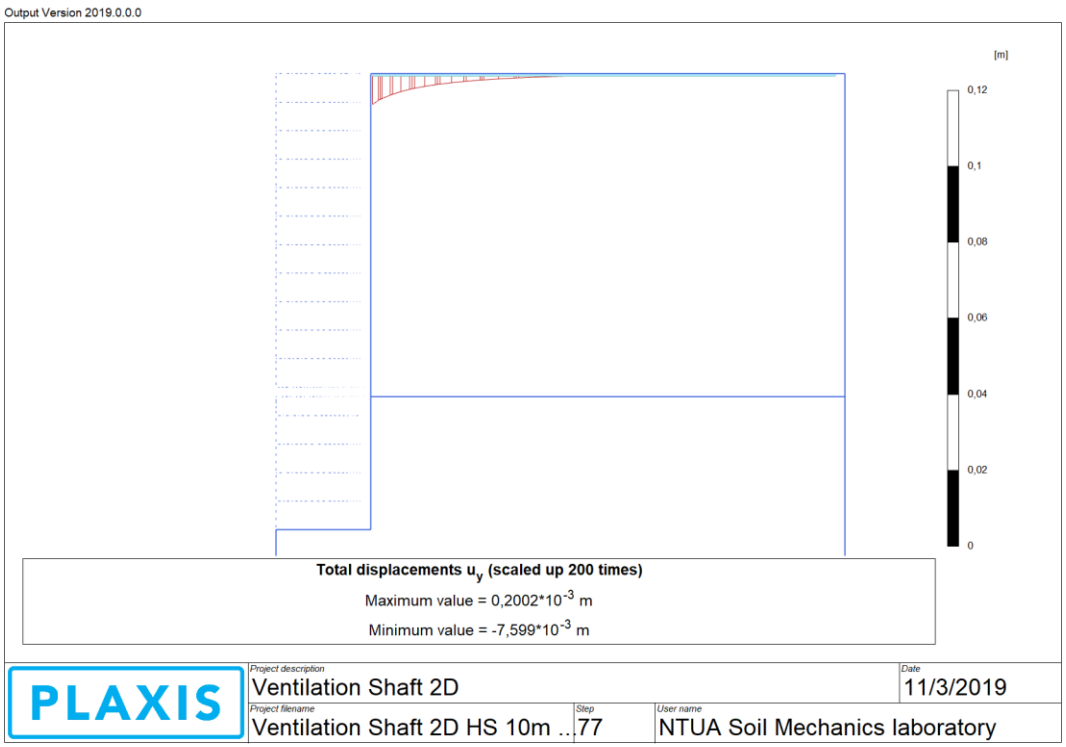

Figure.76 Settlements/Vertical Displacements (u_y) along the ground surface for a distance of 30 meters after the last construction phase.

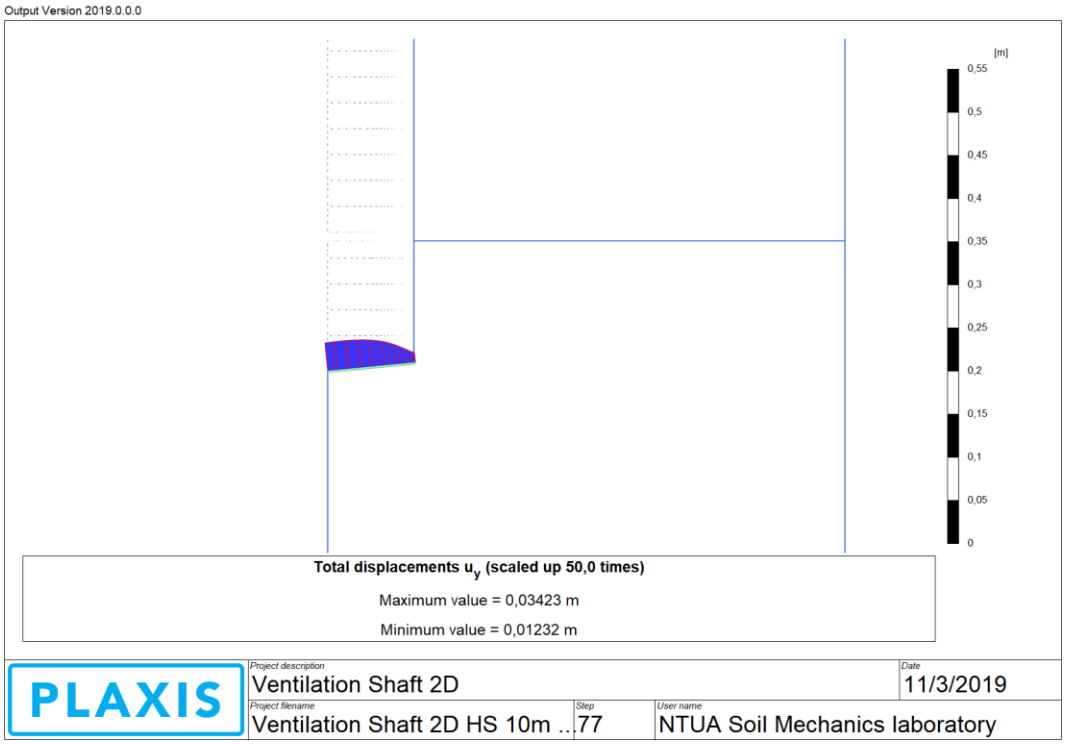

Figure.77 Uplift/ Vertical Displacements (u_y) at the shaft's excavation bottom starting from the axis of axisymmetry.

6.7 TWO-DIMENSIONAL ANALYSIS USING PHASE2 8.0

1. PROJECT SETTINGS

   Like in PLAXIS 2D a new project is created and the basic model parameters are defined. The analysis type is set axisymmetric meaning that the input is 2-dimensional, however the analysis results apply to the3-dimensional problem. The solver type, determining how to compute phase solves the matrix and represent the system of equations defined is the Gaussian Eliminator since the problem is not large and requires a modest amount of computational time.

2. BOUNDARIES

   The first step consists of creating the model once the model limits are set. The model is defined by drawing the boundaries. Closed polylines represent excavation. An excavation boundary defines the final stage of an excavation while intermediate boundaries within the geometrical model represent material boundaries (different material type). All boundaries are modeled by a series of straight line segments defined by x-y coordinates. In this multi stage model, intermediate boundaries within excavations

express different stages of excavation. Material boundaries and stage boundaries can be used interchangeably.

The various separate stages are progressively set up, allowing staged analysis of excavation.

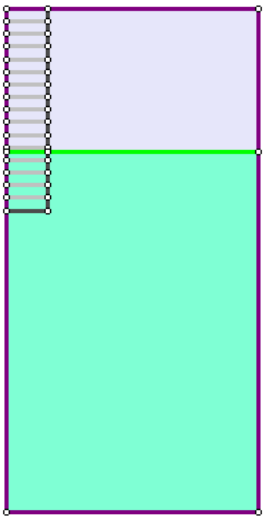

Figure.78 Model definition. Closed polylines represent the sequential excavation stages.

3. MESH

After defining all boundaries, the next step is to create the finite element mesh. First the boundaries must be discretized, subdividing the boundary line segments into discretizations forming the framework of the finite element mesh. The mesh type is set graded producing a good graded mesh using a quadtree nodal insertion technique. The Gradation Factor, set 0,1 by default implies that the average length of the external boundary discretizations is 10 times the average length of the excavation discretizations. The model is discretized indicating in the status bar the actual number of discretizations created.

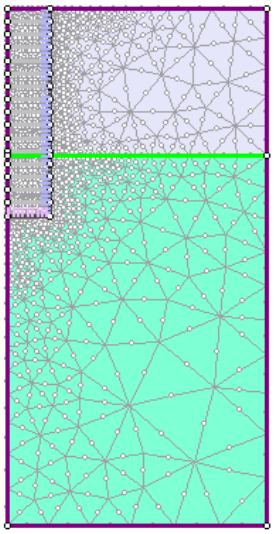

Figure.79 The finite element mesh is created. Boundaries are discretized.

4. DISPLACEMENTS

The problem setting continues by assigning conditions to the contour. Boundaries are set by default to a zero displacement boundary condition. It is common in geotechnical models to set the upper boundary free and the lateral ones, left and right, fixed in the x direction assigning vertical roller symbols. Restraining x, zero x-displacement boundary conditions are applied and the nodes are free to move in the y direction only. Subsequently, the lower edge is fixed in the y direction only, applying zero y-displacement boundary conditions. Nodes restrained are indicated by horizontal roller symbols. The nodes are free to move in the x direction only. The restrain xy option is used at the bottom two corners using a triangular pin symbol.

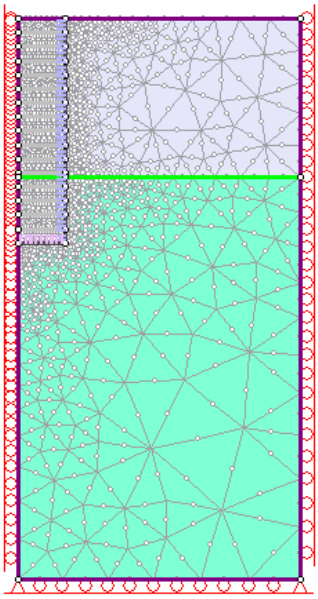

Figure.80 Boundary conditions are assigned to the contour.

5. FIELD STRESSES

The in-situ stress conditions prior to excavation are defined. The gravity field stress option is used to define a gravity stress field which varies linearly with depth as the excavation is near surface. It is assumed that the stress field is aligned with the analysis' section. If the material has initial stress and body force both defined, then the material is in equilibrium and there is no displacement of the top surface. A gravitational field stress with unit weight equal to the material's unit weight and a ground surface elevation equal to the top is used to have the body force and field stress balanced.

6. MATERIALS AND LINERS

Material properties are defined by customizing the soil layers. Anisotropic elastic model is used to define the soil elastic properties requiring Young's Modulus and Poisson's ratio. The failure criterion adopted is the Mohr-Coulomb. Even though an Elastic material does not "fail", the failure criterion allows a degree of overstress to be calculated.

Liners are used to simulate reinforcement, applied in a form of a liner to excavation boundaries. They are used to model the segmented concrete rings and the lean concrete applied at the bottom. Liners are comprised of beam elements corresponding to the edges of finite elements. The Timoshenko Beam formulation is selected which allows for transverse shear deformation effects. Finally, materials and liners are assigned.

6.8 OUTPUTS USING PHASE2 8.0

6.8.1 PHASE2 8.0, DEFORMATION ANALYSIS, MOHR-COULOMB MODEL

Figures 81 to 84 show the deformed mesh, the total displacements, the maximum horizontal and vertical displacements. Proceeding, Figures 85 to 89 show Axial forces, Shear forces, Bending moment, Hoop Axial force and Hoop Bending moment distribution, maximum and minimum values at the last stage.

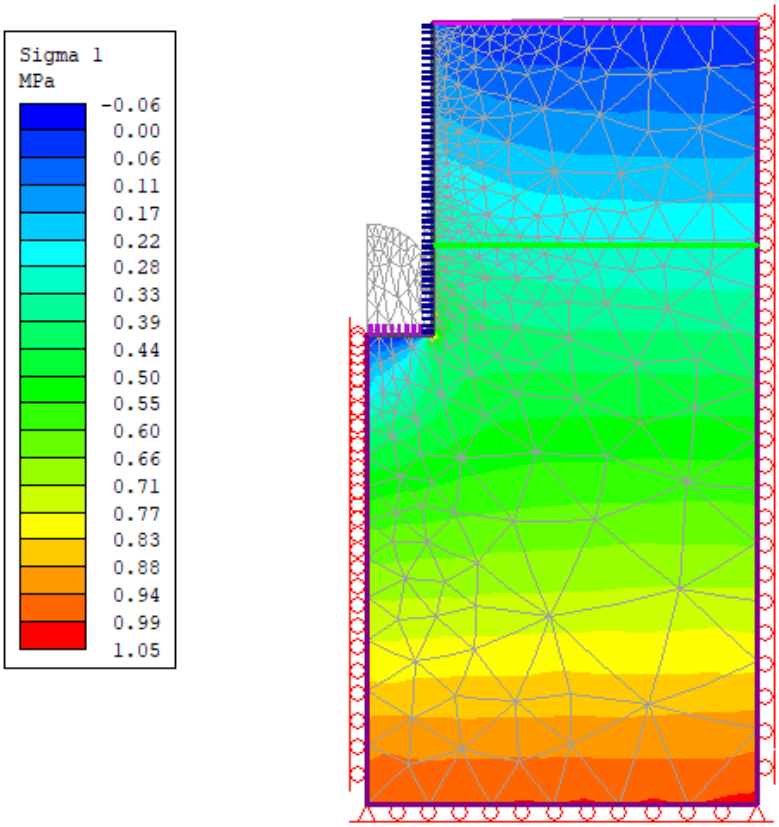

Figure.81 Deformed mesh at the last stage.

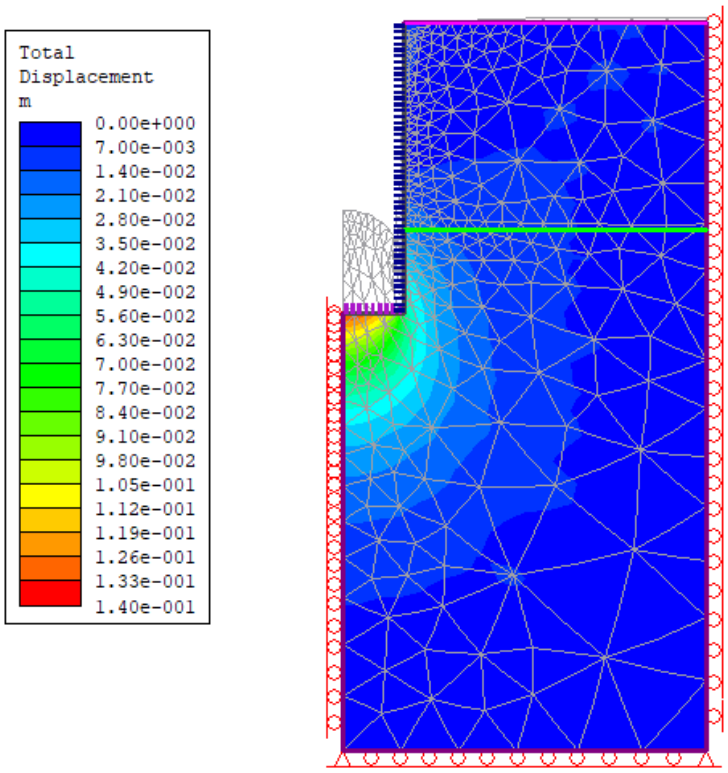

Figure.82 Total Displacements at the last stage.

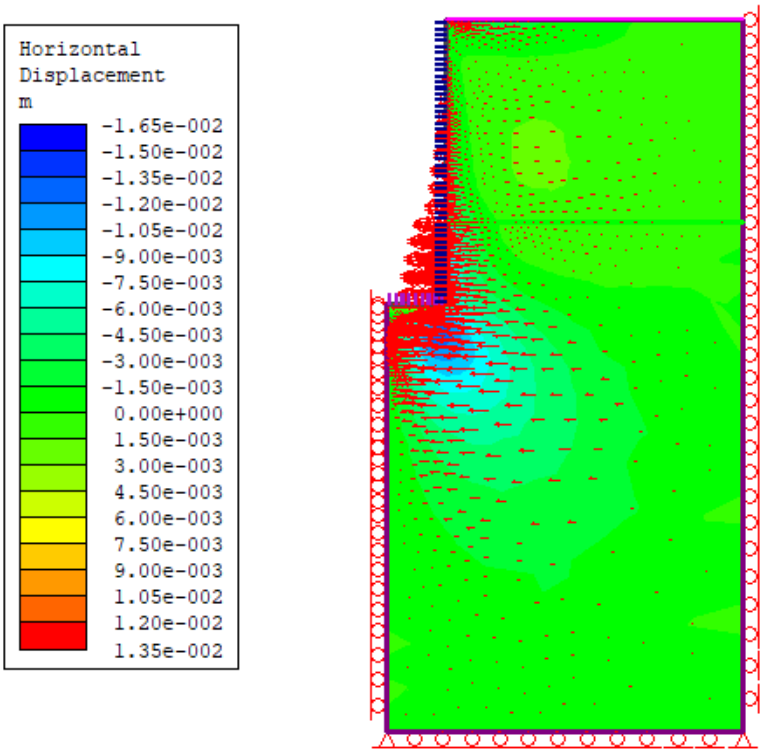

Figure.83 Maximum Horizontal Displacements (u_x) at the last stage.

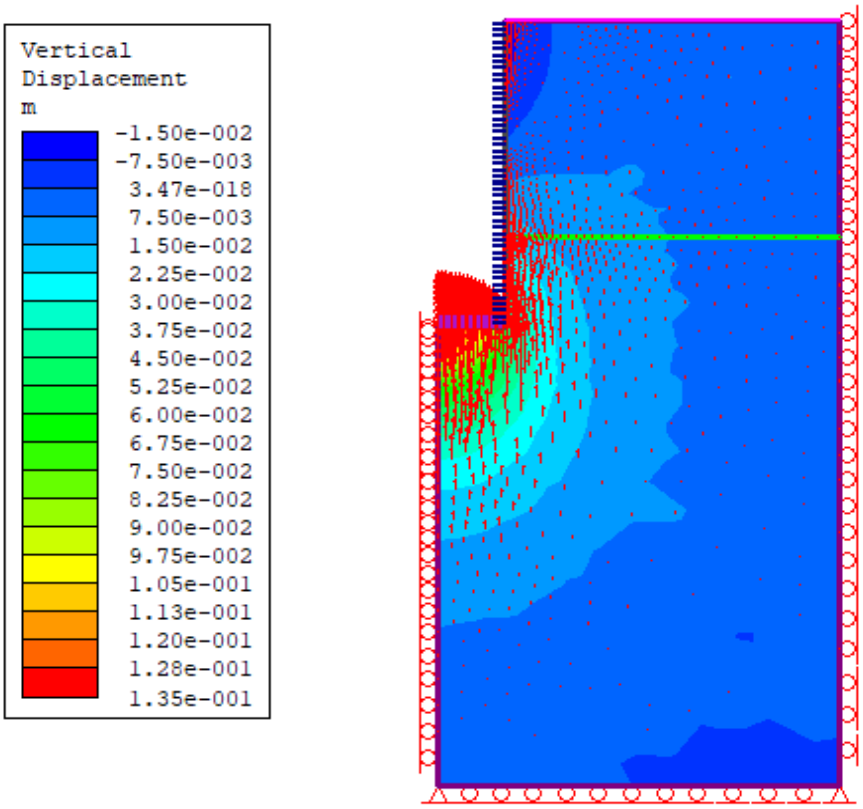

Figure.84 Maximum Vertical Displacements (u_y) at the last stage.

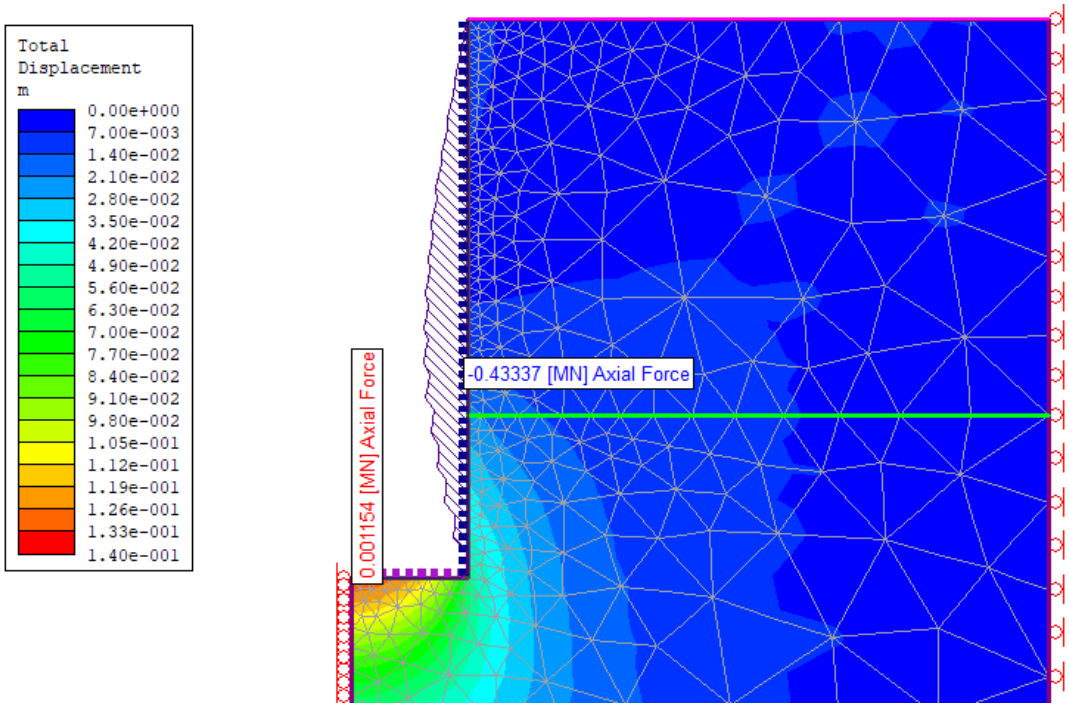

Figure.85 Axial Force (N) distribution, maximum and minimum values at the last stage.

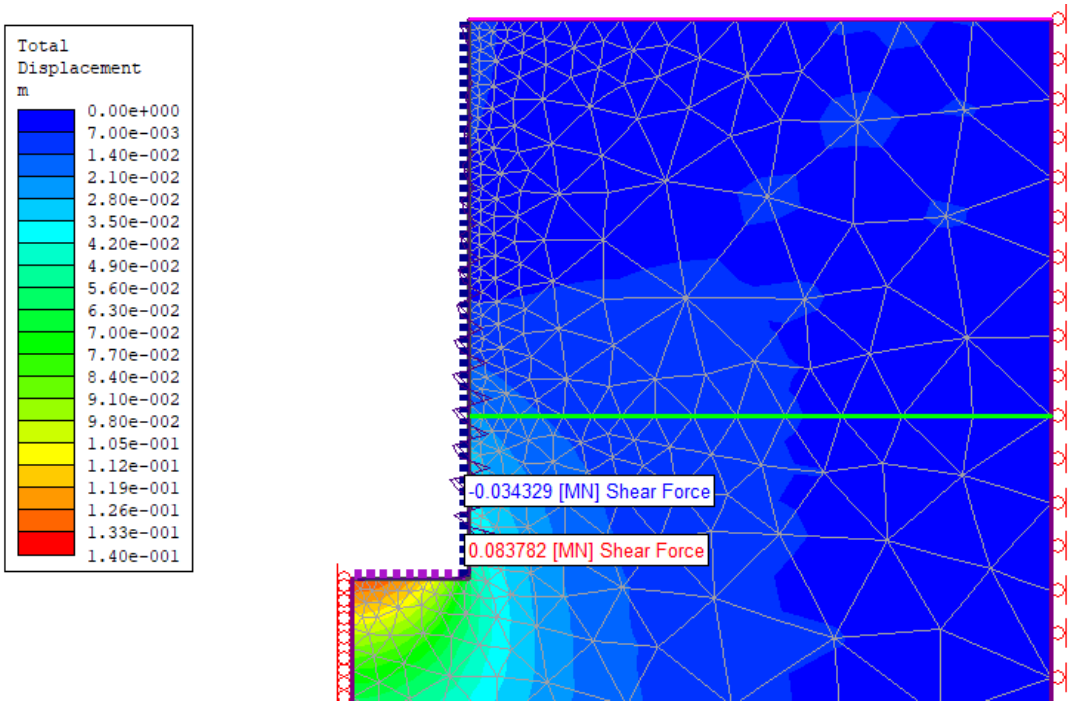

Figure.86 Shear Force (Q) distribution, maximum and minimum values at the last stage.

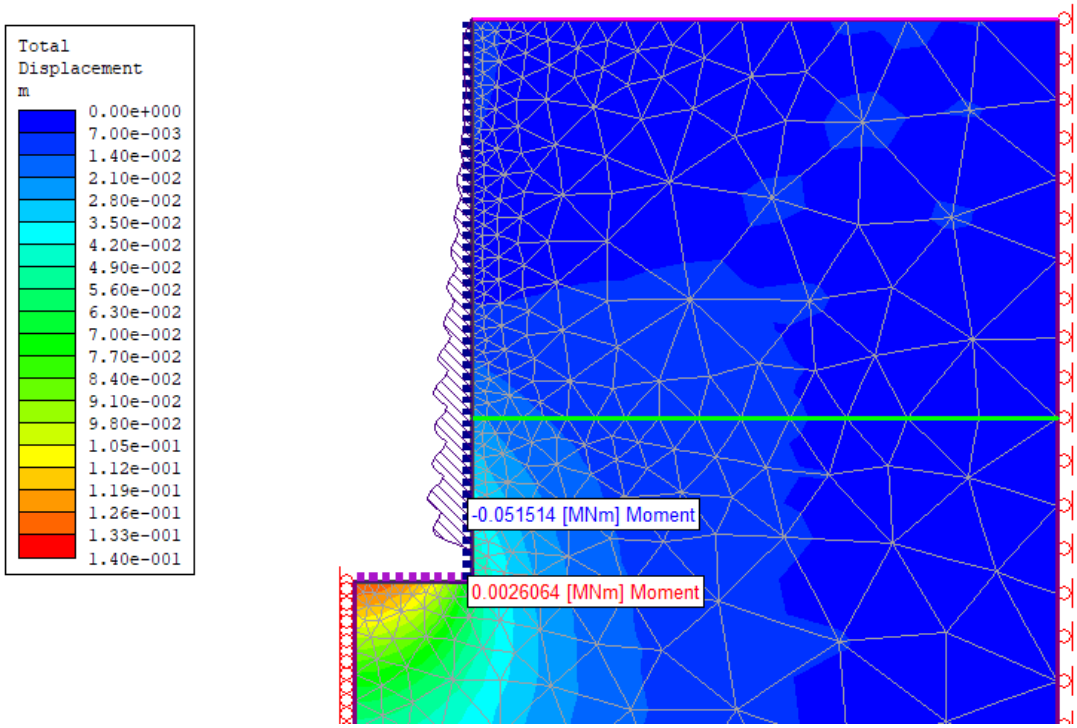

Figure.87 Bending Moment (M) distribution, maximum and minimum values at the last stage.

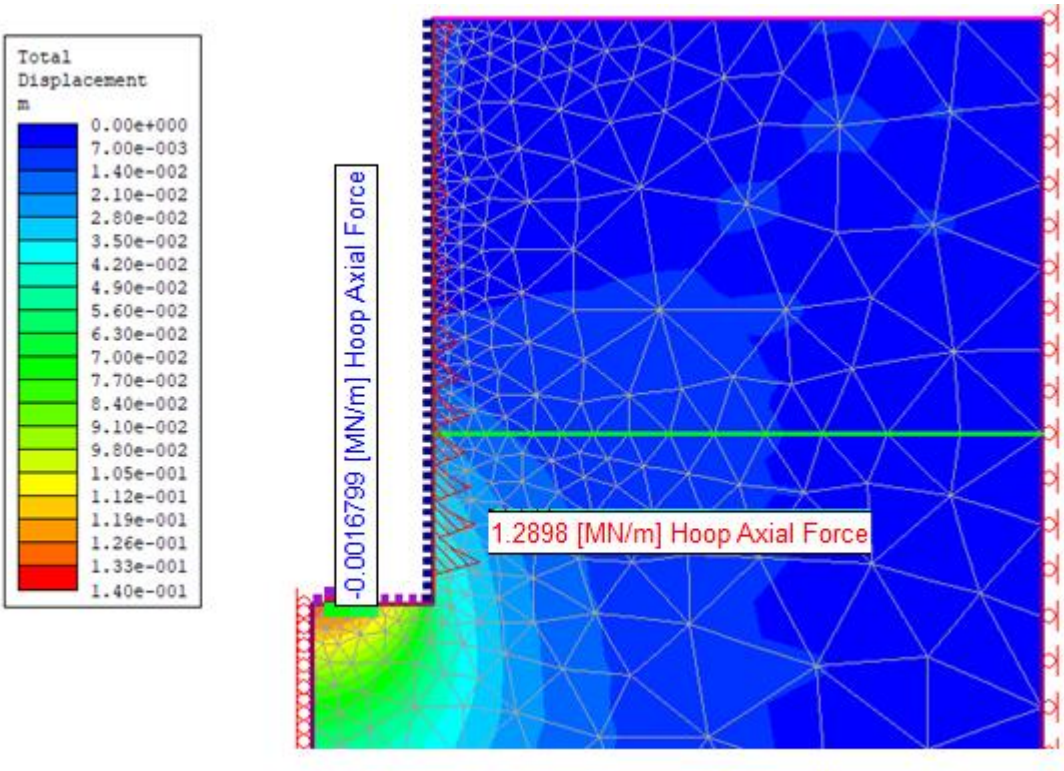

Figure.88 Hoop Axial Force distribution, maximum and minimum values at the last stage.

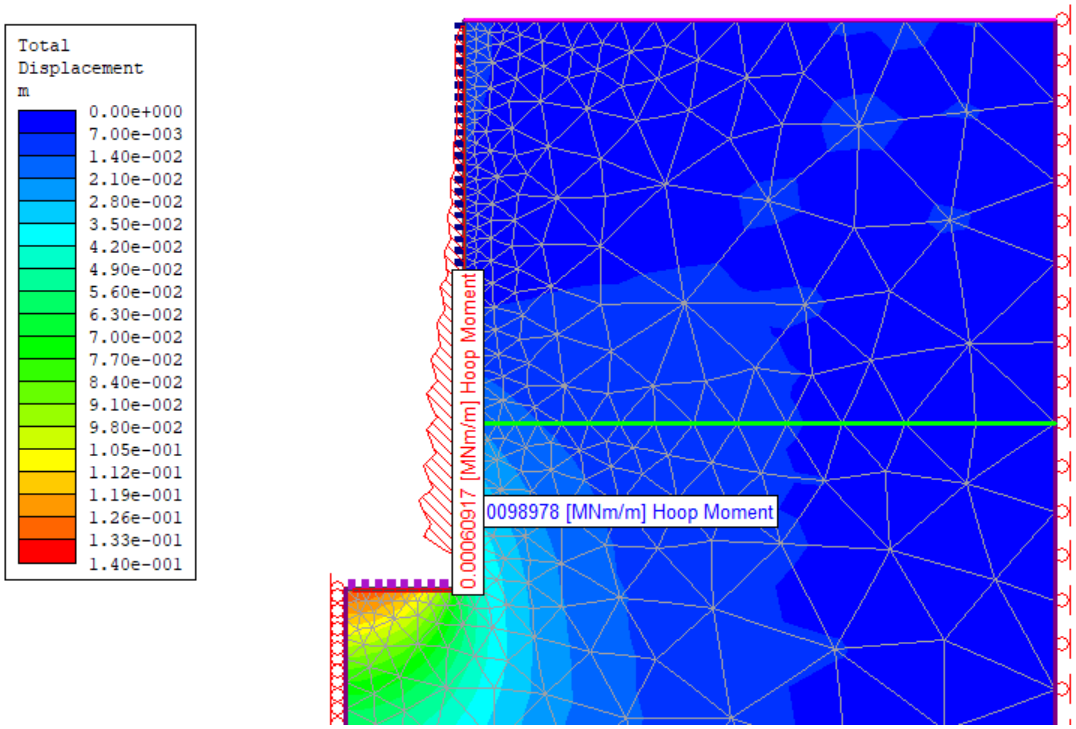

Figure.89 Hoop Bending Moment distribution, maximum and minimum values at the last stage.

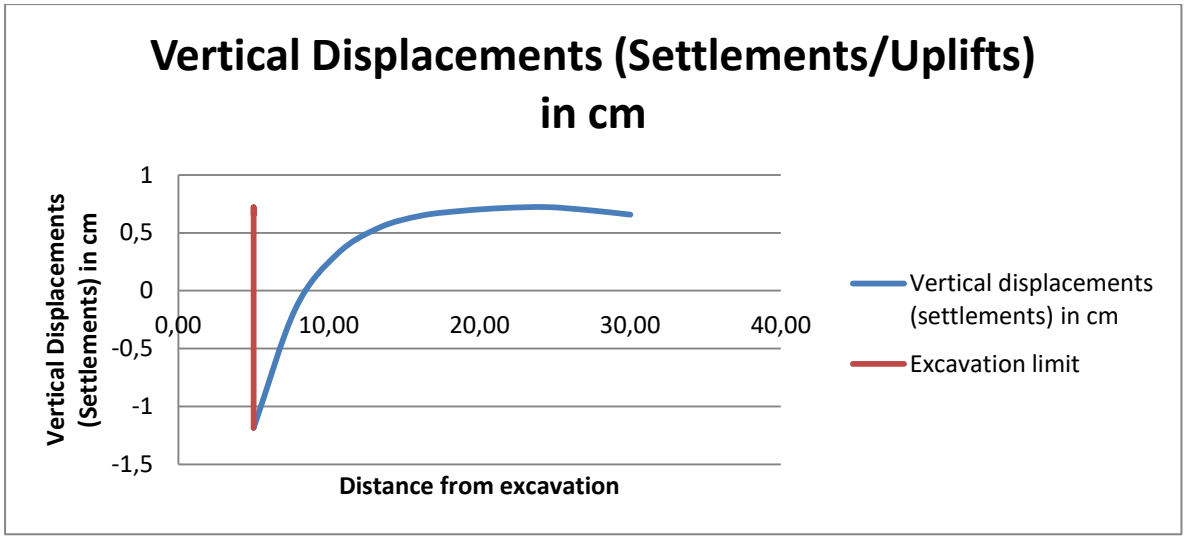

Figure.90 Settlements and Uplifts (Vertical Displacements) expressed in cm adjacent to the excavation at a distance of 30m , starting from the axis of symmetry.

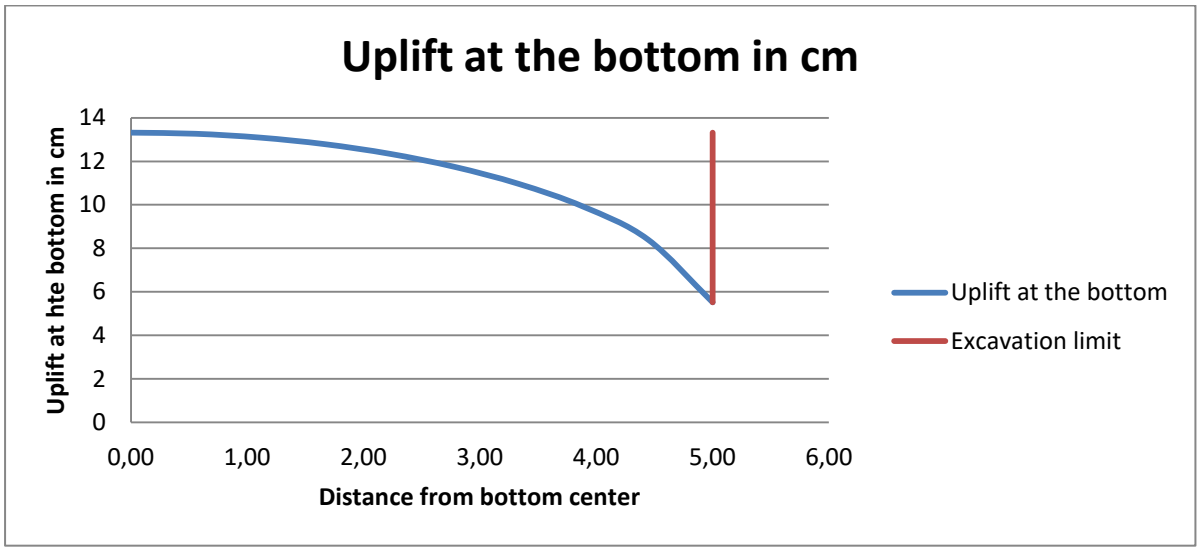

Figure.91 Uplift at the shaft's excavation bottom expressed in cm, starting from the axis of symmetry.

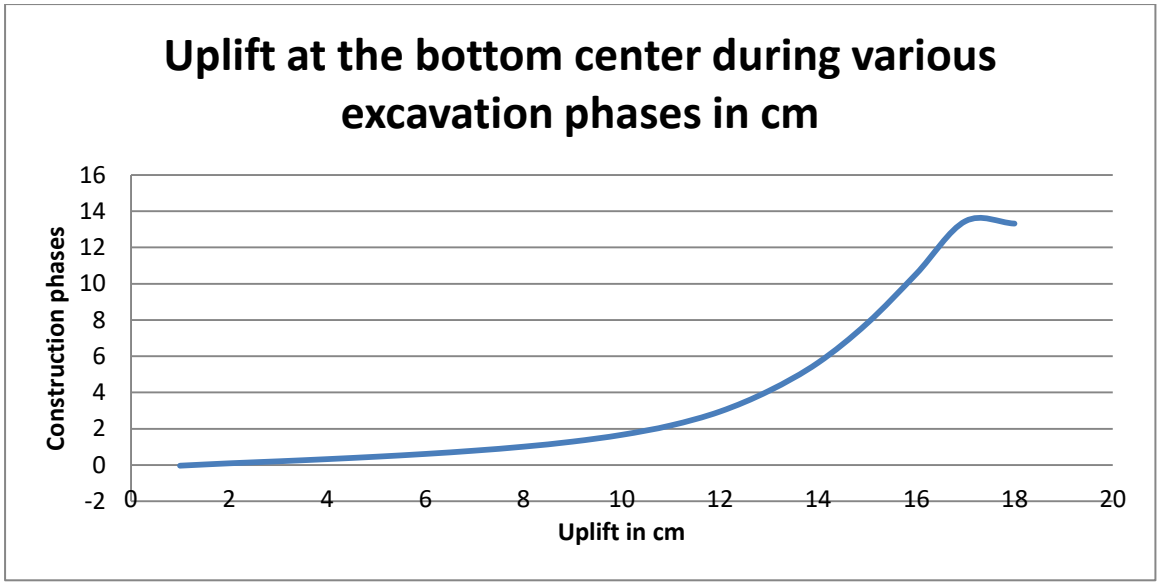

Figure.92 Progressive Uplift at the bottom center during various excavation and construction phases (sequential excavation) expressed in cm.

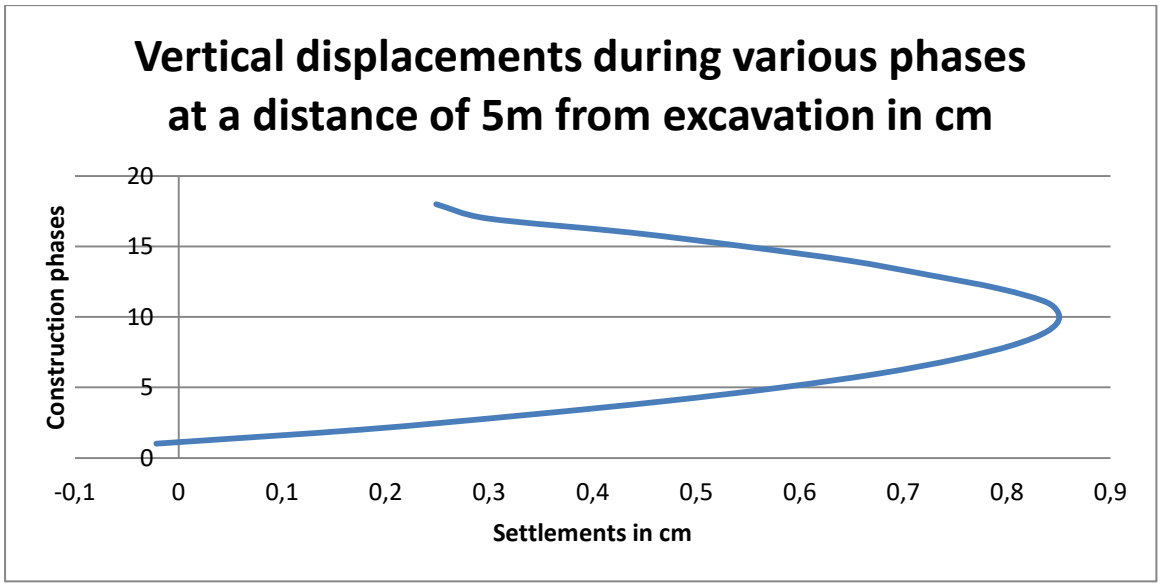

Figure.93 Vertical displacements (settlements) expressed in cm during various excavation/construction phases at a distance of 5 meters from the excavation border.

6.8.2 PHASE2 8.0, STRESS ANALYSIS, MOHR-COULOMB MODEL

Figures 94 to 97 show the deformed mesh, the total displacements, the maximum horizontal and vertical displacements. Proceeding, Figures 98 to 102 show Axial forces, Shear forces, Bending moment, Hoop Axial force and Hoop Bending moment distribution, maximum and minimum values at the last stage.

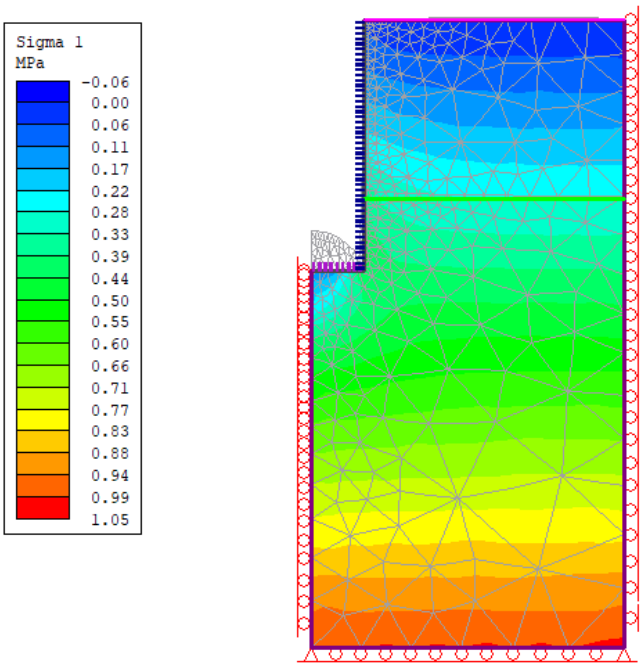

Figure.94 Deformed mesh at the last stage.

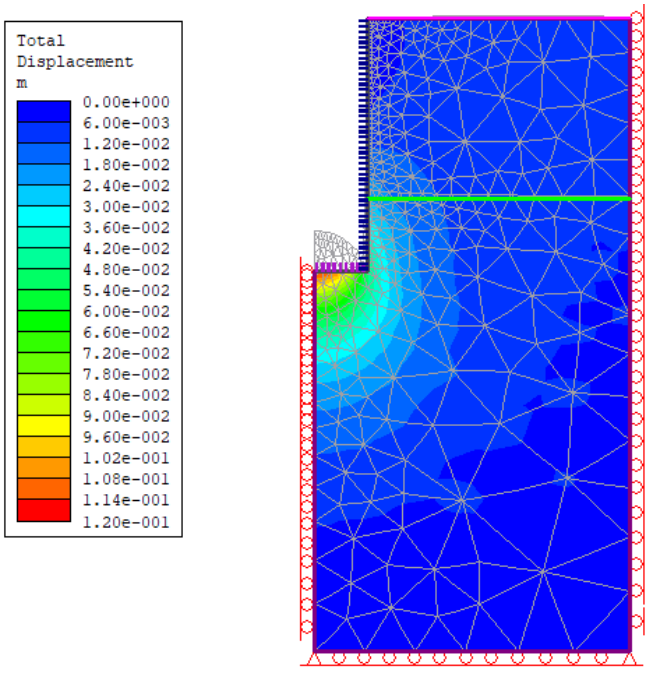

Figure.95 Total Displacements at the last stage.

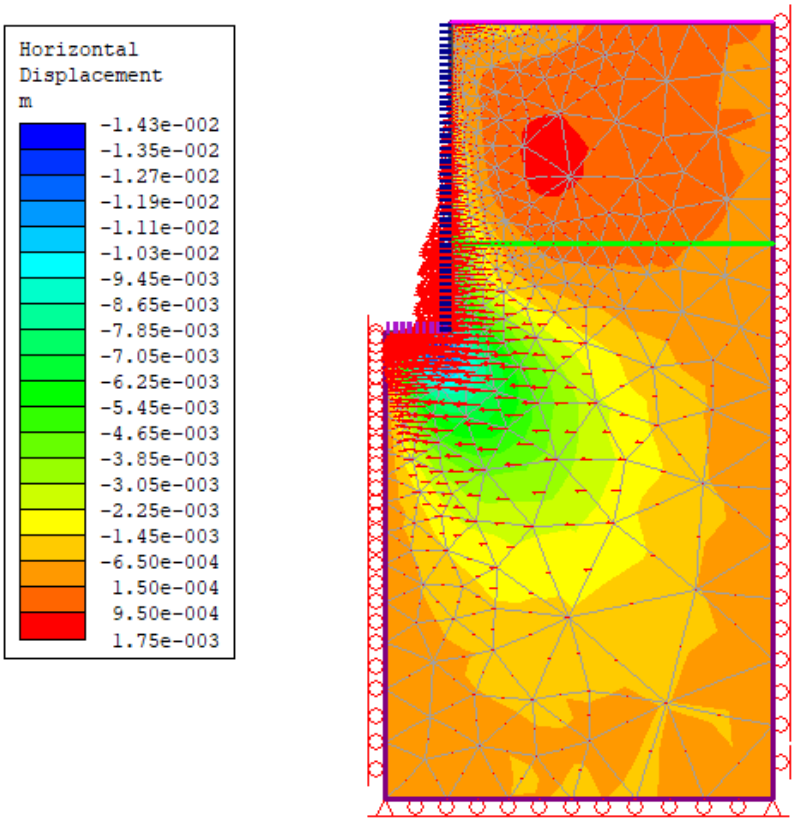

Figure.96 Maximum Horizontal Displacements (u_x) at the last stage.

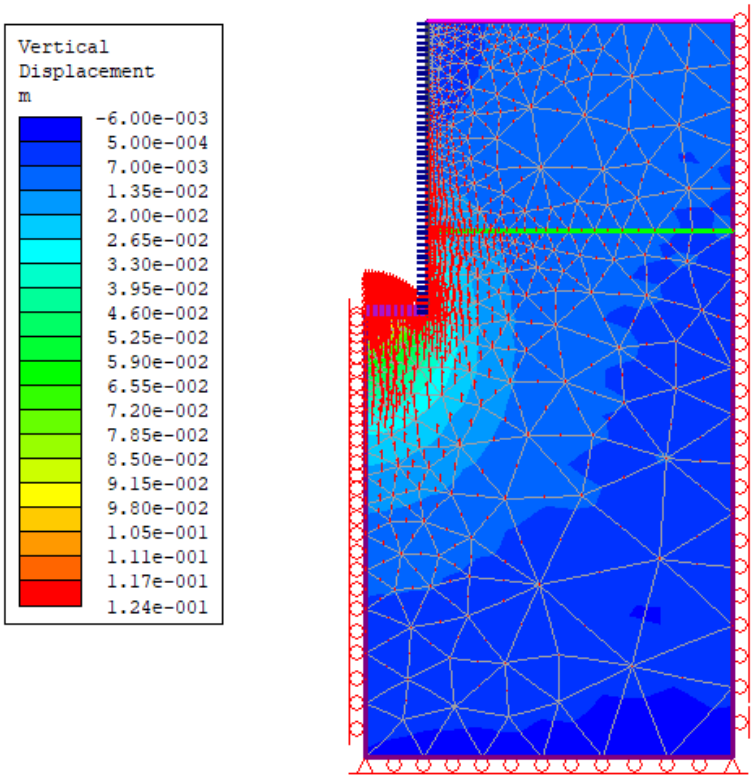

Figure.97 Maximum Vertical Displacements (u_y) at the last stage.

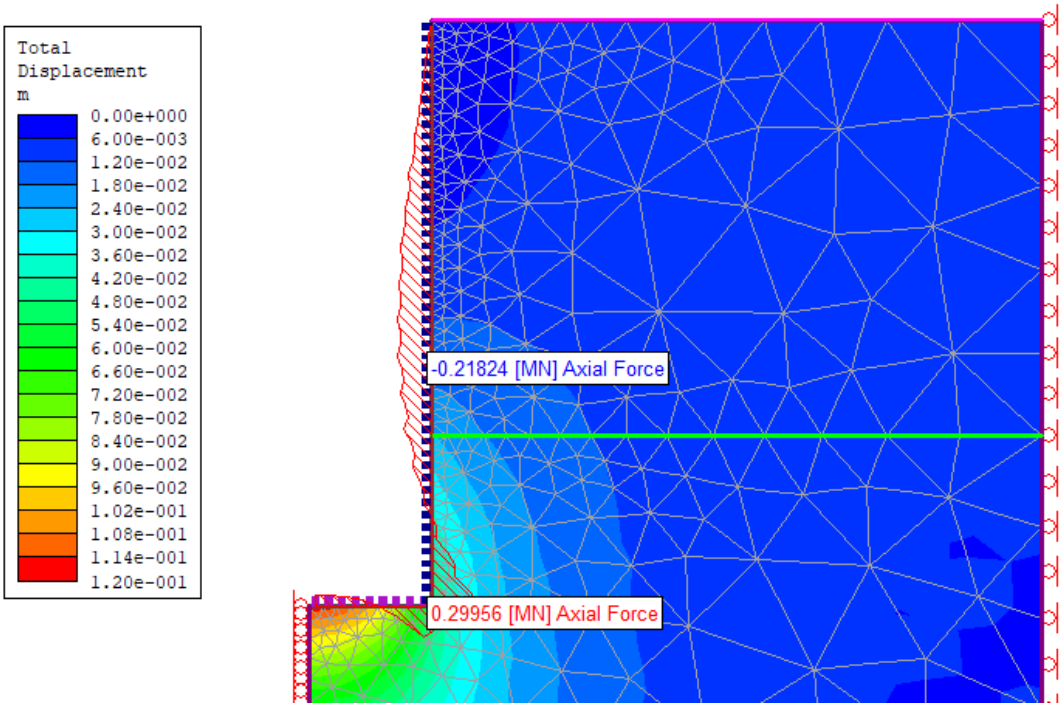

Figure.98 Axial Force (N) distribution, maximum and minimum values at the last stage.

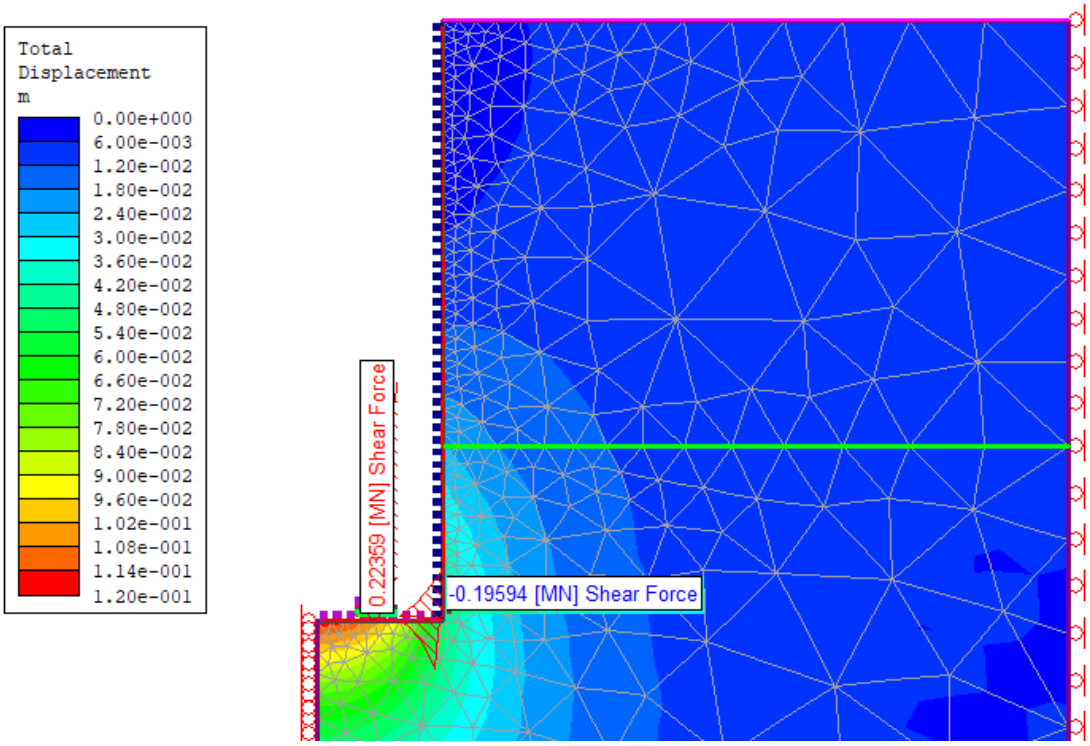

Figure.99 Shear Force (Q) distribution, maximum and minimum values at the last stage.

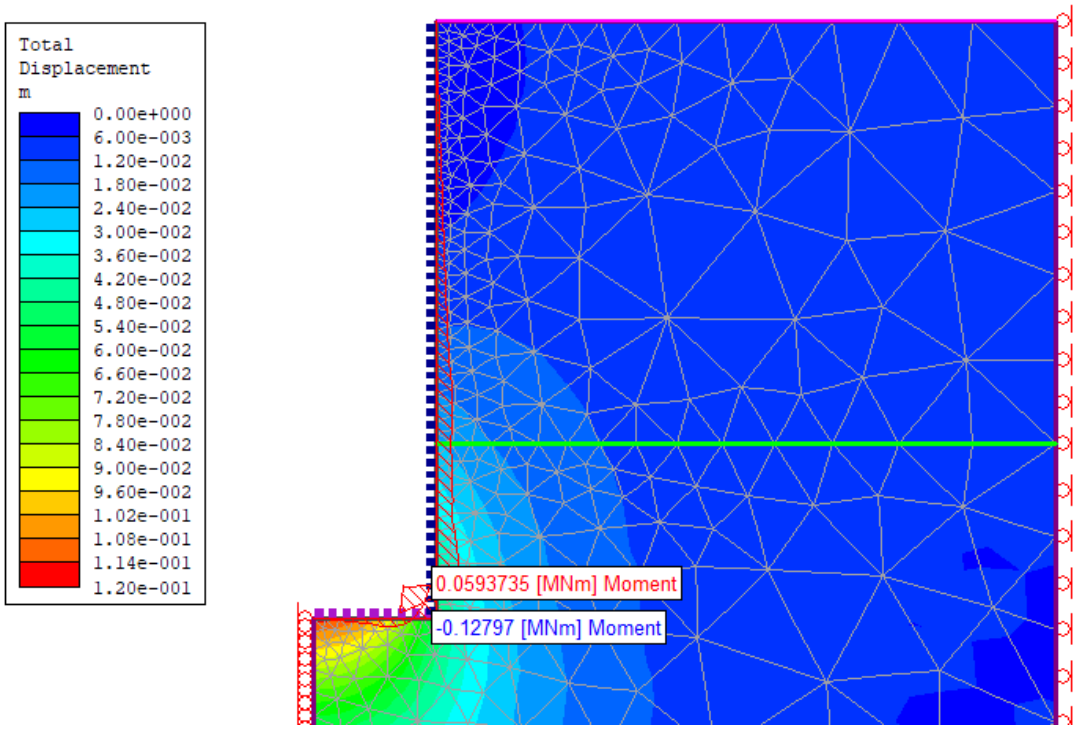

Figure.100 Bending Moment (M) distribution, maximum and minimum values at the last stage.

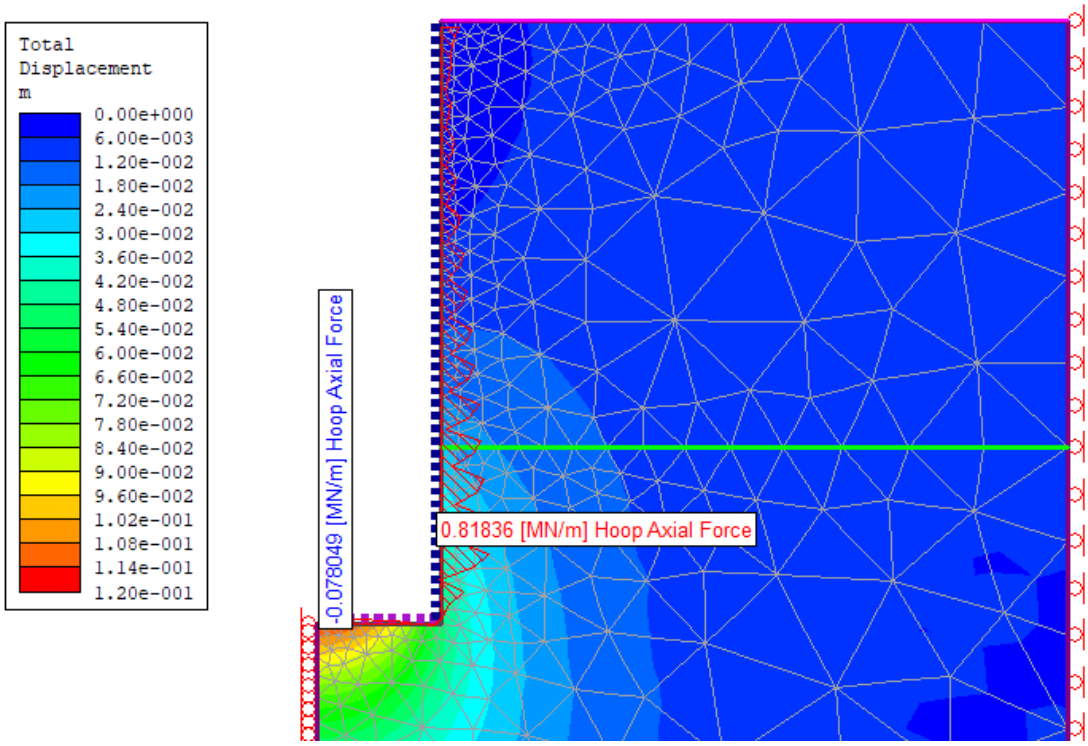

Figure.101 Hoop Axial Force distribution, maximum and minimum values at the last stage.

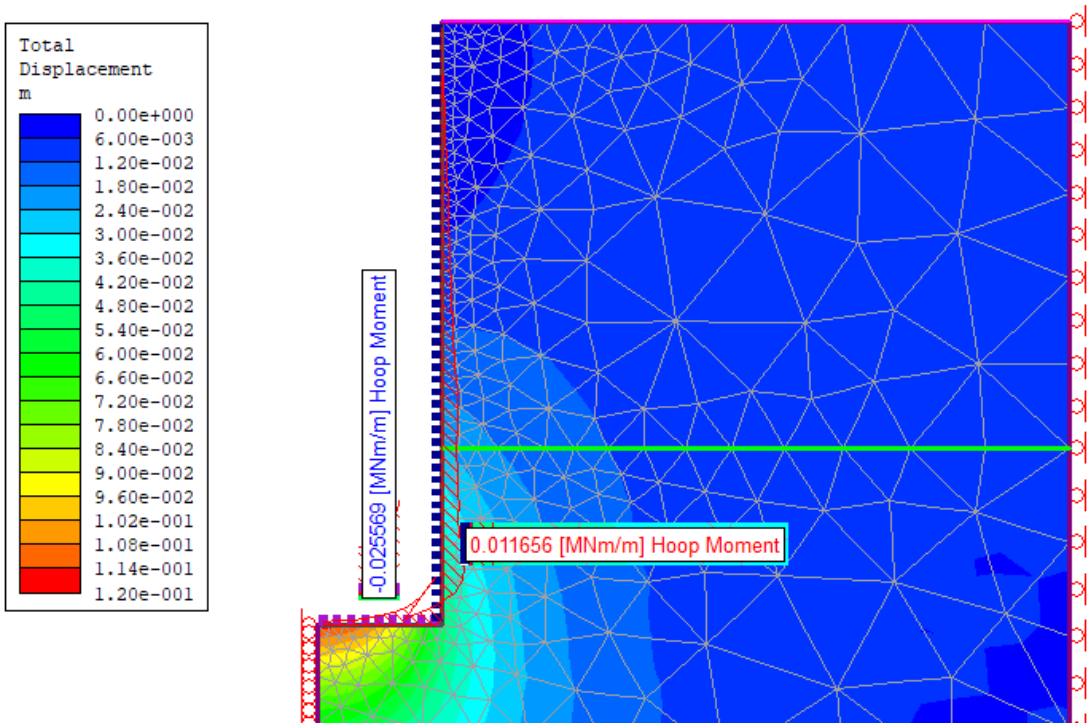

Figure.102 Hoop Bending Moment distribution, maximum and minimum values at the last stage.

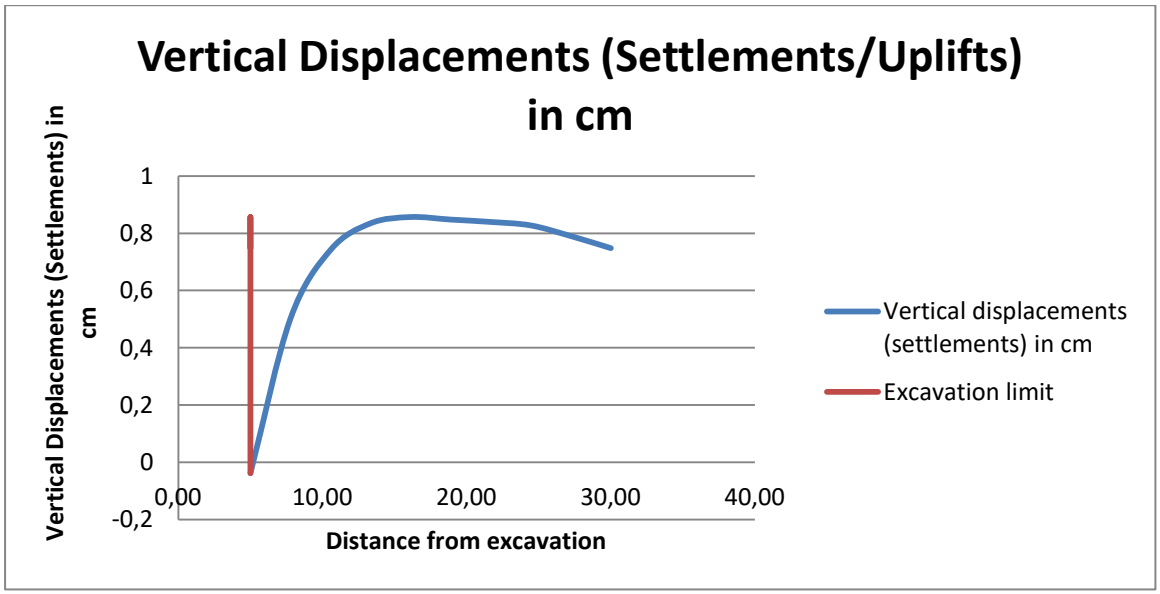

Figure.103 Settlements and Uplifts (Vertical Displacements) expressed in cm adjacent to the excavation at a distance of 30m.

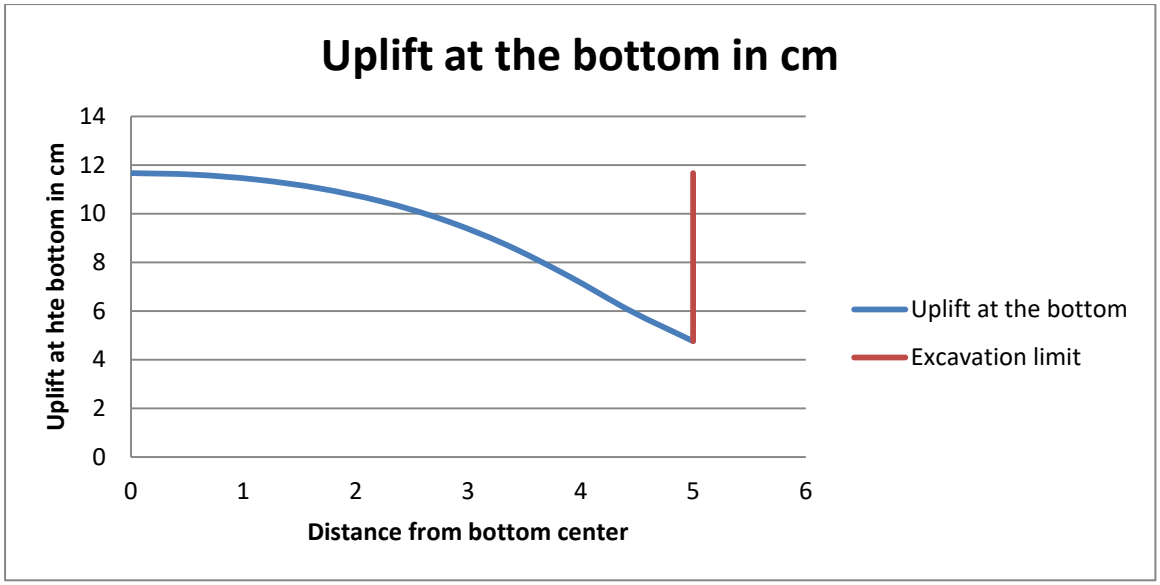

Figure.104 Uplift at the shaft's excavation bottom expressed in cm starting from bottom center.

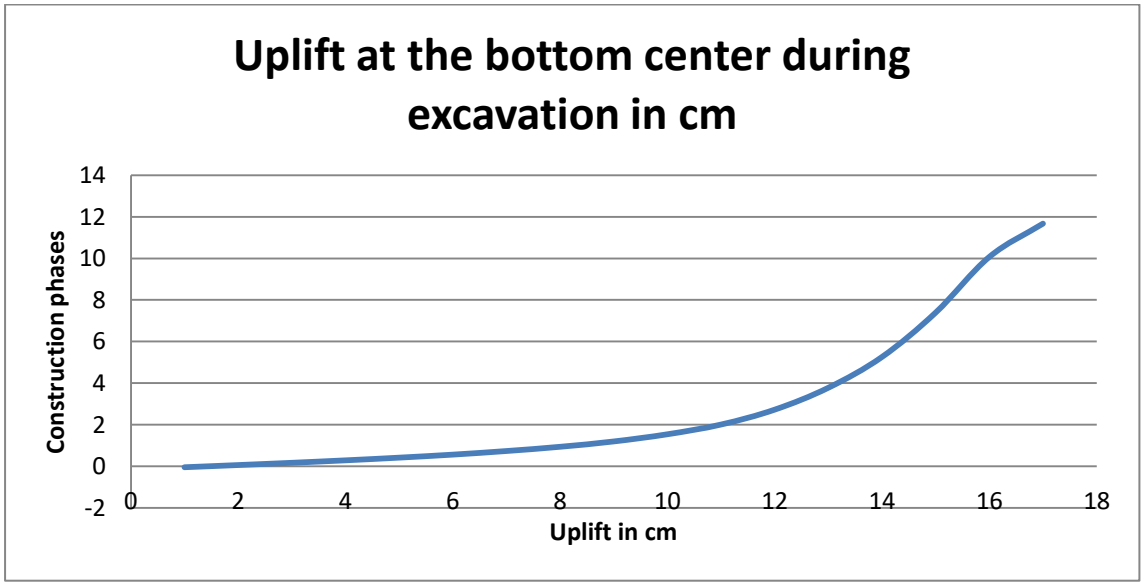

Figure.105 Progressive Uplift at the bottom center during various excavation and construction phases (sequential excavation) expressed in cm.

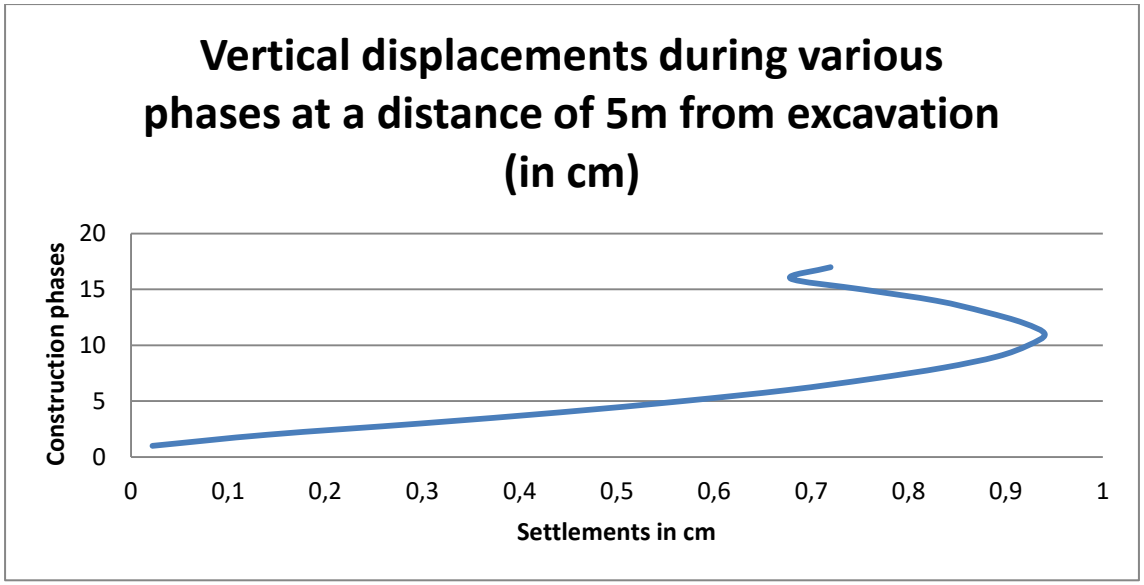

Figure.106 Vertical displacements (settlements) expressed in cm during various excavation/construction phases at a distance of 5 meters from the excavation border.

6.9 COMPARISON OF THE CALCULATION OUTPUTS

The following synoptic table, Table.7 verifies what is written above, implying that in general where the Hardening Soil constitutive model is employed, lower pick values are expected. Percentage variations are not exceeding 100%. The most significant variation occurs comparing the total vertical displacements (uy). Maximum values encountered where the H.S. model is selected are approximately 10 centimeters lower. This can be attributed to the double stiffness model for elasticity that this sophisticated constitutive model is using in combination with isotropic strain hardening.

	PLAXIS 2018 2D					
Maximum and Minimum Values	**M.C. Deform.**	**HS Deform.**	**Percentage Variation |%|**	**MC Stress**	**HS Stress**	**Percentage Variation |%|**
Deformed Mesh (m)	0,1410	0,0451	68%	0,1219	0,0383	69%
Settlements/Uplifts at ground level(m)	$-1,1*10^{-3}$	$-1,1*10^{-3}$	0%	$1,9*10^{-3}$	$0,2*10^{-3}$	89%
	-0,01037	-0,01	4%	$-6,9*10^{-3}$	$-7,6*10^{-3}$	10%
Total Vertical Displ. (u_y) in m	0,1410	0,045	68%	0,1219	0,0383	69%
	-0,0189	-0,01	47%	$-7*10^{-3}$	$-8,1*10^{-3}$	16%
Total Horizontal Displ. (u_x) in m	$1,6*10^{-3}$	$0,8*10^{-3}$	50%	$1,3*10^{-3}$	$1*10^{-3}$	23%
	-0,0588	-0,02	66%	-0,0121	$-3,6*10^{-3}$	70%
Axial Forces (N) KN/m	181,4	66,60	63%	321,1	277,8	13%
	0	-0,337	34%	-169,1	-150,2	11%
Shear Forces (Q) kN/m	18,32	18,93	3%	167,4	147,8	12%
	-40,23	-33,1	18%	-168,8	-147,5	13%
Bending Moments (M) kNm/m	33,01	25,38	23%	80,48	64,96	19%
	-1,5	-0,826	45%	-14,96	-14,72	2%
Hoop Axial Forces (Nz) kN/m	2,36	0,59	75%	-41,3	-82,03	99%
	-1494	-1257	16%	-1361	-1406	3%

Table.7 Comparison of PLAXIS 2D tabulated results.

Comparing the PLAXIS 2D and PHASE2 2-dimensional calculation results can be concluded that ground settlements running PHASE2 are more precautionary as pick values are 554% and 352% higher when respectively, the deformation and stress construction techniques are applied. Concerning the distribution and maximal values of Axial forces, Shear forces and Bending moments, as seen in Table 8 and Table 9 a general conclusion can be drawn. PHASE outputs are higher fluctuating from 56% (Bending moment max. value) to 139% (Axial force max. value) when the deformation construction mode is selected and from 7% (Axial force max value) to 293% (Bending moment min. value) when the stress is selected. On the contrary, Hoop Axial forces exerted on the cylindrical shaft, according to PLAXIS 2D are higher.

Maximum and Minimum Values	**PLAXIS 2D 2018 M.C. Deform.**	**PHASE2 8.0 MC Deform.**	**Percentage Variation |%|**
Deformed Mesh (m)	0,1410	0,1331	5%
Settlements/Uplifts at ground level(m)	$-1,1*10^{-3}$	0,0072	**554%**
	-0,01037		
Total Vertical Displ. (u_y) in m	0,1410	0,1331	5%
	-0,0189	-0,0118	38%
Total Horizontal Displ. (u_x) in m	$1,6*10^{-3}$	0,0059	**269%**
	-0,0588	-0,0152	74%
Axial Forces (N) KN/m	181,4	433,37	**139%**
	0	-1,15	115%
Shear Forces (Q) kN/m	18,32	34,29	87%
	-40,23	-83,78	**107%**
Bending Moments (M) kNm/m	33,01	51,51	56%
	-1,5	-2,6	73%
Hoop Axial Forces (Nz) kN/m	2,36	1,67	29%
	-1494	-1289	14%

Table.8 Comparison of PLAXIS 2D and PHASE2 8.0 tabulated results where the M.C. constitutive model and the deformation construction technique are applied.

Maximum and Minimum Values	**PLAXIS 2D 2018 MC Stress**	**PHASE2 8.0 MC Stress**	**Percentage Variation |%|**
Deformed Mesh (m)	0,1219	0,1166	4%
Bottom Uplift (m)	0,1087	0,116	7%
	0,0499		
Settlements/Uplifts at ground level(m)	$1,9*10^{-3}$	0,0086	**352%**
	$-6,9*10^{-3}$		
Total Vertical Displ. (u_y) in m	0,1219	0,116	5%
	$-7*10^{-3}$	-0,0014	80%
Total Horizontal Displ. (u_x) in m	$1,3*10^{-3}$	0,0011	15%
	-0,0121	-0,0136	13%
Axial Forces (N) KN/m	321,1	299,56	7%
	-169,1	-218,2	28%
Shear Forces (Q) kN/m	167,4	195,94	17%
	-168,8	223,59	33%
Bending Moments (M) kNm/m	80,48	127,97	59%
	-14,96	-59,37	**293%**
Hoop Axial Forces (Nz) kN/m	-41,3	78	90%
	-1361	818,36	39%

Table.9 Comparison of PLAXIS 2D and PHASE2 8.0 tabulated results where the M.C. constitutive model and the stress construction technique are applied.

6.10 SETTLEMENTS

One of the most serious issues confronting the civil engineer during design and construction of an underground project of a relatively limited depth or an open excavation is the effect of the ground movements (settlements) caused during the execution of the project on the existing buildings or other constructions. During the execution of the various excavations, changes in the stress state condition in the soil lead to the occurrence of soil volume losses and the manifestation of vertical and horizontal displacements. These earth movements have the effect of causing in the neighboring buildings and constructions movements, rotations and deformations, potentially leading to damages.

It is of high importance for the designer or the constructor that an estimation is made, as accurately as possible, of the upper territorial movements that may be caused during the construction of a subterranean project. Their possible consequences, on the functionality of the neighboring construction should be taken into account.

According to Anagnostopoulos and Mixalis (2004), settlement of a structure means its vertical movement. As stated based on a large number of observations, the damage caused to buildings is mainly due to the different magnitudes of settlements developed at different points of the foundation, rather than to a certain absolute value of the subsequent settlement. That means that, differential settlements are the ones that cause damages to buildings and constructions.

6.10.1 CRITERIA FOR ALLOWABLE SETTLEMENTS

The criteria for the permissible settlements of buildings, or of general engineering projects, mainly due to their own loads, arose from the correlation between the observed damage to a large number of different types of projects and the corresponding settlement measurements.

Terzaghi and Peck (1948,1967) observed in buildings laying in grained (granular) formations that most of them could safely take differential settlements between the columns, of about 20 mm. However, given that the differential precipitations do not normally exceed 75% of the total settlements, they have proposed as a rule for ordinary buildings on isolate footings, that the safe upper limit of total individual settlement is **25 mm**. For the special case of raft foundations, the above limit is 50 mm.

Skempton and MacDonald (1956) determined the safe limits of the angular rotation and associated them with the safe limits of the maximum individual and differential settlement of different types of building foundations. The following table (Table 10) shows the safe limits of settlements and angular rotations for buildings.

	Isolate Footings	Raft Foundations
Angular Rotation **Maximum Settlement** • Clay • **Sand** Maximum Differential Settlement • Clay • Sand	1/300 3 in (0,076 m) **2 in (0,051 m)** $1^{3/4}$ in $1^{1/4}$ in	1/300 3-5 in 2-3 in

Table.10 Settlements and angular rotation safety limits according to Skempton and MacDonald, 1956 (Anagnostopoulos and Mixalis, 2004).

It should be noted that the above limitations primarily ensure the safety of the building body and not the avoidance of micro-fractions in walls.

6.10.2 SETTLEMENTS EVALUATION

	PLAXIS 2018 2D				PHASE2 8.0	
Maximum and Minimum Values	M.C. Deform.	MC Stress	HS Deform.	HS Stress	MC Deform.	MC Stress
Settlements/Uplifts at ground level(m)	$-1{,}1*10^{-3}$	$1{,}9*10^{-3}$	$-1{,}1*10^{-3}$	$0{,}2*10^{-3}$	0,0072	0,0086
	-0,01037	$-6{,}9*10^{-3}$	-0,01	$-7{,}6*10^{-3}$		

Table.11 Synoptic table of the maximum and minimum values of Vertical Displacements (uy) calculated by the FE analyses.

As seen from the above table Table.11 the numerical maximum and minimum values of vertical displacements are reported from the analyses based on PLAXIS and PHASE. Positive vertical displacements correspond to uplifts, whereas negative values correspond to settlements. As far as settlements are concerned, the calculated values do not exceedsthe aforementioned safety limit.

6.11 ANALYSIS SUMMARY AND OUTPUTS EVALUATION

With a view to accessing the project and the construction technique used to carry it out, an effort is made to evaluate the results of the FE analyses.

I. As it is extensively stated and justified initially, the project is progressively carried out in several repetitive phases. It is evident from the results that regardless of the construction technique, i.e. the application of the segmented concrete rings is made immediately after the excavation of the phase-stage, or the segments are placed at the next stage of excavation, the construction comes to its end and it is implemented as originally studied.

II. As far as the settlements on the ground surface are concerned, the maximum values are observed in the proximity of the excavation as expected. This is apparent from the characteristic curve in Fig. 66 and Fig. 68, corresponding to the cases where the Mohr Coulomb constitutive model is adopted. As the above images indicate, the construction technique followed, affects the direction of the vertical displacements. Distinctively, in the case the Deformation technique is applied, settlements are observed on the surface only, even if the values are not excessive, assuming a maximum value of 0,01 meter. In the case the stress construction technique limits, ground lateral (vertical) deconfinement since a precast concrete ring is placed immediately after the excavation. Consequently, the area affected by settlements is limited in a range of 4 meters from the excavation boundary, a very restrained uplift is observed i.e. vertical displacements receive positive values (maximum value 0,0067 meters).

III. Regarding the overall maximum displacements, they are observed at the bottom of the excavation where a thin 15 cm layer of concrete is utilized, as shown in Fig. 67 and Fig. 69. Where the Mohr Coulomb constitutive model is applied and the deformation construction technique is adopted, the maximum value of the uplift u_{ymax}=0,1410m is more substantial than the case of stress construction technique u_{ymax}=0,1219m.

IV. Observing Fig. 65 where vertical displacements expressed in meters during the excavation and construction procedure are reported, it can be concluded that, if the deformation construction technique is applied, initially during the first excavation phases uplifts of restricted entity are documented. As the project proceeds, the soil behaves differently, and uplifts are turned to settlements as a result of the tension deconfinement. Secondly, as the distance from the excavation limit is growing, the vertical displacements (settlements) diminish, not according a linear distribution. Meaning that, over a distance of 30 meters from the excavation, settlements can be considered negligible and the phenomenon is concluded.

V. Relying on Figures 29 and 38, it can be observed that, the shaft's cylindrical concrete rings are subjected to horizontal ground displacements mainly at the second half of the structure, where it is interacting with the sandy silt earth formation. Depending on the construction technique the entity varies. Characteristically, where the stress construction technique is employed, the maximum value reaches u_x=-0,01219, approximately 5 times less than the deformation construction procedure. All in all, horizontal displacements occurre and are restricted in the stress construction technique. What is written above is confirmed when the Hardening Soil model is applied (Figures 47 and 56). Maximum horizontal displacement values assume lower picks due to the high stiffness on unloading introduced by the constitutive model.

VI. Regarding structural stability of the shaft, Axial Forces (N), Shear Forces (Q), Bending Moments (M) and Hoop Forces (Nz) are studied. Excepting Hoop forces (Nz), developed when the stress construction technique is operated, all values when the Hardening Soil constitutive model is adopted are lower by 15% to 25% on average. This can be attributed to the adopted modulus of elasticity "E" values. Generally, all resulting forces and bending moment values are lower in the deformation construction mode by up to 300% in terms of maximum absolute values and distribution. Furthermore, forces and moments distributions vary on the structure according to the construction technique, meaning that forces and bending moments are exerted differently changing the vulnerability areas of the structure. In particular when the stress method is operated, there is a concentration of axial forces on the bottom layer. Shear forces are concentrated at the bottom having a symmetrical distribution along the last meters of the shaft and lengthwise are to be neglected, as bending moments. It can be concluded that, a concrete layer at the bottom resistant enough to oppose the aforementioned forces and bending moment when the stress construction technique is adopted is required.

VII. Useful conclusions can be drawn with regards to the plastic points graphical representation. Plastic points show the stress points that are in a plastic state, displayed in a plot of the undeformed geometry. Notably, red failure points indicate that the stresses lie on the surface of the failure envelop. Fig. 31 testifies that, if the deformation construction technique is applied a distribution of plastic points is concentrated, once the whole project is completed, over the first half of the vertical concrete support, approximately the first 10 meters of depth. A concentration of plastic points is as well, displayed at the bottom, in the proximity of the vertical support. A probable failure could be demonstrated, due to tensile stresses, in correspondence to those areas. On the contrary, as depicted in Fig. 40, if the stress construction technique is employed, at the end of the construction plastic points are concentrated mainly at the bottom at a depth that exceeds 5 meters and in the proximity of the second half of the earth retaining structure. An imminent failure could be experienced in the vicinity.

VIII. Where the Hardening Soil model is used as the analysis model, both the distribution and the absolute values of the vertical deformations are of limited entity. Distinctively, where the Mohr Coulomb constitutive model is assumed, the maximum lift up is u_{ymax} =0,1410 meters, while where the Hardening Soil is used, the corresponding observed value is u_{ymax}=0,045 meters, namely, 3 times lower. As can be seen from Fig. 66 and Fig. 73 the maximum settlement value is the same, changing only the constitutive model. Assuming the H.S. model during the reload a higher elastic modulus (E) is considered and thus displacements are reduced. Soil Young's modulus, commonly referred to as soil elastic modulus, is an elastic soil parameter and a measure of soil stiffness. The elastic modulus is often used for estimation of soil settlements and elastic deformation analysis.

IX. When the Hardening Soil model is used, Hardening Points might occur. A Hardening Point occurs when a stress state in a point corresponds to the maximum mobilized friction angle that has been previously reached. Assuming that a critical area is where Hardening Points are concentrated, if the deformation construction process is employed, Hardening points create an internal plastic surface (Fig. 49) starting from the lowest point of the vertical support wall meaning that, in that area the maximum resistance offered by the soil (sandy silt) is reached or about to be reached. Diversely if the stress construction procedure is applied, there is a dense concentration of Hardening Points in correspondence to the surface bottom (Fig. 58), where the fine concrete layer is applied contrasting the uplifts.

X. Relaying on the PHASE 2 analyses output, as shown in particular in Fig. 91 and Fig. 104 what is written above can be verified. That means that the most critical phases in the construction process are the penultimate and the last one, where the major bottom uplifts are documented. During the early 12 excavation and project realization stages, uplifts are restrained.

CHAPTER VII
3DIMENSIONALAL ANALYSES USING PLAXIS 3D 2018

7.1 INTRODUCTION

The main scope of the analysis is to simulate the staged excavation procedure and the vertical shaft sequential construction, under 3tridimensional conditions. The analysis is conducted in the presence of groundwater. The various assumptions, model settings and computational results are reported in detail.

7.2 ASSUMPTIONS

- ✓ **Water Flow**
  Water pressures are generated in the soil layers. The main assumption made is the condition of steady flow, that is, the speed of the water flow at any point in the soil does not change with time. The permanent flow state is quite common in nature. If the boundary conditions remain unchanged over a period of time, the water flow in the soil will gradually approach continuous flow conditions.
- ✓ **Full model**
  In the presence of water flow, the axisymmetrical simulation model cannot be used.
- ✓ **Hardening soil Model**
  Geotechnical applications require advanced constitutive models for the simulation of the non-linear behavior of soils. Since soil is a multiphase material, special procedures are required to deal with pore pressures and partial saturation in the soil. Given the interaction between the structure and the surrounding soil, the Hardening Soil constitutive model is adopted.
- ✓ **Water flow at ground level**
  The above assumption is made mainly for simplicity even if it is not the case to find the water table perfectly coincidental with the ground level. In reality it is expected to be at around -2 meters.
- ✓ **kx=ky=kz**
  Coefficients of permeability/hydraulic conductivity have the dimensions of velocity. In such calculations, it is necessary to specify the coefficient of permeability for all drained and/or undrained clusters.
- ✓ **Number of steps**
  Exactly as in the two-dimensional models, the hypothesis of the depth of the excavation step is based on the dimension of the segmented concrete rings i.e. 1,5 meters of height.

- ✓ **Area extension xmin=0, xmax=60, ymin=0, ymax=60 and zmin=0, zmax=60.**
  The above geometrical limitations of the model in terms of width, length and depth respectively are adopted so that the model outputs and deviations influenced by the extension of the model are of minor importance and the effect on the results is slight. A large number of finite elements simulating the soil materials could result in computational inefficiency and in an excessive calculation time.

7.3 ANALYSES OVERVIEW

The 3dimensional analyses performed are briefly presented. To clarify that the calculation steps depending on the analysis type, deformation or stress, are identical as in the bidimensional analyses. Basically, the construction technique and procedure remain invariable, while varying the water flow conditions are varied. As written above dissimilarities are expected in the calculation outcomes', thus the following finite element representations are set up.

No	Water Flow	Analysis Type	Notes
1	YES	Deformation	
2	YES	Stress	
3	YES	Deformation/Stress	Cohesion of first soil layer is implemented.
4	YES	Stress	Dewatering is performed (wells are installed).
5	NO	Stress	

Table.12 Three-dimensional models set up and run as part of the analysis.

The last analysis (analysis no5) is conducted in the absence of water flow, to compare the output results with the ones in the presence of water (analysis no1 and analysis no2). The third analysis is run to evaluate the adaptability of the sequential excavation technique in the presence of water in a soil layer with a more significant cohesion (c=15 kN/m^2). The penultimate model involves the use of dewatering techniques, in particular a group of wells, aiming at lowering the water table, while evaluating the sustainability of the method.

7.4 MODEL SETTINGS

1. PROJECT PROPERTIES

   New project is created defining the basic model parameters. A Full Model is used to simulate the two-layer soil and the shaft in the inside as it is a 3dimensional geotechnical model. 10 node tetrahedral elements are used, being the basic soil elements of the 3D finite element mesh. The default units as suggested by the program are used.

2. SOIL PROPERTIES AND WATER LEVEL

   Once the model parameters are set, soil stratigraphy, soil layer properties and the most critical parameter of the analysis, the water level, are defined through the borehole option.

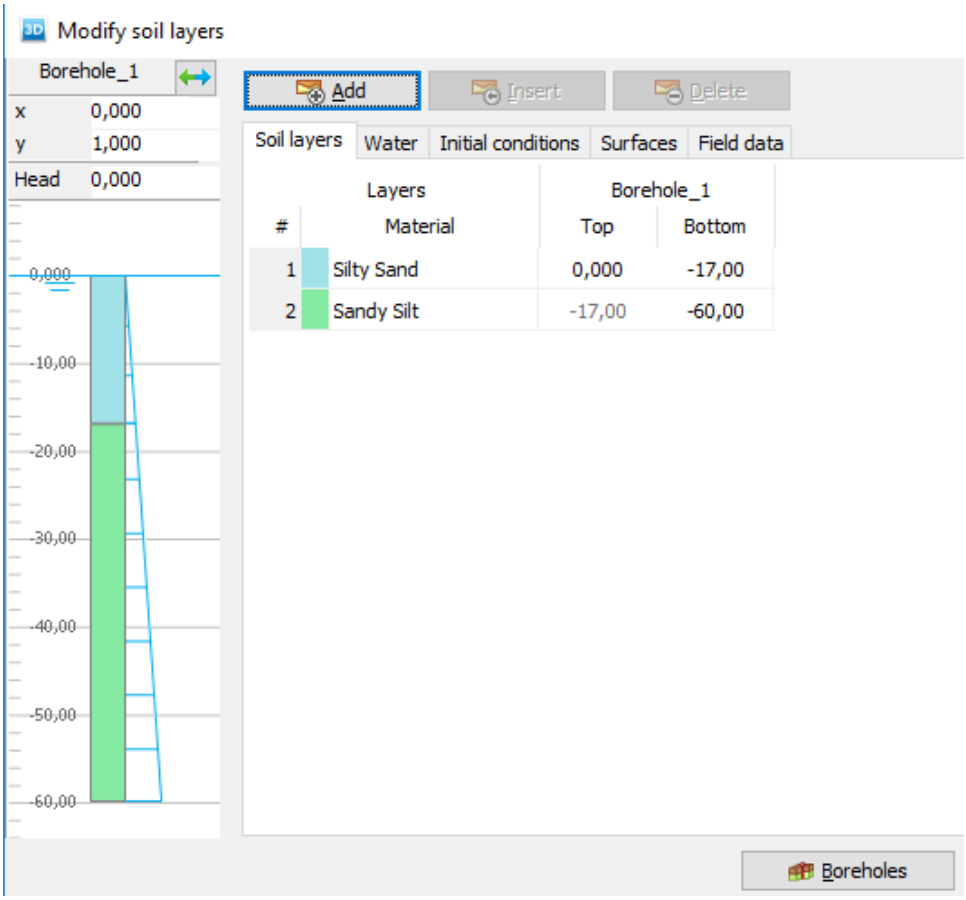

Figure.107 Soil stratification, properties and water level settings.

As far as the water level is concerned, according to the PLAXIS manual, can either be generated according to the information specified in boreholes or can be generated in the flow conditions mode. A water level can be used to

generate external water pressure and to generate pore pressures in soil layers. In the latter case, the water level can act as a phreatic level in partially saturated soil layers as well as pressure head level in aquifer layers. In this case, the borehole water level is chosen as the easiest way to define a water level. A head is specified in a single borehole to create a horizontal water surface that extends to the model boundaries. This water level is, by default, used as the global water level. In principal, a pore pressure distribution underneath this generated water level is hydrostatic.

Pore pressures in soil volumes are generated on the basis of the water conditions assigned to these volumes.

3. STRUCTURES

The structural elements composing the model are defined, forming the basic component of the physical model. The realization of the structure consists of the creation of a vertical cylinder as to simulate the circular shaft. The array option is chosen, shaping the final configuration of the shaft in depth. The vertical cylinder is decomposed into surfaces, the lateral one representing the segmental lining and the internal volume, which is progressively extracted as the excavation proceeds. The external cylinder is selected and the plate is created. As in the two-dimensional analysis, plates are used to simulate the structures.

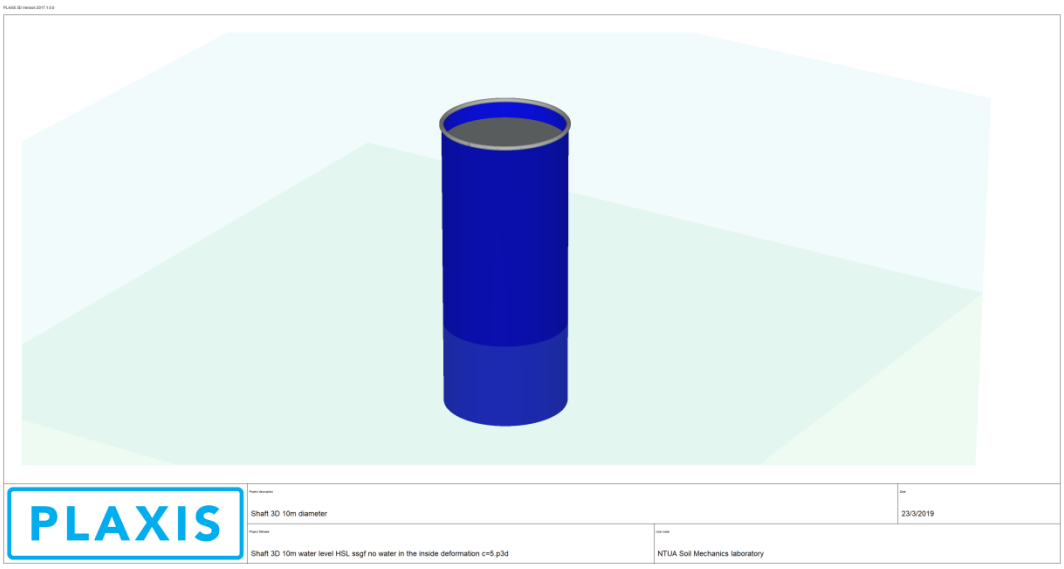

Figure.108 Physical model of the shaft in 3D space.

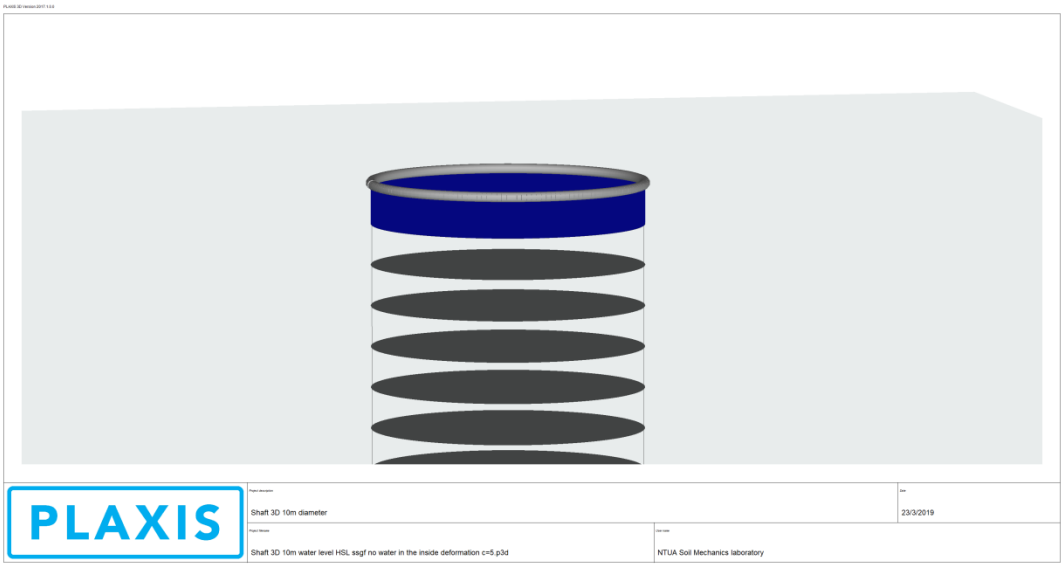

Figure.109 One of the vertical cylinders composing the structure.

4. INTERFACES

Interfaces are created and added to allow for a proper modeling of soil structure interaction. Interfaces are simulating a cohesionless (c=0) thin zone of intensely shearing material at the contact between the structural element and the surrounding soil.

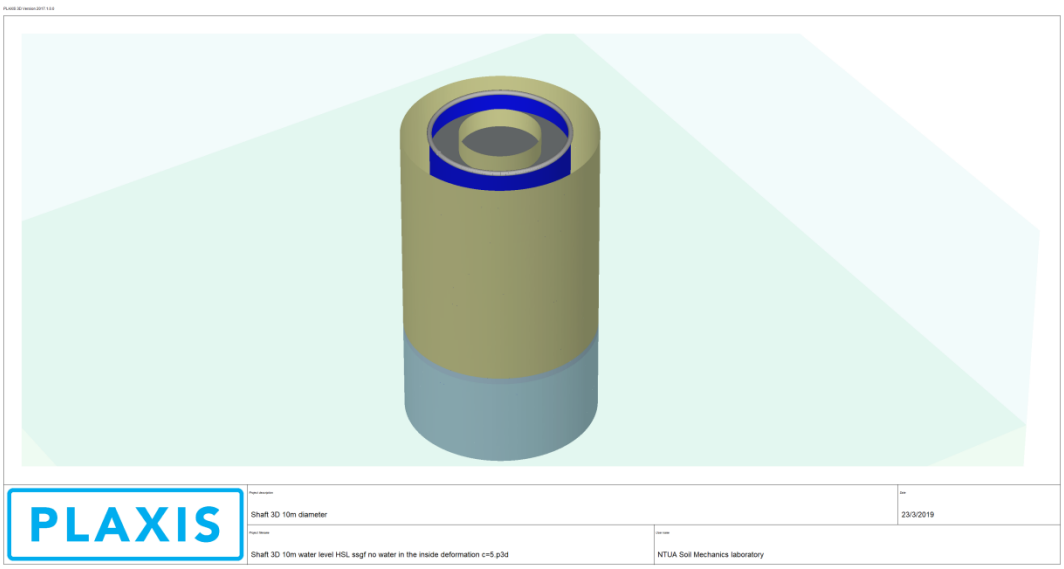

Figure.110 Negative (-) and positive (+) interfaces adjacent to the plates.

In situations involving groundwater flow and consolidation, interface elements can contribute to the flow of groundwater and thereby influence the pore pressure distribution. Therefore interface permeabilities are relevant in such

situations. Flow in interface elements may involve flow across the element as well as flow in the interface longitudinal direction.

5. MESH

Mesh generation consists of the division of the volume into elements. The composition of finite elements is called a mesh. The mesh must be dense enough for accurate calculation, thus is selected to be fine.

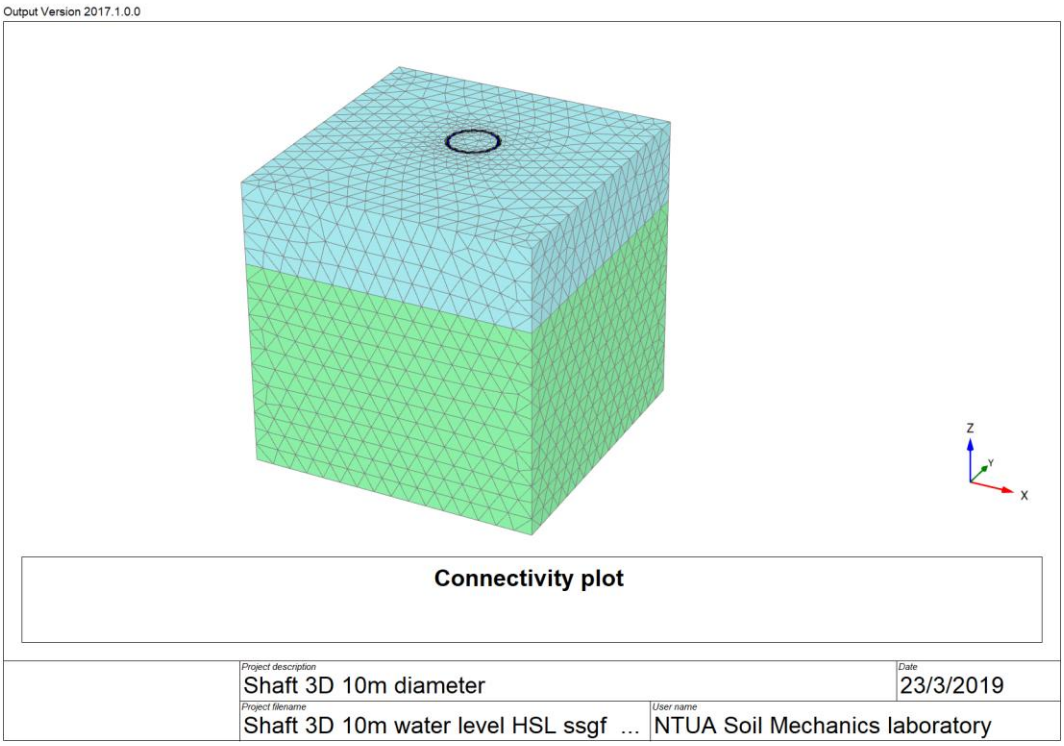

Figure.111 3dimensional generated Mesh Output.

6. FLOW BOUNDARY CONDITIONS

Water pressures i.e. pore pressures in finite element stress points and external water loads, are calculated on the basis of the water conditions as defined for a calculation phase. The various types of pore pressures can be previewed by selecting the stress menu. The phreatic level or external water level can be seen when the phreatic water level option is active in the geometry menu.

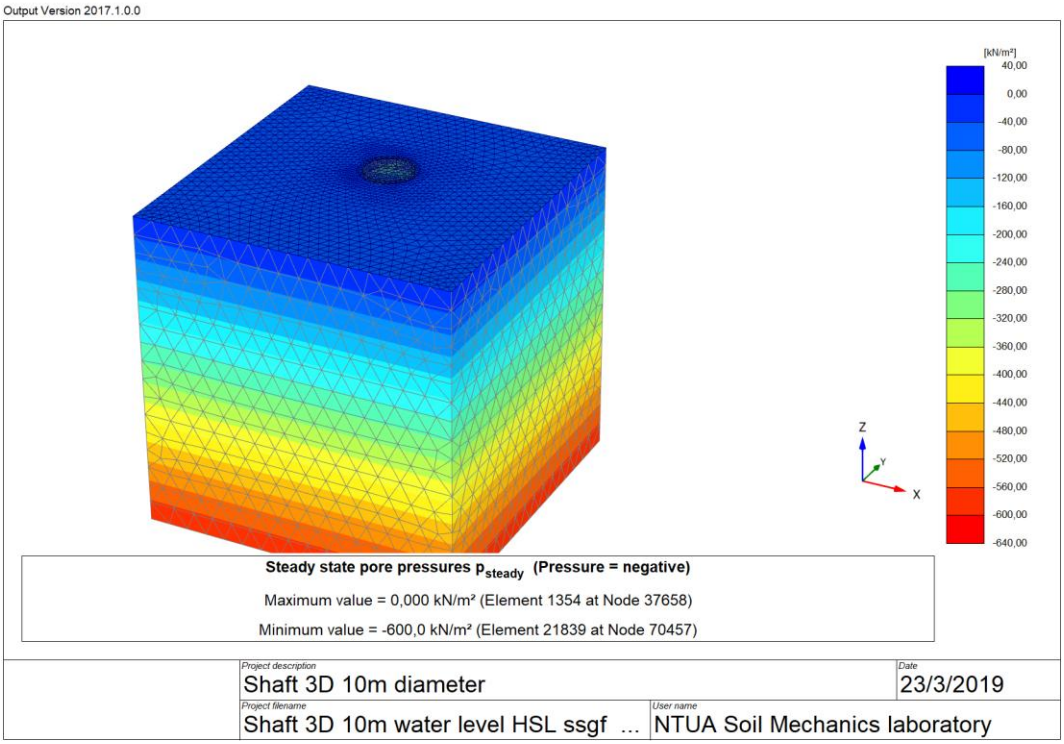

Figure.112 Preview phase, steady state pore pressures, psteady.

By default the bottom of the boundary of the model is closed. The prescribed groundwater head on external geometry boundaries is, by default, derived from the position of the general phreatic level, at least when the general phreatic level is outside the active geometry.

7. STAGED CONSTRUCTION

Finite element calculations are divided into several calculation phases, modeling the excavation and the subsequent construction phases.

The calculation type selected in the initial Phase is to K_0 procedure, meaning the direct generation of initial effective stresses, pore pressures and state parameters. In PLAXIS, initial stresses may be generated by using the K_0 procedure or by using gravity loading. The K_0 procedure is particularly suitable in cases with a horizontal surface and with all soil layers and phreatic levels parallel to the surface. In such a case, the equilibrium is systematically satisfied as vertical stresses=gravity weight, horizontal stresses=lateral reaction forces along the model boundaries.

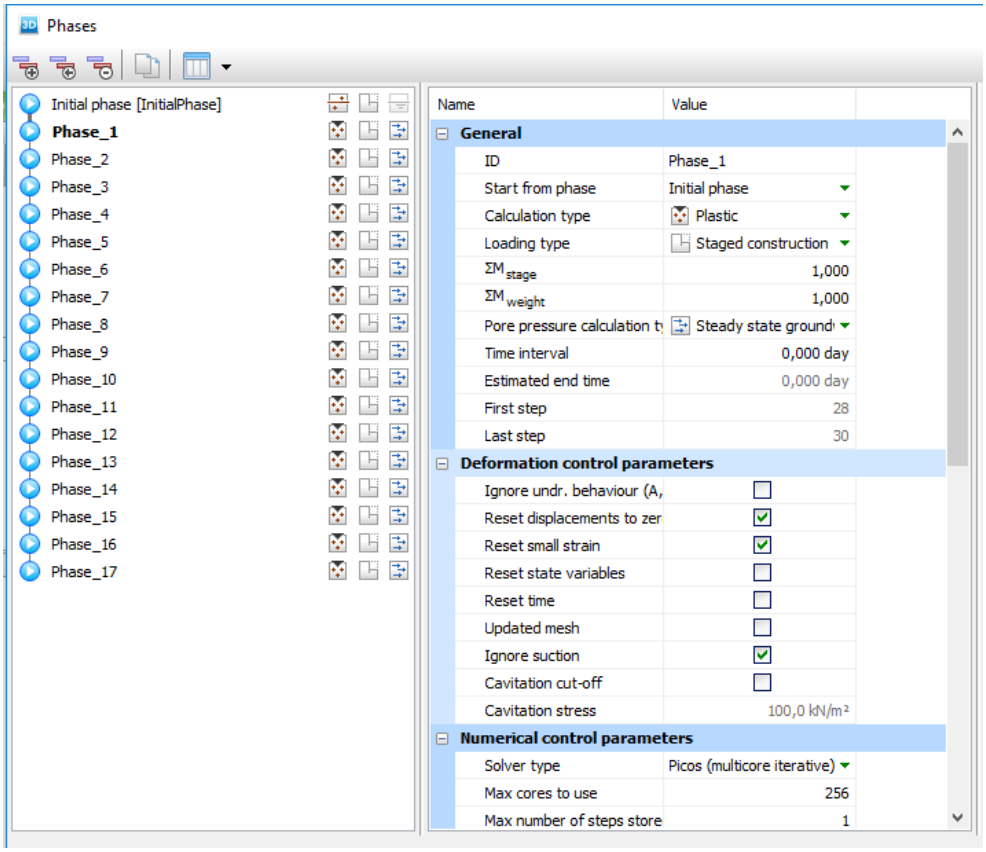

Figure.113 Initial phase and stage construction phases.

Initially, all soil volumes are active and all structural elements are inactive. Progressively, soil volumes and structural objects are respectively deactivated and activated to simulate the project realization procedure. Attention should be paid to setting all excavated soil volumes dry. In addition to the global water pressure distribution it is possible to remove water pressures from individual groups of volumes in order to make them dry. Deactivation of water can be done independently from the soil itself. Hence, if the soil is deactivated and the water level is above the excavation level, then there is still water in the excavated area. If it is the intension to simulate a dry excavation then the water must be explicitly deactivated. The water pressure in adjacent soil volumes is not affected and may be required to be changed.

This implies that, if the soil is deactivated and the water level is above the excavation level, then there is still water in the excavated area. The dry clusters behave as non-porous materials. As a result, neither initial nor excess pore pressure is taken into account and flow is not possible through the cluster.

7.5 OUTPUTS USING PLAXIS 3D

The main graphical representations refer to the deformations, stresses and resulting forces in plates.

7.5.1 DEFORMATIONS

Connectivity plot is a plot of the mesh in which the element connections are clearly visualized. It is the result of the meshing process. The plot is particularly of interest when interface elements are included in the mesh. Interface elements are composed of pairs of nodes in which the nodes in the pair have the same coordinates.

7.5.2 STRESSES

Stress and strain diagrams can be used to visualize the development of stresses (stress path) or strains (strain path) or the stress-strain behavior of the soil in a particular stress point. These curves are useful to analyze the local behavior of the soil. Stress-strain diagrams represent the idealized behavior of the soil according to the selected soil model. Since soil behavior is stress dependant and soil models do not take all aspects of stress dependency into account, stress paths are useful to validate previously selected model parameters.

7.5.3 RESULTING FORCES IN PLATES

It is possible to display the structural forces in a wall structure that is composed of volume elements with an assigned dataset with concrete properties. The structural forces are calculated by integrating the results in the stress points along the region perpendicular to the cross section line. When a plate is displayed, axial forces N_1 and N_2, shear forces Q_{12}, Q_{23} and Q_{13} and moments M_{11}, M_{22} and M_{12} are available. These forces represent the actual forces at the end of the calculation step. Axial forces are positive when they generate tensile stresses. The sign of bending moments and shear forces depend on the plate's local system of axes.

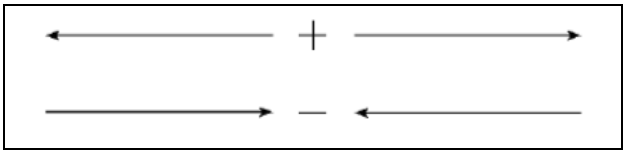

Figure.114 Sign convention for axial forces in beams and plates (Plaxis3D-2-Reference-Manual.pdf).

As shown in Figure.115, the first and second direction (1,2) lie in the plane of the plate whereas the third direction is perpendicular to the plate.

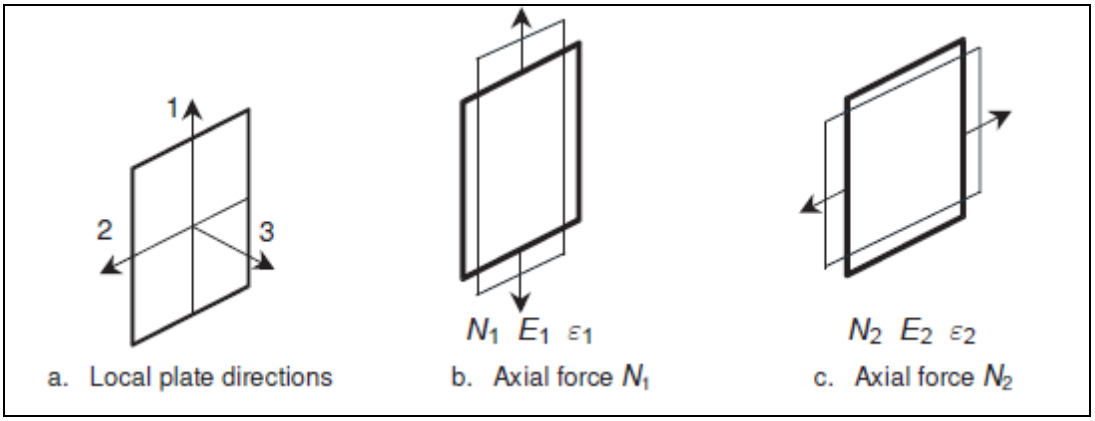

Figure.115 Positive Axial forces in plates (Plaxis3D-2-Reference-Manual.pdf).

The Axial Force N1 is the axial force in the first direction. The Axial Force N2 is the axial force in the second direction.

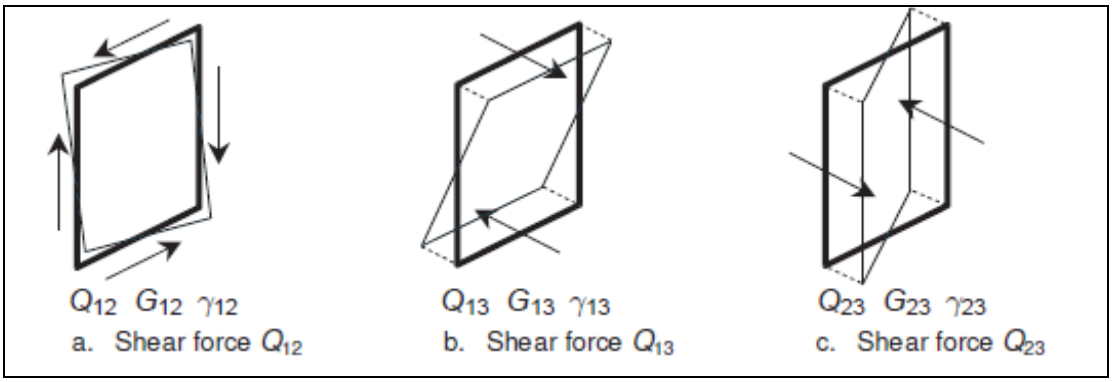

Figure.116 Positive Shear forces in plates (Plaxis3D-2-Reference-Manual.pdf).

The Shear Force Q12 is the in-plane. The Shear Force Q13 is the shear force perpendicular to the plate over the first direction, whereas the Shear Force Q13 is the shear force perpendicular to the plate over the second direction (Figure 116).

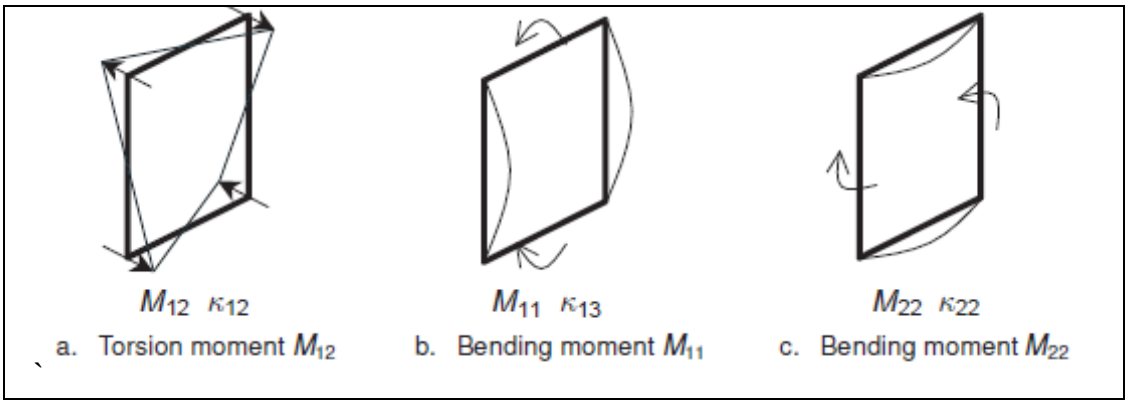

Figure.117 Positive Bending Moments in plates (Plaxis3D-2-Reference-Manual.pdf).

The Bending Moment M1 is the bending moment due to the bending over the second axes. Around the second axis the Bending Moment M22 is the bending moment due to bending over the first axis (around the first axis).

The Torsion Moment M12 is the moment according to transverse shear force (Figure 117).

7.5.4 PLAXIS 3D, DEFORMATION ANALYSIS, HARDENING SOIL MODEL IN WATER FLOW CONDITIONS

As reported in Figures 118 and 119, the calculation fails at the 6th phase, meaning that 7,5 meters have been excavated before the critical condition is reached. A failed calculation is indicated by a cross mark in a red tube. Characteristically, the prescribed ultimate state is not reached and the soil body collapses, meaning that a collapse load has been reached. At the end of the calculation the defined state is not reached and the calculation is not considered to be successful. A successful calculation is indicated by a check mark in a green circle.

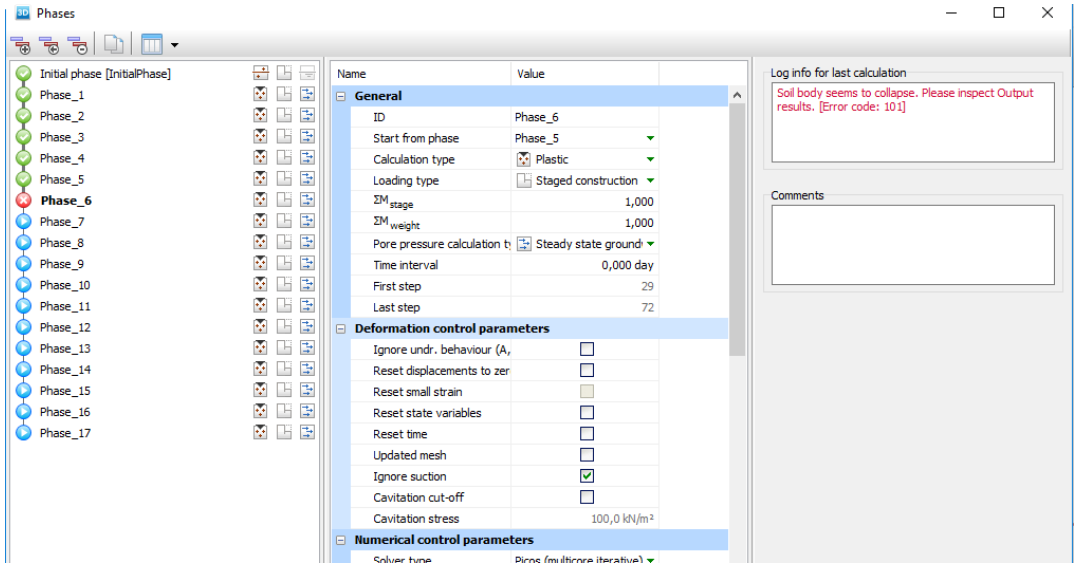

Figure.118 Executed phases and phase collapsed phase.

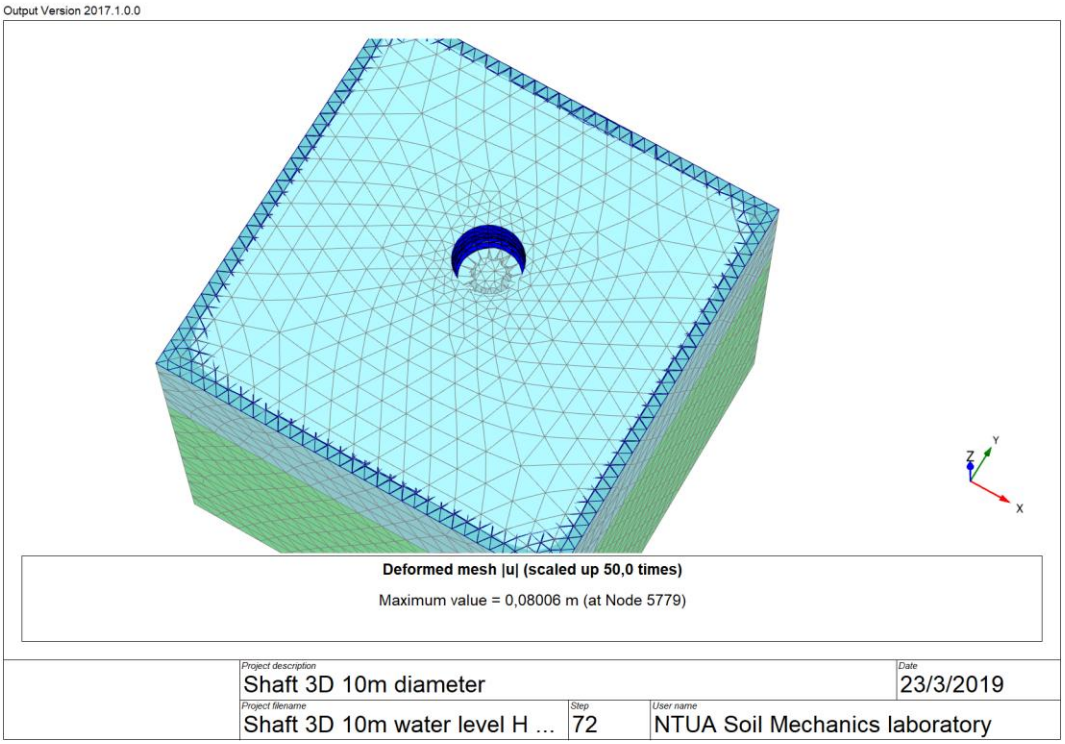

Figure.119 Deformed mesh at the failure stage, where soil body collapses.

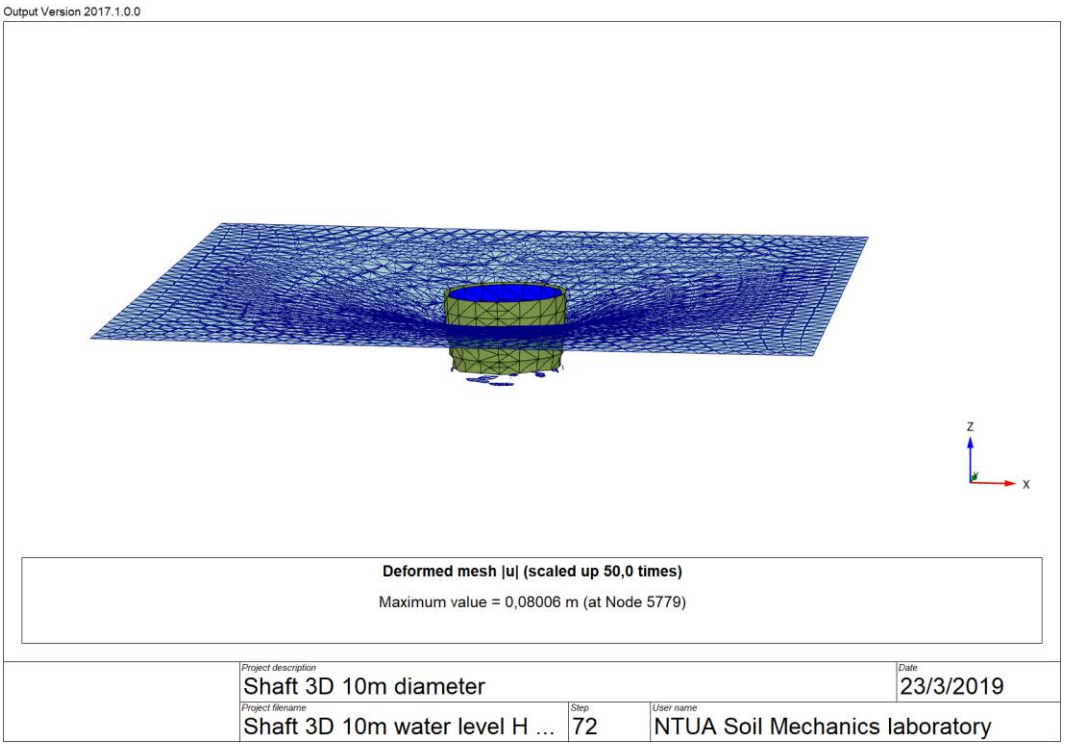

Figure.120 Deformed mesh at the failure stage, where soil body collapses. Soils are hidden.

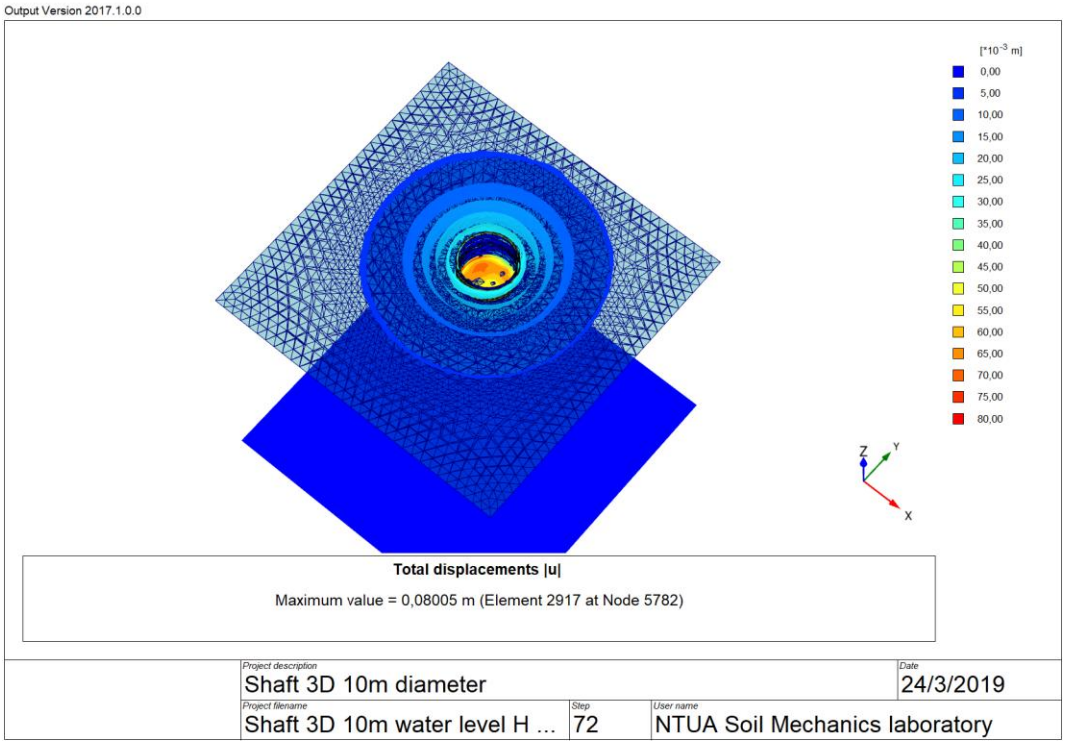

Figure.121 Total displacements (absolute value) at the failure stage.

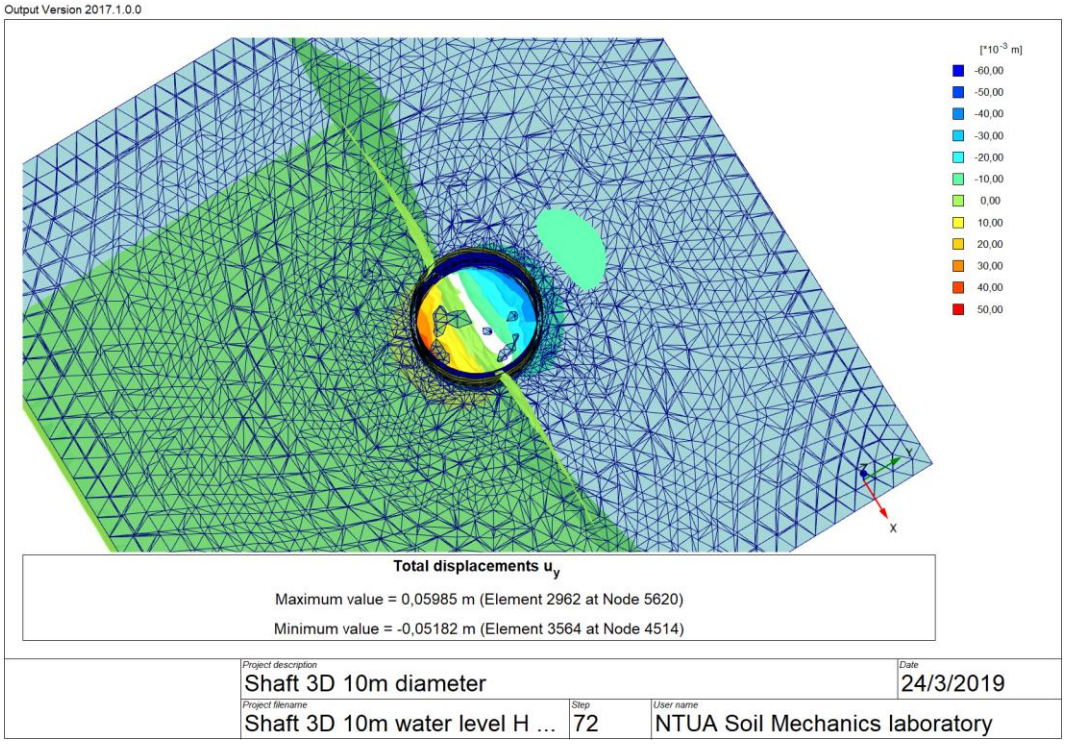

Figure.122 Maximum vertical displacements at the failure stage.

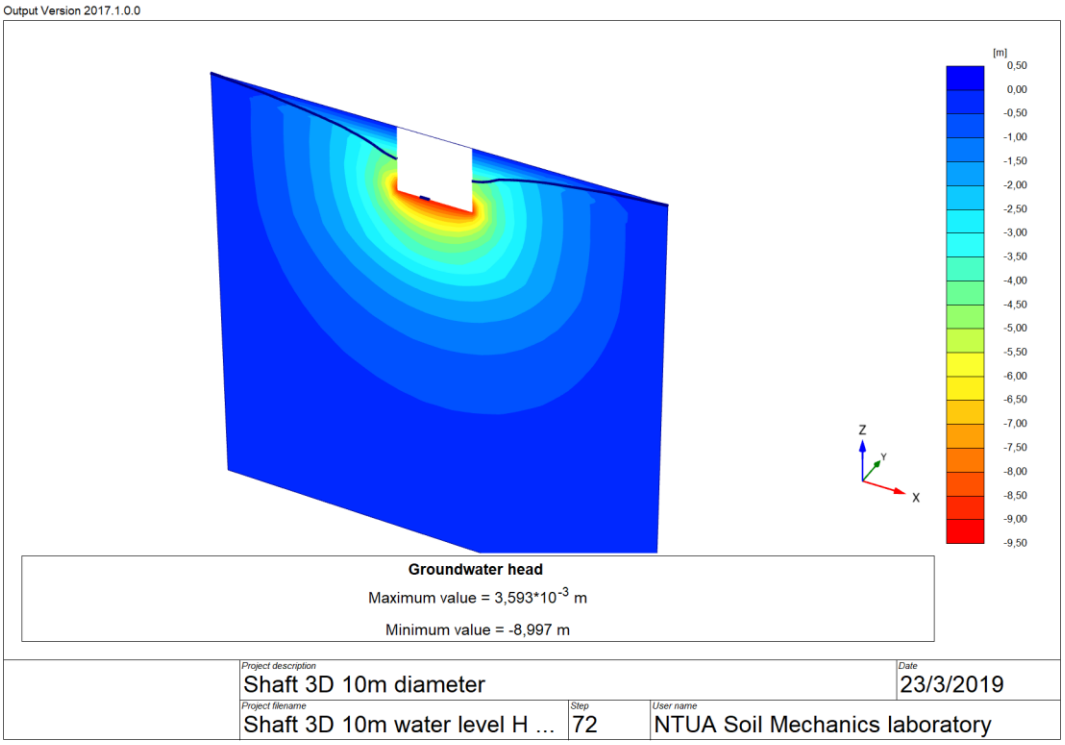

Figure.123 Groundwater head at the failure stage.

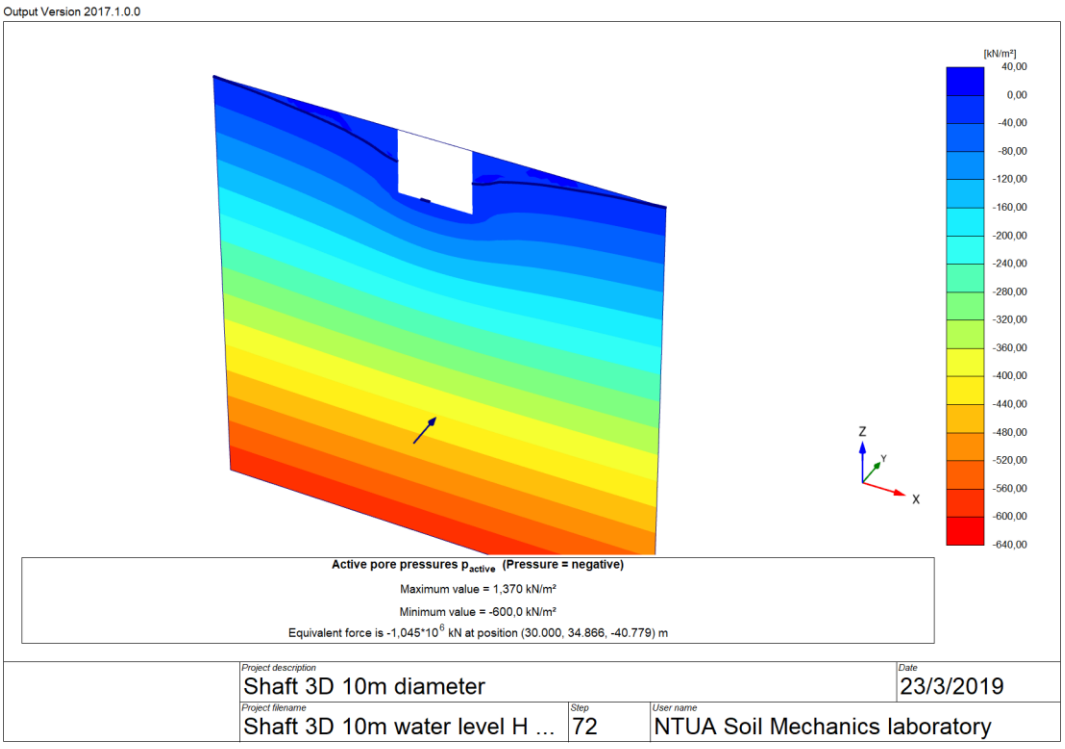

Figure.124 Active pore pressures pactive (pressures=negative) at the failure stage.

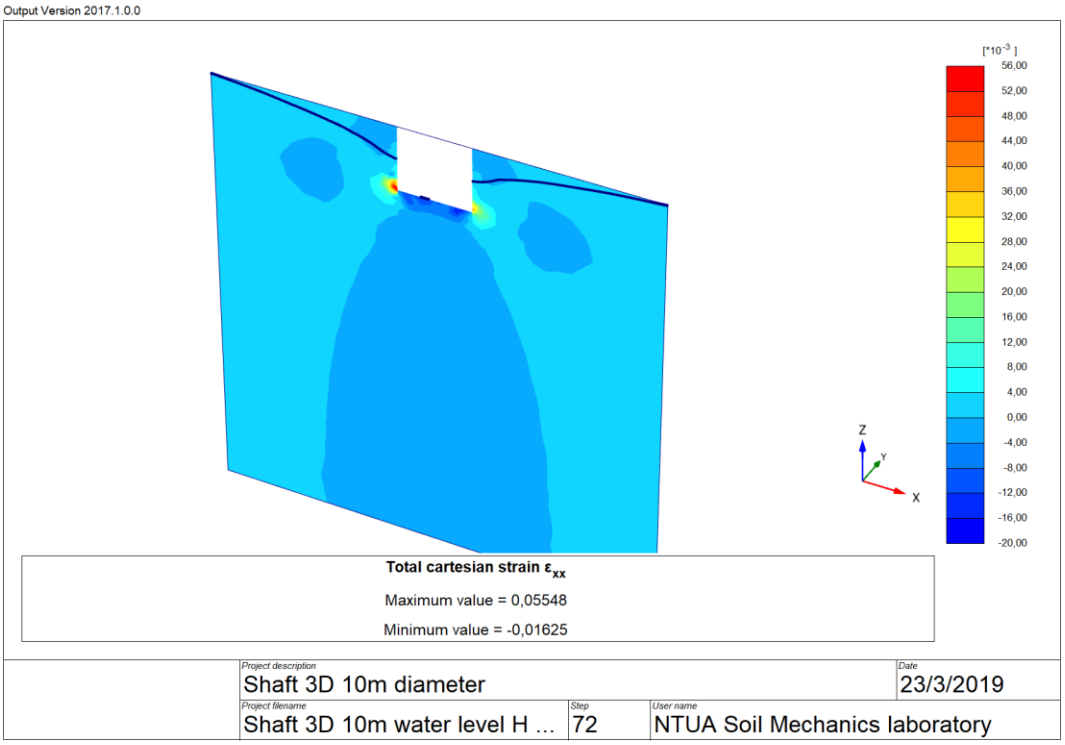

Figure.125 Total Cartesian strain εxx at the failure stage.

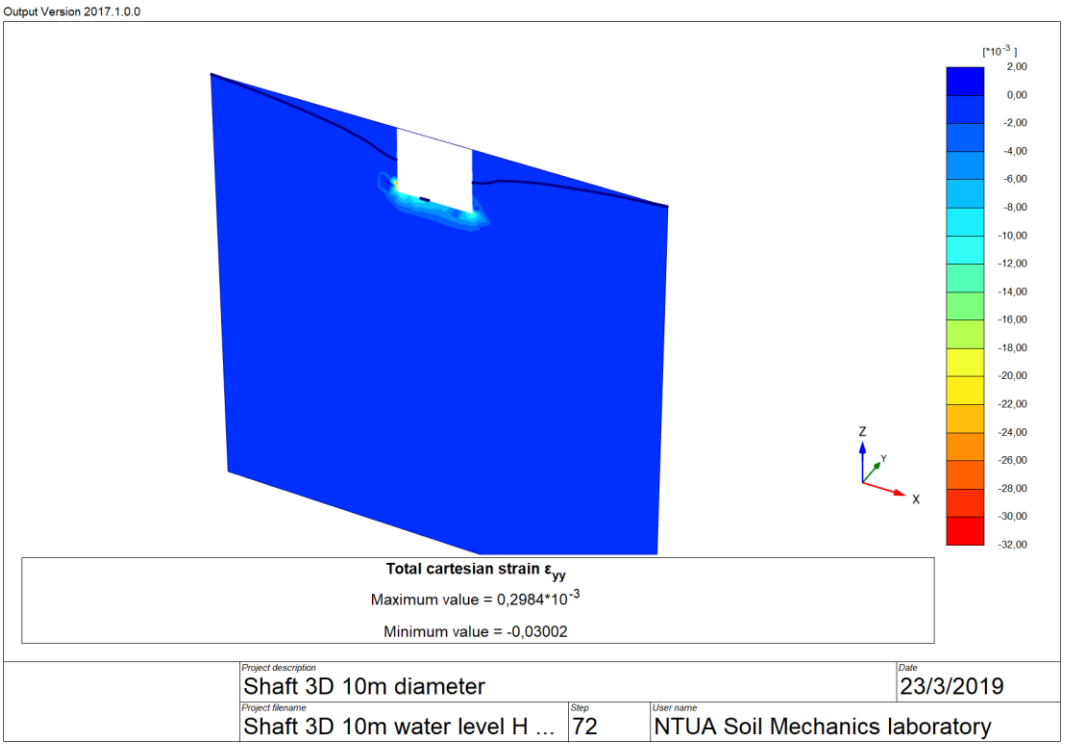

Figure.126 Total Cartesian strain εyy at the failure stage.

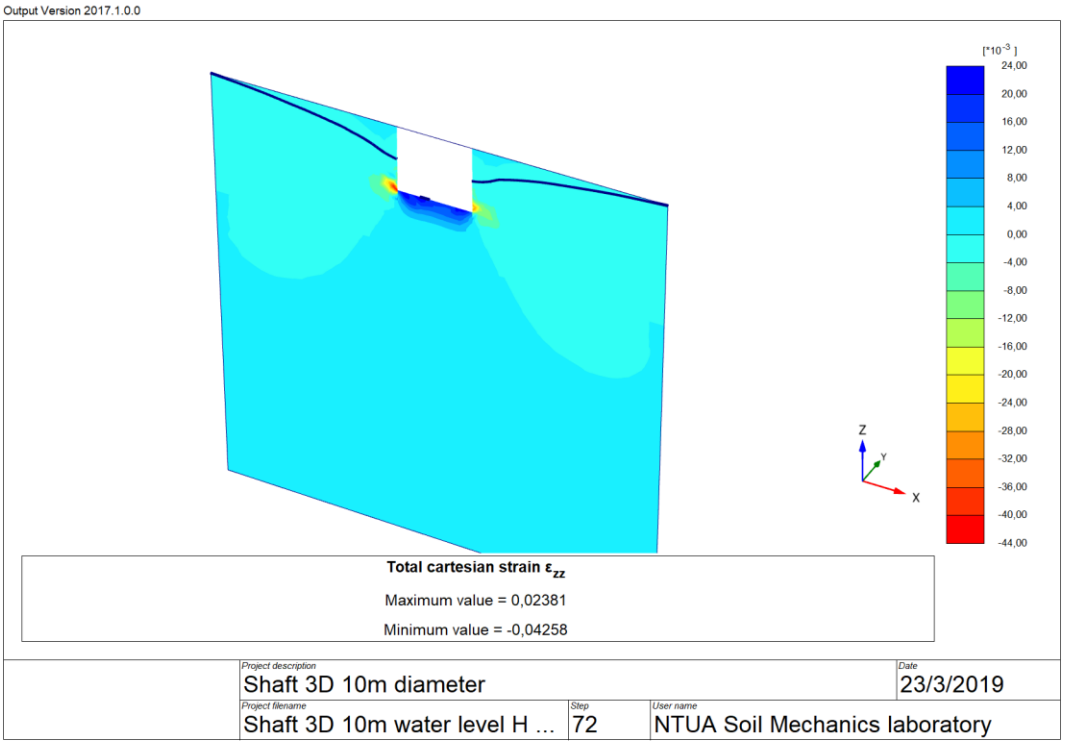

Figure.127 Total Cartesian strain ε_{zz} at the failure stage.

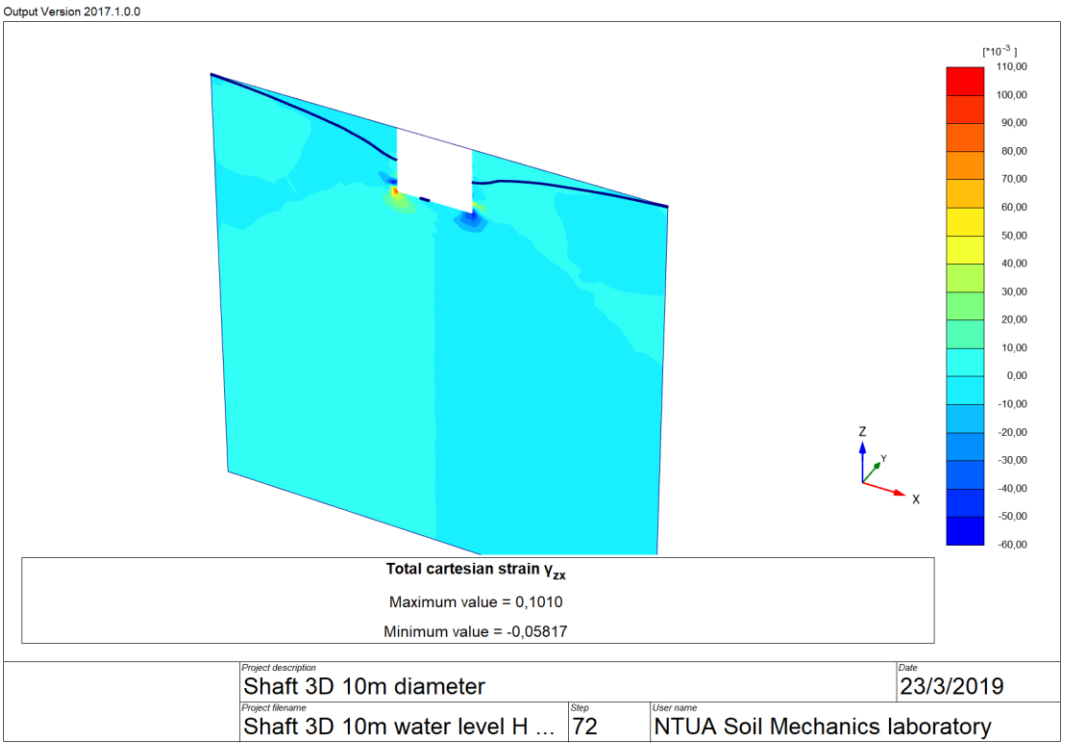

Figure.128 Total Cartesian strain γ_{zx} at the failure stage.

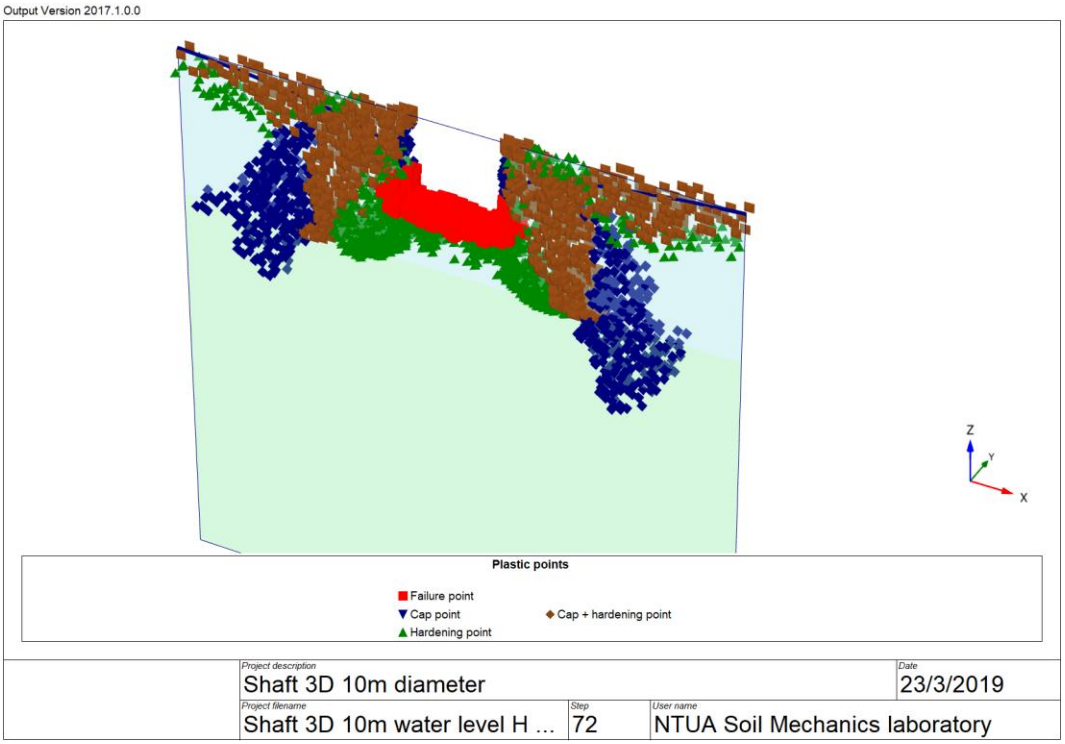

Figure.129 Plastic points at the failure stage including, Failure points in red, Cap Points in blue, Hardening Points in green and Cap + Hardening Points in brown.

Figure 130 indicates that there are no plastic points on the structure, meaning that the failure is to be attributed to the underlying soil.

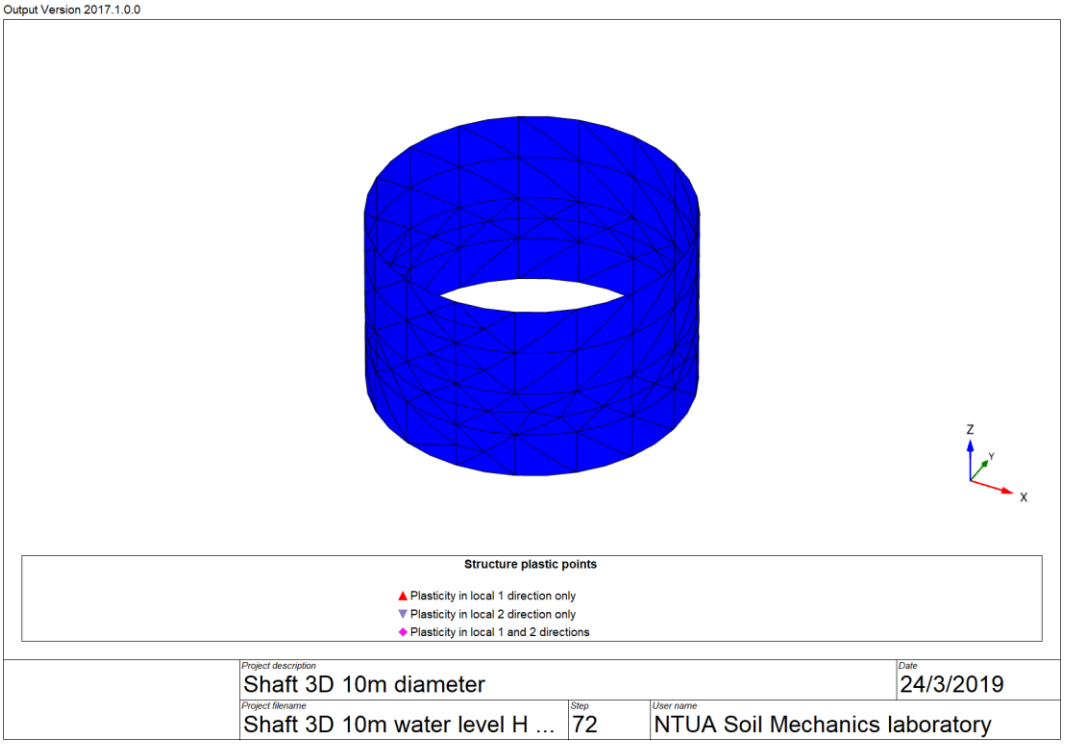

Figure.130 Plastic Points on structure.

Axial forces N_2 maximum values (the relative graphical representation is reported in the following scheme) are dominating over the axis forces N_1 in Figure 131.

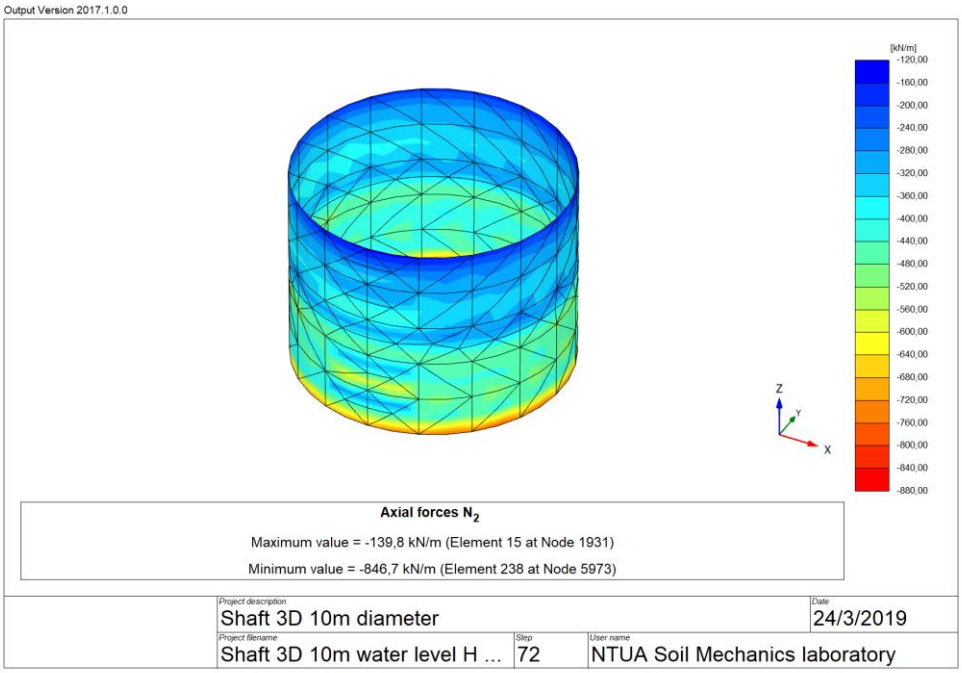

Figure.131 Axial forces N_2 distribution, maximum and minimum values at the failure stage.

Q_{12}, Q_{23} and Q_{13} have similar values fluctuation even if the distribution is dissimilar due to the direction they are applied. Q_{13} presents the maximum values in Figure 132.

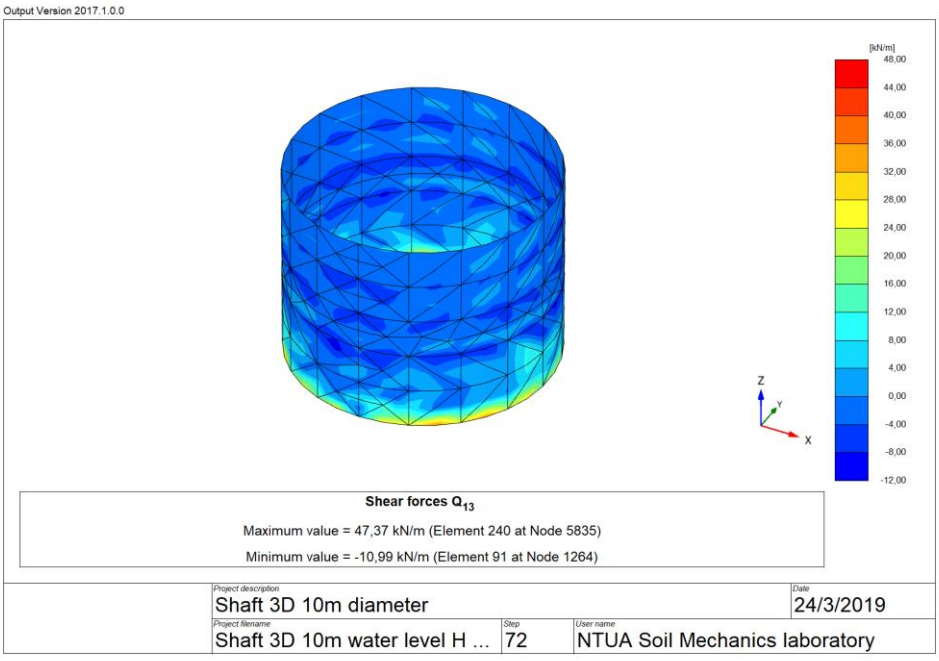

Figure.132 Shear Forces Q_{13} distribution, maximum and minimum values at the failure stage.

M11, M12 and M22 have similar values even if the distribution is dissimilar due to the direction in the space that they are applied. M22 presents the maximum values in Figure 133.

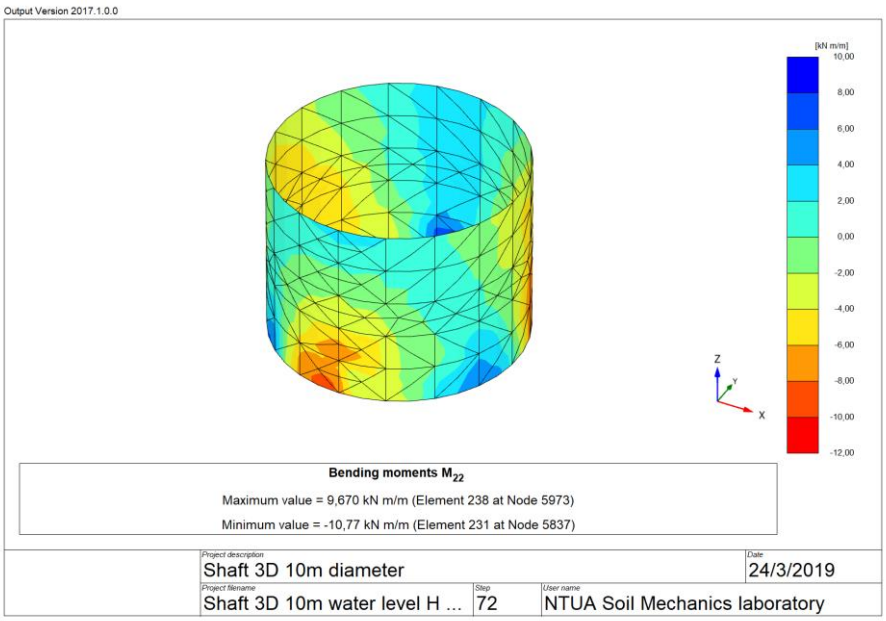

Figure.133 Bending Moments M22 distribution, maximum and minimum values at the failure stage.

7.5.5 PLAXIS 3D, STRESS ANALYSIS, HARDENING SOIL MODEL IN WATER FLOW CONDITIONS

Applying the stage construction technique, the calculation is failed at the 6th phase, meaning that the ultimate state is not reached and the soil body collapses as shown in Figures 135 and 136.

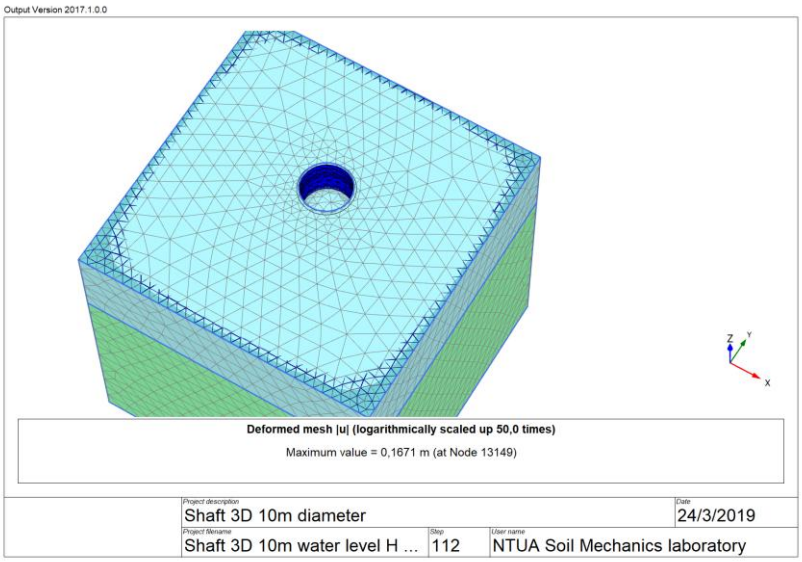

Figure.134 Deformed mesh at the failure stage, where soil body collapses.

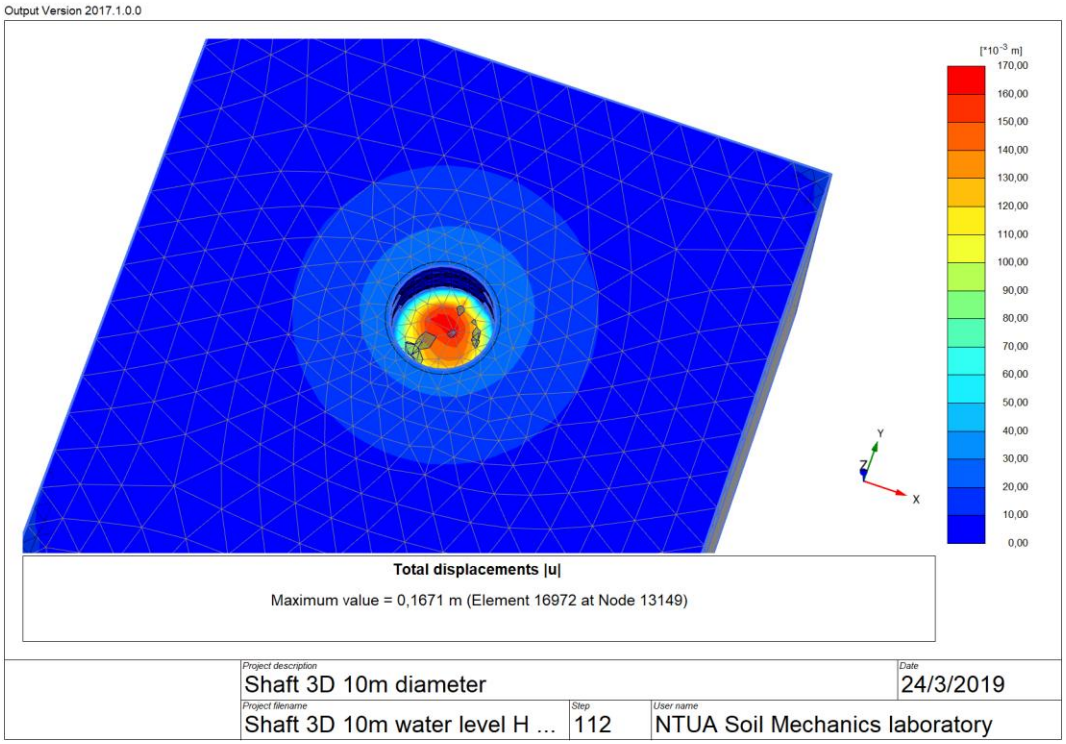

Figure.135 Total displacements (absolute value) at the failure stage.

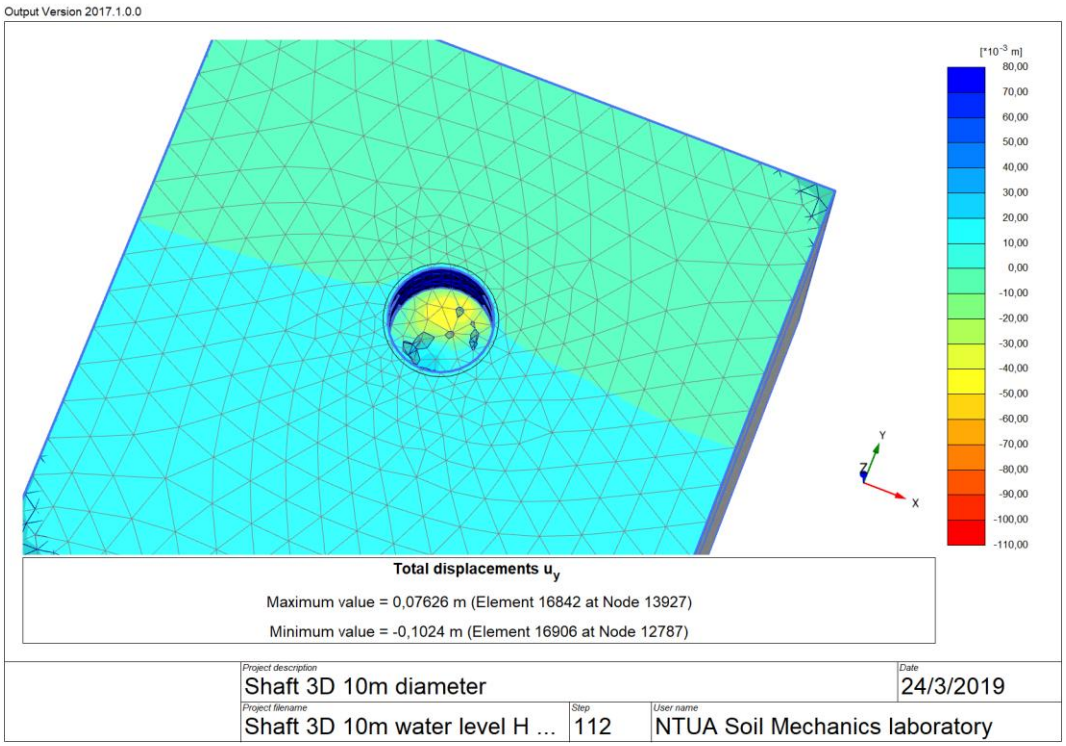

Figure.136 Maximum Vertical Displacements at the failure stage.

.

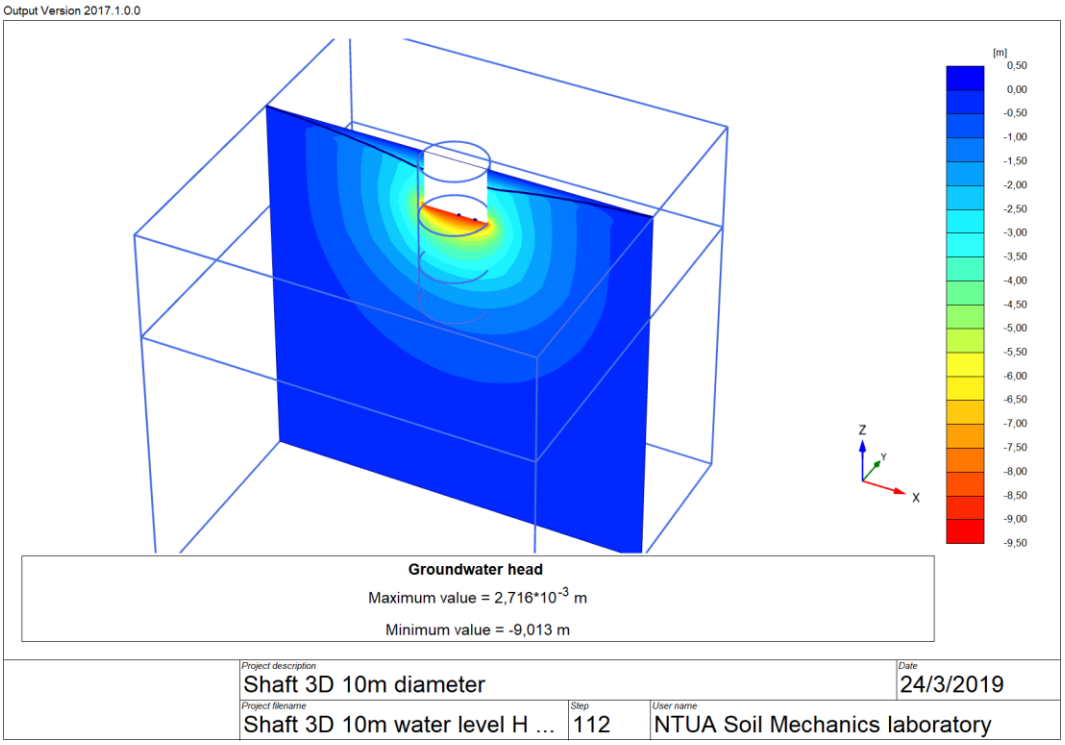

Figure.137 Groundwater head at the failure stage.

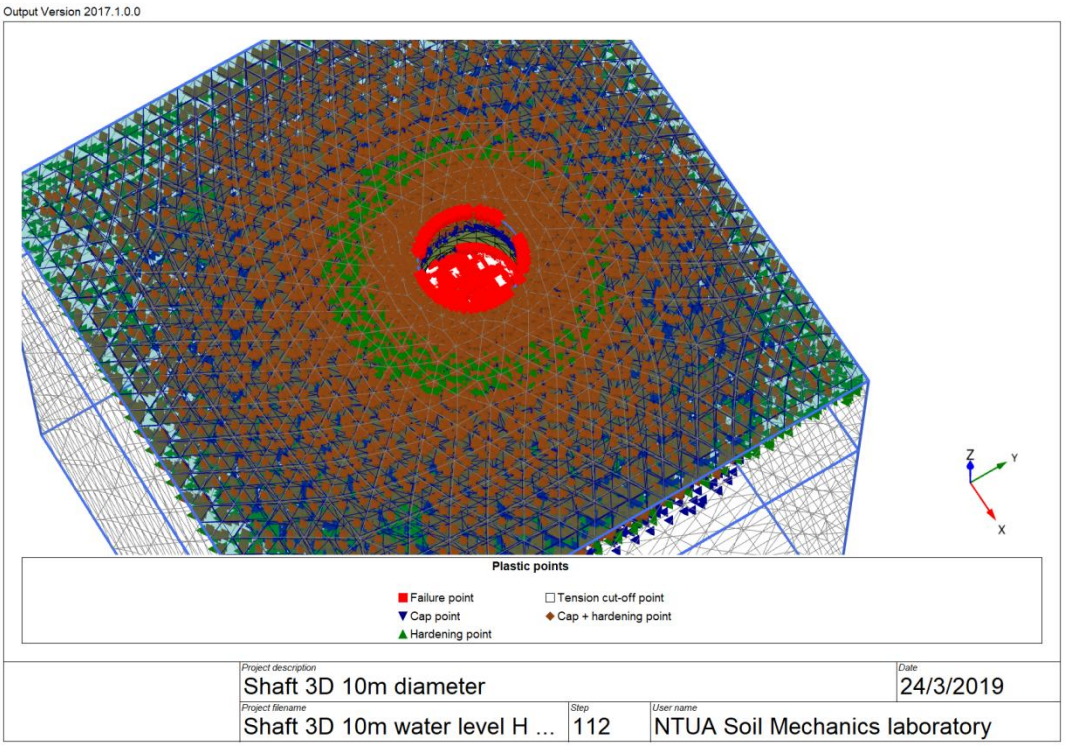

Figure.138 Plastic points at the failure stage including, Failure points in red, Cap Points in blue, Hardening Points in green and Cap + Hardening Points in brown.

7.6 CURVES

Curve points give an overview of the nodes and stress points that are preselected for the generation of curves, with an indication of their coordinates. The points selected in the structure view can be used to generate curves related to resulting structural forces. The points should be selected after selecting the structure.

Another quantity that can be presented in a curve is the pore pressure. The quantity is available for selected nodes as well as stress points. In the pore pressure subtree stresses, p_{active}, p_{steady} or p_{excess} can be selected. Pore pressures are expressed in the units of stress.

Force displacement curves can be used to visualize the relationship between the development of a structural force quantity and a displacement component of a certain point in the geometry. A structural force quantity can only be selected for nodes being selected after the calculation.

7.6.1 PLAXIS 3D, DEFORMATION ANALYSIS, HARDENING SOIL MODEL IN WATER FLOW CONDITIONS

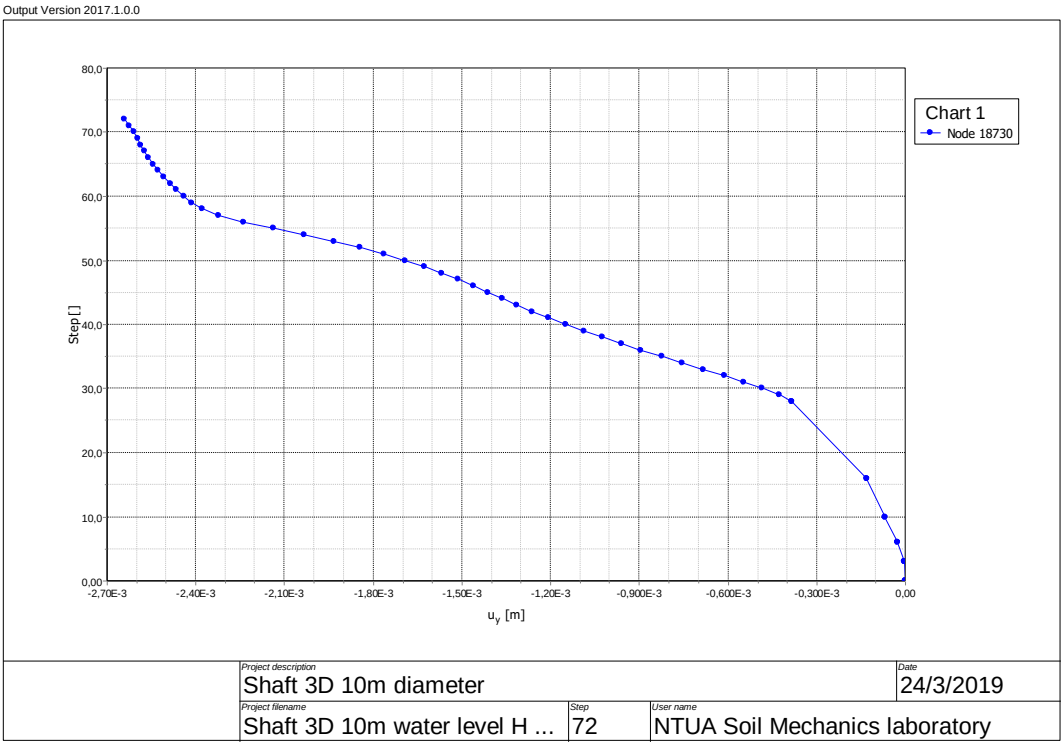

Figure.139 Progressive Vertical Displacements at the bottom center from the first stage until the failure excavation and construction phase expressed in meters.

Three points are selected as node points in the analysis namely (35,35,0-37.5,35,0-40,35,0) at the ground surface from the excavation border, each one 2,5 meters apart from the previous one, for a total distance of 5 meters to evaluate the absolute total displacements (max. u_x, uy, uz) and to represent them diagrammatically until the failure stage. It should be noticed that, the trend of the diagrams are similar and as the distance increases, values are decreasing, as expected. All the absolute vertical displacements documented at the ground surface until the failure stage are relatively small, reaching the maximum value of 2,5 centimeters for the point (3846) adjacent to the shaft as shown in Figure 140..

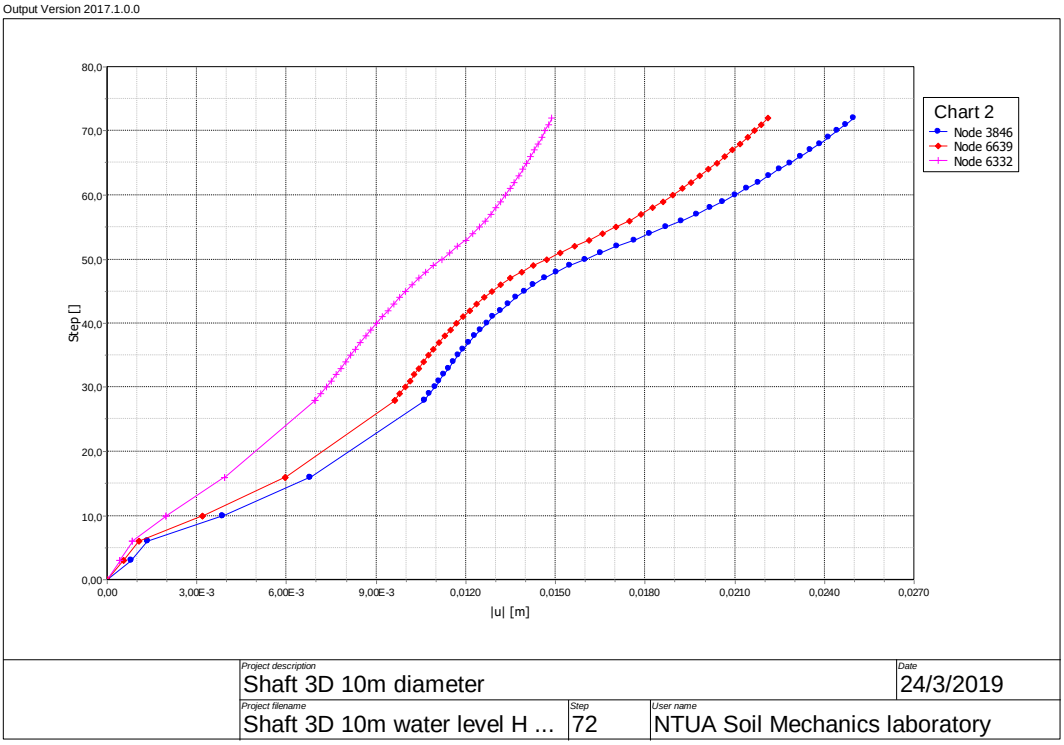

Figure.140 Trend of Absolute Total Displacements for 3 points from the first until the failure stage along the ground surface at a distance at a relative distance of 2,5 meters, the first lying on the shaft's border.

7.7 CONSTRUCTION TECHNIQUE EVALUATION

The subject of the present analysis is the study of the influence of the soil formation on the application of the construction technique used in the presence of an aquifer. Obvious factors influencing the development of deformations in the ground are cohesion (c), modulus of Elasticity (E) and the Poisson's ratio (v). With a view to assessing the above construction method, in the upper formation an increased value of soil cohesion is considered. The hypothetical formation is generally referred to as Soil1 with a characteristic value of c=15 kN/m^2. The results focus on evaluating the maximum extends of excavation and simultaneous support employing segmented concrete rings.

	Failing at stage	Succeed until stage	Max depth reached
Silty Sand const. Stress c=5 kPa	6^{th}	5^{th}	>7,5m
Silty Sand const. Deformation c=5 kPa	6^{th}	5^{th}	>7,5m
Soil 1 const. Stress c=15 kPa	14^{th}	13^{th}	>19,5m
Soil 1 const. Deformation c=15 kPa	14^{th}	13^{th}	>19,5m

Table.13 Maximum depth and stage reached depending on soil cohesion.

Observing the above calculation results presented in Table 13, it is evident that the cohesion is of great influence in the adoption of this specific construction technique in the presence of water flow. The first soil layer where c=15 kN/m^2 allows the shaft construction safely. The excavation and construction proceed until stage 14^{th}, meaning that an approximated depth of 20 meters is reached and supported. The maximum displacements values, as the deformed mesh shows, are |u|=3,215 meters at the collapsing stage and |u|=0,5 at the penultimate stage. As Figure 141 testifies, at the 14^{th} phase, irrespective of the construction technique being stress or deformation, based on the program outputs a mass of soil seems to collapse, meaning that there is an imminent failure. Failure points are represented in red, Cap points in blue, Hardening points in green and Cap+ Hardening points in brown. The failure is to be expected at the bottom where there is a vast concentration of failure points.

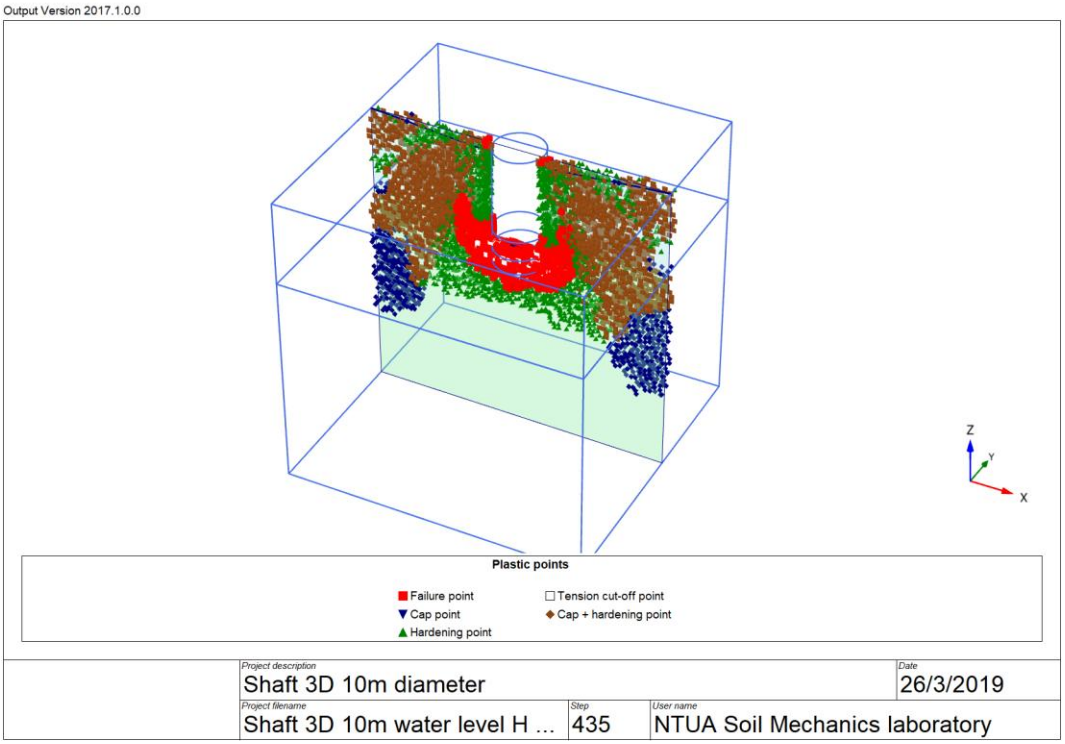

Figure.141 Plastic points at the failure stage (Phase 14) applying the Deformation construction technique, the cohesion of the upper formation is c=15 kN/m^2.

7.8 DEWATERING

7.8.1 PORE PRESSURES

The scope of the model is to represent an effective soil response i.e. the relationship between the stress and the strains associated with the soil skeleton. The presence of pore pressures significantly influences the soil response. In many cases it is sufficient to analyze either the long term (drained) response or the short term (undrained) response without considering the time dependent development of pore pressures. Under undrained conditions, excess pore pressures are generated as a result of stress changes. The dissipation of these excess pore pressures with time can be analyzed in a consolidation calculation.

In the pore pressure a further division is made between steady state pore pressure p_{steady} and excess pore pressure p_{excess}.

$$p_{water}=p_{steady}+p_{excess}$$

Excess pore pressures are pore pressures that occur as a result of the stress changes in undrained materials. In this respect, changes in stress may be a result of a change in hydraulic conditions or consolidation. Hence, excess pore pressures are a result of a deformation analysis.

7.8.2 CONSOLIDATION CALCULATION

As stated above, a consolidation calculation is usually conducted when it is necessary to analyze the development and dissipation of excess pore pressure. In consolidation analysis, the flow boundary conditions define where excess pore pressures may dissipate through the model boundary and hence, it affects the excess pore pressures only. In a ground flow or fully coupled analysis, the flow boundary conditions define where pore water may flow into or out of the soil and hence, it affects the total pore pressures in these cases. Consolidation without additional loading until a desired degree of consolidation, specified by the degree of consolidation parameter is reached. By default, the degree of consolidation parameter is set to 90%.

7.9 EMPLOYMENT OF WELLS

The following analysis is conducted while attempting to lower the water table, during the excavation process and successive installation of segmented rings composing to shaft's skeleton.

Dewatering, discussed previously in Chapter III in detail, is conceived in the present model as a series of phases where wells are active, in pumping out water (Figure 142). To underline that, the model is set in a manner that flow is continuous during all stages with only the lower limit to be impermeable while permeability coefficients are established at the beginning. Wells are continuously pumping out water pointing to lower progressively the height of the free surface, characteristically:

Step	**Phase**	**h_{min} set to:**
1	Initial Phase	
2	Wells 1	h_{min}=-4,0m
3	Consolidation	
4	Wells 2	h_{min}=-8,0m
5	Consolidation	
6	Wells 3	h_{min}=-12,0m
7	Consolidation	
8	Wells 4	h_{min}=-16,0m
9	Consolidation	
10	Wells 5	h_{min}=-20,0m
11	Consolidation	
12	Various construction phases	h_{min}=-20,0

Table.14 Phases proceeding excavation and construction.

The flow rate Q=0,03 m^3/s and the maximum well depth z_{max}=-16m are assigned constant values during the simulation procedure. Intermediate consolidation phases, as indicated above, are set between well phases. Consolidation according to PLAXIS 3D is a time dependent analysis of deformation and excess pore pressure and an input of soil permeability is required. The minimum excess pore pressure value, is selected at the loading type menu and set |p-stop|=1 kN/m^2 .Practically, this kind of sequential procedure is selected hoping to eliminate excess pore pressures, a consequence of the flow induced by the dewatering method, as the analysis is not time dependent and excess pore pressures need time to dissipate. This line of action, aims to lower the water head so that more suitable conditions are set. During the various project phases, wells continue to extract water at a constant rate until failure. The construction technique selected is 'Stress' as previous experience shows that little difference with the 'deformation' method.

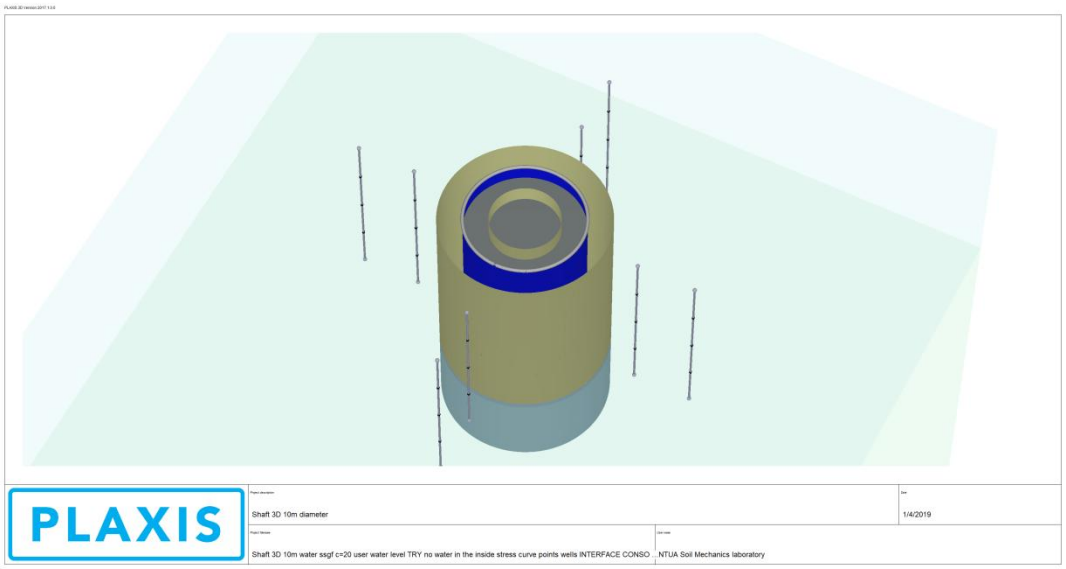

Figure.142 Group of wells and the hypothetical phases.

Application of this particular dewatering technique, results to failure of the excavation at the 10^{th} stage, meaning that 13,5 meters are successfully excavated and constructed before the collapse phase is reached. The failed stage is indicated in the calculation procedure by a cross mark in a red tube in Figure 143. As the annotation message shows soil body collapses, meaning that the initially conceived project cannot be successfully completed.

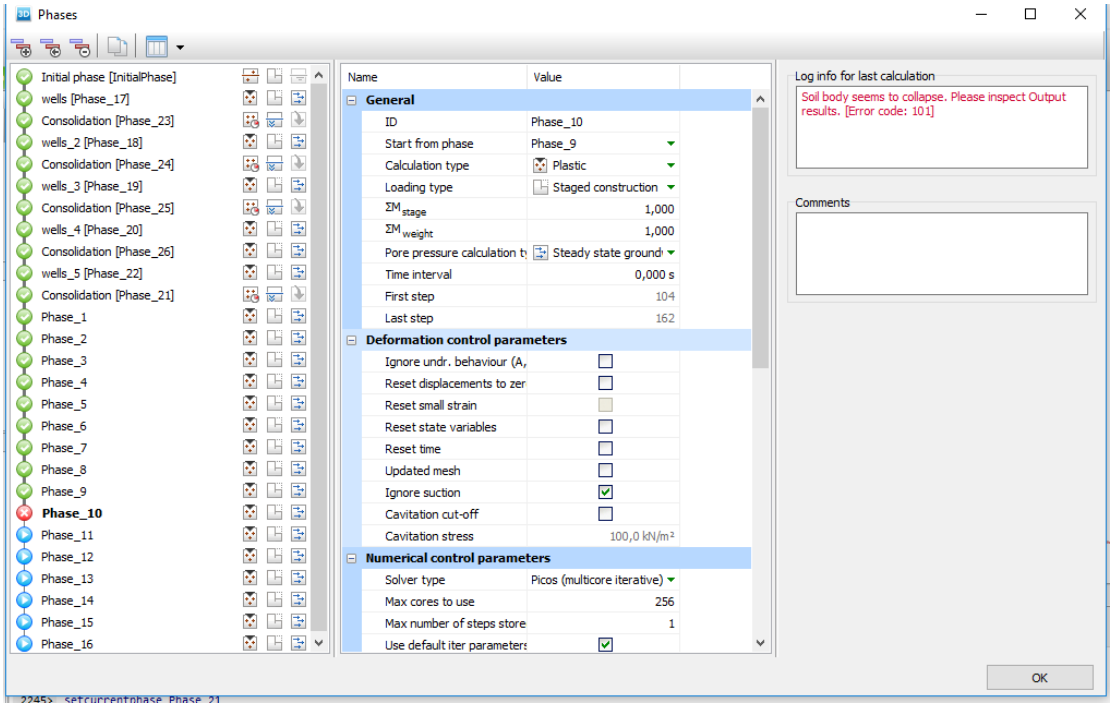

Figure.143 Executed phases and collapse phase.

7.10 OUTPUTS EMPLOYING WELLS

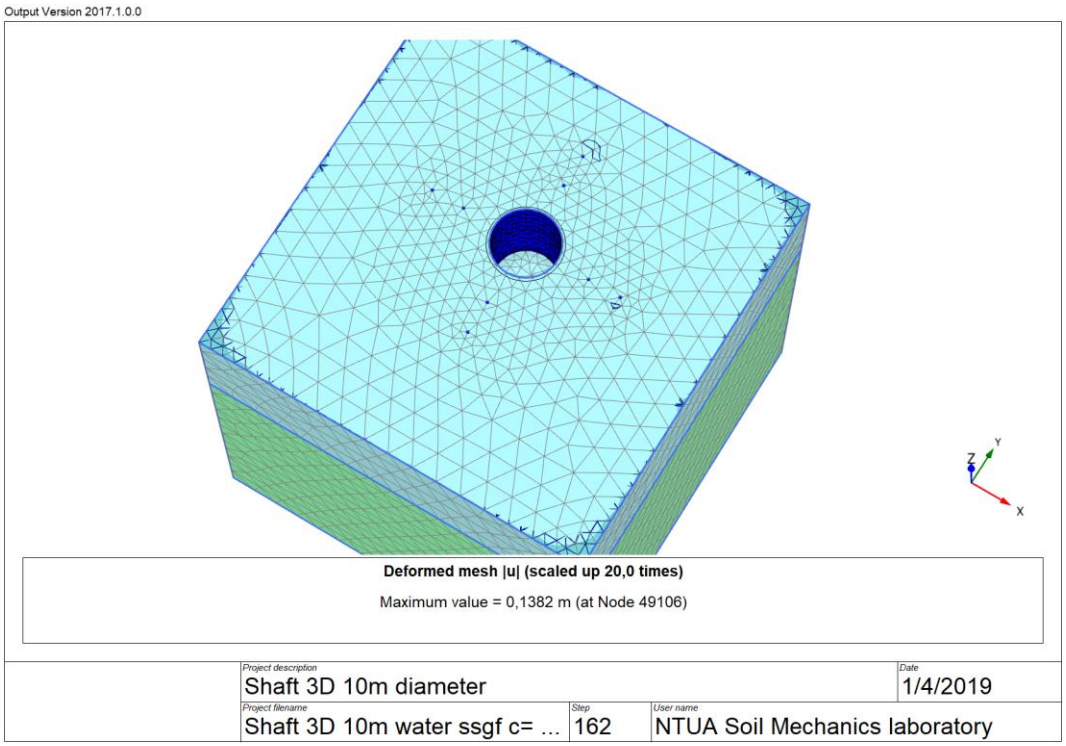

Figure.144 Deformed mesh at the failure stage, where body soil collapses.

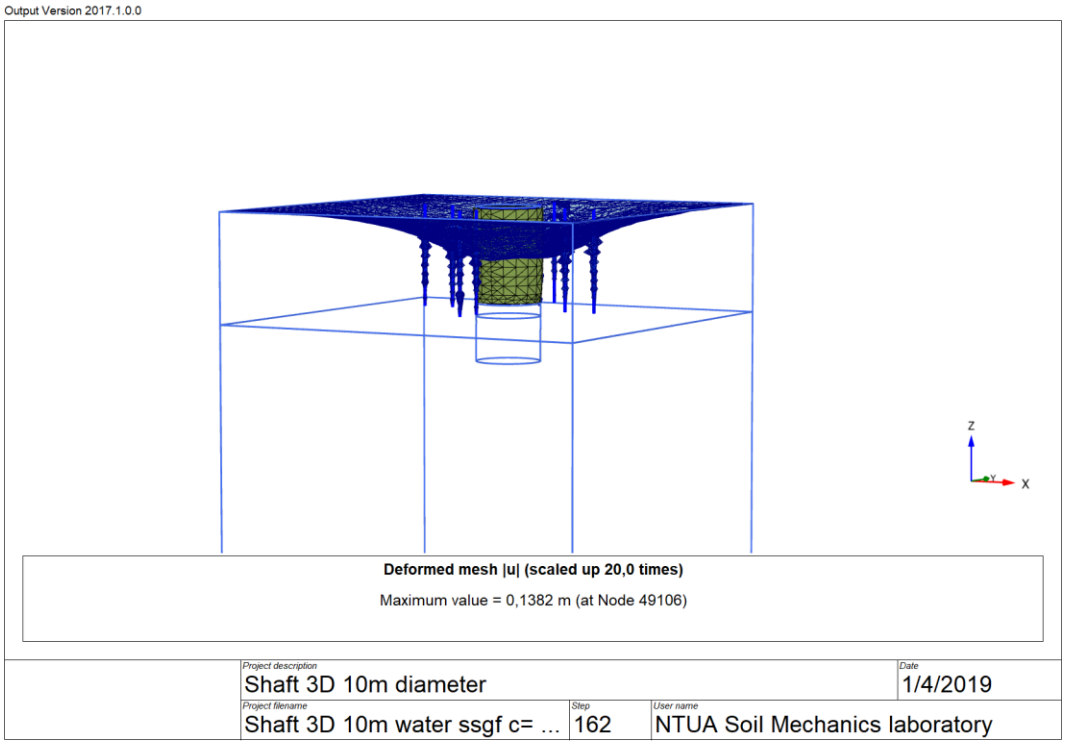

Figure.145 Deformed mesh at the failure stage, where soil body collapses. Soils are hidden.

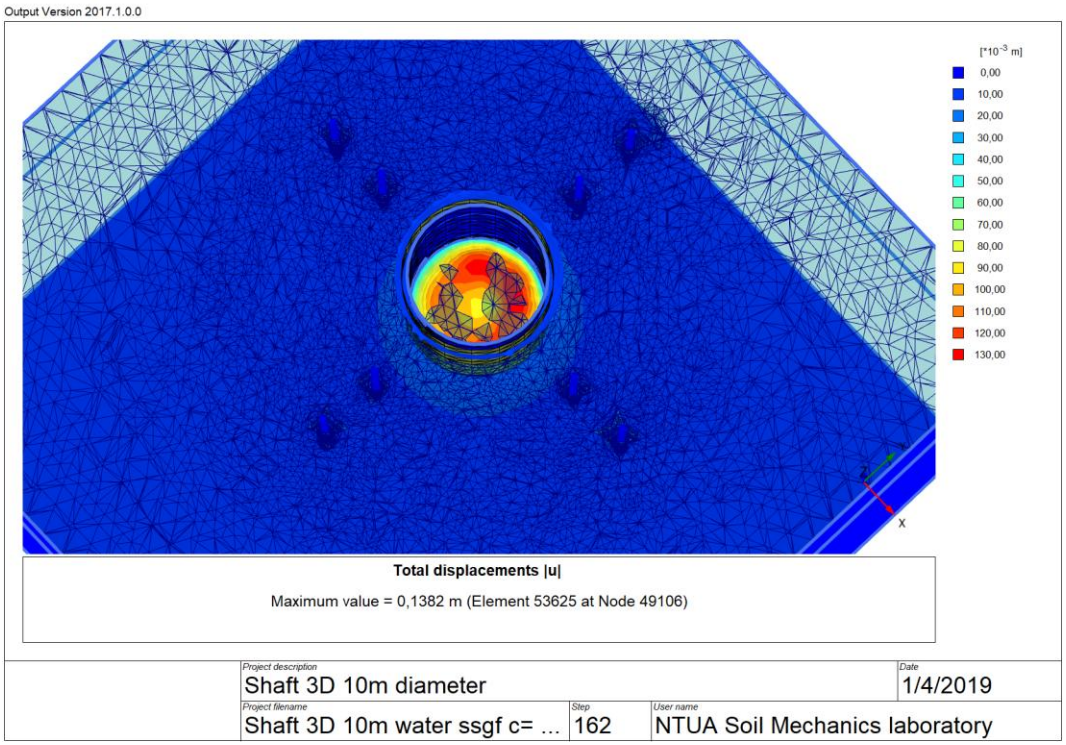

Figure.146 Total Displacements (absolute value) at the failure stage.

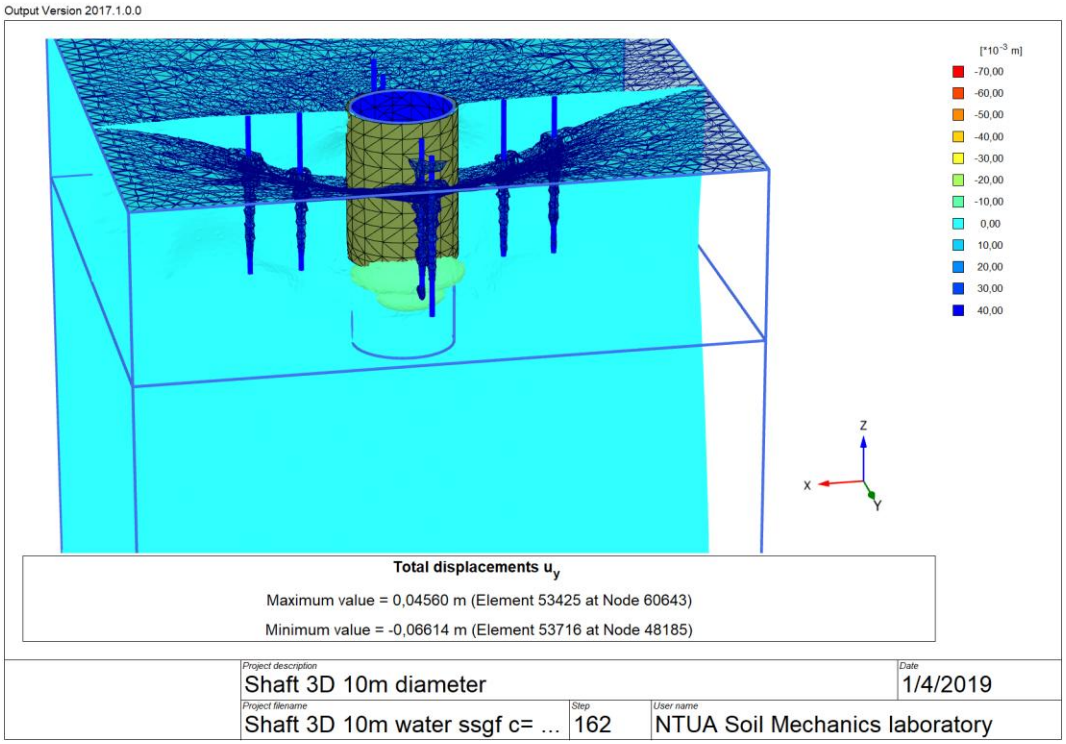

Figure.147 Maximum vertical displacements (u_y) at the failure stage.

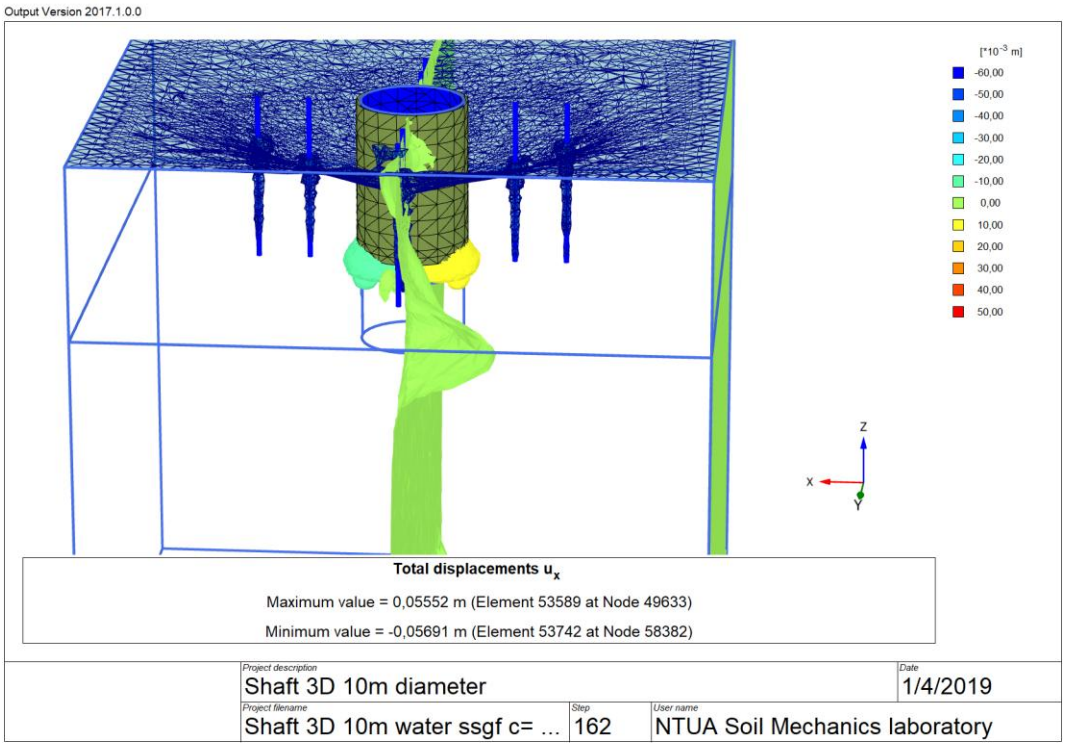

Figure.148 Maximum horizontal displacements (u_x) at the failure stage.

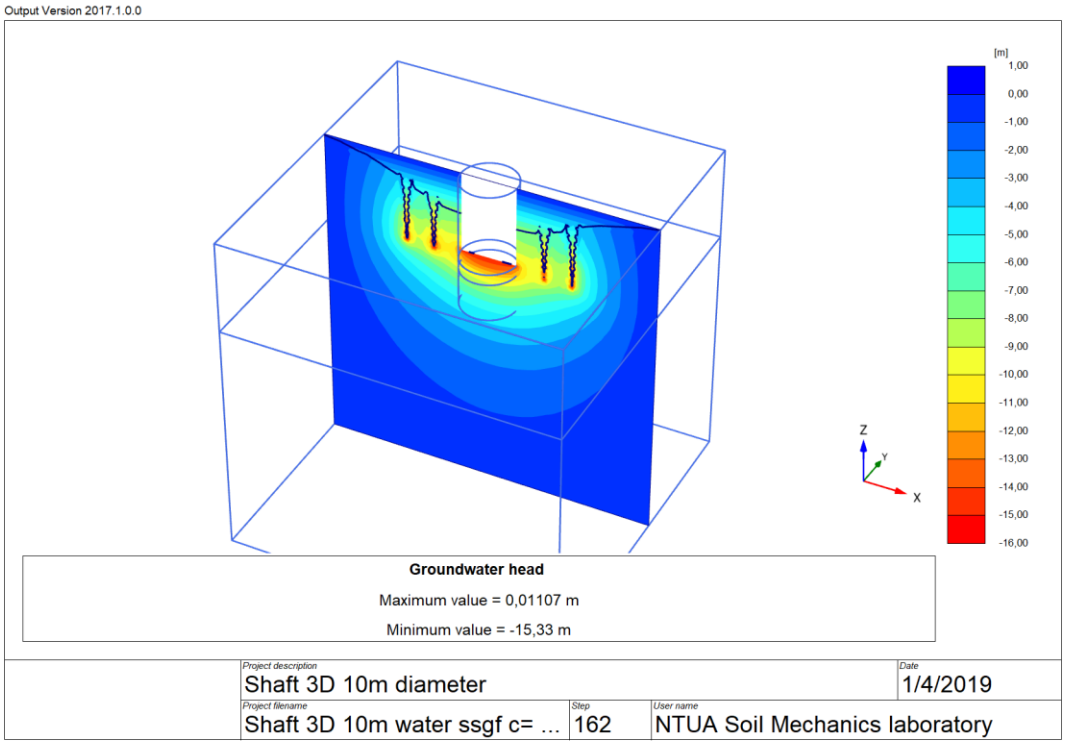

Figure.149 Groundwater head at the failure stage.

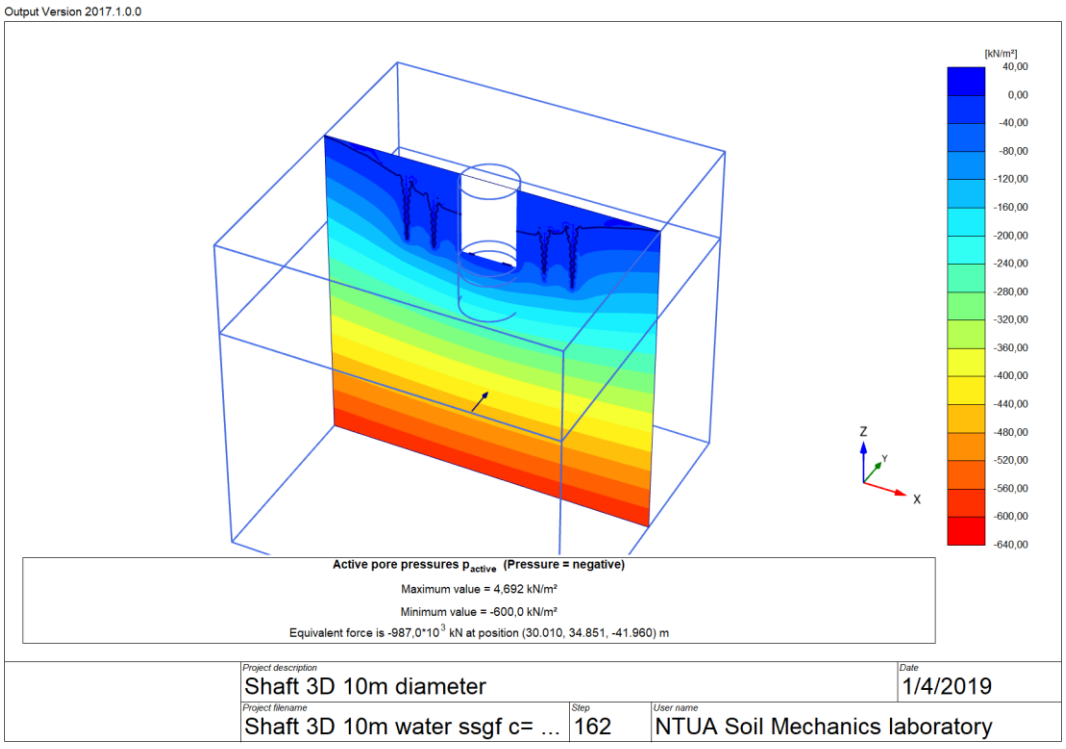

Figure.150 Active pore pressures p_{active} (pressures=negative) at the failure stage.

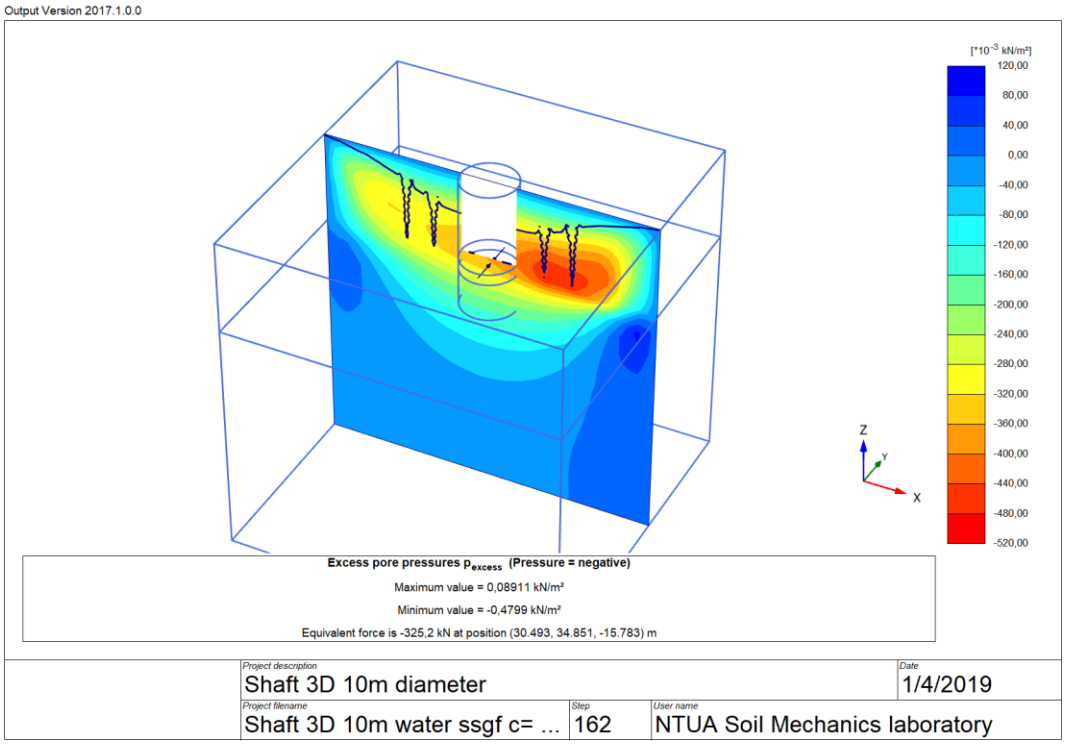

Figure.151 Excess pore pressure pexcess (pressure=negative) at the failure stage.

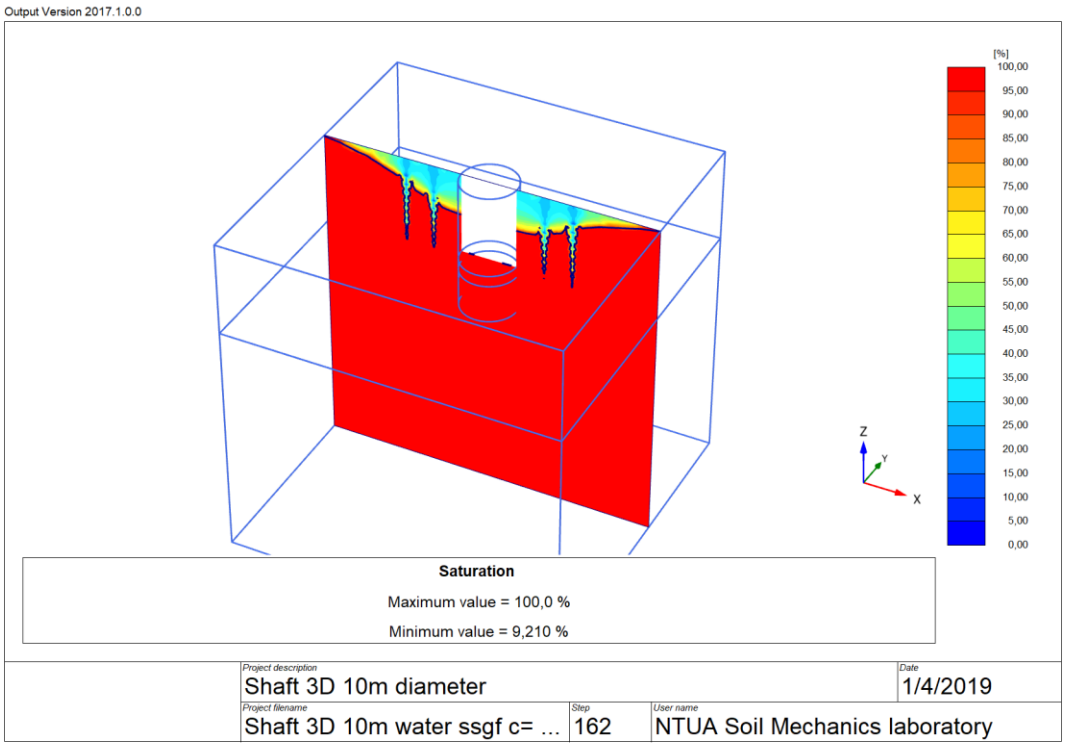

Figure.152 Saturation at the failure stage.

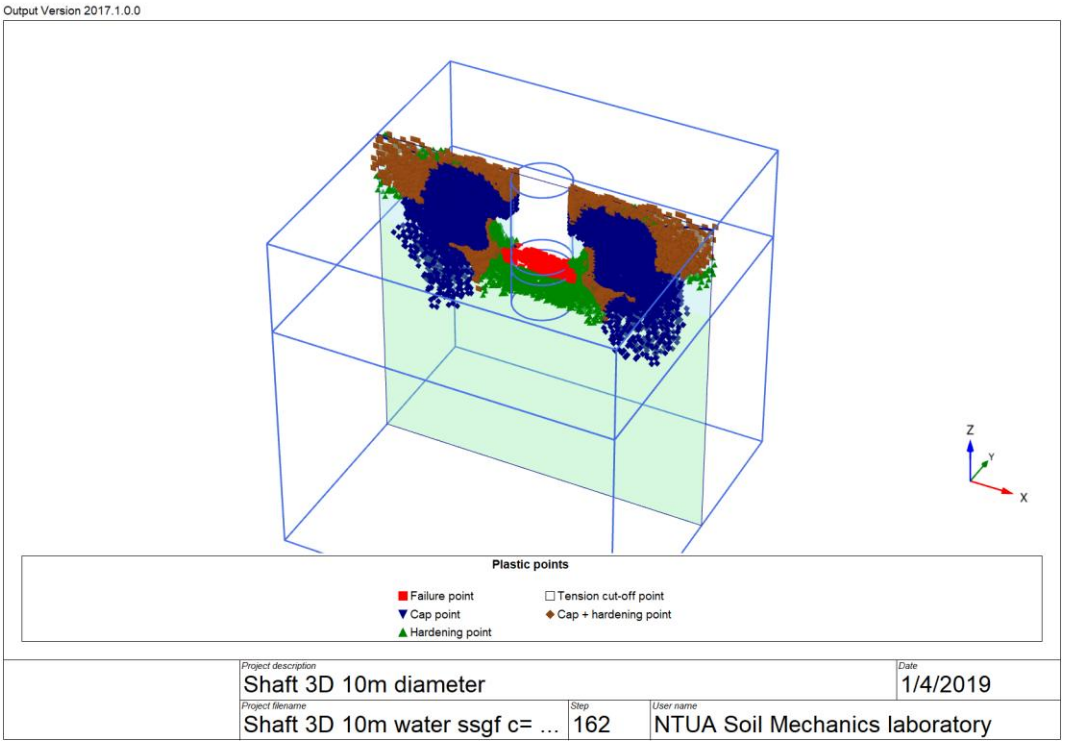

Figure.153 Plastic points at the failure stage, including Failure points, Cap points, Hardening points and Cap+ Hardening points.

Figures 144 to 152 represent displacement and pore pressure built up during construction while from Figure 153 it can be concluded that, there is a concentration of plastic points at the bottom of the excavation when the 10th simulation phase is reached, meaning that the failure is to be observed in the silty sand formation. Force distribution in the shaft is shown in Figures 154 & 155.

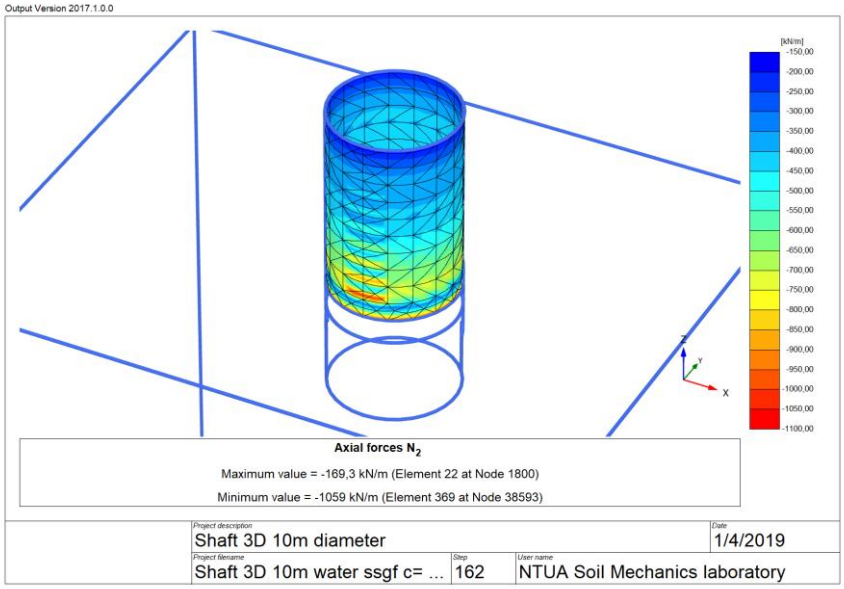

Figure.154 Axial Forces N2 distribution, maximum and minimum values at the failure stage.

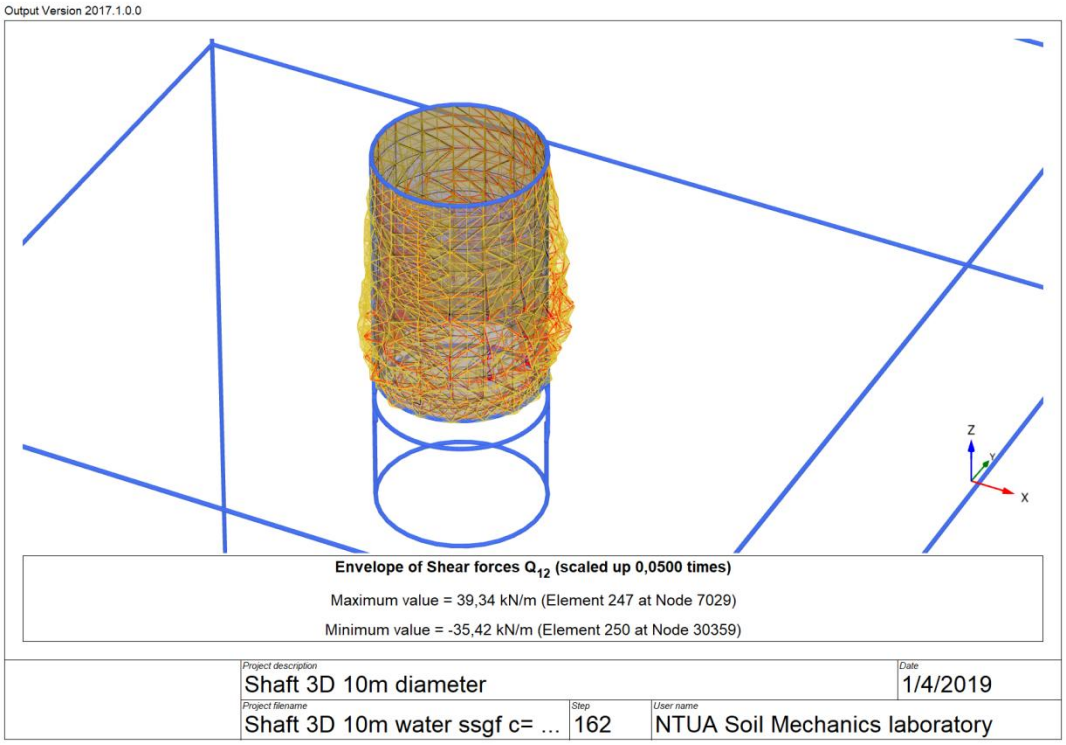

Figure.155 Envelope of the Shear forces Q_{12} at the failure stage.

To complete the analysis 3 points are selected at the ground surface for the generation of displacement curves. The points are at a distance of 0, 2,5 and 5 meters respectively from the excavation border. Vertical displacements are represented diagrammatically until the failure stage. As the output indicates, vertical displacements are of minor importance with pick values not exceeding 1 millimeter.

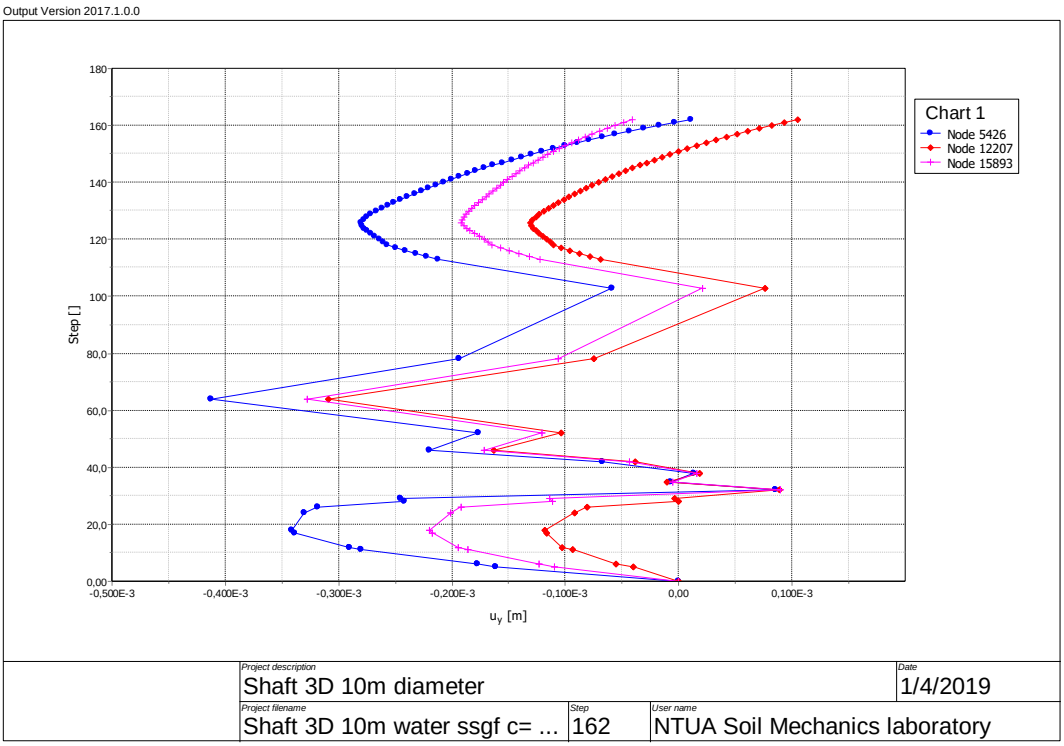

Figure.156 Trend of vertical displacement (u_y) for 3 points at the ground surface from the first until the failure stage expressed in meters.

7.11 PLAXIS 3D, STRESS ANALYSIS, HARDENING SOIL MODEL IN DRY CONDITIONS

With the main aim to compare the results and understand the PLAXIS 3D program, a three-dimensional analysis of the model is additionally carried out in the total absence of groundwater flow, meaning in dry conditions. The Hardening soil constitutive model and the" Stress" construction technique are selected.

The analysis is under 2D conditions already described in the Chapter VI employing PLAXIS 2D and PHASE2 8.0. As expected from the previous results, the project in dry conditions is successfully carried out, without encountering any particular complications in several repetitive phases. The results of the 3D analysis are presented in the following Figures 157 to 164.

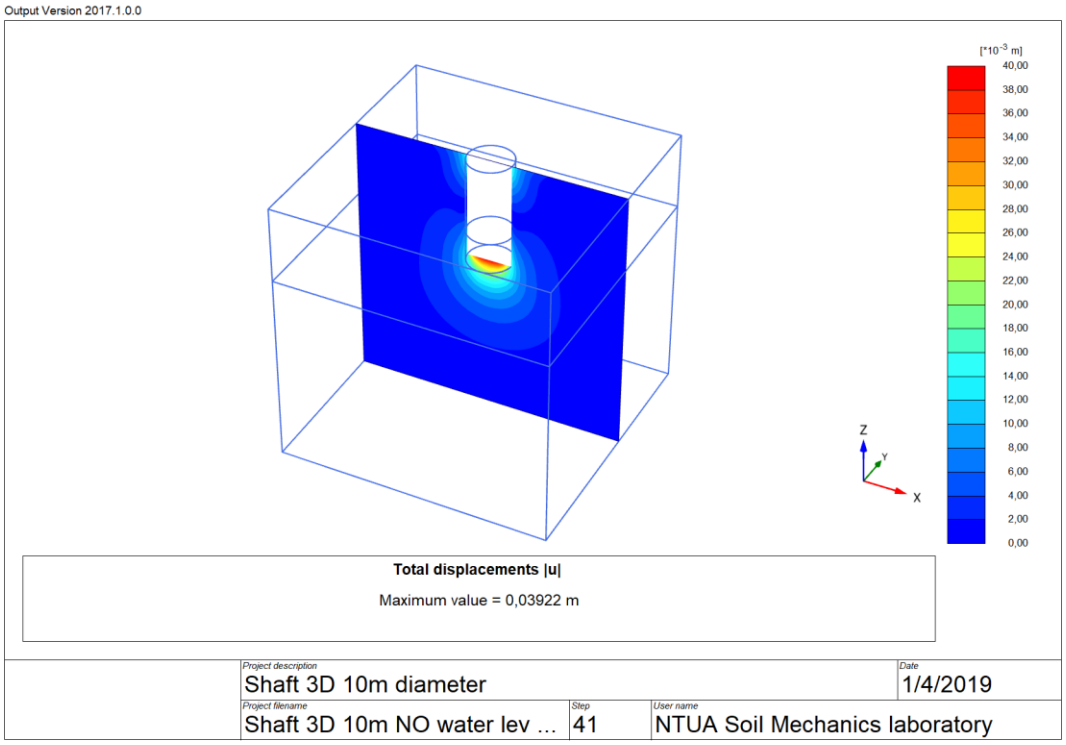

Figure.157 Total Displacements |u| absolute value at the last stage (project concluded).

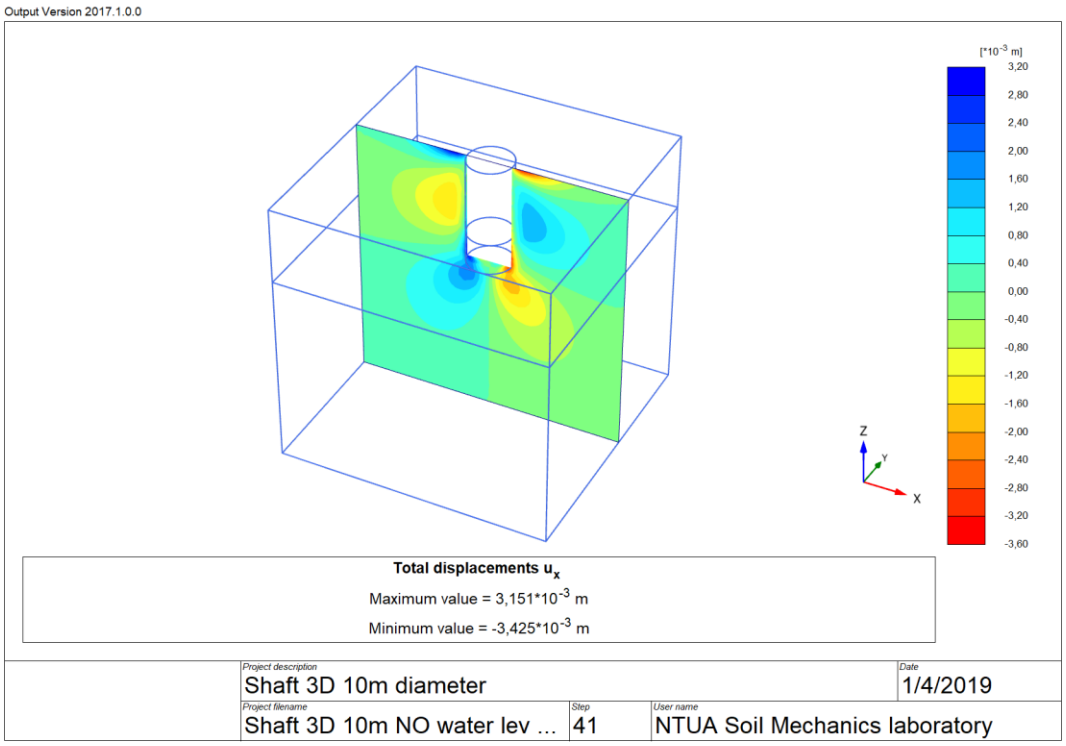

Figure.158 Horizontal Displacements (u_y) at the last stage (project concluded).

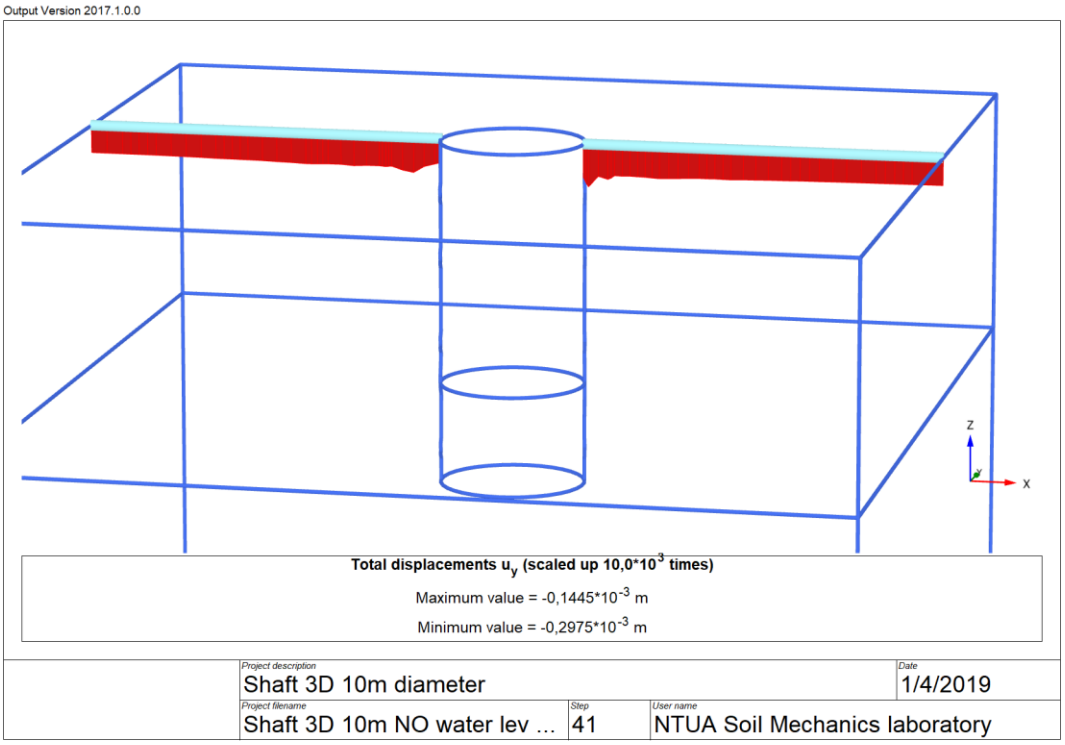

Figure.159 Cross section of Settlements (Vertical Displacements) expressed in meters adjacent to the excavation.

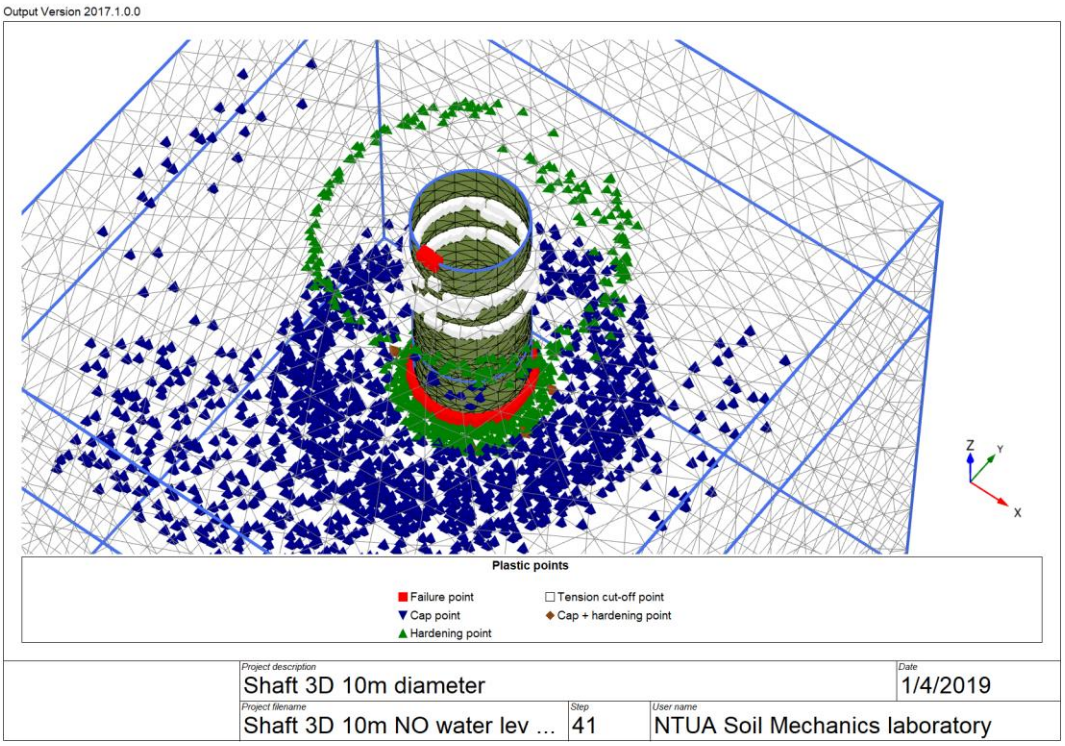

Figure.160 Plastic points at the last stage (project concluded) including Failure points, Cap points, Hardening points and Cap+ Hardening points.

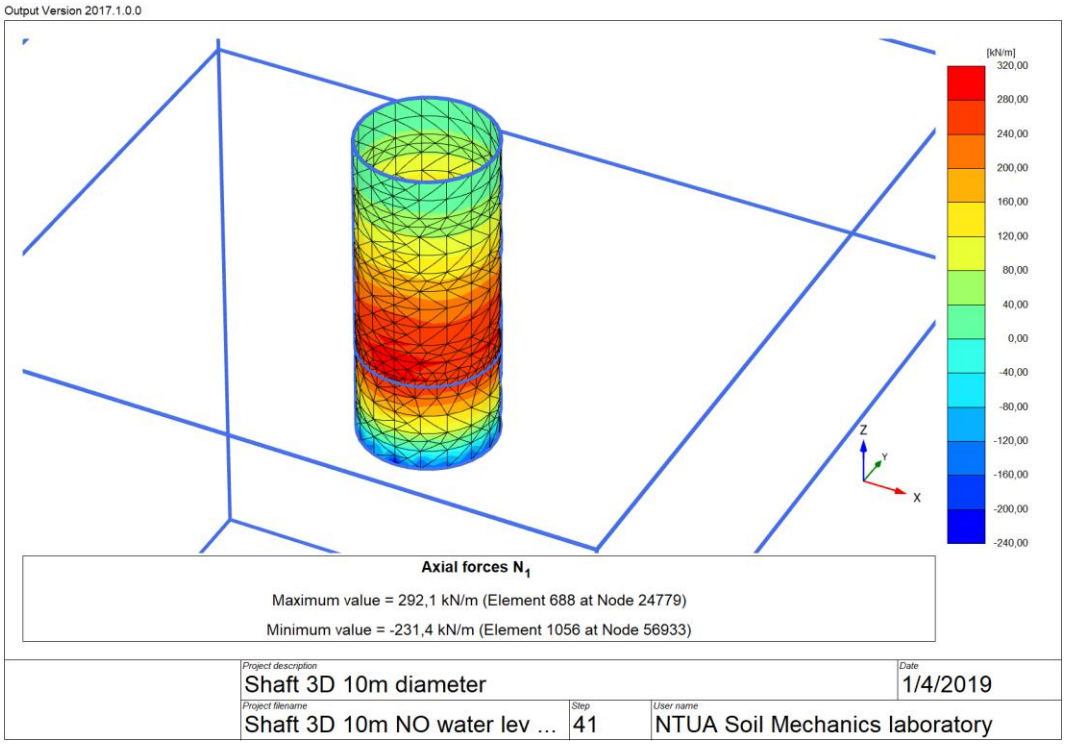

Figure.161 Axial forces N_1 distribution, maximum and minimum values at the last stage (project concluded).

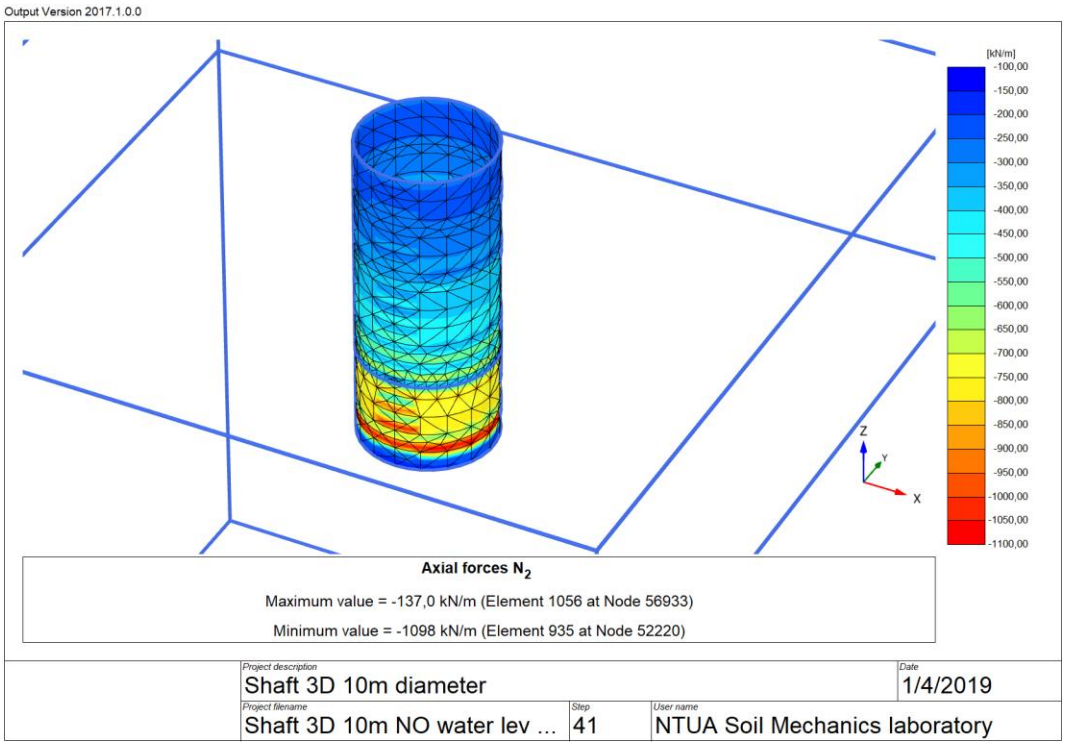

Figure.162 Axial forces N_2 distribution, maximum and minimum values at the last stage (project concluded).

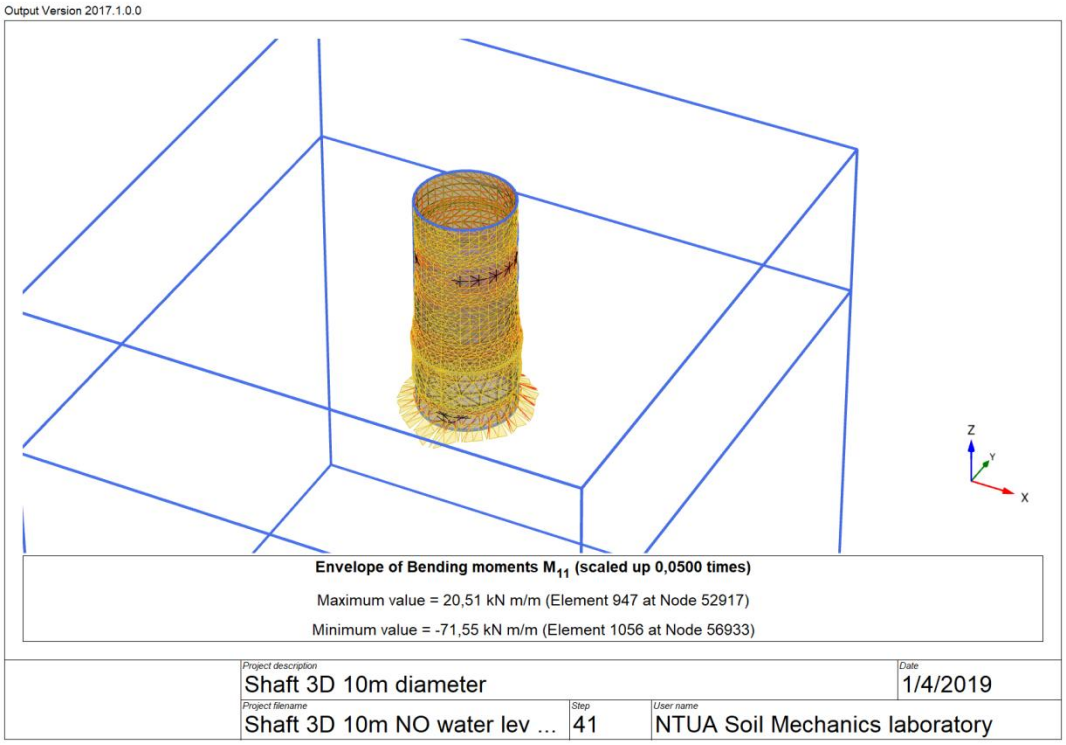

Figure.163 Envelop of Bending Moment M_{11} at the last stage (project concluded).

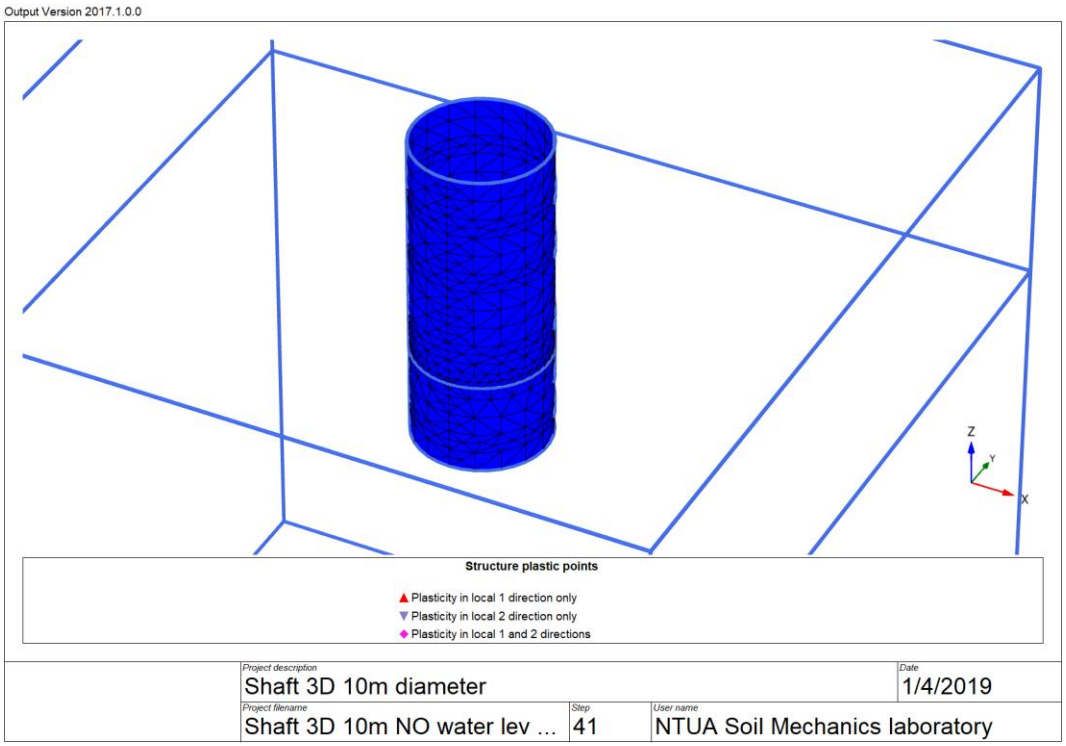

Figure.164 Structure Plastic points at the last stage (project concluded).

7.12 COMPARISON OF THE CALCULATION OUTPUTS

PLAXIS 3D HS Stress	Maximum and Minimum Values
Deformed Mesh (m)	0,03922
Bottom Uplift (m)	**0,03922**
Settlements/Uplifts at ground level (m)	$-0{,}298*10^{-3}$
	$\mathbf{-0{,}145*10^{-3}}$
Total Vertical Displ. (uy) in m	$3{,}3*10^{-3}$
	$\mathbf{-3{,}5*10^{-3}}$
Total Horizontal Displ. (ux) in m	$3{,}16*10^{-3}$
	$\mathbf{-3{,}43*10^{-3}}$
Axial Forces N_1 in KN/m	**292,1**
	-231,4
Axial Forces N_2 in KN/m	-137
	-1098
Shear Forces Q_{12} in KN/m	34,72
	-47,24
Shear Forces Q_{23} in KN/m	25,1
	-25,79
Shear Forces Q_{13} in KN/m	34,08
	-232,5
Bending Moment M_{11} in KNm/m	20,51
	-71,55
Bending Moment M_{22} in KN/m	4,12
	-10,81
Bending Moment M_{12} in KN/m	4,08
	-4,57

Tab.15 Synoptic table of the maximum and minimum output values of the 3-dimensional analysis in dry conditions using PLAXIS 3D 2018.

Comparing the 2-dimensional analysis in dry conditions running PLAXIS 2D and the 3-dimensional analysis running PLAXIS 3D it can be concluded that there is, where the comparison can be made, a certain affinity in the results i.e. maximum values of deformed mesh, bottom uplift, horizontal displacements (ux) and bending moments. Excessive absolute percentage variations are encountered in correspondence to the maximum values of settlements at the surface (5106%) and the overall maximum total vertical displacements (1000%). Even though, these numbers are not alarming as the entities are of the order of a few millimeters and settlement limitations are not surpassed. It should be mentioned that variances may occur as in the 2-dimensional axisymmetric analysis simplifications are made and the study is conducted in the plane and not in the space.

Maximum and Minimum Values	**PLAXIS 2018 3D HS Stress**	**PLAXIS 2018 2D HS Stress**	**Percentage Variation |%|**
Deformed Mesh (m)	0,03922	0,0383	2,43%
Bottom Uplift (m)	0,03922	0,0342	12,8%
Settlements/Uplifts at ground level (m)	$-0{,}298*10^{-3}$	$0{,}2*10^{-3}$	32%
	$-0{,}145*10^{-3}$	$-7{,}6*10^{-3}$	**5,106%**
Total Vertical Displ. (u_y) in m	$3{,}3*10^{-3}$	0,0383	**1000%**
	$-3{,}5*10^{-3}$	$-8{,}1*10^{-3}$	**131%**
Total Horizontal Displ. (u_x) in m	$3{,}16*10^{-3}$	$1*10^{-3}$	68%
	$-3{,}43*10^{-3}$	$-3{,}6*10^{-3}$	17%
Axial Forces N_1 in KN/m	292,1	277,8	5%
	-231,4	-150,2	35%
Shear Forces Q in KN/m	34,72	147,8	**332%**
	-47,24	-147,5	**212%**
Bending Moment M_{11} in KNm/m	20,51	-14,72	26%
	-71,55	64,96	9%

Table.16 Comparison of PLAXIS 3D and PLAXIS 2D tabulated results where the H.S. constitutive model and the stress construction technique are applied.

7.13 CONCLUSIONS

I. From the analyses carried out in the present chapter, it is evident that regardless of the construction technique i.e. the application of the segmented concrete rings is done immediately after the excavation of the phase/stage (Deformation technique) or at the next stage of excavation (Stress technique), the construction in the presence of water flow is failing. Precisely at the 6^{th} stage, meaning that as approximately 7,5 meters are excavated and supported the structural integrity of the shaft is guaranteed. Once that depth is exceeded, a body of soil collapses.

II. The employment of wells, selected and installed as a dewatering technique directing to lower the groundwater table is of benefit to the construction process. In fact, in the presence of a group of wells (8 wells), applied in a shape of a cross, each one pumping out $Q=0,03m^3/s$ and having a maximum depth of -16 meters, simulation indicates that body soil collapses at a later stage, precisely at the 10^{th} stage. It can be concluded that the excavation and subsequent support continues without particular difficulties for another 6 meters.

III. Plastic points as extensively described above, depict the stress points that are in a plastic state displayed in a plot of undeformed geometry. They indicate the stresses that lie on the failure envelop, meaning that failure is imminent in these areas. As in the 2-dimensional analyses where the Stress construction technique is employed, plastic points are mainly concentrated at the bottom.

IV. Surface settlements, are of minor importance to the designer even if, due to the water table lowering, are expected. As already demonstrated where the Hardening Soil constitutive model is used values of vertical deformations assume values of restrained entity.

V. Regarding structural stability, as Fig. 130 indicates there are no plastic points displayed before the failing stage. The most critical area is detected at the bottom not affecting the structure itself.

CHAPTER VIII
THESIS CONCLUSIONS AND FURTHER RESEARCH

A computer aided study is performed to investigate the realization and the subsequent effects of an 24 meters deep sequential excavation and construction of a ventilation shaft composted of segmented concrete rings. The lateral and base vertical displacements are examined. The analyses are performed both in dry conditions and in the presence of a groundwater table at ground level. Two-dimensional models simulating the cylindrical shaft are developed to satisfy the axisymmetric configuration of this particular underground structure and to allow the measurements of the earth effects acting on the shaft. All assumptions regarding the selected soil parameters are justified and where necessary, bibliographical references are made. Moreover, 3D analyses are performed to simulate the water flow and an effort to lower the water table utilizing wells is made. No safety factor is calculated as the results imply the stability or instability of the structure. The results, outcomes of various finite element method softwares are compared. Based on this study, the following conclusion can be drawn.

8.1 THESIS CONCLUSIONS

I. FINITE ELEMENT ANALYSIS-AXISYMMETRY

The Finite Element method is widely used for analyzing geotechnical problems, producing realistic results and being of great value to civil engineering problems. Even if geotechnical problems involve three dimensional structures necessitating a three dimensional analysis, this is not always a practical proposition. An axisymmetric analysis is conducted, clearly reducing the size of the problem and the number of finite elements needed to represent the model. An axisymmetric model is used for circular shafts with a uniform radial cross section around the central axis, where the deformation and stress state are assumed to be identical in any radial direction. Two-dimensional analyses are performed applying commercial finite element software, in particular PLAXIS 2D 2018 and PHASE2 8.0.

II. CIRCULAR SHAFT

It can be concluded that a circular shaft generally in dry conditions is structurally stable. The earth loads applied to this geometry place the support in ring under compression, reducing the reinforcement in the structural elements. A circular structure is preferred as it is structurally stable, minimizing the ground displacements during excavation. As part the thesis, in the dry analyses, an axisymmetric model is used for shafts with a uniform radial cross section around the central axis. As the 2-dimensional results testify in dry conditions, the shaft's cylindrical concrete rings are subjected to horizontal ground displacements mainly at the lower half of the structure. In the presence of water flow, where the 3-

dimensional analyses are carried out, regardless of the construction technique (deformation or stress construction technique), the project fails. Precisely at the 6^{th} stage, meaning that approximately 7,5 meters are excavated and successfully retained. As soon as that depth is exceeded, body soil collapses is evident, implying an imminent failure.

III. CONSTRUCTION TECHNIQUE

As the analyses' results indicate, if the deformation construction technique is applied uplifts of restricted entity are displayed during the first excavation phases, transformed into settlements in the following phases as a result of the deconfinement. Generally, all resulting forces and bending moment values are lower in the deformation construction mode in terms of maximum absolute values and distribution. Moreover, forces and bending moments are exerted differently on the structure depending on the construction technique.

IV. CONSTITUTIVE MODEL

Regarding the structural stability of the shaft, with the only exception of Hoop Forces (Nz) developed when the stress construction technique is operated, all values of forces and movements on the shaft are lower (15% to 25% on average) when the H.S. model is adopted. Furthermore when the H.S. model is used both the distribution and the absolute values of the vertical deformations are limited.

V. SETTLEMENTS

The construction technique adopted affects the direction of the vertical settlements. Where the deformation technique is applied settlements (not uplifts) are observed on the surface. On the other hand, where the stress construction technique is selected, ground lateral (vertical) deconfinement is limited. According to criteria in the international bibliography for the permissible settlements of buildings, all induced settlements are acceptable and the area affected by settlements is limited in a range of 4 meters from the excavation boundary.

VI. BOTTOM UPLIFT

The major undesirable effect encountered is the vertical displacements at the bottom of the excavation, representing the overall maximum displacement. Where the Mohr Coulomb constitutive model is applied and the deformation construction mode is adopted, the maximum value of the uplift is more substantial (u_y=0,1410m) than the case of stress construction mode (u_y=0,1219m) based on the PHASE2 analyses' results. Last but not least, in the presence of water flow, ground surface settlements are also of minor importance.

VII. DEWATERING

The employment of wells, selected and installed as a dewatering technique, aiming to lower the ground water table, is of benefit to the project permitting the excavation and sequential support to continue for an extra 6 meters compared to water flow conditions.

VIII. PLASTIC POINTS

Plastic points show the stress points that are in a plastic state displayed in a plot of the deformed geometry. In dry conditions, if the deformation construction technique is applied, a distribution of plastic points is concentrated over the first half of the vertical concrete support, as well as, at the bottom in the proximity of the vertical support. Diversely, if the stress construction technique is employed, plastic points are concentrated mainly at the bottom at a depth that exceeds 5 meters, in the proximity of the shaft. In the presence of water flow, as in the 2-dimensional analyses conducted in dry conditions, where the stress construction technique is employed, plastic points are mainly concentrated at the bottom of the shaft.

8.2 RECOMMENDATIONS FOR FUTURE WORK

Following the foregoing work that more research is needed to establish an overall accepted design methodology for cylindrical shafts in the presence of water flow. Recommendations for further research based on the results of this thesis consist of the investigation of dewatering techniques so that deep excavations are constructed in the presence of water without the danger of imminent soil collapse. This would contribute to the development of a more rational design methodology for shafts in the presence of water flow and a more advanced evaluation of the applicability of the theoretical methods. Alternative shaft construction techniques could also be evaluated comparing the reliability of each method.

BIBLIOGRAPHY

[Online]. Available: https://www.revolvy.com/page/Shaft-(civil-engineering) [Accessed in 22/10/2018].

Abbo, A. J., Lyamin, A. V., Sloan, S. W., & Hambleton, J. P. (2011). A C2 continuous approximation to the Mohr–Coulomb yield surface. International Journal of solids and Structures, 48(21), 3001-3010.

Aye, T. T., Tong, M. S. Y., Yi, K. H., & Arunasoruban, E. (2014). Design and Construction of Large Diameter Circular Shafts. Underground Singapore, Singapore.

Boyce G.M. in J.Rush (2012). "Shaft Design and Construction ". Tunnel Business Magazine TBM. https://tunnelingonline.com/shaft-design-and-construction/ [accessed in 12/11/2018].

Brinkgreve, R.B.J., Kumarswamy, S., Swolfs, W.M. (2018). Plaxis 3D 2018 (General Info, Tutorial, Reference, Material Models and Scientific Manual). Delft, Netherlands.

Brinkgreve, R.B.J., Kumarswamy, S., Swolfs, W.M., Zampich, L., Ragi Manoj, N., (2018). Plaxis 2D 2019 (General Info., Tutorial, Reference, Material Models and Scientific Manual). Delft, Netherlands.

Cheng, Y. M., & Hu, Y. Y. (2005). Active earth pressure on circular shaft lining obtained by simplified slip line solution with general tangential stress coefficient. (Chinese journal of geotechnical engineering).

Chiesa G. (1994). Idraulica delle acque di falda. Dario Flacovio Editore. EAN 9788877582164.

Chini, S. A., & Genauer, G. (1997). Excavation Support Systems for Construction Operations. Journal of Construction Education, 2(3), 156-170.

Datta, Sahashi K. Gulhati Manoj (2005).Geotechnical engineering. Tata McGraw-Hill Education, 2005.

Dias, C.C. and Gomes, A.T. and Vaunat, Jean (2013). Shafts by the Sequential Excavation Method: Mechanical vs Hydro-mechanical calculations. Advances in Unsaturated Soils - Proceedings of the 1st Pan-American Conference on Unsaturated Soils, PanAmUNSAT 2013, 501-506.

Faustin, N. E., Elshafie, M. Z., & Mair, R. J. (2018). Case studies of circular shaft construction in London. Proceedings of the Institution of Civil Engineers-Geotechnical Engineering, 171(5), 391-404.

Harter, T. (2003). Water well design and construction. UCANR Publications.

Holl, G. W. & Fairon, E. G. (1973). A review of some aspects of shaft design. Journal of the South African Institute of Mining and Metallurgy, 73 pp. 309-324.

Humes, Tunnel and shaft solutions. Available: https://www.holcim.com.au/sites/australia/files/atoms/files/hu-tunnel-sharf-solutions-iss3.pdf [Online].

Hutton, D. V. (2004). Fundamentals of finite element analysis. McGraw-hill. ISBN 0-07-112231-1 (ISE).

Kim, K. Y., Lee, D. S., Cho, J., Jeong, S. S., & Lee, S. (2013). The effect of arching pressure on a vertical circular shaft. Tunnelling and underground space technology, 37, 10-21.

Kumagai, Toshio, Kouzou Ariizumi, and Atsuo Kashiwagi. (1999). "Behaviour and analysis of a large-scale cylindrical earth retaining structure." Soils and foundations 39.3: 13-26.

Lade, V.P. (2005). Overview of Constitutive Models For Soils. Geotechnical Special Publication. 1-34. 10.1061/40771(169)1.

Logan, D. L. (2011). A first course in the finite element method. Cengage Learning. ISBN-13-978-0-495-66825-1.

Meftah, A., Benmebarek, N., & Benmebarek, S. (2018). Numerical study of the active earth pressure distribution on cylindrical shafts using 2D finite difference code. Journal of Applied Engineering Science & Technology, 4(2), 123-128.

Muramatsu, M., and Y. Abe. (1996). "Considerations in shaft excavation and peripheral ground deformation." Geotechnical Aspects of Underground Construction in Soft Ground: 173-178.

Papadopoulos D. (2014). Analysis of a circular ventilation shaft with 2D and 3D finite element models (FEM), NTUA.

Phase 2. Model Reference Manual (2005). Rocscience.

Potts, D. M. & Zdravkovic, L., (2001). Finite element analysis in geotechnical engineering: application (Vol. 2). Thomas Telford.

Salgado, R., Bandini, P., & Karim, A. (2000). Shear strength and stiffness of silty sand. Journal of Geotechnical and Geoenvironmental Engineering, 126(5), 451-462.

Schanz, T., Vermeer, P. A., & Bonnier, P. G. (1999). The hardening soil model: formulation and verification. Beyond 2000 in computational geotechnics, 281-296.

Venkatramaiah, C. (1995). Geotechnical engineering. New Age International.

Wong, R. C. K., & Kaiser, P. K. (1988). Design and performance evaluation of vertical shafts: rational shaft design method and verification of design method. Canadian Geotechnical Journal, 25(2), 320-337.

Zhang, X.P., Lu, M, Zhao, Z (2013). Vertical shaft design optimization for underground space development, pp 367-372.

Αναγνωστόπουλος Α. & Μιχάλης Η. (2004). Σημειώσεις Αντιστηρίξεων και Καθιζήσεων λόγω εκσκαφών. Ε.Μ.Π.

Καββαδας Μ. (2005). Στοιχεία εδαφομηχανικής, Μόνιμη Υδατική Ροή διαμέσου του εδάφους. (www.civilntua.gr~kavvadas).